

USAAMRDL-TR-75-19



AD-A013 407

**FLIGHT TESTING OF A FAN-IN-FIN ANTITORQUE AND
DIRECTIONAL CONTROL SYSTEM AND A COLLECTIVE FORCE
AUGMENTATION SYSTEM (CFAS)**

**SIKORSKY AIRCRAFT DIVISION
UNITED TECHNOLOGIES CORPORATION
Stratford, Conn. 06602**

12

June 1975

Final Report for Period April 1972 - May 1974

Approved for public release;
distribution unlimited.

DDC
RECEIVED
JUL 30 1975
RECEIVED
B

Prepared for

**EUSTIS DIRECTORATE
U. S. ARMY AIR MOBILITY RESEARCH AND DEVELOPMENT LABORATORY
Fort Eustis, Va. 23604**

**Best
Available
Copy**

EUSTIS DIRECTORATE POSITION STATEMENT

The results of this flight demonstration program support the technical feasibility of using the fan-in-fin concept as an alternate antitorque and directional control device for single-rotor helicopters in the general size and weight range of the flight vehicle. The applicability of the results is influenced by the consideration that only the empennage (including the fan) was peculiar to the demonstrated concept in contrast to a helicopter initially designed to include the fan-in-fin concept. Since this report accurately portrays the program, results similar to those demonstrated could reasonably be expected in new aircraft designs of the same general size and weight as the demonstrator helicopter.

Mr. James P. Whitman of the Systems Support Division served as the Project Engineer and Contracting Officer's Technical Representative for this effort. Messrs. Harry L. Murray and Duane R. Simon served as the Assistant Contracting Officer's Technical Representative and Government Evaluation Pilot, respectively.



DISCLAIMERS

The findings in this report are not to be construed as an official Department of the Army position unless so designated by other authorized documents.

When Government drawings, specifications, or other data are used for any purpose other than in connection with a definitely related Government procurement operation, the United States Government thereby incurs no responsibility nor any obligation whatsoever; and the fact that the Government may have formulated, furnished, or in any way supplied the said drawings, specifications, or other data is not to be regarded by implication or otherwise as in any manner licensing the holder or any other person or corporation, or conveying any rights or permission, to manufacture, use, or sell any patented invention that may in any way be related thereto.

Trade names cited in this report do not constitute an official endorsement or approval of the use of such commercial hardware or software.

DISPOSITION INSTRUCTIONS

Destroy this report when no longer needed. Do not return it to the originator.

UNCLASSIFIED

SECURITY CLASSIFICATION OF THIS PAGE (When Data Entered)

REPORT DOCUMENTATION PAGE		READ INSTRUCTIONS BEFORE COMPLETING FORM	
1. REPORT NUMBER USAAMRDL-TR-75-19	2. GOVT ACCESSION NO.	3. RECIPIENT'S CATALOG NUMBER	
4. TITLE (and Subtitle) FLIGHT TESTING OF A FAN-IN-FIN ANTITORQUE AND DIRECTIONAL CONTROL SYSTEM AND A COLLECTIVE FORCE AUGMENTATION SYSTEM (CFAS)		5. FUNDING NUMBERS Final Report Apr 1972 - May 1974	
6. AUTHOR(s) Wilfried H. Meier, William P. Groth, David R. Clark, David Verzella		7. PERFORMING ORG. REPORT NUMBER SER-67015	
8. PERFORMING ORGANIZATION NAME AND ADDRESS Sikorsky Aircraft Division United Technologies Corporation Stratford, Connecticut 06602		9. PROGRAM ELEMENT, PROJECT, TASK AREA & WORK UNIT NUMBERS 63204A 1F163204D157 00 013 EK	
10. CONTROLLING OFFICE NAME AND ADDRESS Eustis Directorate, U. S. Army Air Mobility Research & Development Laboratory, Fort Eustis, Virginia 23604		11. REPORT DATE June 1975	
12. MONITORING AGENCY NAME & ADDRESS (if different from Controlling Office)		13. NUMBER OF PAGES 201	
14. DISTRIBUTION STATEMENT (of this report) 12 205p.		15. SECURITY CLASS. (of this report) UNCLASSIFIED	
16. DISTRIBUTION STATEMENT (of the abstract entered in Block 20, if different from Report)		17a. DECLASSIFICATION/DOWNGRADING SCHEDULE	
17. DISTRIBUTION STATEMENT (of the abstract entered in Block 20, if different from Report) 16 DA-1-F-163204-D-157			
18. SUPPLEMENTARY NOTES 17 1-F-163204-D-15700			
19. KEY WORDS (Continue on reverse side if necessary and identify by block number) HELICOPTERS SHROUDED PROPELLERS ANTITORQUE ROTORS CONTROL, DIRECTIONAL DUCTED FANS ANTITORQUE CONCEPTS CONTROL FEEL AUGMENTATION			
20. ABSTRACT (Continue on reverse side if necessary and identify by block number) A research flight test program was conducted to determine the characteristics of the fan-in-fin antitorque and directional control concept compared with a conventional tail rotor in the areas of stability, control, power requirements, aerodynamics, and overall aircraft performance. For the program, the tail rotor of Sikorsky's S-67 Blackhawk helicopter was replaced by a ducted fan, mounted in a new vertical tail. The modified aircraft was flight tested under a test plan that provided direct comparison with the baseline aircraft.			

DD FORM 1 JAN 73 1473 EDITION OF 1 NOV 68 IS OBSOLETE
S/N 0102-014-6601UNCLASSIFIED
SECURITY CLASSIFICATION OF THIS PAGE (When Data Entered)

323 800

UNCLASSIFIED

SECURITY CLASSIFICATION OF THIS PAGE (When Data Entered)

(Cont'd)
p 173A) The fan-in-fin demonstrated that its advantages in compactness and increased safety in ground operation can be realized without significant performance penalty or unpredictable impact on handling qualities. ^{At 160 KTS} Some shortcomings were experienced by this configuration, but test results confirmed that the fan-in-fin is an acceptable alternate to the tail rotor in applications where the reduction in operational hazards provided by the fan is essential. The measured performance indicated a decrease of about 3 KTAS in top speed to 190 KTAS, and a reduction in hover gross weight of about 1 1/2 percent. Fan stress and vibration levels remained within acceptable limits throughout the flight envelope. A substantial improvement in maneuvering capability in hover and at low speeds is possible because the fan is designed to higher thrust levels than the tail rotor and is not subject to the stress limitations that applied to the tail rotor. Likewise, autorotation and sideslip envelopes are greatly expanded, the former because of the increased control range available and the latter because of the removal of the stress limitations. The fan itself performed well over the entire flight envelope. No instabilities were detected, and no reversal phenomena or other aerodynamic problems were encountered. Throughout the ground and flight tests, the mechanical reliability of the fan was good.

Handling qualities with the fan-in-fin in flight, with one exception, were similar to those with the tail rotor at comparable gross weights and center-of-gravity positions. The one exception was a decrease in lateral directional stability at high speeds, with a resulting noticeable softness in yaw and difficulty in maintaining precise yaw trim. This characteristic has also been displayed by other helicopters equipped with yaw control and antitorque fans; the reason for it has been identified, but has yet to be corrected. Increasing the vertical tail area does not appear to be the cure. A better understanding of the air flow pattern around the fan is needed.

At low negative fan thrust levels, fan thrust response to control inputs was sluggish, rendering directional control in the taxi mode unsatisfactory. This is an aerodynamic problem of the fan when operating at moderate negative thrust. In addition, the negative thrust from the fan at reduced rotational speeds was judged inadequate, and for this reason autorotational roll-on landings were not performed. This is a control range problem and can be corrected.

Some of the low-speed maneuvers were associated with strong pitching motion of the aircraft, especially in light winds. The problem was diagnosed as main rotor downwash impingement on the horizontal stabilator (11 inches forward of that in the tail rotor configuration), possibly complicated by deflection of the fan wake over the left stabilator. One flight without the stabilator verified this assessment.

Although acoustical fan data were acquired and the fan acoustical signature was lower in sound pressure level than the tail rotor, an observer may judge it to be louder.

Concurrently with the fan-in-fin flight test program, a collective force augmentation system (CFAS) was evaluated on the S-67 helicopter. System description and flight test results are contained in Appendix D of this report. The purpose of CFAS is to keep main rotor loads within acceptable limits during high-speed maneuvering flight by introducing a force-feel cue to the pilot's collective control stick. Flight tests ^{proved} the CFAS ~~proved it~~ capable of providing the pilot with the proper force cues to maneuver the helicopter to the boundary of the main rotor load limit. X

UNCLASSIFIED

SECURITY CLASSIFICATION OF THIS PAGE (When Data Entered)

PREFACE

This report presents the results of a research flight test program for a fan-in-fin helicopter, and compares the fan-in-fin to the aircraft equipped with a tail rotor. Sikorsky Aircraft was the prime contractor and used the S-67 Blackhawk for the conversion. Hamilton Standard, Division of United Aircraft Corporation, the fan subcontractor, designed and built two ducted fan units: one for ground and one for flight testing. Fan static ground tests were conducted, operating for 80.9 hours on Sikorsky's tail rotor test stand. A 6.1-hour tie-down test verified fan design and air-frame compatibility. The flight test program totaled 29 flight hours and comprised a fan shakedown phase, a rudder/fan optimization phase, flight tests for comparison with the tail rotor configuration, and an evaluation phase conducted by the U. S. Army.

The program was conducted at the Contractor's facility for the Eustis Directorate, U. S. Army Air Mobility Research and Development Laboratory, Fort Eustis, Virginia, under Contract DAAJ02-72-C-0050, DA Project 1F-163204D157.

Mr. J. Whitman and Mr. H. Murray were the Army technical representatives, Mr. D. Simon was the Army project pilot and Mr. J. Nedin was the contractor's project task manager.

CONTENTS

	<u>Page</u>
PREFACE	1
LIST OF ILLUSTRATIONS	5
LIST OF TABLES	12
INTRODUCTION	13
SCOPE OF PROGRAM	15
DESIGN APPROACH AND DESCRIPTION OF TEST AIRCRAFT	16
Program Objectives	16
S-67 General Information	16
Fan-in-Fin Design Approach and Constraints	17
Specific Design Aspects, S-67 Fan-in-Fin	18
TEST PROCEDURES AND TECHNIQUES	34
Maneuver Techniques	34
RESULTS AND DISCUSSION	36
Aircraft Performance	36
Fan Static Performance	52
Fan Forward Flight Performance	62
Fan Inlet Behavior	72
S-67 Fan-in-Fin Handling Qualities	94
Acoustic Signature	145
Implications for S-67 Flight Envelope	147
OPERATIONAL POTENTIAL	150
Applications	150
Reliability and Maintainability	151
Abrasion	152
CONCLUSIONS AND RECOMMENDATIONS	153
Limits of Comparison	153
Conclusions	153
Recommendations	155
LIST OF REFERENCES	156

CONTENTS (CONTINUED)

	<u>Page</u>
APPENDIX A. FAN DESIGN AND DESCRIPTION	157
Fan Design Approach	157
Fan Design and Operation	158
Fan Blade Characteristics	158
Excerpts from Fan Specification	162
APPENDIX B. RUDDER EVALUATION	165
Description	165
Flight Tests	165
Conclusion	165
APPENDIX C. ACOUSTIC EVALUATION	166
Isolated Fan Noise	166
Aircraft Tie-Down Tests	172
Flight Noise Survey Tests	176
APPENDIX D. EVALUATION OF A COLLECTIVE FORCE AUGMENTATION SYSTEM . .	185
Preface	185
Foreword	185
Introduction	185
Scope of Program	186
System Description	187
Results and Discussion	193
Conclusions and Recommendations, CFAS	198
LIST OF SYMBOLS	199

LIST OF ILLUSTRATIONS

<u>Figure</u>		<u>Page</u>
1	The S-67 Blackhawk Helicopter With Tail Rotor	14
2	The Modified S-67 Blackhawk Helicopter With Fan-in-Fin . . .	14
3	General Arrangement, S-67 Fan-in-Fin Configuration	19
4	General Arrangement, S-67 Tail Rotor Configuration	21
5	Inboard Profile, S-67 Fan-in-Fin Configuration, Fin and Fan Installation	23
6	S-67 Fan-in-Fin, Upper and Lower Vertical Tail Surfaces With Fan Cusp	31
7	Qualitative Representation of Airflow Around Fan and Cusped Trailing Edge	32
8	S-67, Comparison of Tethered IGE Hover Performance, Nondimensional, Main Rotor Tip Mach Number $M = 0.615$, Wheel Height 10 ft, $h/D = 0.395$	37
9	S-67, Comparison of Tethered IGE Hover Performance, Power vs Gross Weight, SLS, 104% N_R , $h/D = 0.395$	38
10	S-67, Comparison of Tethered OGE Hover Performance, Nondimensional	40
11	S-67, Comparison of Tethered OGE Hover Performance, Nondimensional, With Boundaries of Uncertainty (from Figure 10)	41
12	S-67, Comparison of Measured Tethered OGE Hover Performance, Power vs Gross Weight, and Calculated S-67 Main Rotor Performance, SLS, 104% N_R	43
13	Comparison of OGE Hover Ceilings, Standard Temperature, 104% N_R , Sikorsky Data for S-67 Tail Rotor Configuration, Calculated and Test Data for S-67 Fan-in-Fin	46
14	Test Stand Measurements, Thrust vs Power Characteristics of the Isolated Shrouded Fan and Tail Rotor, SLS, 104% N_R . .	48
15	S-67 Fan-in-Fin Forward Flight Performance, Total Power vs Tip Speed Ratio, Nondimensional	49
16	S-67 Fan-in-Fin Forward Flight Performance, Main Rotor Power vs Tip Speed Ratio, Nondimensional	50

LIST OF ILLUSTRATIONS (CONTINUED)

<u>Figure</u>		<u>Page</u>
17	S-67 Fan-in-Fin Forward Flight Performance, Shaft Power vs Forward Speed, SLS, 104% N_R	51
18	Fan Module With Simulated Fin Center Section Installed on Sikorsky Tail Rotor Test Stand	53
19	Fan Shroud Geometry	54
20	Fan Shaft Power vs Blade Angle, SLS, 104% N_R , Static	55
21	Comparison of Measured and Predicted Fan Module Performance, Static Thrust vs Blade Angle, SLS, 104% N_R	56
22	Comparison of Measured and Predicted Fan Module Performance, Static Thrust vs Power, SLS, 104% N_R	57
23	Comparison of Measured and Predicted Static Fan Module Thrust, Rake Survey Data	59
24	Fan Performance in Hover, Thrust vs Power, SLS, 104% N_R . . .	61
25	Fan Power, Thrust, and Blade Angle vs Forward Speed; GW = 16,200 lb, Density Altitude 3,000 ft	63
26	Fan Thrust Measurement in Trimmed Level Flight: GW = 16,200 lb, Density Altitude 3,000 ft	64
27	Station location of Measured Thrust Vector Center; GW = 16,200 lb, Density Altitude 3,000 ft	65
28	Fan Input Power vs Sideslip and Speed; GW = 16,200 lb, Density Altitude 3,000 ft	66
29	Fan Thrust vs Sideslip and Speed; GW = 16,200 lb, Density Altitude 3,000 ft	67
30	Fan Blade Pitch Angle vs Sideslip and Speed; GW = 16,200 lb, Density Altitude 3,000 ft	68
31	S-67 Fan-in-Fin Aircraft, Approximately 10 Deg Left Sideslip From Trim at 180 KIAS, Fan Inlet Side	70
32	Schematic of Static Test Module With Pressure Tap Azimuths .	73
33	Variation of Fan Inlet Pressure Field With Fan Static Thrust	74

LIST OF ILLUSTRATIONS (CONTINUED)

<u>Figure</u>		<u>Page</u>
34	Variation of Thrust Component of Inlet Lip Section With Changing Blade Angle; Wind Velocity = 0	76
35	Variation of Fan Inlet Pressure Field, Simulated Forward and Rearward Flight, Positive Fan Thrust, Blade Angle = 25 deg, Wind Velocity = 35 Knots	77
36	Variation of Components of Inlet Lip Suction With Simulated Aircraft Heading at High Thrust; Wind Velocity = 35 Knots . .	79
37	Variation of Fan Inlet Pressure Field, Simulated Sideslip Conditions, Positive Fan Thrust, Blade Angle = 25 deg, Wind Velocity = 35 Knots	80
38	Variation of Fan Inlet Pressure Field, Simulated Quartering Flight at 35 Knots, Positive Fan Thrust, Blade Angle = 25 deg	81
39	Variation of Fan Inlet Pressure Field, Simulated Forward, Rearward, and Sideward Flight at 35 Knots, Negative Fan Thrust, Blade Angle = -25 deg	82
40	Variation of Fan Inlet Pressure Field, Simulated Sideslip Conditions, Negative Fan Thrust, Blade Angle = -25 deg, Wind Velocity = 35 Knots	83
41	Comparison of Predicted and Measured Inlet Pressures, Static Thrust	85
42	Comparison of Predicted and Measured Inlet Pressures; Airspeed = 35 Knots	86
43	Typical Fan Wake Velocity Profiles	88
44	Fan Inlet and Tufts at 140 KIAS	89
45	Fan Cusp and Tufts at 160 KIAS	90
46	Fan Exhaust and Tufts at 140 KIAS	91
47	Fan Inlet and Tufts at 80 KIAS	92
48	Comparison of Critical Azimuth in Hover, 20-ft Wheel Height	95
49	Comparison of Critical Azimuth in Hover, 100-ft Wheel Height	97

LIST OF ILLUSTRATIONS (CONTINUED)

<u>Figure</u>		<u>Page</u>
50	S-67 Fan-in-Fin, Left Hover Turn	100
51	S-67 Tail Rotor, Left Hover Turn	101
52	S-67 Fan-in-Fin, Right Hover Turn	102
53	S-67 Tail Rotor, Right Hover Turn	103
54	Comparison of Side-Flight Characteristics, 20-ft Wheel Height	105
55	Comparison of Side-Flight Characteristics, 100-ft Wheel Height	106
56	Comparison of Low-Speed Forward and Rearward Flight Characteristics, 20-ft Wheel Height	108
57	Comparison of Low-Speed Forward and Rearward Flight Characteristics, 100-ft Wheel Height	109
58	Comparison of Level Flight Controllability, Control Positions	110
59	Comparison of Level Flight Controllability, Aircraft Attitudes	111
60	Comparison of Static Lateral Directional Stability, 80 KIAS, Level Flight	113
61	Comparison of Static Lateral Directional Stability, 80 KIAS, Partial Power Descent	114
62	Comparison of Static Lateral Directional Stability, 80 KIAS, Climb	115
63	Comparison of Static Lateral Directional Stability, 140 KIAS, Level Flight	116
64	Comparison of Static Lateral Directional Stability, 140 KIAS, Partial Power Descent	117
65	Comparison of Static Lateral Directional Stability, $V_{max} = 190$ KTAS, Level Flight	118
66	Comparison of Static Lateral Directional Stability, $V_{max} = 190$ KTAS, Partial Power Descent	119

LIST OF ILLUSTRATIONS (CONTINUED)

<u>Figure</u>		<u>Page</u>
67	Comparison of Static Lateral Directional Stability, Dive at 111% Q, 209 KTAS	120
68	Variation of Sideslip With Pedal Position, S-67 Fan-in-Fin . .	121
69	S-67 Fan-in-Fin, Level Flight 120 KIAS, 1-inch 1/2-sec Right Pedal Pulse	124
70	S-67 Tail Rotor, Level Flight 120 KIAS, 1-inch 1/2-sec Right Pedal Pulse	125
71	S-67 Fan-in-Fin, Level Flight 120 KIAS, 1-inch 1/2-sec Left Pedal Pulse	126
72	S-67 Tail Rotor, Level Flight 120 KIAS, 1-inch 1/2-sec Left Pedal Pulse	127
73	S-67 Fan-in-Fin, Level Flight 160 KIAS, 1-inch 1/2-sec Right Pedal Pulse	128
74	S-67 Tail Rotor, Level Flight 160 KIAS, 1-inch 1/2-sec Right Pedal Pulse	129
75	S-67 Fan-in-Fin, Level Flight 160 KIAS, 1-inch 1/2-sec Left Pedal Pulse	130
76	S-67 Tail Rotor, Level Flight 160 KIAS, 1-inch 1/2-sec Left Pedal Pulse	131
77	S-67 Fan-in-Fin, Level Flight 180 KIAS, 1-inch 1/2-sec Right Pedal Pulse	132
78	S-67 Tail Rotor, Level Flight 180 KIAS, 1-inch 1/2-sec Right Pedal Pulse	133
79	S-67 Fan-in-Fin, Level Flight 180 KIAS, 1-inch 1/2-sec Left Pedal Pulse	134
80	S-67 Tail Rotor, Level Flight 180 KIAS, 1-inch 1/2-sec Left Pedal Pulse	135
81	Comparison of Maneuvering Capability	137
82	Comparison of Directional Control Response With Airspeed . . .	138
83	Comparison of Lateral Control Response With Airspeed	139

LIST OF ILLUSTRATIONS (CONTINUED)

<u>Figure</u>		<u>Page</u>
84	Comparison of Maneuvering Stability Characteristics at 80 KIAS	141
85	Comparison of Maneuvering Stability Characteristics at 140 KIAS	142
86	Comparison of Maneuvering Stability Characteristics at 177 KIAS	143
87	S-67 Sideslip vs Speed Envelope	148
A-1	Fan Assembly	159
A-2	Fan Blade Characteristics, $C_{L_1} = 0.9$	160
C-1	Fan and Tail Rotor Perceived Noise Levels vs Thrust, Exit Side, -45-deg Azimuth (45 deg Off Tip Path Plane), 500-ft Distance	167
C-2	Calculated Lobal Patterns (Constant Noise Levels) for the Isolated Fan and Tail Rotor, Thrust = 1000 lb	168
C-3	Fan-in-Fin, Test Stand, PNdB vs Fan Blade Pitch Angle, Exit Side, -135-deg Azimuth (45 deg Off Fan Tip Path Plane), 500-ft Distance	169
C-4	Fan-in-Fin, Test Stand, PNdB vs Fan Blade Pitch Angle, +180-deg Azimuth (On Fan Tip Path Plane), 500-ft Distance	170
C-5	Fan-in-Fin, Test Stand, PNdB vs Fan Blade Pitch Angle, Intake Side, +135-deg Azimuth (45 deg Off Fan Tip Path Plane), 500-ft Distance	171
C-6	Fan-in-Fin, Test Stand, Sound Pressure Level vs Frequency, Exit Side, -135-deg Azimuth (45 deg Off Fan Tip Path Plane), 500-ft Distance, 2997 RPM	173
C-7	Fan-in-Fin, Test Stand, Relationship Between Fan Blade Pitch Angle, Rotational Speed, and Total Thrust, SLS, 104% N_R	174
C-8	Fan-in-Fin, Test Stand, 1/10 Octave Band Spectra Comparison With Tail Rotor at 1000 lb Thrust, 2997 RPM Fan, 1214 RPM Tail Rotor, 500-ft Distance	175
C-9	Fan-in-Fin, Comparison of Perceived Noise Level vs Fan Thrust Between Test Stand and Aircraft Tie-Down Tests, -45-deg Azimuth, 2997 RPM, 500-ft Distance	177

LIST OF ILLUSTRATIONS (CONTINUED)

<u>Figure</u>		<u>Page</u>
C-10	Comparison of S-67 Aircraft Perceived Noise Levels in Hovering Flight, 100-ft Altitude, at 500-ft Distance	178
C-11	S-67 Aircraft Sound Pressure Level vs Distance, 80-KIAS Fly-Over	179
C-12	S-67 Aircraft Sound Pressure Level vs Distance, 120-KIAS Fly-Over	181
C-13	S-67 Aircraft Sound Pressure Level vs Distance, 175-KIAS Fly-Over	183
D-1	CFAS Block Diagram	188
D-2	Typical Stick Force Characteristic	189
D-3	Cruise Guide Force Characteristic	190
D-4	CFAS Control Panel	191
D-5	CFAS Controls Schematic	192
D-6	CFAS Worst Case Hardover	193
D-7	CFAS Flight Test Evaluation Results	195

LIST OF TABLES

<u>Table</u>		<u>Page</u>
1	Principal Dimensions and Characteristics, S-67 Aircraft, Tail Rotor Configuration	25
2	Principal Dimensions and Characteristics, S-67 Aircraft, Fan-in-Fin Configuration	27
3	Comparison of Tethered IGE Hover Performance, SLS, $h/D = 0.395$, $104\% N_R$; From Figure 9	39
4	Comparison of Tethered OGE Hover Performance, SLS, $104\% N_R$; From Figure 12	42
5	Total Thrust Capability, Aircraft Installation (Calculated From Static Fan Module Test Results)	58
6	Yaw Displacement After One Second, One Inch Pedal Input . . .	136
7	Adverse Yaw Comparison: Change in Sideslip 1-1/2 Seconds After A 2-Inch Lateral Step Input	140
8	Comparison of Measured Total Aircraft Noise in Hover OGE, 100-ft Wheel Height, at 500-ft Distance	146
9	Comparison of Measured Total Aircraft Noise During Fly-Over at 200-ft Altitude	146

INTRODUCTION

For helicopters, the single main rotor/tail rotor arrangement has developed into the most extensively used configuration. The tail rotor has proved to be an efficient and reliable device for main rotor torque reaction and directional control. However, the large-scale deployment of such helicopters has exposed the tail rotor's susceptibility to damage in ground operations and as a hazard to personnel.

In 1970, the U. S. Army sponsored studies of advanced anti-torque concepts to evaluate the merits of alternate approaches to the tail rotor (References 1 and 2). The shrouded fan-in-fin emerged as the most promising concept with respect to performance, at the same time offering protection for its rotating parts as well as safety to personnel. Actual flight testing of a fan-in-fin helicopter was at that time in progress in France, adding further encouragement to the practicality of the concept. Therefore, the U. S. Army instituted a follow-on program, and Sikorsky Aircraft was awarded a research contract for flight evaluation of a helicopter with a fan-in-fin, which is the subject of this report.

Figures 1 and 2 show the S-67 helicopter before and after modification.

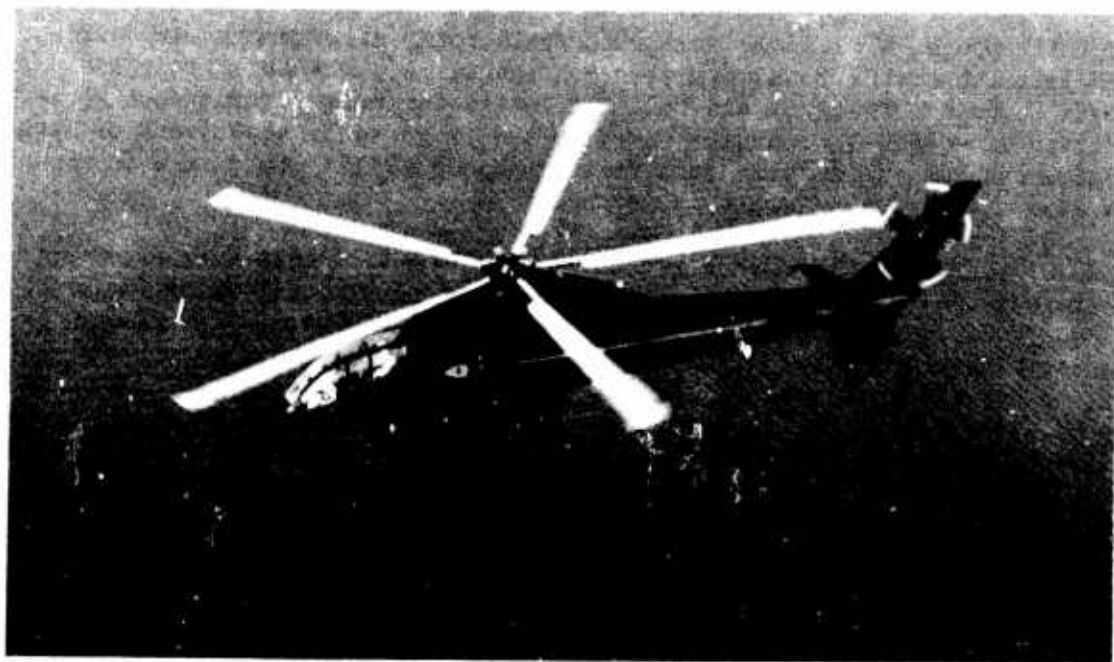


Figure 1. The S-67 Blackhawk Helicopter With Tail Rotor.



Figure 2. The Modified S-67 Blackhawk Helicopter With Fan-in-Fin.

SCOPE OF PROGRAM

The fan-in-fin research flight test program included preliminary design, detail design, fabrication, ground and flight test of the fan-in-fin helicopter antitorque system, as well as baseline flight testing of the helicopter with the tail rotor prior to modification.

The preliminary design included careful study of constraints imposed by the existing airframe and hardware, extensive trade-offs of fan power requirements, fan weight and associated yaw inertia, fan thrust levels, fan size, tip speed, blade twist, duct depth and inlet shape, as well as fin size and shape. A 1/12 scale wind tunnel model test aided in verification of stability predictions.

Detail design included stress analysis of the aft sections of the helicopter as modified, fin structural design, flight controls design, fan detail design, and design of a special fan test module simulating the fin for the ground whirl stand tests.

Aircraft parts, in particular fin and shroud, were made on "soft" tooling. The two fans were fabricated to typical prototype standards, with solid aluminum blades and a gearbox milled out of solid magnesium stock. The two fans built under the program show minor differences in the lubrication system, because the whirl stand version is rotated 94 deg in pitch from the aircraft installation position.

Ground tests of the number one fan on the Sikorsky tail rotor whirl stand included lubrication tests, gear pattern check, stress and motion surveys, precession tests, a duct pressure survey, and performance tests with and without external airflow up to 35 knots. The number two fan underwent a tie-down and system integrity test in the aircraft.

The flight test program consisted of fan shakedown, flow pattern observations with tufts, rudder bias optimization, handling qualities evaluation, performance measurements, and Government pilot evaluation flights.

DESIGN APPROACH AND DESCRIPTION OF TEST AIRCRAFT

PROGRAM OBJECTIVES

The primary objectives of the program were to evaluate the performance, handling qualities, and acoustic characteristics of the fan-in-fin aircraft configuration; to compare these characteristics with those of the tail rotor configuration; and to correlate fan performance and fan inlet behavior with predictions to verify the methodology used. Secondary program objectives included the evaluation of a rudder as part of the fan-in-fin aircraft flight control system and the evaluation of a collective force augmentation system, discussed in Appendix D.

S-67 GENERAL INFORMATION

The S-67 is a single main rotor, twin turbine engine helicopter designed as an attack helicopter. Figure 1 shows the S-67 tail rotor configuration used for baseline comparison flying. The dynamic components are from various models of the S-61/SH-3 series of helicopters. However, the normal rotational speed of the drive system is increased by 4% on the S-67 compared to the S-61/SH-3 series. The normal operating rotational speed of the S-67 dynamic system is referred to as 104% N_R throughout this report and applies to both the tail rotor and the fan-in-fin configuration.

The five-bladed main rotor is fully articulated and uses the low twist (-4 deg), swept-tip blades of the S-61F (NH-3A). The rotor head is faired, but the arms and oscillating masses of the bifilar vibration absorber protrude outside the fairing. The narrow, low drag fuselage accommodates the two crew members in tandem arrangement, pilot in rear and copilot in front, and offers a six-place cabin in the center section that was used for the test instrumentation. The main landing gear is retractable. The aircraft is configured with wings to unload the rotor in high-speed maneuvers. The wings are fitted with speed brakes to improve deceleration, reduce dive speed, and control dive angles. The large, all-movable horizontal stabilator is linked to the main rotor longitudinal cyclic controls. The main rotor controls are hydraulically boosted by primary and auxiliary servos.

In the baseline configuration, the aircraft is equipped with a five-bladed tail rotor with a diameter of 10 feet 7-1/4 inches. This tail rotor is a standard SH-3D/-3H production item. It is installed on the upper vertical fin, and its drive train includes the tail drive shaft, intermediate gearbox, pylon shaft and tail gearbox. The upper and the lower vertical fins of the tail rotor aircraft are cambered to unload the tail rotor in high speed flight. The tail rotor control system incorporates a negative gradient spring and a yaw servo. This yaw servo is referred to as "yaw auxiliary servo" throughout this report for two reasons: it is housed in the same hydraulic module that accommodates the main rotor auxiliary servos, and in the fan-in-fin configuration it becomes truly an auxiliary servo, the fan being operated by a separate actuator.

FAN-IN-FIN DESIGN APPROACH AND CONSTRAINTS

The conversion of the S-67 into fan-in-fin configuration was carried out within a number of constraints. The approach taken is discussed in Appendix A of this report, which contains pertinent fan design parameters and a detailed fan description. The most significant constraint was that the modification had to be restricted to the tail of the aircraft aft of the rear manufacturing break of the tailcone (Station 619, see Figure 3) to minimize program cost. The other constraints and their impact on the fan-in-fin aircraft configuration need to be discussed individually.

Yaw Control Criteria

The substitution of a shrouded fan for the tail rotor to provide main rotor torque compensation and directional control offered an opportunity to improve the yaw control capability of the S-67. The principal yaw control requirements for helicopters are specified in MIL-H-8501A (Reference 3), sections 3.3.5 and 3.3.6. The S-67 in tail rotor configuration does not meet these requirements.

For a fan-in-fin aircraft configuration, the full pedal displacement yaw control requirement in hover, section 3.3.5 of MIL-H-8501A, is more demanding than the control requirement during hovering flight in a 35-knot wind, section 3.3.6.

Preliminary design studies showed that within the constraints of available power and aircraft center-of-gravity range, fan thrust produced by full pedal displacement was always less than that required by MIL-H-8501A. Available thrust would not meet requirements due to rapidly increasing yaw inertia, which resulted from the increased fan size and weight associated with increasing thrust available. Although the resulting design solution does not meet the MIL-H-8501A requirement, it is still better than the tail rotor configuration, in that it exhibits greater directional control response.

However, it proved feasible to design for the yaw maneuver requirements when hovering in a 35-knot wind, section 3.3.6 of Reference 3. This criterion was therefore adopted to determine the design thrust level and to size the fan.

Power Available

The power available to the fan was determined from the ratings of the existing tail drive system components as 835 SHP transient peak (never to be exceeded) and 350 SHP maximum continuous power. To avoid overtorquing the drive shaft, the fan was designed to generate the maximum thrust required to meet the adopted maneuver design criteria at 4000 feet altitude, 95°F and at Design Gross Weight requiring only 673 SHP, which corresponds to 835 SHP at SLS conditions for the same blade pitch angle setting. This power limit proved to be the most important factor in determining the diameter of the fan.

Aircraft Yaw Inertia

Because of the wings and the large tail surfaces, the inertia of the S-67 aircraft around the yaw axis (I_{ZZ}) is relatively high. The large yaw inertia was further increased by the fan weight (332 lb).

The high inertia and the difficulty to achieve the high fan thrust levels with the available power dictated that the fan be installed as far forward as practical to minimize the contribution of the fan weight to aircraft inertia. The latter increases with the square of the distance between fan and aircraft center of gravity, while the fan thrust requirements decrease linearly with that distance.

Fan Blade Pitch Angle Actuator

The high fan blade pitch angle control moments that result from the solid aluminum blade design and the choice of the feathering axis to coincide with the 50% chord line require significantly more force capability in the control system than the tail rotor. To avoid design and development of a special servo, a CH-53 two-stage tail rotor servo with enlarged bore is used to operate the fan blade pitch change mechanism. This actuator imposed design constraints on the fan gearbox, required a large hemispherical fairing on the fan exhaust side, and its force and stroke characteristics imposed an upper limit on the allowable value of the fan total activity factor.

Sense of Rotation

Sikorsky tail rotors conventionally rotate so that the blades move upwards in the forward part of the tail rotor disk. This arrangement avoids the loss of tail rotor performance if the main rotor downwash starts to immerse the tail rotor disk, a condition typically experienced during translation into forward flight. Careful analysis showed that a fan would probably be as adversely affected as a tail rotor under the same conditions. Therefore, the same sense of rotation was chosen for the fan as for the tail rotor.

Owing to the sense of rotation of the S-67 tail drive shaft, the choice of an aerodynamically favorable tail rotor direction of rotation coupled with the constraint on the position of the tail rotor drive shaft forced a gear arrangement whereby the fan bevel gear is on the left and the fan rotor on the right side of the aircraft centerline. This introduces an increase in the weight of the fan gearbox and contributes to the overall depth of the fan assembly.

SPECIFIC DESIGN ASPECTS, S-67 FAN-IN-FIN

The general arrangement of the S-67 fan-in-fin and tail rotor configurations may be compared by reference to Figures 3 and 4. Details of the fan installation are shown on Figure 5. In addition, Tables 1 and 2 list the principal dimensions and characteristics for the S-67 in the fan-in-fin and tail rotor configurations.

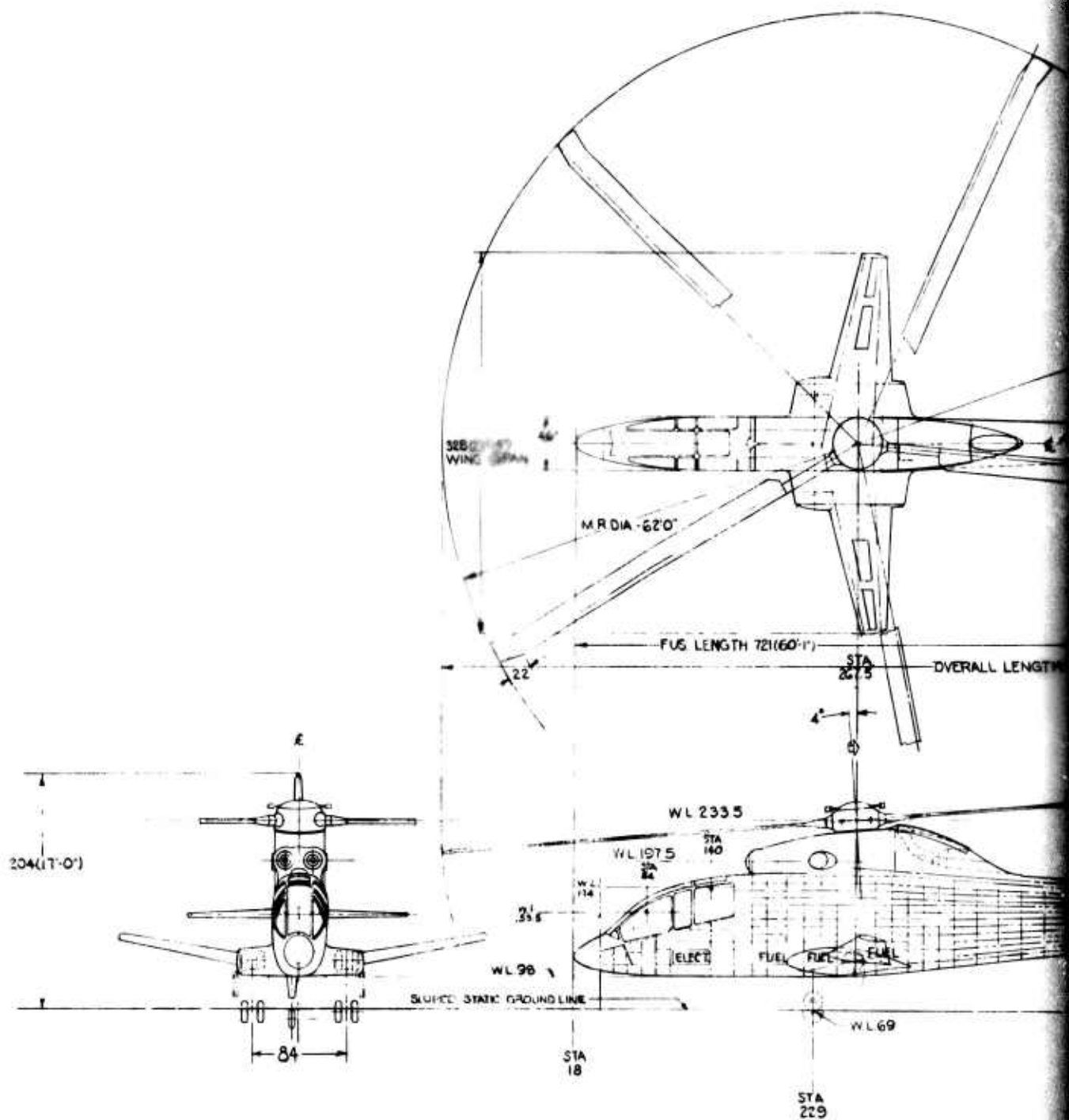
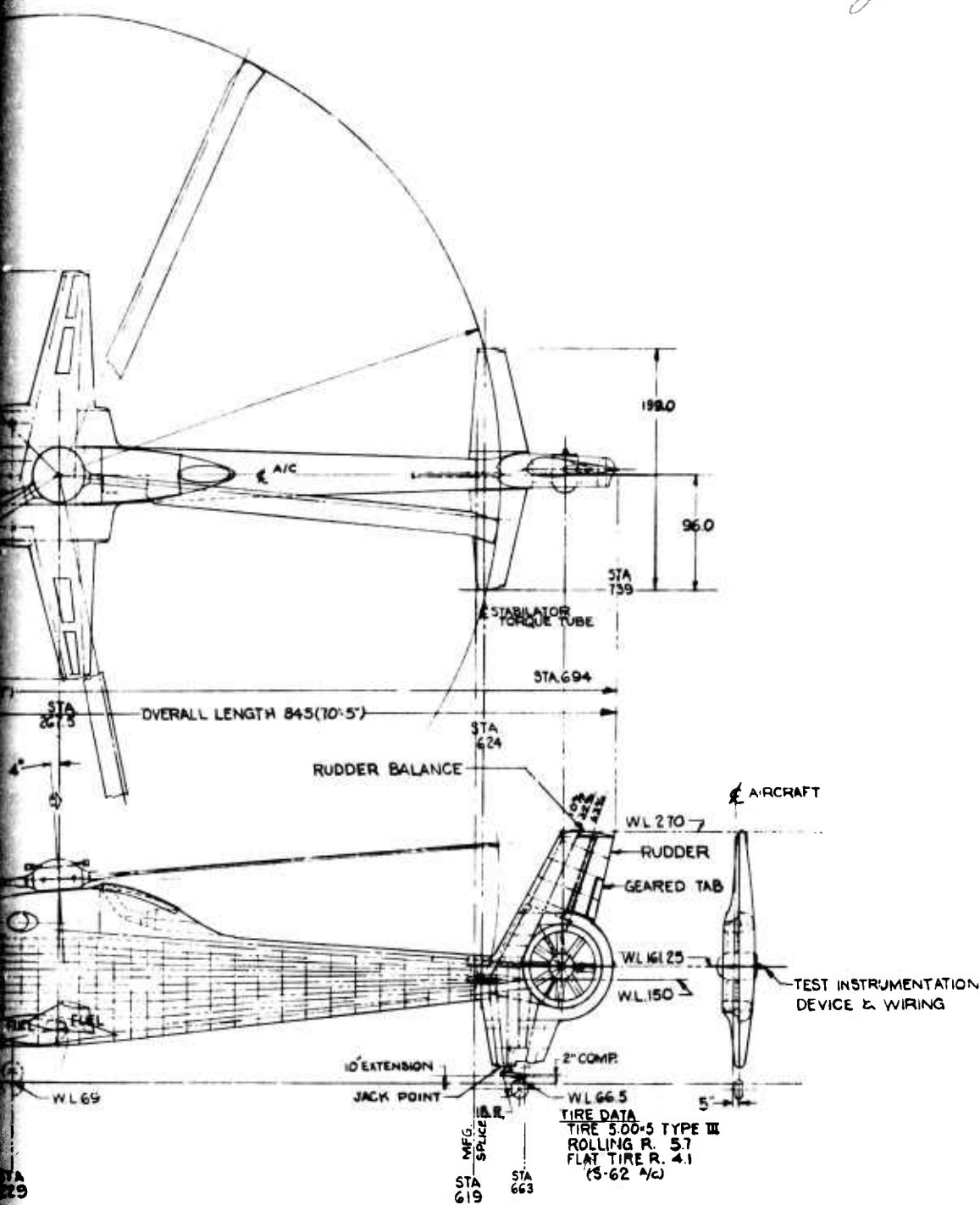


Figure 3. General Arrangement, S-67 Fan-in-Fin Configuration.

2



•PRECEDING PAGE BLANK-NOT FIDGES.

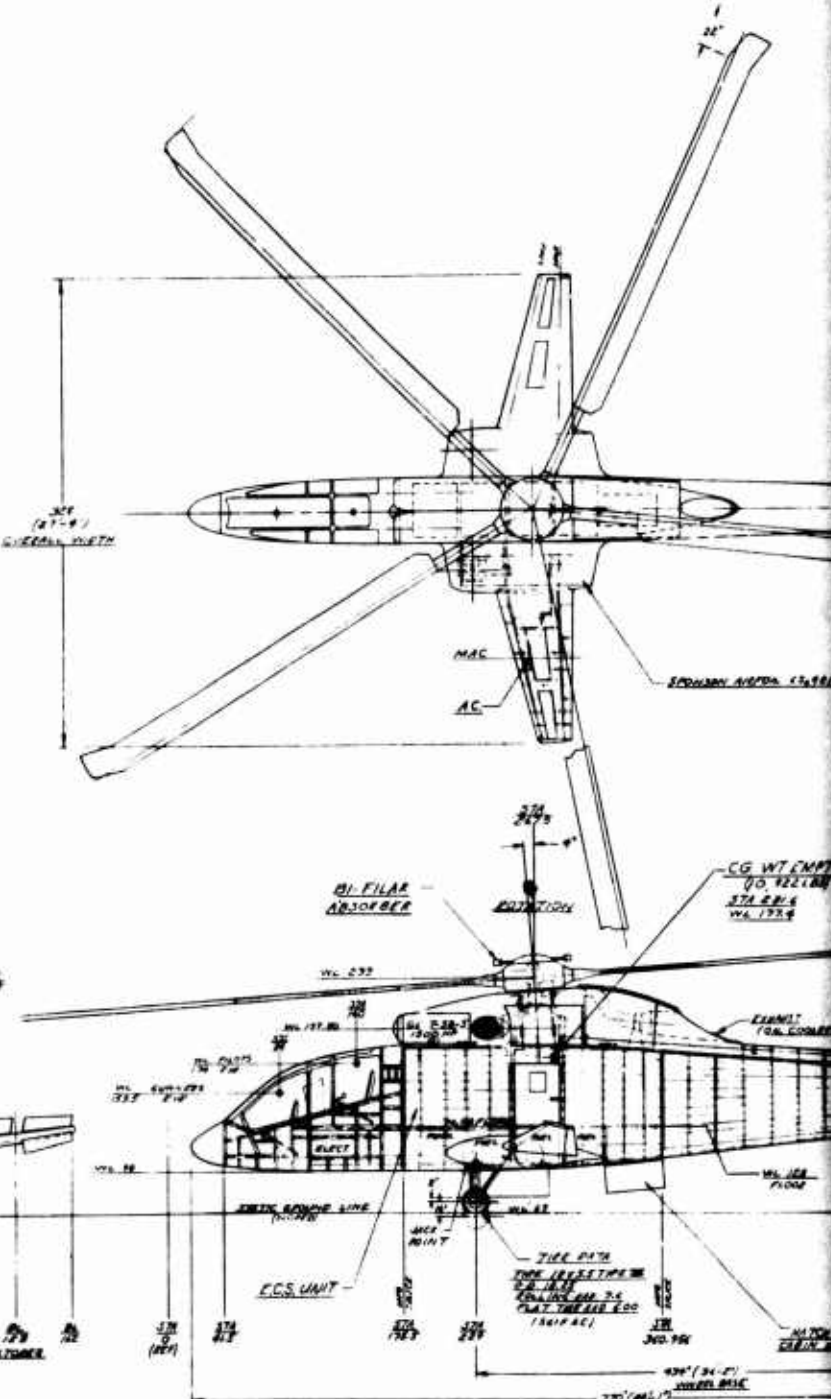
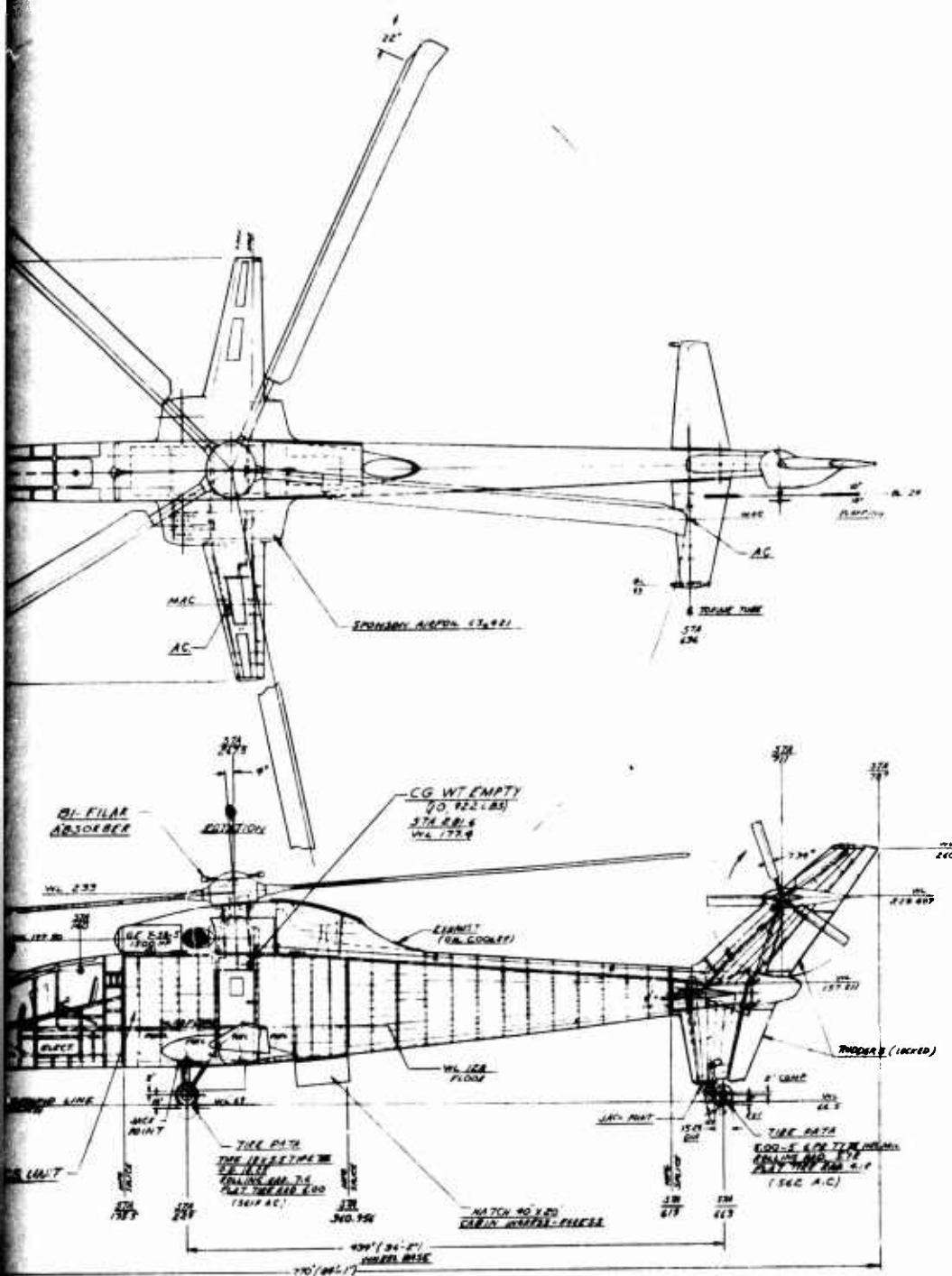


Figure 4. General Arrangement, S-67 Tail Rotor Configuration.

2



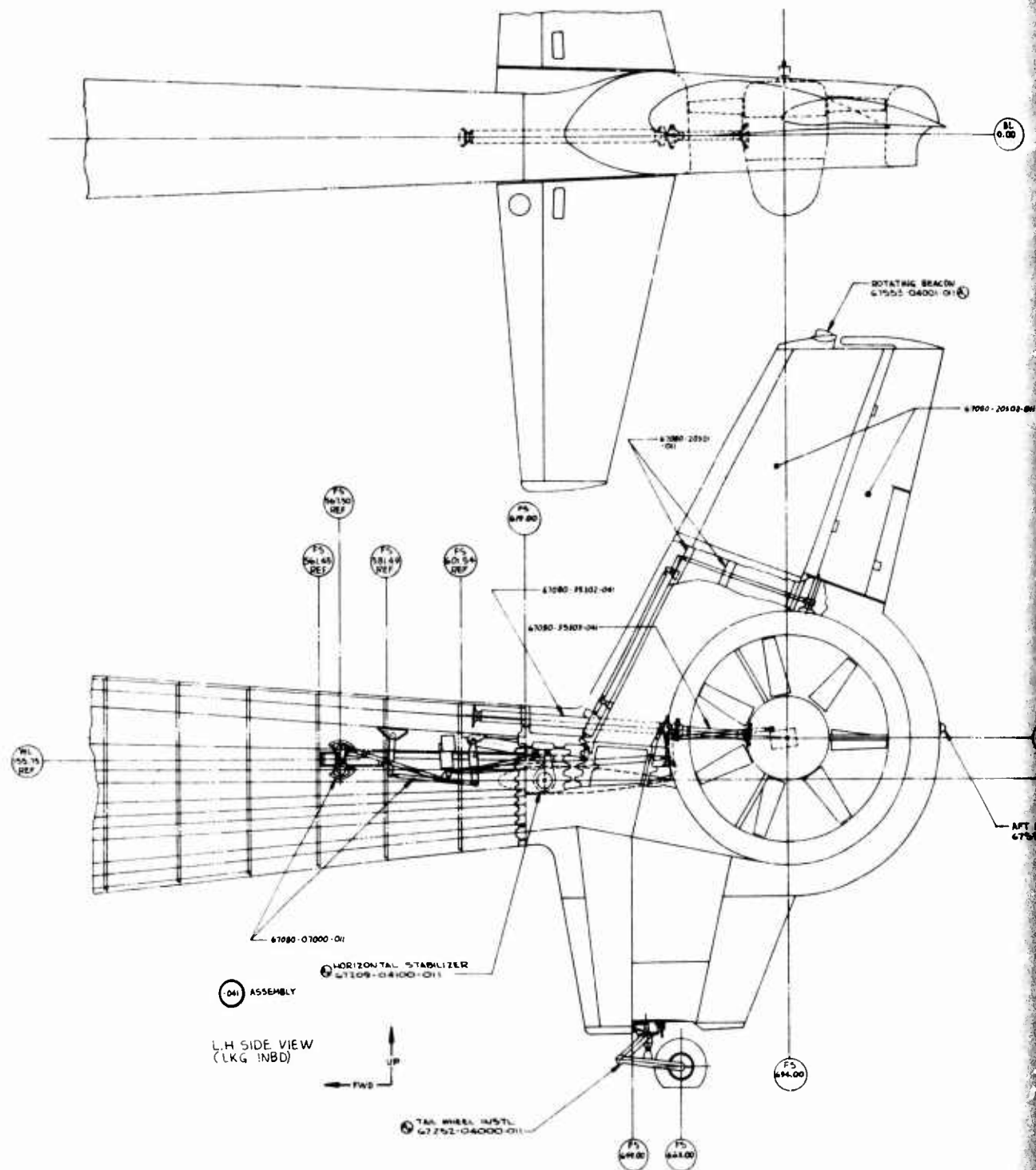


Figure 5. Inboard Profile, S-67 Helicopter Configuration, Fin and Fan Installation.

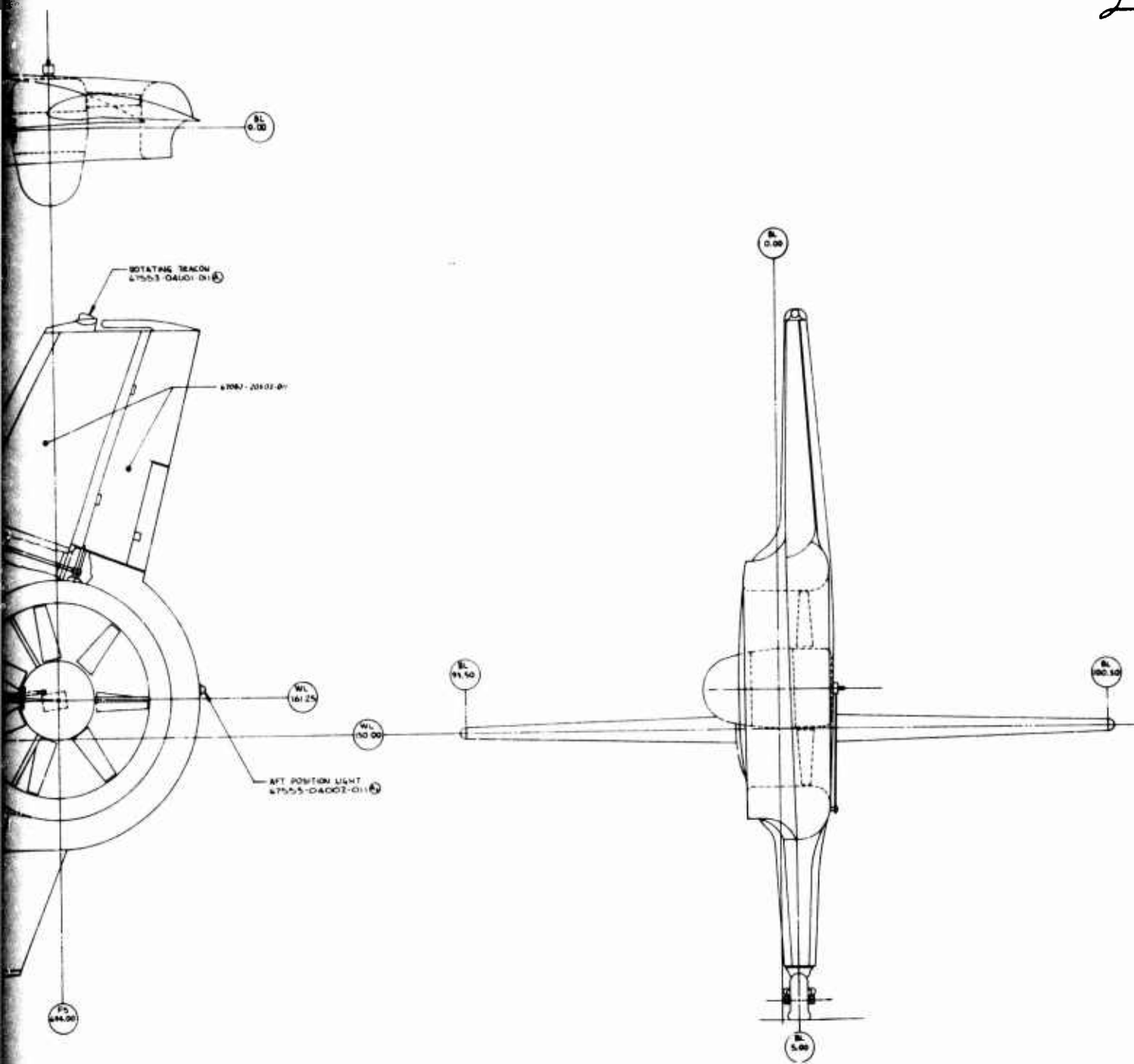


TABLE 1. PRINCIPAL DIMENSIONS AND CHARACTERISTICS,
S-67 AIRCRAFT, TAIL ROTOR CONFIGURATION

Main Rotor

Diameter	62 ft
Normal tip speed (104% N_R of S-61/ SH-3 series aircraft)	686 ft/sec
Disc area	3019 ft ²
Solidity	0.0781
Number of blades	5
Blade chord	1.52 ft
Blade twist	-4 deg
Airfoil section	NACA 0012 MOD
Articulation	Full flapping and lagging
Tip sweep	20 deg

Tail Rotor

Diameter	10 ft 7-1/4 in.
Normal tip speed (104% N_R of S-61/ SH-3 series aircraft)	718 ft/sec
Disc area	87.9 ft ²
Solidity	0.1843
Number of blades	5
Blade chord	0.612 ft
Blade twist	0 deg
Airfoil section	NACA 0012 MOD
Pitch flap coupling	45 deg

Fuselage

Overall length	64 ft 1 in.
Overall height	16 ft 3 in.
Overall width	27 ft 4 in.
Wheel tread	7 ft
Wheel base	36 ft 2 in.

Stabilator

Root chord	4 ft 2 in.
Tip chord	2 ft
Taper ratio	0.48
Area	50 ft ²
Span	15 ft 6 in.
Aspect ratio	4.8
Airfoil (root)	NACA 0015
Airfoil (tip)	NACA 0012

TABLE 1 - Continued

Vertical Fin

Root chord	7 ft 6 in.
Tip chord (upper)	2 ft 10 in.
Tip chord (lower)	3 ft 9 in.
Taper ratio (upper)	0.62
Taper ratio (lower)	0.5
Total area	68.7 ft ²
Aspect ratio	2.65
Airfoil section (upper)	NACA 4415
Airfoil section (lower root)	NACA 4415
Airfoil section (lower tip)	NACA 4421

Wing

Root chord	4 ft 6 in.
Tip chord	1 ft 11.5 in.
Overall span	27 ft 4 in.
Total exposed area	58 ft ²
Total equivalent area	98 ft ²
Incidence	8 deg
Dihedral	10 deg
Quarter chord sweep	10 deg 45 min
Taper ratio (exposed)	0.44
Aspect ratio (overall)	8.0
Airfoil section (root)	NACA 4415
Airfoil section (tip)	NACA 4412

Propulsion System

Engines	Two CT58-140-2
Takeoff power (each)	1500 hp
Military power	1400 hp
Normal power	1250 hp
Transmission rating: 111% Q	2800 hp limited to 5 min
100% Q	2500 hp, limited to 30 min
86% Q	2160 hp, maximum continuous

Loading Conditions

Design gross weight	16,300 lb
Empty weight	13,373 lb
Maximum gross weight capability	20,780 lb
Center-of-gravity range	258 in. to 276 in.

TABLE 1 - Concluded

Inertias	
I_{XX}	7800 slug-ft ²
I_{YY}	59,000 slug-ft ²
I_{ZZ}	53,000 slug-ft ²
I_{XZ}	3300 slug-ft ²

TABLE 2. PRINCIPAL DIMENSIONS AND CHARACTERISTICS,
S-67 AIRCRAFT, FAN-IN-FIN CONFIGURATION

Main Rotor	
Diameter	62 ft
Normal tip speed (104% N_R of S-61/ SH-3 series aircraft)	686 ft/sec
Disc area	3019 ft ²
Solidity	0.0781
Number of blades	5
Blade chord	1.52 ft
Blade twist	-4 deg
Airfoil section	NACA 0012 MOD
Articulation	Full flapping and lagging
Tip sweep	20 deg
Fan	
Diameter	4 ft 8 in.
Normal tip speed	732 ft/sec
Disc area	17.1 ft ²
Solidity	.398
Number of blades	7
Blade chord	5.0 in.
Blade twist ($r/R = .4$ to 1.)	31.8 deg
Activity factor per blade	135.7
Airfoil section	NACA 16 series
Hub diameter ratio	0.4
Number of vanes	3
Vane chord	8.75 in. root/6.50 in. tip
Vane twist	0. deg
Vane airfoil section	NACA 16020 (1 degree incidence)
Polar moment of inertia	35.2 in. lb sec ² @ 2997 RPM

TABLE 2 - Continued

Fuselage

Length	60 ft 1 in.
Height	17 ft
Width	27 ft 4 in.
Wheel tread	7 ft
Wheel base	36 ft 2 in.

Stabilator

Root chord	4 ft 5.4 in.
Tip chord	2 ft
Taper ratio	0.48
Area	52 ft ²
Span	16 ft 1 in.
Aspect ratio	4.97
Airfoil (root)	NACA 0015
Airfoil (tip)	NACA 0012

Vertical Fin

Root chord (upper (W.L. 204.5))	5 ft 8 in.
Root Chord (lower)	5 ft 6.5 in.
Tip chord (upper)	3 ft 10 in.
Tip chord (lower)	3 ft 9 in.
Total area	58.9 ft ² (excluding fan)
Airfoil section (upper root)	NACA 6421
Airfoil section (upper tip)	NACA 4415
Airfoil section (lower fin)	NACA 0021
Incidence (upper fin only)	2 deg trailing edge left

Wing

Root chord	4 ft 6 in.
Tip chord	1 ft 11.5 in.
Overall span	27 ft 4 in.
Total exposed area	58 ft ²
Total equivalent area	98 ft ²
Incidence	8 deg
Dihedral	10 deg
Quarter chord sweep	10 deg 45 min
Taper ratio (exposed)	0.44
Aspect ratio (overall)	8.0
Airfoil section (root)	NACA 4415
Airfoil section (tip)	NACA 4412

TABLE 2 - Concluded

Propulsion System

Engines	Two CT58-140-2
Takeoff power (each)	1500 hp
Military power	1400 hp
Normal power	1250 hp
Transmission rating: 111% Q	2800 hp, limited to 5 min
100% Q	2500 hp, limited to 30 min
86% Q	2160 hp, maximum continuous

Loading Conditions

Design gross weight	16,030 lb
Empty weight	13,792 lb
Maximum gross weight capability	20,780 lb
Center-of-gravity range	258 in. to 276 in.

Inertias

I_{XX}	7800 slug-ft ²
I_{YY}	63,500 slug-ft ²
I_{ZZ}	61,530 slug-ft ²
I_{XZ}	3300 slug-ft ²

Fin Design

The general appearance of the lower vertical fin is maintained for the fan-in-fin aircraft. It was, however, designed without camber and incidence. The lower fin is most effective in autorotation and part-power descent, and by keeping the airfoil symmetrical, the negative fan thrust requirements in this phase of flight could be minimized. The upper fin, effective in cruise and high power climbs, is cambered and set at two degrees incidence to unload the fan in forward flight. Because of reduced sweep, the aerodynamic center of the upper fin in the fan configuration is further forward than in the tail rotor configuration. This is compensated for by a corresponding increase in fin area. The upper fin incorporates a rudder. Additional information concerning the rudder is contained in Appendix B.

The fan is installed on the extended centerline of the tail drive shaft and towards the trailing edge of the fin. In this position, the transient interference effect known as lift droop experienced on surface areas aft of the fan (Reference 4) is minimized. Accommodating the deep fan duct as far aft as possible, in a fin with minimum side area and with lowest possible drag, led to the cusped fuselage termination shown in Figure 6. The rationale for this design is apparent from the sketches of the flow fields in hover and in forward flight shown in Figure 7. In hover, the well-defined trailing edge establishes a fixed dividing line between the flow fields on the fan inlet and on the fan exhaust side. The concave cut-out in the fan rim structure, the cusp, minimizes the area of flow separation around the fan exhaust. In forward flight, the concave cusp in the fan rim structure permits the flow to remain attached almost all around the fan exhaust flow column, reducing the extent of the region of flow separation and the base drag of the deep fan assembly. Furthermore, the well-defined trailing edge reduces the intensity of any vortex shedding that might induce tail shake. Flow visualization studies in the wind tunnel and inflight observation of tufts verify the rationale used in developing this configuration.

Flight Controls

Yaw control is provided by fan and rudder, both operated by the pilot's and copilot's pedals. The control linkage for both fan and rudder is common from the pedals through the yaw axis auxiliary servo, a mixing unit providing collective to yaw coupling, and cables to a bellcrank in the tail section. From this point on, fan and rudder controls are separate. The fan control linkage incorporates a variable gain device permitting the pilot to vary the fan blade angle range. It is electrically operated and adjustable from the cockpit with a gain range of zero to 100%. The rudder control linkage incorporates an electrically operated bias actuator, permitting the neutral position of the rudder to shift either left or right, with a bias range of ± 8 deg. Since there is no power boost for the rudder except the forward yaw auxiliary servo, a tab is provided to reduce rudder control loads.

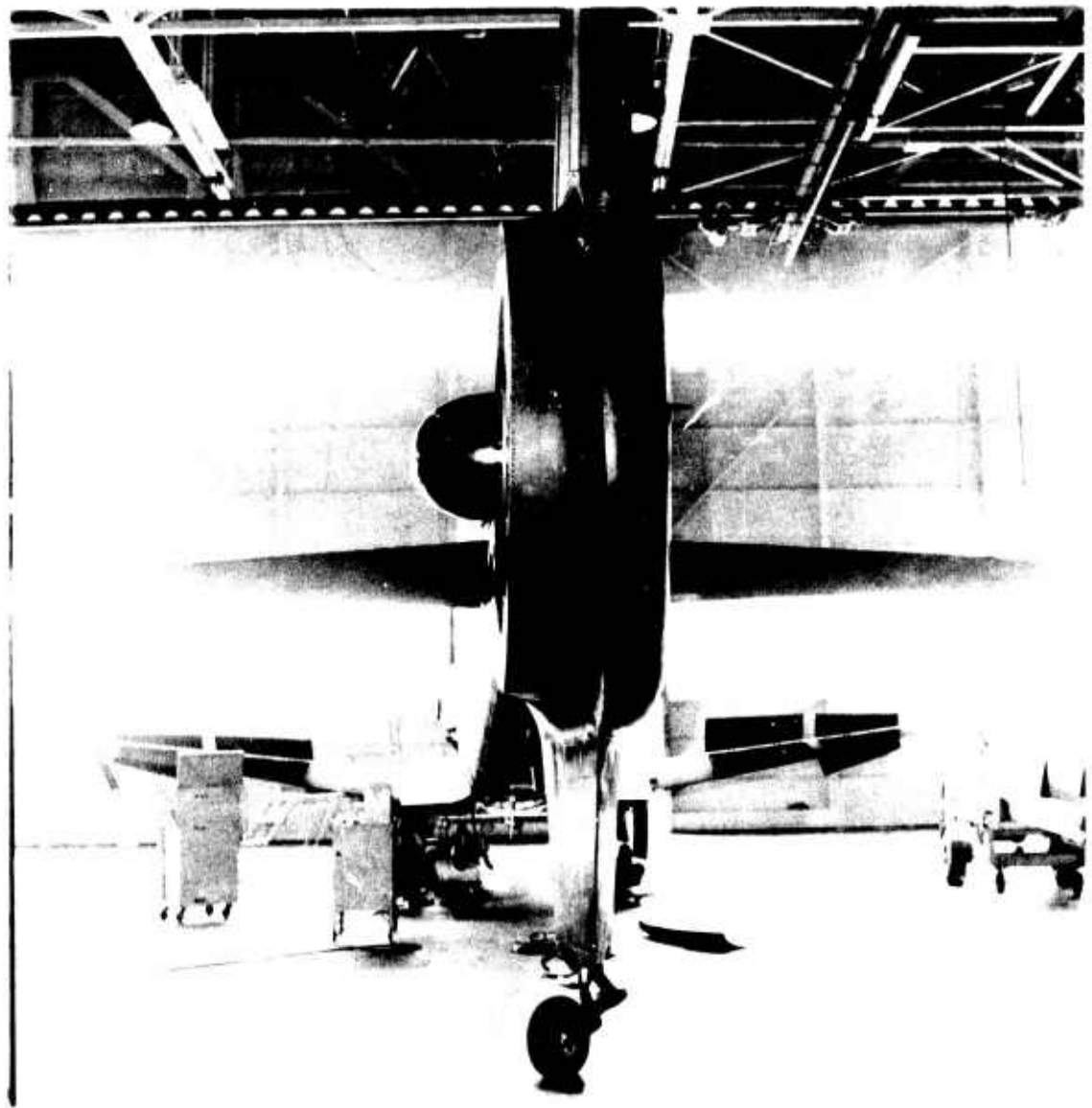
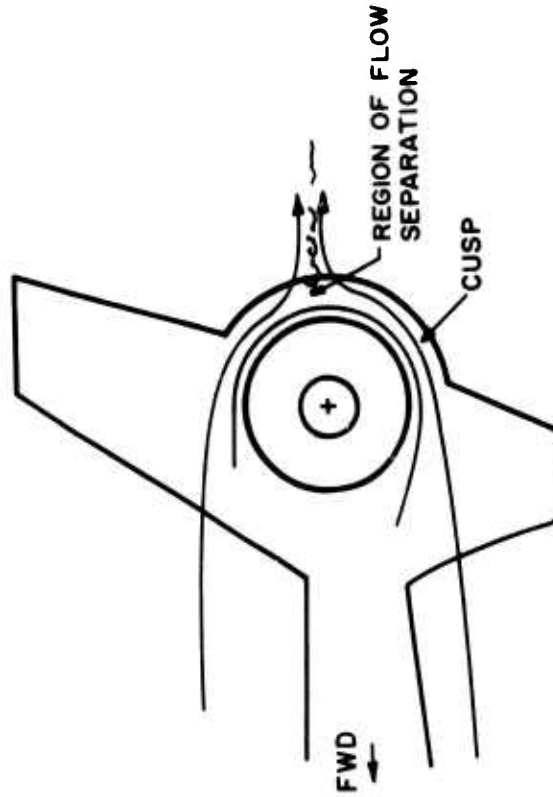


Figure 6. S-67 Fan-in-Fin, Upper and Lower Vertical Tail Surfaces With Fan Cusp.

FORWARD FLIGHT CONDITION

SIDE VIEW OF FAN AND CUSPED TRAILING EDGE, FAN EXHAUST SIDE



HOVER CONDITION

TOP VIEW OF FAN AND FIN

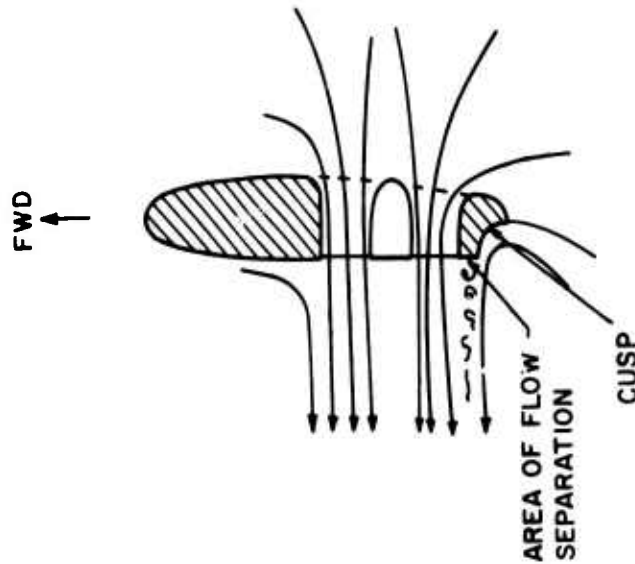


Figure 7. Qualitative Representation of Airflow Around Fan and Cusped Trailing Edge.

Horizontal Stabilator

To minimize aircraft yaw inertia, the fan had to be installed as far forward as practical. As a consequence, the stabilator had to be moved forward 11 inches. A comparison of the top views of the two aircraft configurations, Figures 3 and 4, shows considerably more overlap between main rotor tip path plane and horizontal stabilator for the fan-in-fin.

The right side stabilator span is increased by 7 inches through insertion of a stationary airfoil along the fuselage. This was done to adapt the existing contour of the right-hand stabilator root to the contour of the new vertical tail, and to compensate in part for the reduced stabilator moment arm by increasing its area.

Fan Location

The fan centerline is 17 inches forward and 62-1/4 inches below the centerline of the tail rotor on the baseline aircraft.

The forward shift in fan location demands about 4% increased fan thrust over the tail rotor to compensate for the same main rotor torque.

Stability Augmentation System (SAS)

The aircraft is equipped with a Stability Augmentation System (SAS) incorporating pitch, roll and yaw channels. It provides short-term damping and control throughout the entire speed (including hover) and altitude range, and can be engaged or disengaged manually at any time during flight. For comparison flying with the tail rotor as well as during the fan-in-fin flight test program, the SAS was switched off to prevent it from masking any effects associated with conversion from tail rotor to fan.

Collective-to-Yaw Coupling

The fan-in-fin configuration has the same collective-to-yaw mechanical coupling as the tail rotor configuration. The coupling ratio was originally determined for the S-61 helicopter at a mission gross weight of 18,000 lb. The coupling is provided to compensate automatically for changes in antitorque requirements due to changes in main rotor torque. The coupling ratio was not changed for the fan-in-fin configuration despite the higher pedal sensitivity.

TEST PROCEDURES AND TECHNIQUES

The flight test program had two major phases. During the initial fan shake-down phase, the flight envelope for the aircraft was established and explored with the emphasis on flight safety, including stress and vibration surveys. After verification that the fan did not impose any structural or vibration limits anywhere in the flight envelope, a second phase was initiated. This included handling qualities and performance evaluation for a direct comparison with the tail rotor configuration baseline data.

MANEUVER TECHNIQUES

Critical Azimuth

These tests were performed with the nose of the aircraft initially heading into the wind and executing a right turn in 45 deg azimuth increments (aircraft heading relative to wind) in hover.

Static Lateral/Directional Stability

These tests were performed by trimming the aircraft for ball-in-the center in level flight. Then, with the collective fixed and maintaining a steady airspeed, the aircraft was stabilized at incremental sideslip angles on both sides of trim. Excessive, uncomfortable roll attitudes and slip angles beyond any flight requirement were designated sideslip limiting factors. Partial power descents and autorotation sideslips were performed in a similar manner.

Maneuver Stability

These tests were performed by trimming the aircraft in coordinated level flight at the desired airspeed and then rolling the aircraft to incremental bank angles in both directions. Collective control was fixed and airspeed was held constant by bleeding off altitude during the maneuver.

Directional Short Period Damping

These tests were performed by displacing the rudder control approximately 1 inch for a duration of 1/2 second and returning the rudder control to the trim position while recording the subsequent aircraft response.

Adverse Yaw Characteristics

These tests were performed by trimming the aircraft into a 3-deg bank angle turn with the ball in the center and introducing a 2-inch lateral step input in the opposite direction from the bank angle. Tests were performed both with the pedals fixed and using the pedals for maintaining the trim sideslip angle.

Directional Control Power, Directional and Lateral Control Sensitivities

Single-axis control step inputs of varying magnitudes up to 1.5 inches of

control were applied, using mechanical fixtures to obtain the desired control input size. The inputs were held until the rate peaked or until recovery was deemed necessary by the pilot.

Single Engine Failure

These tests were performed in a hover and during 20 knots forward flight at a 40-foot wheel height. At the light test gross weight, the collective was lowered to perform the landing maneuver.

Level Flight Performance

This test was conducted at a constant coefficient of weight by increasing altitude as fuel was burned off. Temperature variations were taken into account by varying main rotor speed to maintain a constant referred rotor speed.

Tether Hover Performance

These tests were conducted at 10-foot and 100-foot wheel heights for constant coefficient of power levels by adjusting engine torque for pressure altitude variations. Temperature variations were taken into account by varying main rotor speed to maintain a constant referred rotor speed ($N_R/\sqrt{\theta}$).

Low-Speed Forward, Sideward, and Rearward Flight

These tests were performed using a calibrated pace vehicle where accurate airspeed determination was not practical with the aircraft airspeed system.

Autorotation Maneuvers

These tests were performed at 80 and 120 KIAS with speed brakes closed and up to 165 KIAS with speed brakes open.

RESULTS AND DISCUSSION

AIRCRAFT PERFORMANCE

Hover Performance

Hover performance of the S-67 tail rotor and fan-in-fin configurations was evaluated in ground effect (IGE) and out of ground effect (OGE) by means of the tethered hover technique. The tethered hover performance of the tail rotor configuration was first assessed OGE by Sikorsky Aircraft and then again OGE and IGE during evaluation of the S-67 as an attack helicopter by the U. S. Army Aviation Systems Test Activity (USAASTA). The fan-in-fin configuration was tested IGE and OGE by Sikorsky Aircraft.

The tethered hover technique is predicted upon a significant sampling of data points acquired on repeated flights to establish a reliable mean value. The repeatability within one flight (precision of individual data points) has been demonstrated to be within $\pm 3\%$ of main rotor thrust. However, between flights, particularly with long time intervals and changes in equipment, personnel, and aircraft condition, significant systematic errors can be introduced. Experience has shown that these effects can shift the apparent results by as much as $6\frac{1}{2}\%$ between individual flights. Insufficient tethered hover flying was conducted to establish a reliable mean value, so the data must be considered as inconclusive.

IGE Hover Performance

Figure 8 shows the nondimensionalized IGE tethered hover performance for the fan-in-fin and tail rotor configurations, at a main rotor tip Mach number of 0.615 and a ratio of main rotor height/diameter (h/D) of 0.395 (necessary to assure adequate clearance between ground and tail wheel). The data show a small increase in total power required to hover for the fan-in-fin as compared to the tail rotor configuration. At low total power, gross weight capability of the fan-in-fin configuration is reduced by about 2.4%; at high total power, gross weight capability is reduced by only about 0.3% when compared with the tail rotor configuration.

Figure 9 shows total power, main rotor power, and antitorque device power vs gross weight for the tail rotor and fan-in-fin configurations at sea level standard conditions. Total power levels and gross weight are based on the values shown in Figure 8. Fan power and tail rotor power were measured. Main rotor power for the fan-in-fin configuration was also measured. Main rotor power for the tail rotor configuration was not measured, but has been deduced by subtracting tail rotor power and drive system power losses from total power.

It is most meaningful to compare the performance of the two configurations at equal main rotor power levels. Table 3 shows how the two configurations compare at two different main rotor power levels, 1,900 MRHP and 2,200 MRHP. The data are based on Figure 9. As can be seen, the gross weights are quite comparable at 1,900 MRHP; at 2,200 MRHP, the difference is much larger,

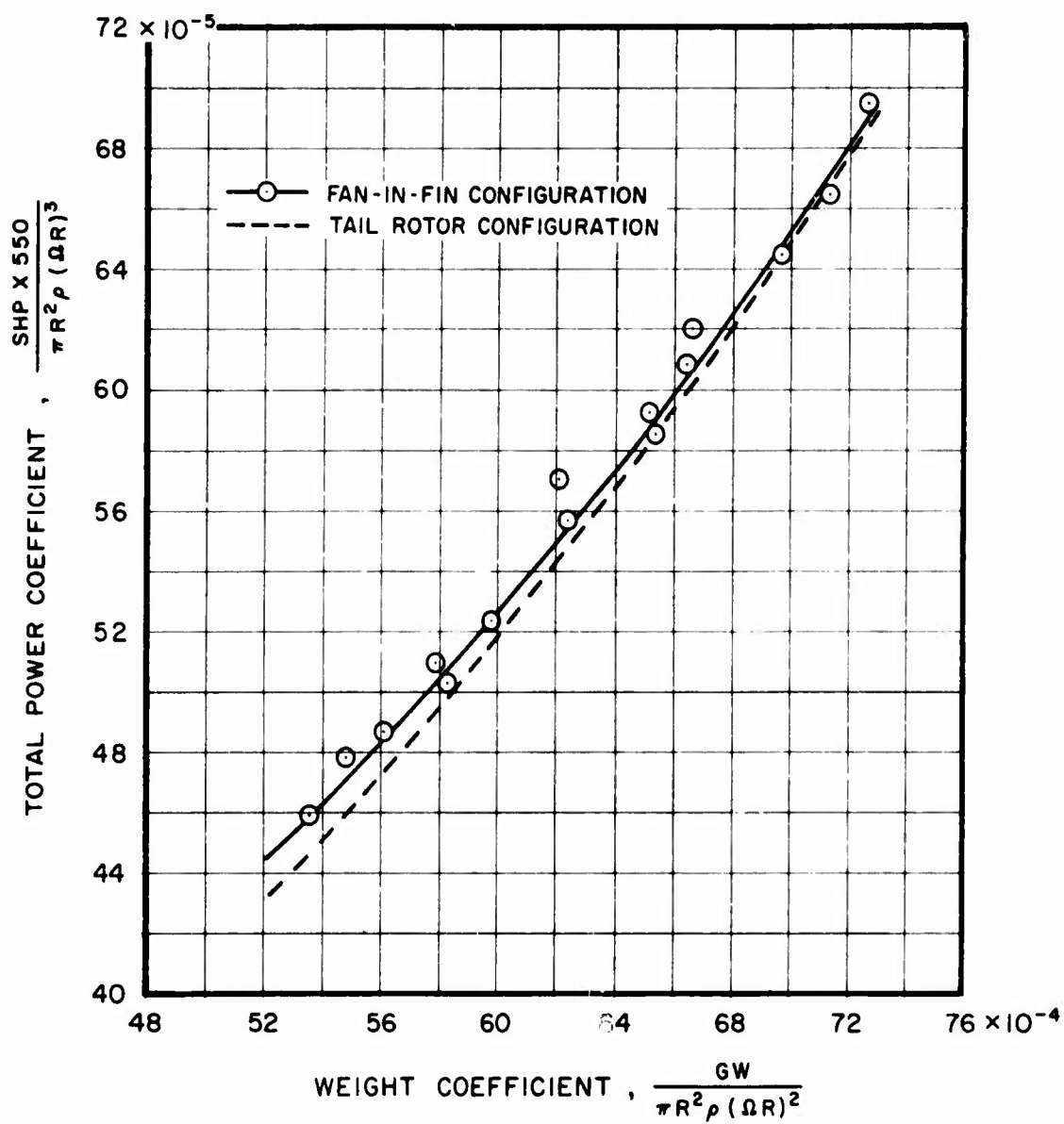


Figure 8. S-67, Comparison of Tethered IGE Hover Performance, Nondimensional, Main Rotor Tip Mach Number $M = 0.615$, Wheel Height 10 ft, $h/D = 0.395$.

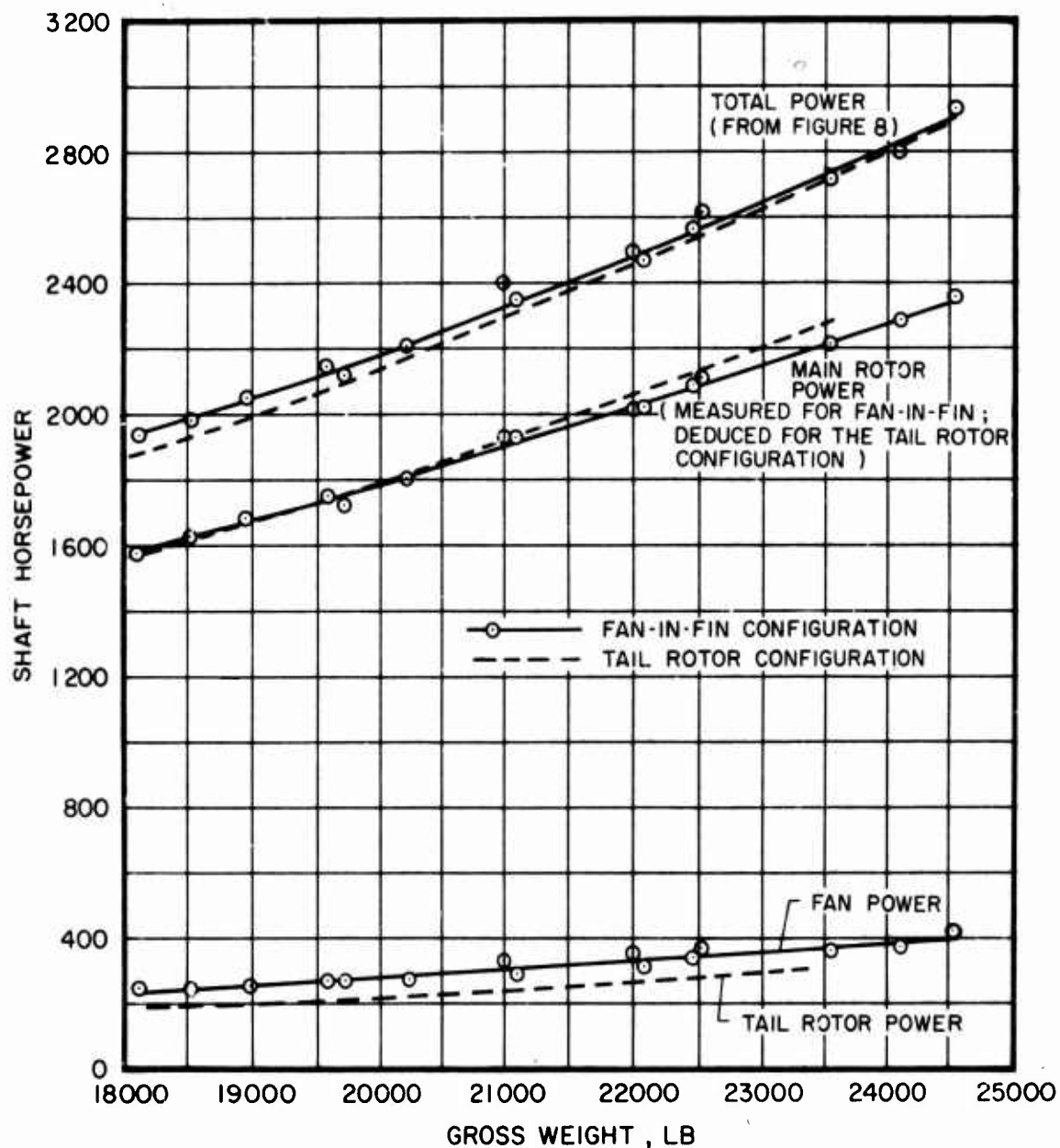


Figure 9. S-67, Comparison of Tethered IGE Hover Performance, Power vs Gross Weight, SLS, 104% N_R , $h/D = 0.395$.

although well within the expected range of systematic error usually observed for the tethered hover technique.

TABLE 3. COMPARISON OF TETHERED IGE HOVER PERFORMANCE, SLS, $h/D = 0.395$, $104\% N_R$; FROM FIGURE 9.

Configuration	Tail rotor	Fan-in-fin	Tail rotor	Fan-in-fin
Main rotor power, MRHP	1,900	1,900	2,200	2,200
Total power, SHP	2,270	2,330	2,620	2,700
Drive system and accessory losses, HP	130	130	130	135
Tail rotor power, HP	240	-	290	-
Fan power, HP	-	300	-	365
Gross Weight, lb	20,840	21,000	22,930	23,400

OGE Hover Performance

Figure 10 shows nondimensionalized tethered hover performance data for the fan-in-fin configuration, comparable data for the tail rotor configuration as obtained by Sikorsky Aircraft and USAASTA, and one free-hover data point for the fan-in-fin configuration. The two sets of tail rotor configuration data were taken under seemingly identical conditions; both sets of data are within the range of systematic error observed for the tethered hover technique and must be considered valid. It must be concluded, therefore, that there is no absolute data reference against which the measured fan-in-fin performance data can be compared.

Figure 11 is identical to Figure 10 but boundaries of uncertainty have been applied to the tethered hover test data corresponding to the potential $6\text{-}1/2\%$ systematic error on rotor thrust (or weight coefficient). The boundaries for the tail rotor configuration are established by adding $6\text{-}1/2\%$ (weight coefficient) to the Sikorsky data and subtracting $6\text{-}1/2\%$ from the USAASTA data. The boundaries for the fan-in-fin configuration are $6\text{-}1/2\%$ higher and lower than the test data. There is considerable overlap of the bands of uncertainty between the test results for the two configurations. The fan-in-fin free hover performance point shown on Figures 10 and 11 is within the boundary of uncertainty of the fan-in-fin tethered hover data.

The magnitude of uncertainty indicates that use of the tethered hover technique with insufficient data sampling does not permit a reliable comparison of hover performance between the two configurations.

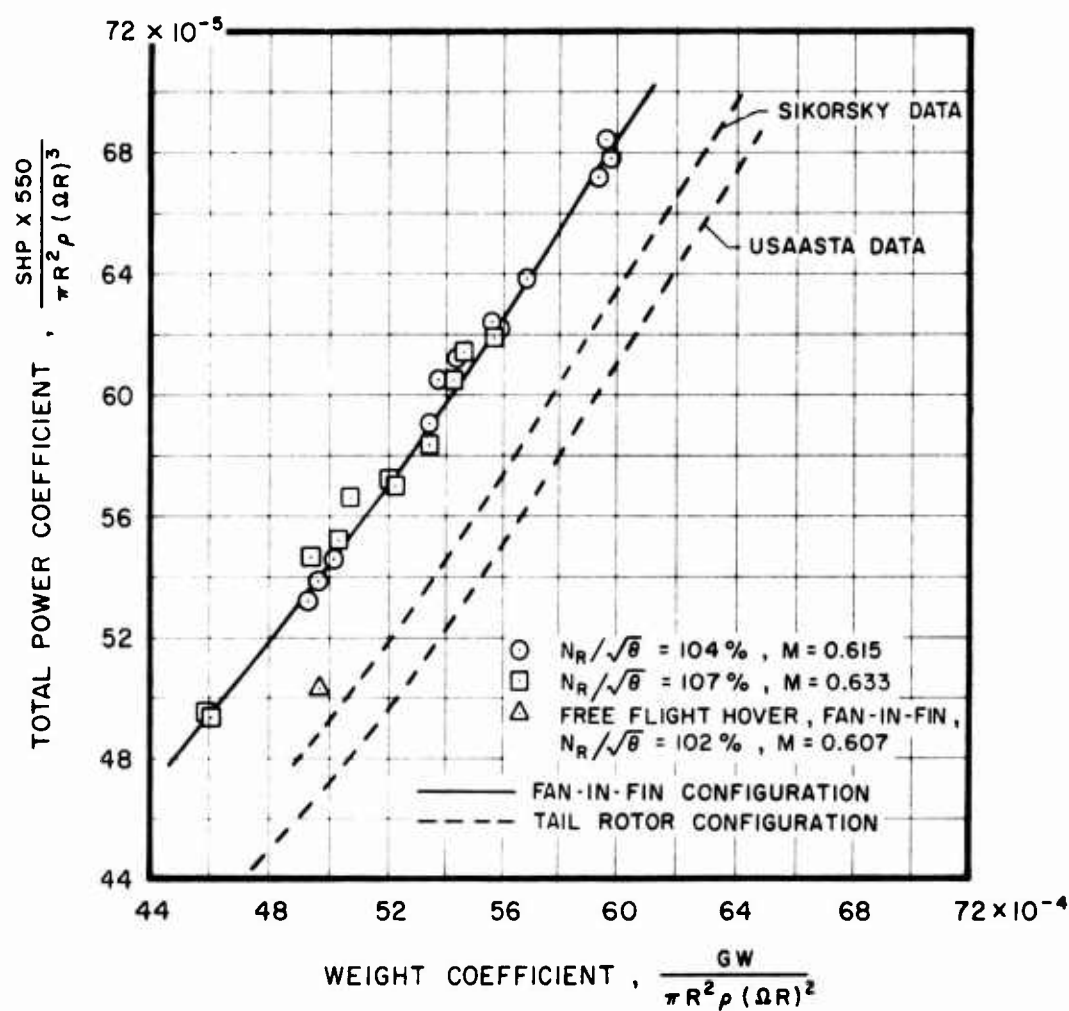


Figure 10. S-67, Comparison of Tethered OGE Hover Performance, Nondimensional.

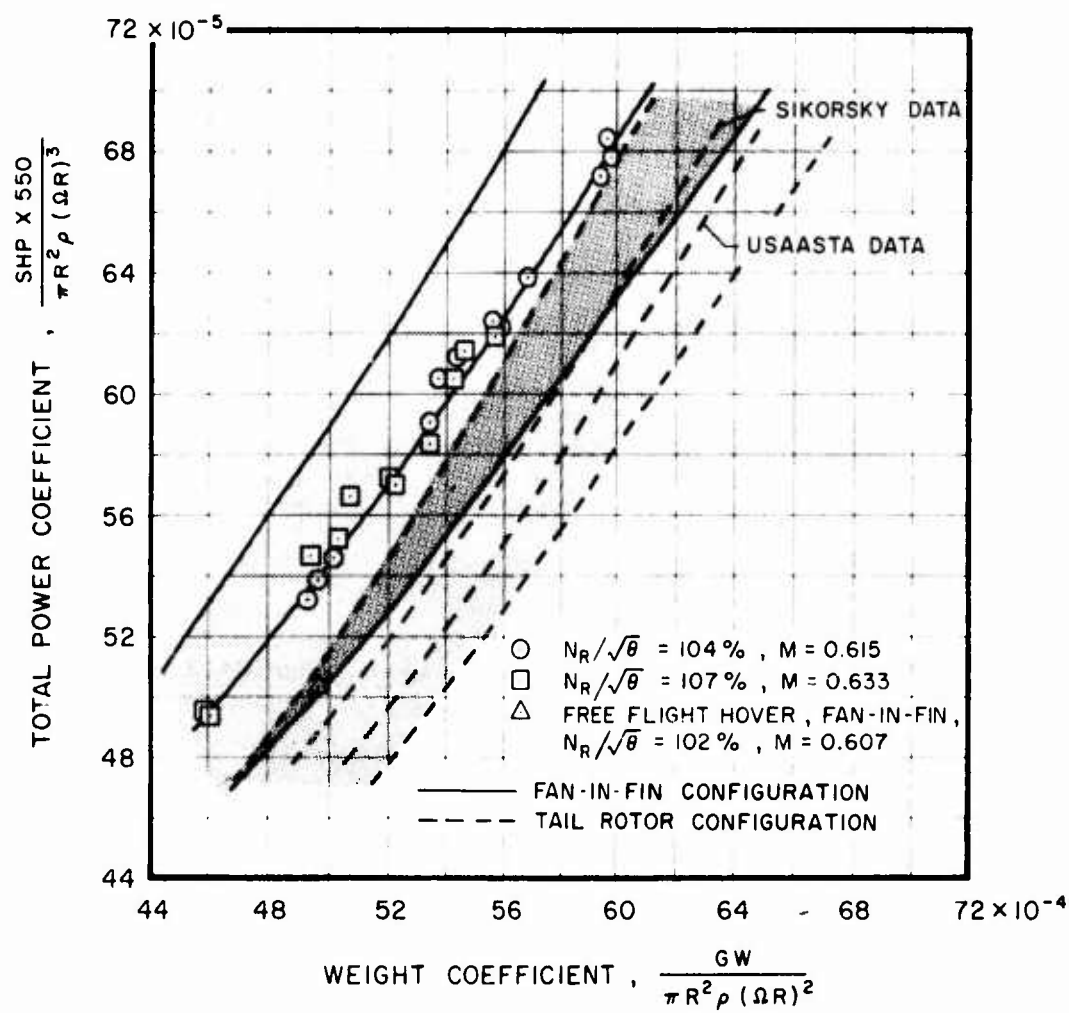


Figure 11. S-67, Comparison of Tethered OGE Hover Performance, Nondimensional, With Boundaries of Uncertainty (from Figure 10).

Figure 12 shows total power, main rotor power and antitorque power vs gross weight for the S-67 tail rotor and fan-in-fin configuration, derived from the tethered hover performance data shown in Figures 10 and 11, for SLS and 104% N_R , with the tail rotor configuration data being the Sikorsky test data. The individual data points plotted in Figure 12 are the result of analytically computed S-67 main rotor performance data that show excellent correlation in main rotor performance with the Sikorsky tethered hover performance measurement of the tail rotor configuration. The hover performance computation employs the Sikorsky main rotor performance computer program substantiated by whirl stand tests (of comparable rotors; the S-67 rotor was not whirl tested). Based on this correlation between measured and computed main rotor performance, the S-67 tethered hover performance data measured by Sikorsky will be adopted as S-67 tail rotor configuration reference data.

In Table 4, the tethered hover performance as measured for the fan-in-fin and tail rotor configurations (Sikorsky test data) are compared at two levels of main rotor power, 1,900 MRHP and 2,200 MRHP (Table 4A), and at two levels of gross weight, 17,070 lb and 20,200 lb (Table 4B). The data are taken from Figure 12. A substantial decrease in gross weight is apparent for the fan-in-fin configuration, but this difference is within the boundaries of uncertainty described previously. On no other occasion throughout the entire flight test program was there any evidence of such a large difference in performance between the two aircraft configurations.

TABLE 4. COMPARISON OF TETHERED HOVER PERFORMANCE,
SLS, 104% N_R : FROM FIGURE 12.

4A. Comparison at Equal Levels of Main Rotor Power.

Configuration	Tail Rotor (Sikorsky Data)	Fan-in- Fin	Tail Rotor (Sikorsky Data)	Fan-in- Fin
Main rotor power, MRHP	1,900	1,900	2,200	2,200
Total power, SHP	2,280	2,325	2,660	2,680
Drive system and accessory losses, HP	120	125	130	130
Tail rotor power, HP	260	-	330	-
Fan power, HP	-	300	-	350
Gross Weight, lb	18,150	17,070	20,200	19,180

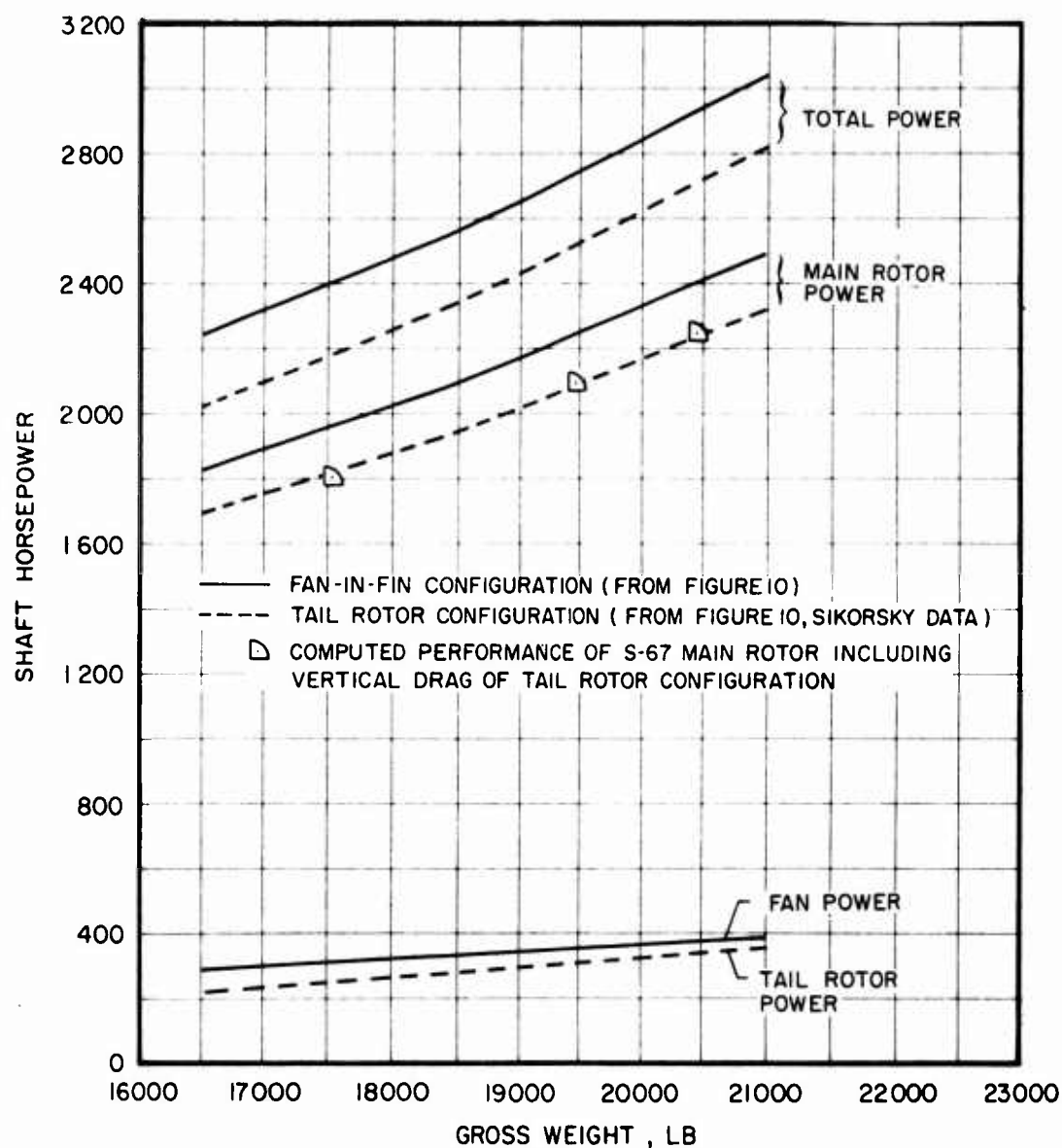


Figure 12. S-67, Comparison of Measured Tethered OGE Hover Performance, Power vs Gross Weight, and Calculated S-67 Main Rotor Performance, SLS, 104% N_R .

4B. Comparison at Equal Gross Weights.

Configuration	Tail Rotor (Sikorsky Data)	Fan-in- Fin	Tail Rotor (Sikorsky Data)	Fan-in- Fin
Gross Weight, lb	17,070	17,070	20,200	20,200
Drive system and accessory losses, HP	120	125	130	130
Tail rotor power, HP	230	-	330	-
Fan power, HP	-	300	-	370
Main rotor power, MRHP	1,760	1,900	2,200	2,370
Total power, SHP	2,110	2,325	2,660	2,870

Although the test data appear as inconclusive, the possibility of contributing factors must be investigated, in particular the consequences of aircraft configuration changes and the possible existence of interference between fan wake and main rotor downwash. In the fan-in-fin configuration, the horizontal stabilator is 11 inches closer to the main rotor than in the tail rotor configuration. The difference in vertical drag resulting from this change in stabilator position is at most 200 pounds, determined by using a standard aerodynamic load analysis and verified independently by observing differences in longitudinal cyclic positions required to trim the two S-67 configurations. Adverse interference between fan and main rotor wakes, if any, would result in some small loss of thrust over the aft portion of the main rotor disc and would also appear in differences in main rotor longitudinal cyclic. However, the differences in main rotor longitudinal cyclic positions can be attributed to the increased vertical drag of the repositioned stabilator alone and do not indicate any identifiable interference.

The large difference observed in tethered hover performance between the tail rotor and fan-in-fin configurations cannot, therefore, be rationally explained. Consequently, it is believed that it is a manifestation of the uncertainty of the method when based on insufficient data sampling.

Free flight hover performance was not assessed during the fan-in-fin program, but one reliable free hover performance data point is available. Additional free hover points have been recorded and are more optimistic than the one plotted in Figure 10, but are less reliable, primarily because of strong winds, uncertain wind azimuth, uncertain altitude above ground, and uncertain fuel state. However, the available free hover data support the conclusion that the fan-in-fin OGE hover performance would be better than measured during the tethered hover tests.

Analytical Assessment

Since the OGE tethered hover tests for the fan-in-fin configuration are inconclusive, the difference in hover performance capability between the two configurations should also be determined by means of an incremental approach. The incremental approach, using analytical means as well as test data, is inherently more reliable and accurate when investigating small differences between large numbers that are known to have uncertainties larger than the difference that is to be determined. Therefore, the following assumptions are made to compare the OGE hover performance capability of the two aircraft configurations:

- . The Sikorsky OGE tethered hover performance test data correlated with calculated performance will be used as tail rotor configuration reference data.
- . Main rotor performance and main rotor response to control inputs are the same for both configurations.
- . The power required by the two antitorque devices will be used as measured during the OGE tethered hover tests at similar main rotor power levels, thus accounting for the difference in moment arms between fan and tail rotor.
- . A download of 200 pounds on the horizontal stabilator will be assumed for the fan-in-fin configuration as a result of vertical drag on the repositioned stabilator, including any small interference effects that might exist.
- . Accessory power and drive system losses are equal for both configurations.

On the basis of these assumptions, Figure 13 shows the OGE hover ceilings for the two configurations for standard temperature at the specification takeoff rating of the engines or at the transmission power limit. The tail rotor configuration data are based on the Sikorsky test data shown in Figures 10, 11, and 12 that correlate well with calculated aircraft hover performance. The calculated fan-in-fin configuration data are derived from the tail rotor configuration data by means of an incremental approach on the basis of the assumptions listed above. As can be seen, the calculated hover gross weight of the S-67 fan-in-fin is about 1-1/2% (200-300 pounds) less than that of the S-67 tail rotor configuration at the same rated total power levels and pressure altitudes. Also indicated on Figure 13 is the result of the S-67 fan-in-fin configuration OGE tethered hover tests (from Figure 12). When using the calculated fan-in-fin hover performance capability on Figure 13 as a reference, the performance obtained from the test appears pessimistic but it is within the boundaries of uncertainty associated with the test technique.

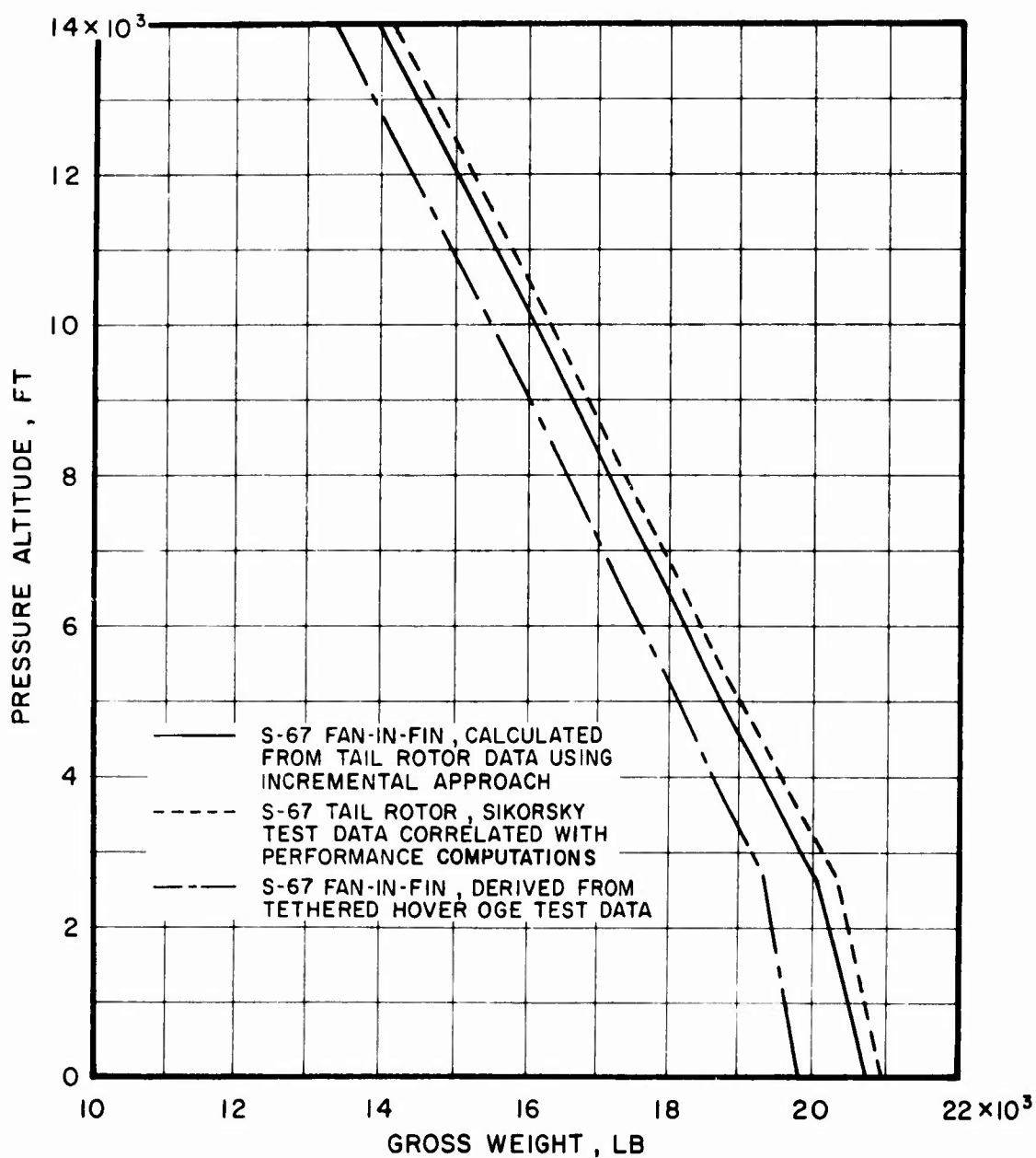


Figure 13. Comparison of OGE Hover Ceilings, Standard Temperature, 104% N_R , Sikorsky Data for S-67 Tail Rotor Configuration, Calculated and Test Data for S-67 Fan-in-Fin.

Comparison of Fan and Tail Rotor Thrust/Power Characteristics

Figures 12 and 14 provide an interesting comparison between the performance of the fan and the tail rotor when installed on the aircraft (Figure 12) or on the test stand (Figure 14). In Figure 14, tail rotor performance data was measured with a simulated SH-3 fin, which is smaller than the S-67 fin; fan data was obtained with the simulated fin module described later in Fan Static Performance that lacks the upper and lower vertical fins. The test stand data, Figure 14, indicates that fan power is about 50% higher than tail rotor power over the entire thrust range. However, when comparing the required power for the two antitorque devices at the same main rotor power in flight (Figure 12), it can be deduced that the fan requires about 40 SHP more than the tail rotor for low main rotor power levels and less than that with increasing main rotor power levels. This indicates that for increasing antitorque thrust requirements, the fan benefits from increased thrust generated on the vertical fin while the tail rotor suffers from increasing blockage caused by the large vertical fin.

Forward Flight Performance

Figures 15, 16 and 17 compare the nondimensional and dimensional steady level flight performance for the fan-in-fin and tail rotor configurations. A comparison of total power required versus airspeed indicates a reduced speed capability of 3 KTAS for the fan-in-fin when both configurations are operating at the same power and gross weight.

The minor difference in total power required at a given flight speed is necessary to provide extra propulsive force to overcome the increased drag of the fan-in-fin configuration and to supply the inherently higher power for the fan relative to the tail rotor. Throughout the forward flight range shown in Figures 15, 16, and 17, the fan power is approximately 10-15 SHP (12-19%) higher than the tail rotor power. The remaining difference in total power is attributed to the increased parasite drag (estimated to be approximately 1 ft² equivalent flat plate drag) and momentum drag of the fan configuration. Differences in performance due to aircraft trim drag, attributable to differences in fin design or location of fan or tail rotor, are negligible because of only minor differences in pitch and yaw trim attitudes of the two aircraft.

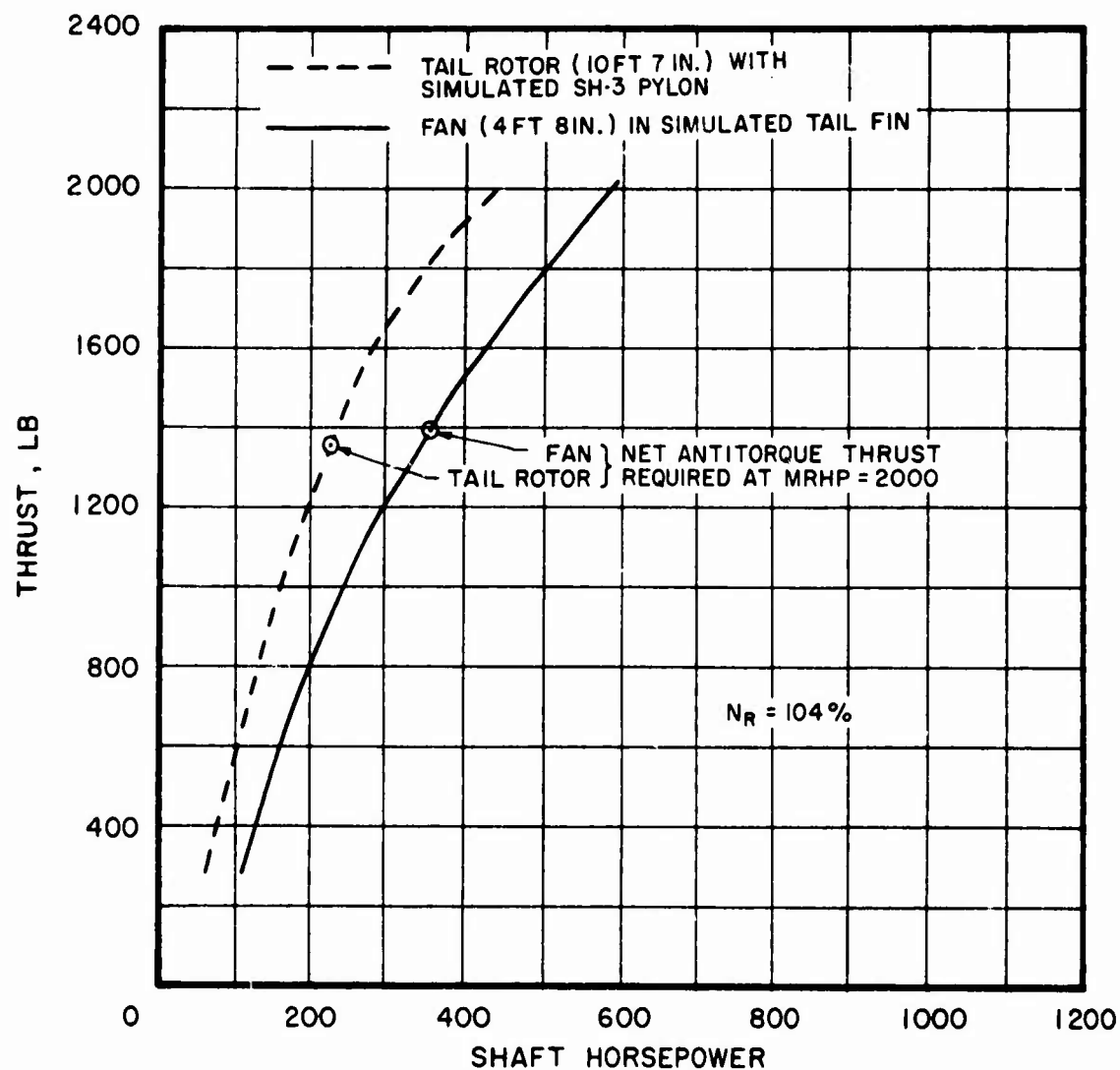


Figure 14. Test Stand Measurements, Thrust vs Power Characteristics of the Isolated Shrouded Fan and Tail Rotor, SLS, 104% N_R .

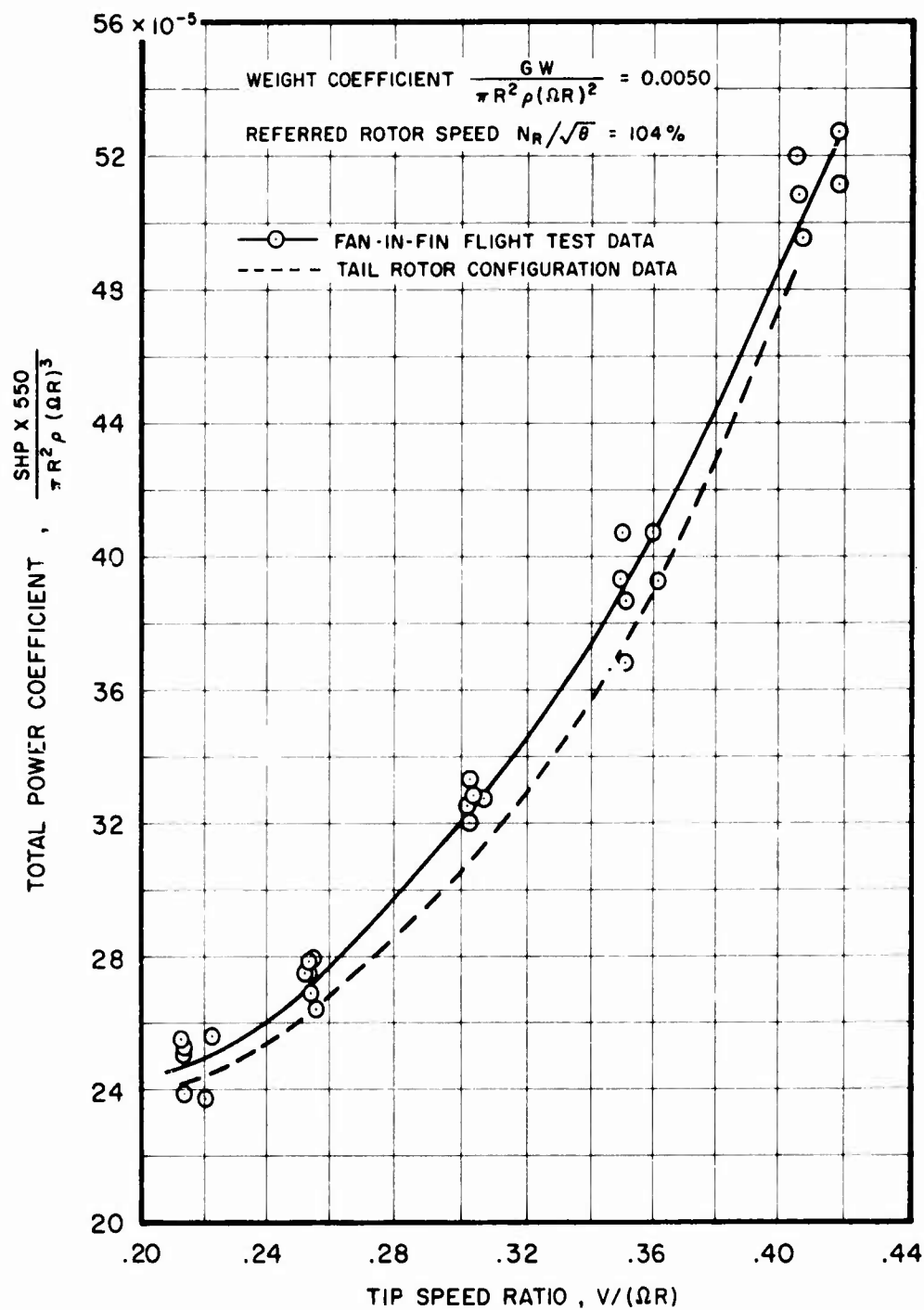
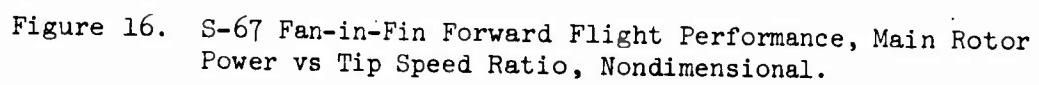


Figure 15. 3-67 Fan-in-Fin Forward Flight Performance, Total Power vs Tip Speed Ratio, Nondimensional.



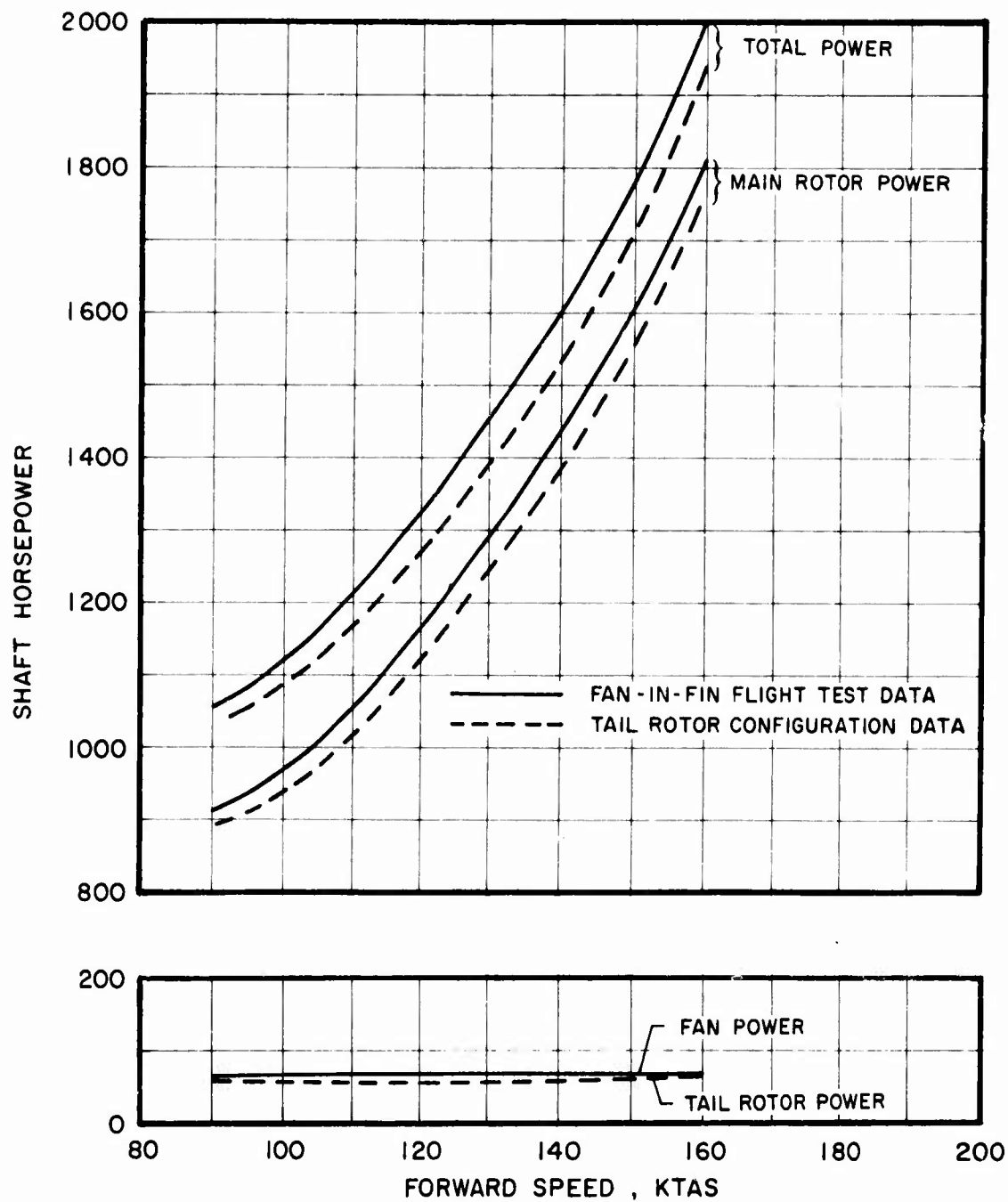


Figure 17. S-67 Fan-in-Fin Forward Flight Performance, Shaft Power vs Forward Speed, SLS, 104% N_R .

FAN STATIC PERFORMANCE

Test Arrangement

Static performance of the fan was evaluated on the Sikorsky tail rotor test stand. Figure 18 shows the fan module mounted in the efflux of the blower installation used to generate crosswind conditions. The tests included force (thrust) measurement data covering the entire blade angle operating regime and rake survey data at two fan blade angles.

Figure 19 shows the shroud geometry for the fan in top view. This shroud is part of the fan assembly and was installed in the simulated fin module as well as in the aircraft by means of three load cells capable of measuring the axial component of force generated by the fan and inlet lip. These three load cells measure only fan thrust and induced forces acting on the inlet lip and cannot sense the force on the surrounding surface. The total thrust force in the axial direction (relative to the fan) was measured by a single load cell that is part of the test facility. The difference between the sum of the loads measured on the three fan load cells and that on the single test facility load cell may then be attributed to thrust generated on the surface surrounding the fan shroud.

The module used for the static tests modelled the area around the inlet but did not extend to the extremities of the upper and lower surfaces of the aircraft's vertical tail. Analysis had shown that the contribution of the upper and lower fins was very small; hence the absence of the influence of the surfaces on the fan inflow thrust was negligible. Consequently, it was not modelled. The leading and trailing edges of the module represent the fin of the aircraft although the fuselage is not simulated, in order to evaluate low-speed flight conditions in all directions by means of the blower installation.

Force Measurements

The results of the force measurement test are presented in Figures 20, 21, and 22. Figures 20 and 21, respectively, show the power absorbed by the fan and the total thrust generated by the fan, as functions of fan blade angle (at 0.75 fan blade radius station), normalized for sea level standard conditions and 2997 RPM ($104\% N_R$). Figure 22 shows the predicted fan thrust, the thrust measured by the three fan load cells, and the thrust measured by the single test stand load cell as functions of fan input shaft power at $104\% N_R$, sea level standard conditions. At high positive thrust levels, the agreement between predicted and measured performance is fairly good. At negative and low positive thrust levels, there are considerable deviations from the predictions. These will be discussed in the section on Fan Inlet Behavior.

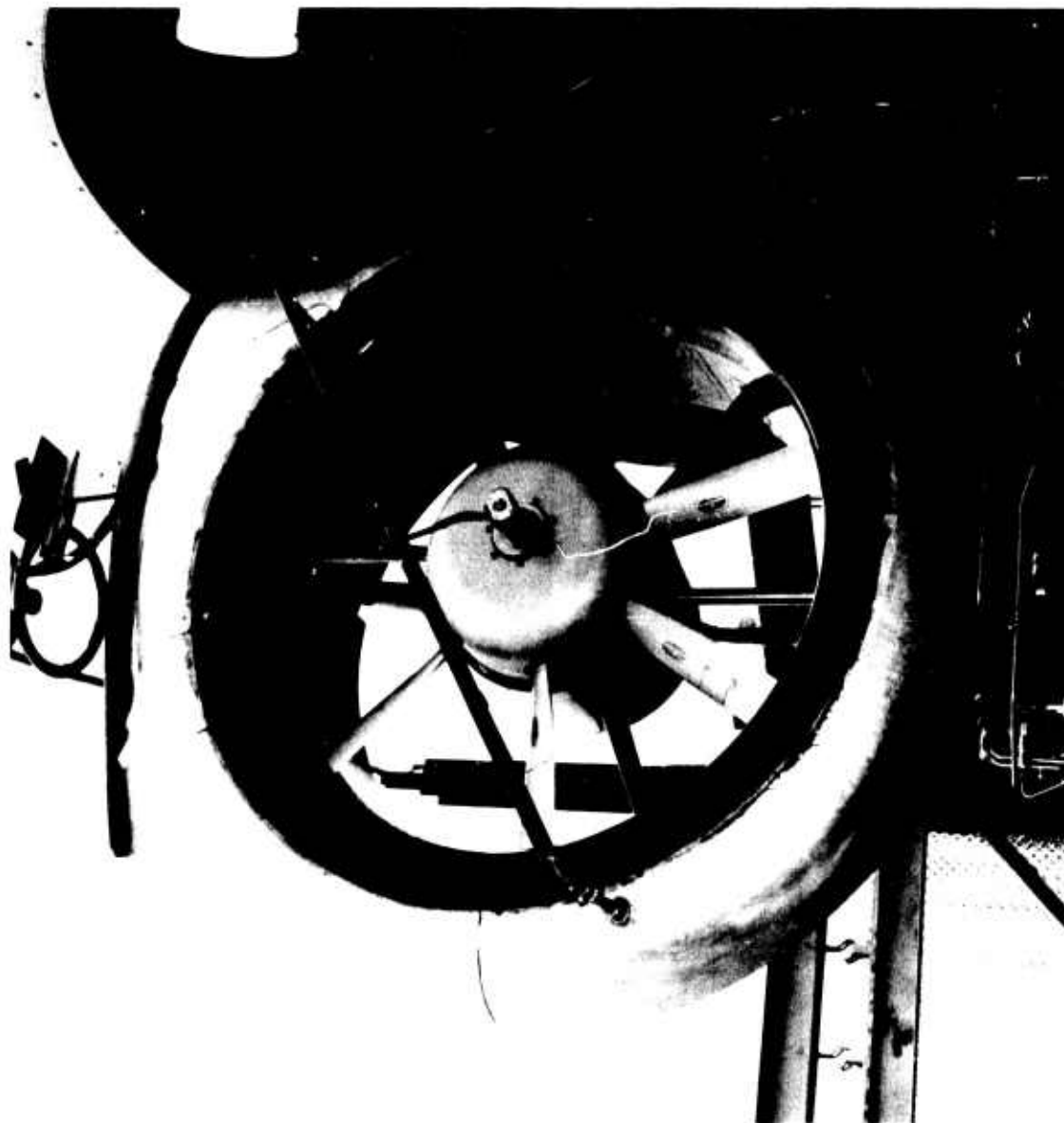
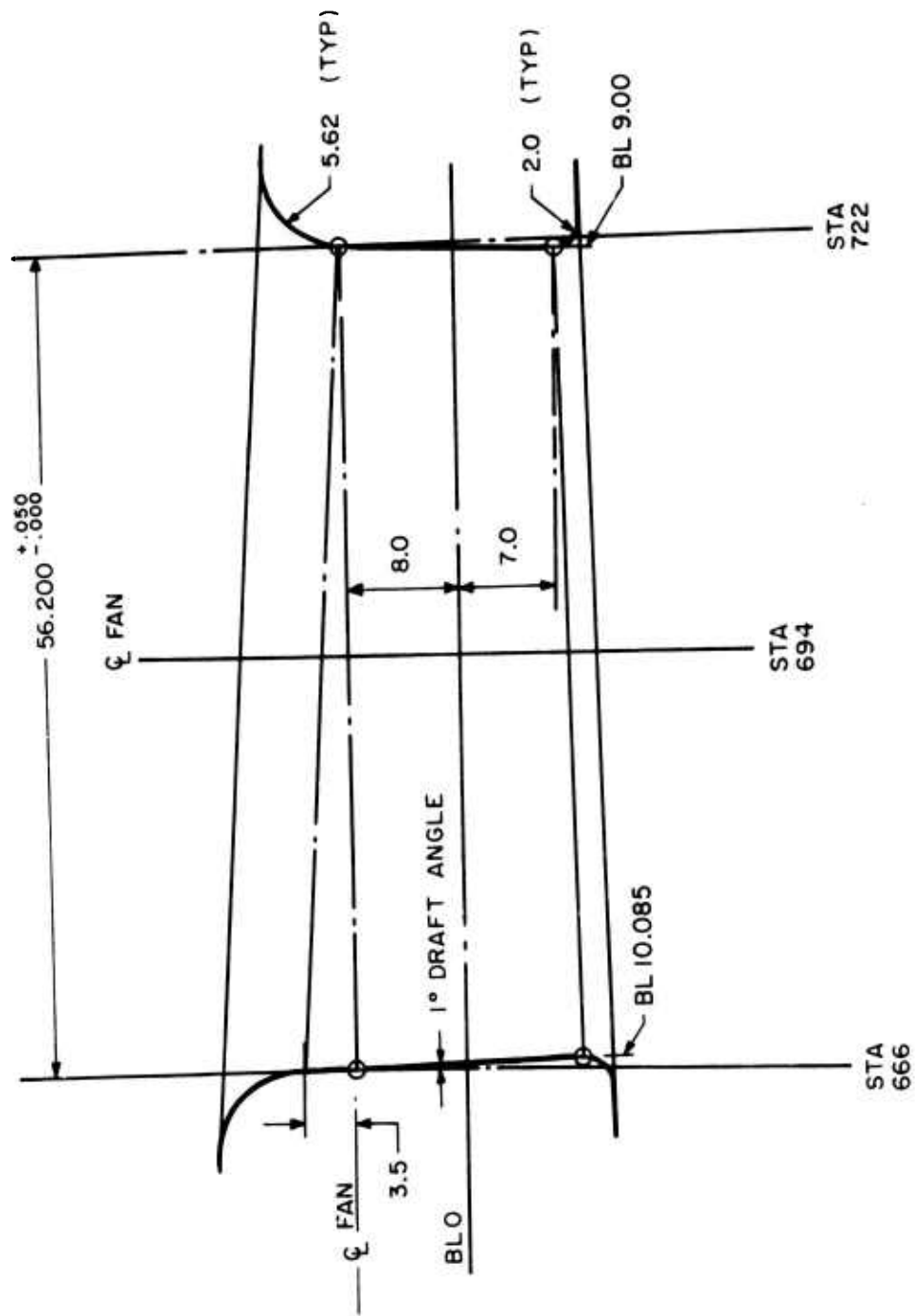


Figure 16. Fan Module With Simulated Fin Center Section Installed on Nikorsky Tail Rotor Test Stand.



(ALL DIMENSIONS IN INCHES)

Figure 19. Fan Shroud Geometry.

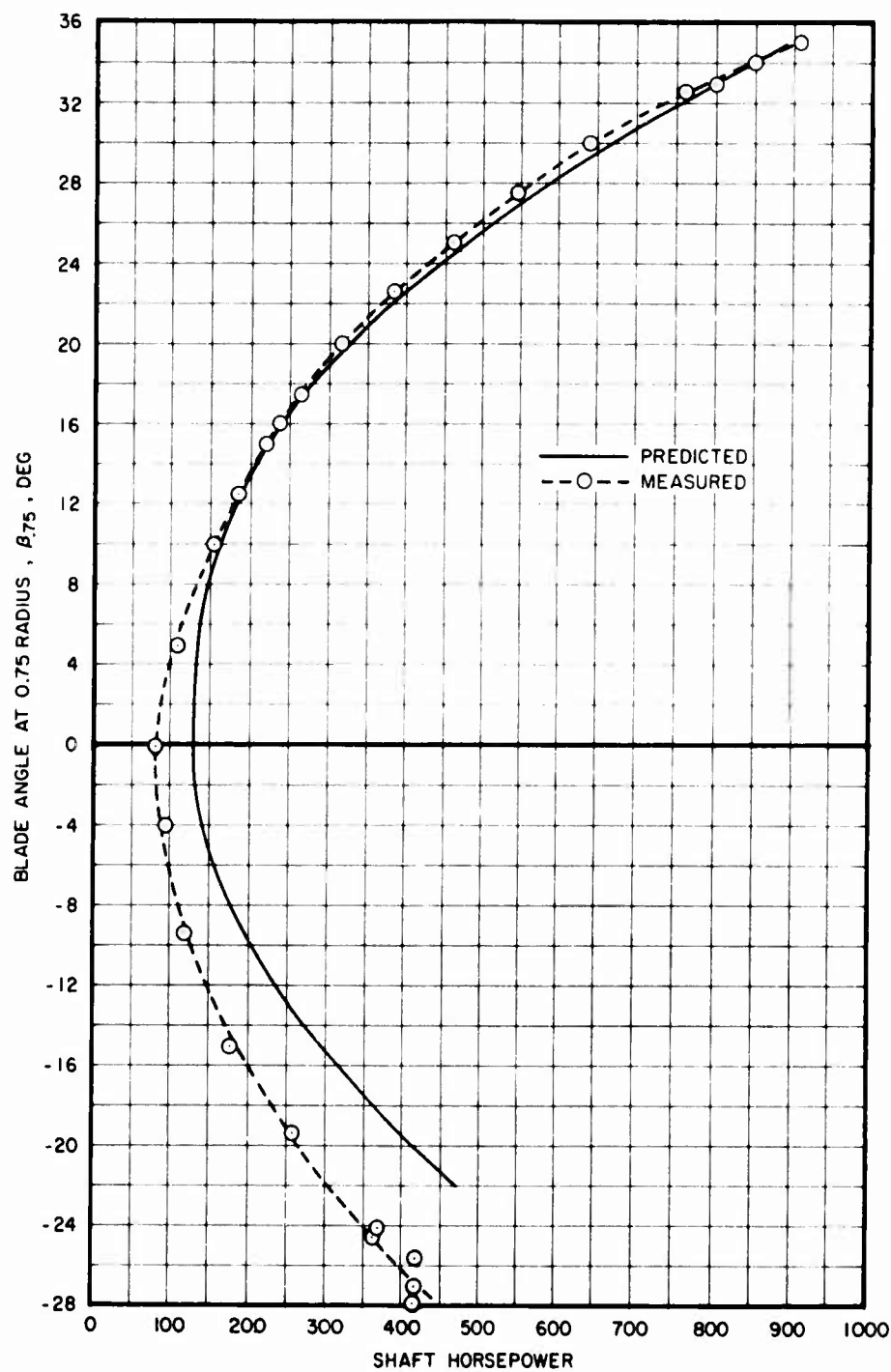


Figure 20. Fan Shaft Power vs Blade Angle, SLS, 104% N_R , Static.

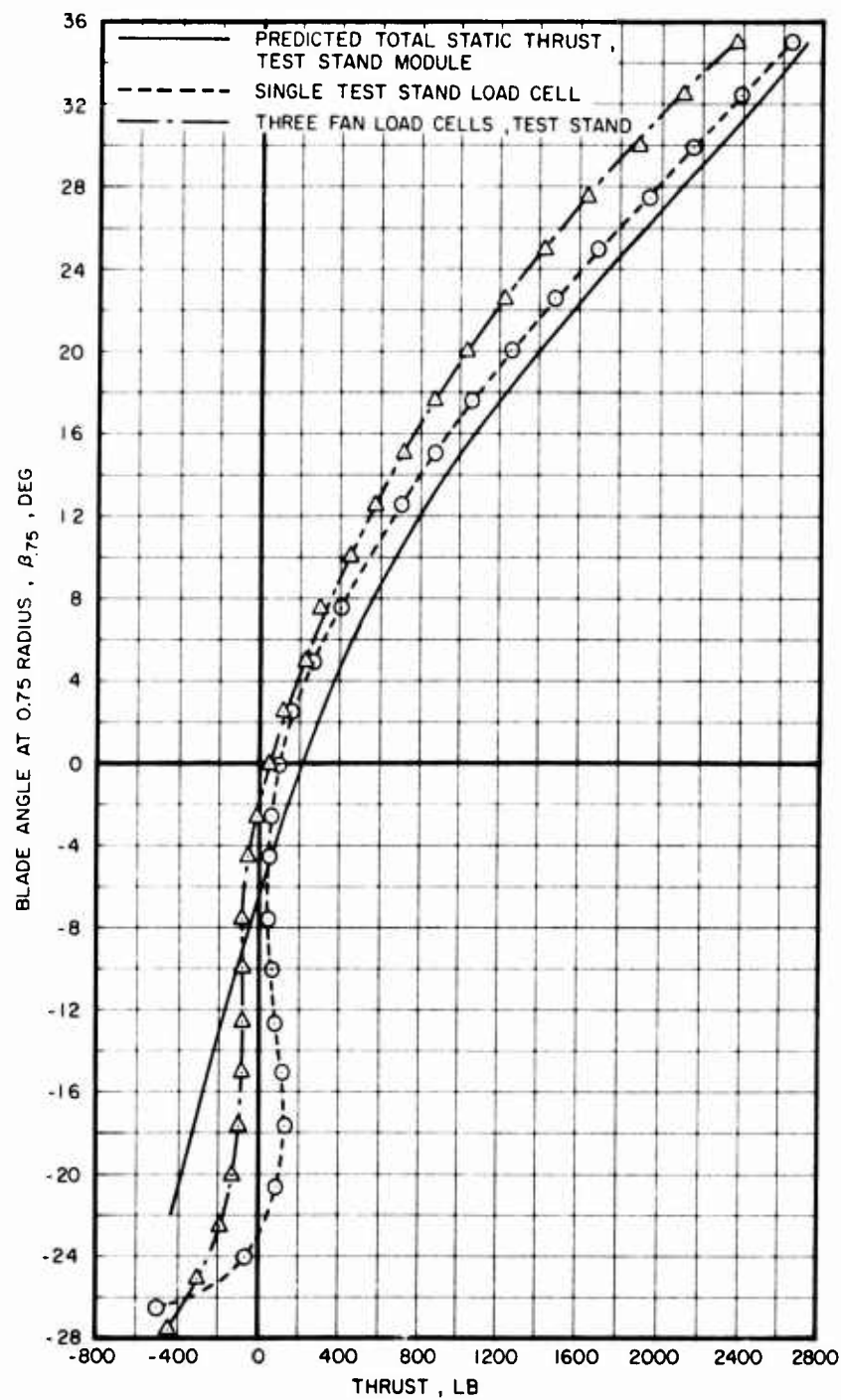


Figure 21. Comparison of Measured and Predicted Fan Module Performance, Static Thrust vs Blade Angle, SLS, 104% N_R .

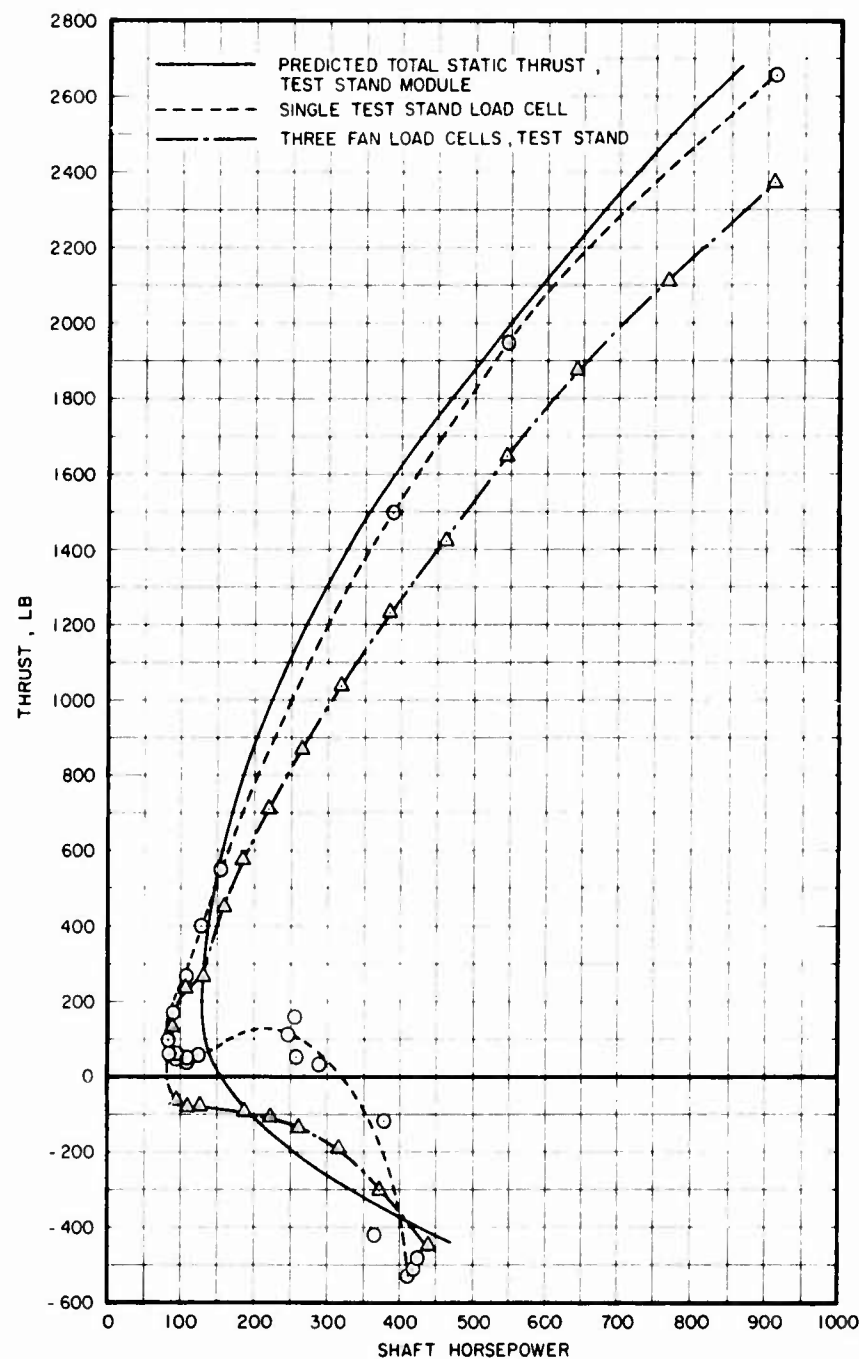


Figure 22. Comparison of Measured and Predicted Fan Module Performance, Static Thrust vs Power, SLS, 104% N_R .

Table 5 presents the thrust capability of the fan-in-fin installation on the S-67 aircraft projected on the basis of the results of the static fan module tests. The total thrust values are calculated for SLS and 4000 ft, 95°F conditions at 104% N_R , and correspond to the actual rigging employed for the fan on the aircraft throughout the flight test program.

TABLE 5. TOTAL THRUST CAPABILITY, AIRCRAFT INSTALLATION
(Calculated From Static Fan Module Test Results)

<u>Condition</u> (104% N_R)	<u>Thrust, lb</u>
SLS, maximum static	2620
SLS, maximum in 35 knots side flight	2140
SLS, maximum negative	-435
4000 ft 95°F, maximum static	2100
4000 ft 95°F, maximum in 35 knots right side flight	1720
4000 ft 95°F, maximum negative	-350

Pressure Survey Data

The flow velocities in the fan wake (as derived from measured wake rake pressures) were determined to support the assumptions on mass flow that were made for thrust predictions.

A survey rake was mounted downstream of the fan. The basic rake data were acquired as delta pressure in inches of water and then converted to elemental fan thrust coefficients in order to compare directly with calculations. Rake surveys were made at two fan blade pitch angle settings.

The rake data were then used to predict net thrust. This was done by converting the elemental pressure ratios (P_{STATIC}/P_{TOTAL}) to elemental exit velocities and using momentum relationships to integrate the fan thrust. The thrust generated by the inlet and the surface surrounding the inlet was calculated (see section Fan Inlet Behavior) and added to obtain total thrust. The results shown in the summary plot, Figure 23, indicate good agreement with predicted thrust.

It can be concluded from the rake data that both the fan and the inlet were producing the predicted thrust levels.

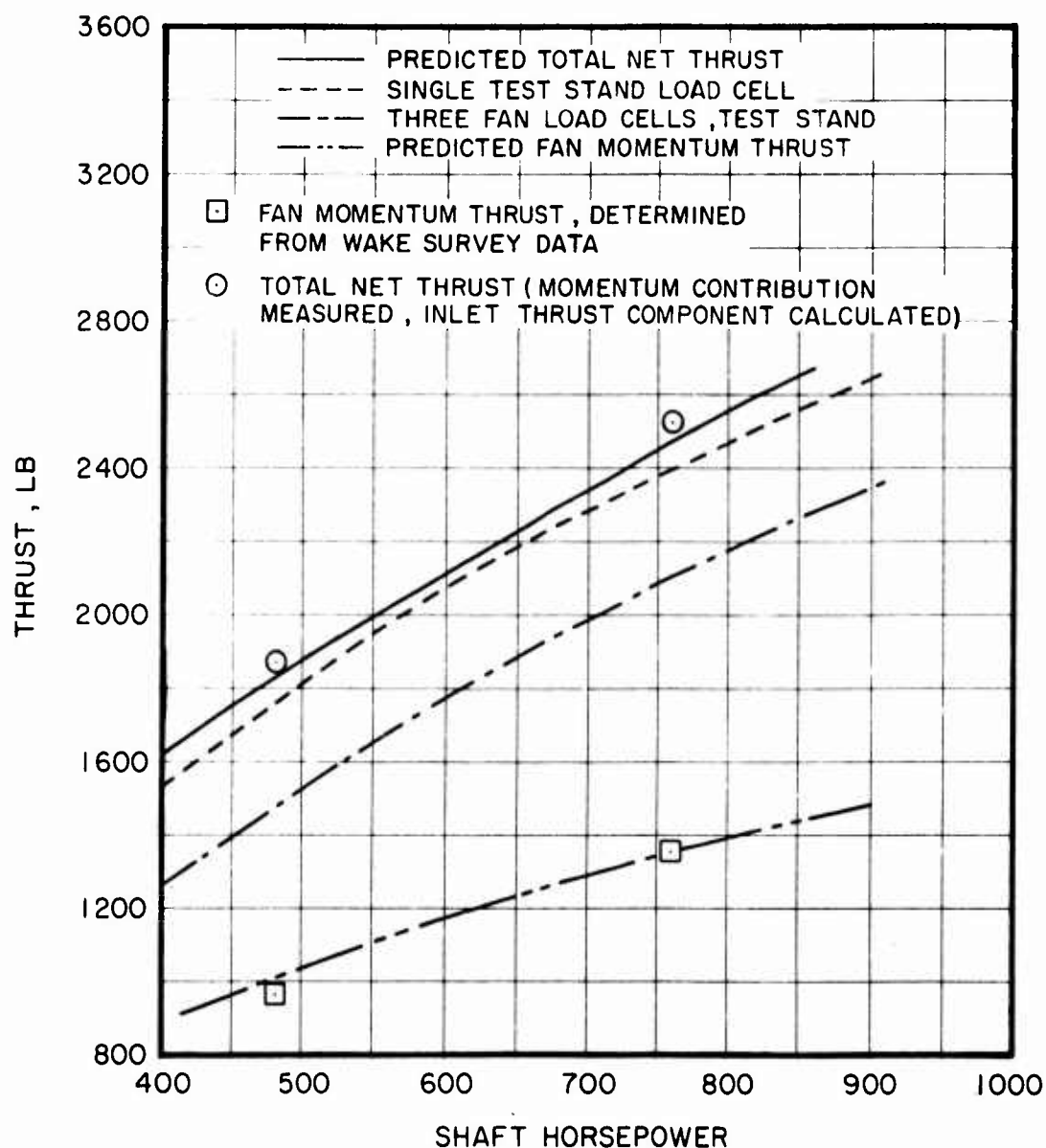


Figure 23. Comparison of Measured and Predicted Static Fan Module Thrust, Rake Survey Data.

Hover Tests

In Figure 24, the in-flight performance of the fan in hover is compared with the static test stand measurements in terms of net thrust versus shaft power. Thrust measurements were obtained with the three fan load cells, so they do not include the thrust generated outside the inlet lip on the fin. The data were obtained during tethered hover tests and are normalized for sea level standard conditions and 104% N_R (2997 RPM).

As can be seen, the in-flight performance of the fan is approximately 3% below the performance obtained on the test stand. This is probably a consequence of the flow field induced by the main rotor, the presence of the horizontal stabilator that was not part of the static test module, and possible differences in the calibration of the torque measurement instrumentation between the test stand drive shaft and the aircraft tail drive shaft.

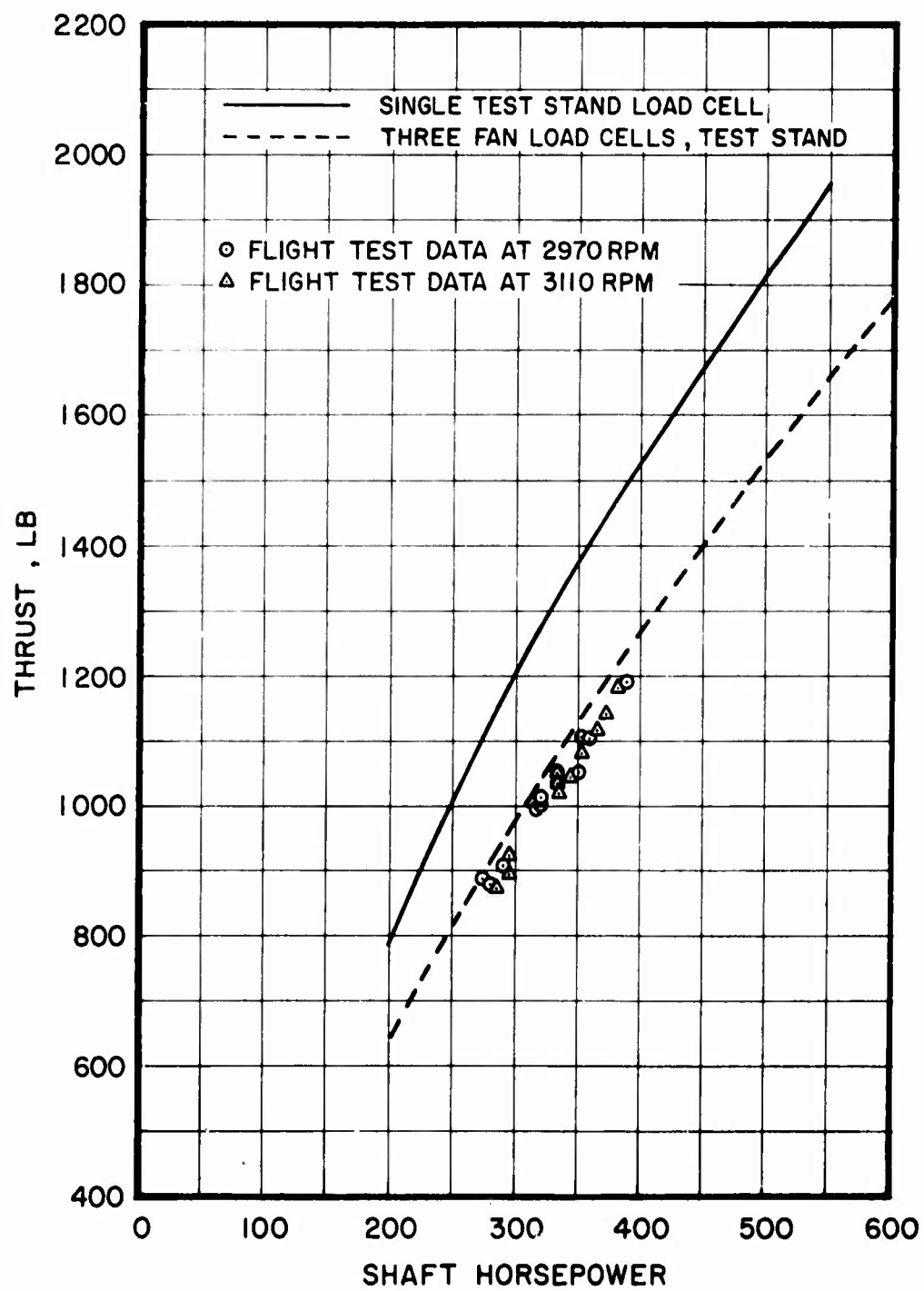


Figure 24. Fan Performance in Hover, Thrust vs Power, SLS, 104% N_R .

FAN FORWARD FLIGHT PERFORMANCE

Fan performance in forward flight was assessed by measuring fan blade pitch angle, input drive shaft torque, and individual load cell forces.

Figure 25 shows fan power required, measured total fan thrust, and fan blade pitch angle as functions of true airspeed, at a gross weight of approximately 16,200 lb and a density altitude of approximately 3000 feet. As can be seen, the measured fan thrust shows a marked increase with airspeed above about 120 KTAS that is not reflected by an increase in either the required power or the fan blade pitch angle setting. The increased thrust can be attributed directly to increasing inlet lip effectiveness with airspeed. Figure 26 shows the thrust readings obtained from the three individual cells, corrected for tail drive shaft torque reaction. The upper forward cell measures higher thrust than the lower forward cell, which would be expected as a consequence of higher inlet lip thrust generated there by the general flow field under the main rotor. Both the upper and lower forward cell measurements verify the increasing inlet lip effectiveness with airspeed. It is interesting to note that the aft load cell measures negative thrust over the entire speed range above 40 knots. This is the result of the presence of a stagnation region on the aft portion of the inlet lip, as will be shown in the following section, Fan Inlet Behavior.

Figure 27 shows the location of the center of the fan and inlet lip thrust vector, based on the data presented in Figure 26. Although there is considerable scatter in the data, it is apparent that with increasing airspeed, the center of the thrust vector moves forward. At about 140 KTAS, it is forward of the fan itself and is in fact slightly forward of the inlet lip, indicating again dominance of the inlet at higher flight speeds. However, if the total thrust induced by the fan on the inlet and the surface surrounding the inlet were taken into account, the actual center of the total thrust vector would be further forward than indicated in Figure 27 for the inlet and fan alone. This is supported by the data taken at speeds as low as 35 kts on the static test stand and presented in Figure 36.

Figures 28, 29, and 30, respectively, show the fan input power, fan thrust as measured by the three load cells, and fan blade pitch angles as functions of sideslip at airspeeds of approximately 88 KTAS, 146 KTAS, and 180 KTAS. The data show that fan thrust and blade angle have stable variation over the sideslip angles at all speeds. The fan power shows a peculiarity in right sideslip that becomes more pronounced at high speed. The dip apparent in the fan power required curve at about 7-1/2 deg right sideslip is believed to be caused by a stabilator root vortex shedding from the fixed stabilizer section used to adapt the horizontal stabilator to the modified fuselage contour.

The behavior of the fan in left sideslip conditions is of particular interest. Measured thrust, power required and fan blade pitch angle indicate that left sideslips (nose right) are far less demanding on fan thrust than right sideslips. The reason for this is that in left sideslip conditions the flow separates on the right side of the upper vertical fin. As a result of the subsequent loss of fin effectiveness, very little thrust change is necessary to achieve large left sideslip angles. This flow separation is

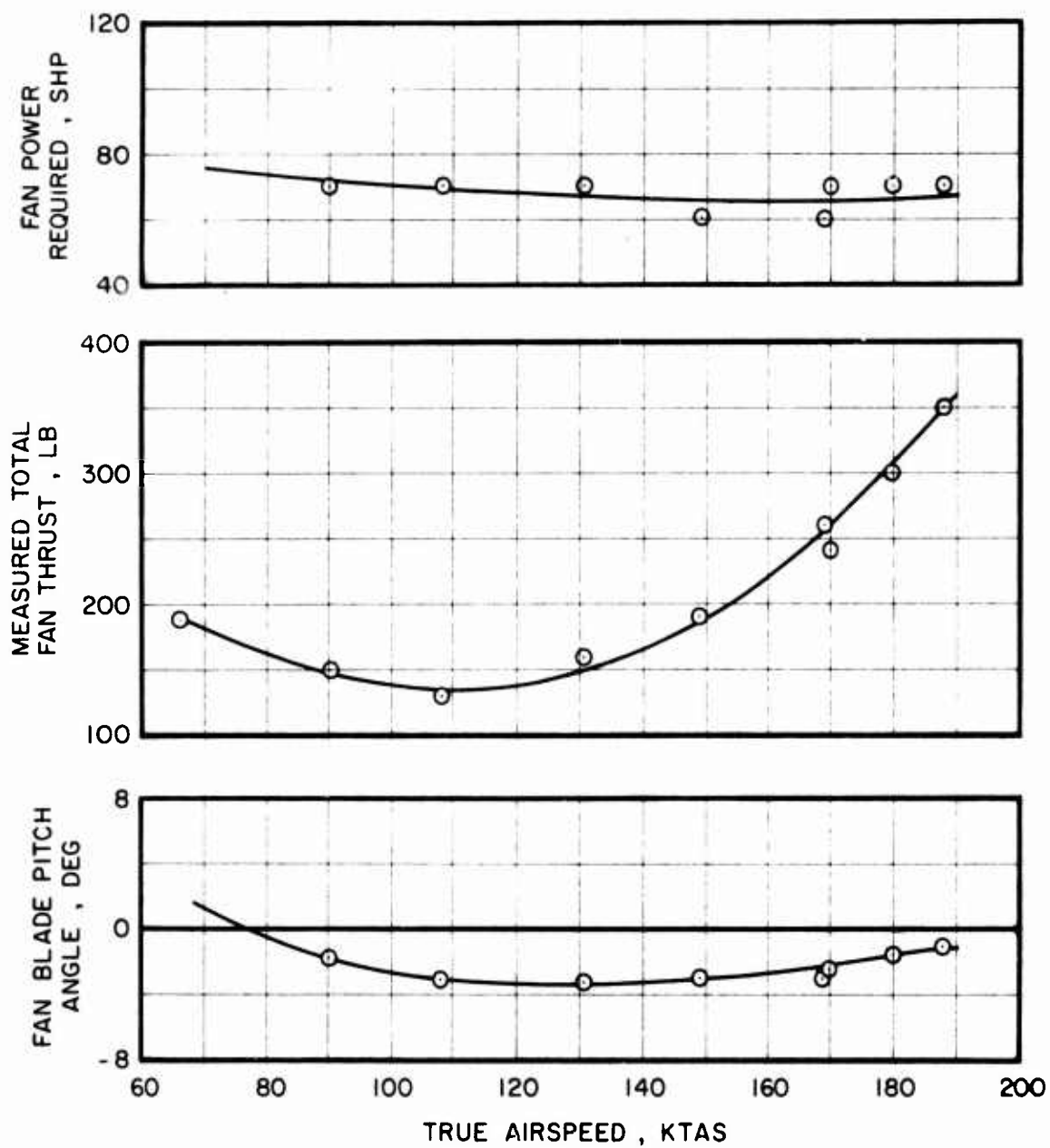


Figure 25. Fan Power, Thrust, and Blade Angle vs Forward Speed; GW = 16,200 lb, Density Altitude 3,000 ft.

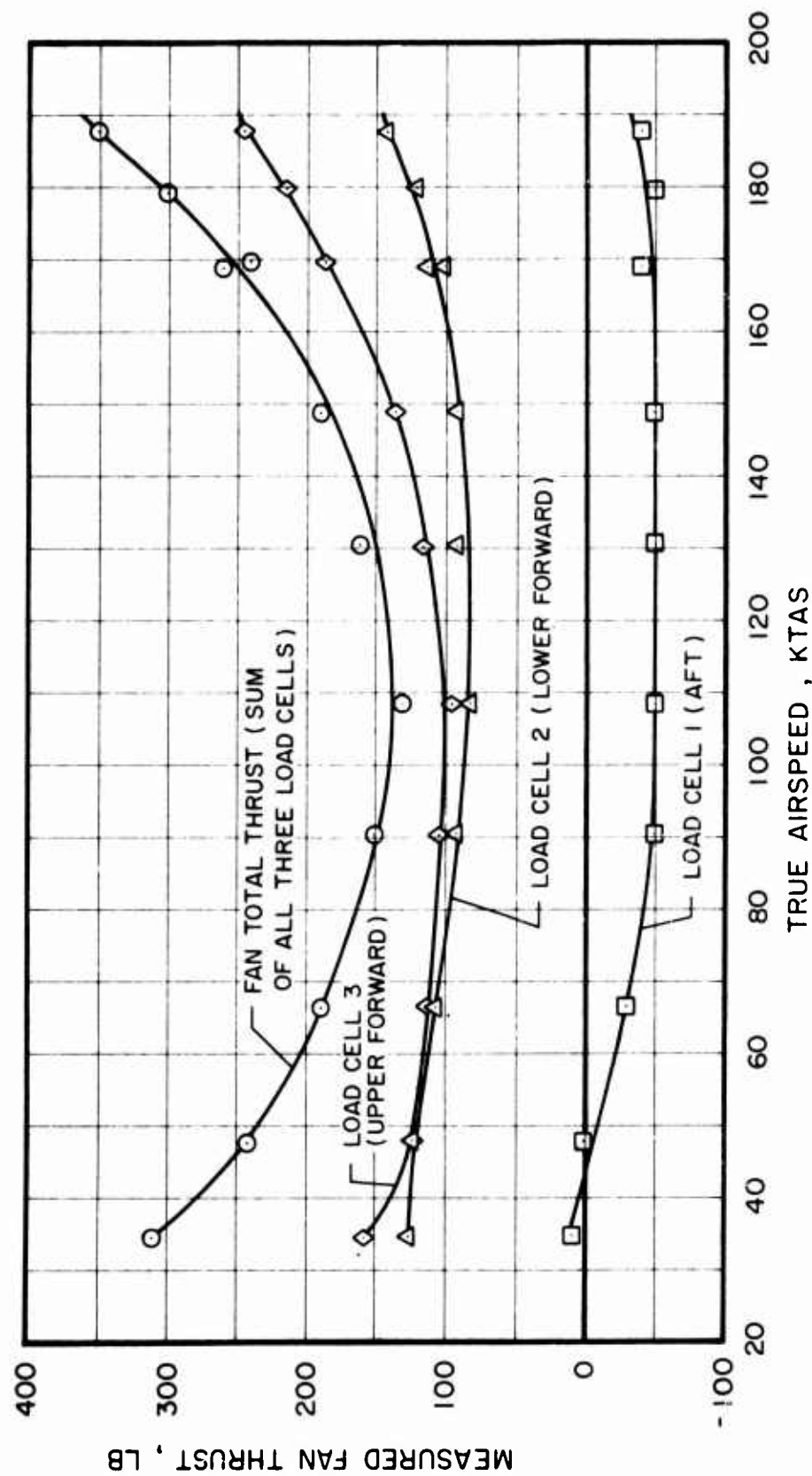


Figure 26. Fan Thrust Measurement in Trimmed Level Flight; GW = 16,200 lb, Density Altitude 3,000 ft.

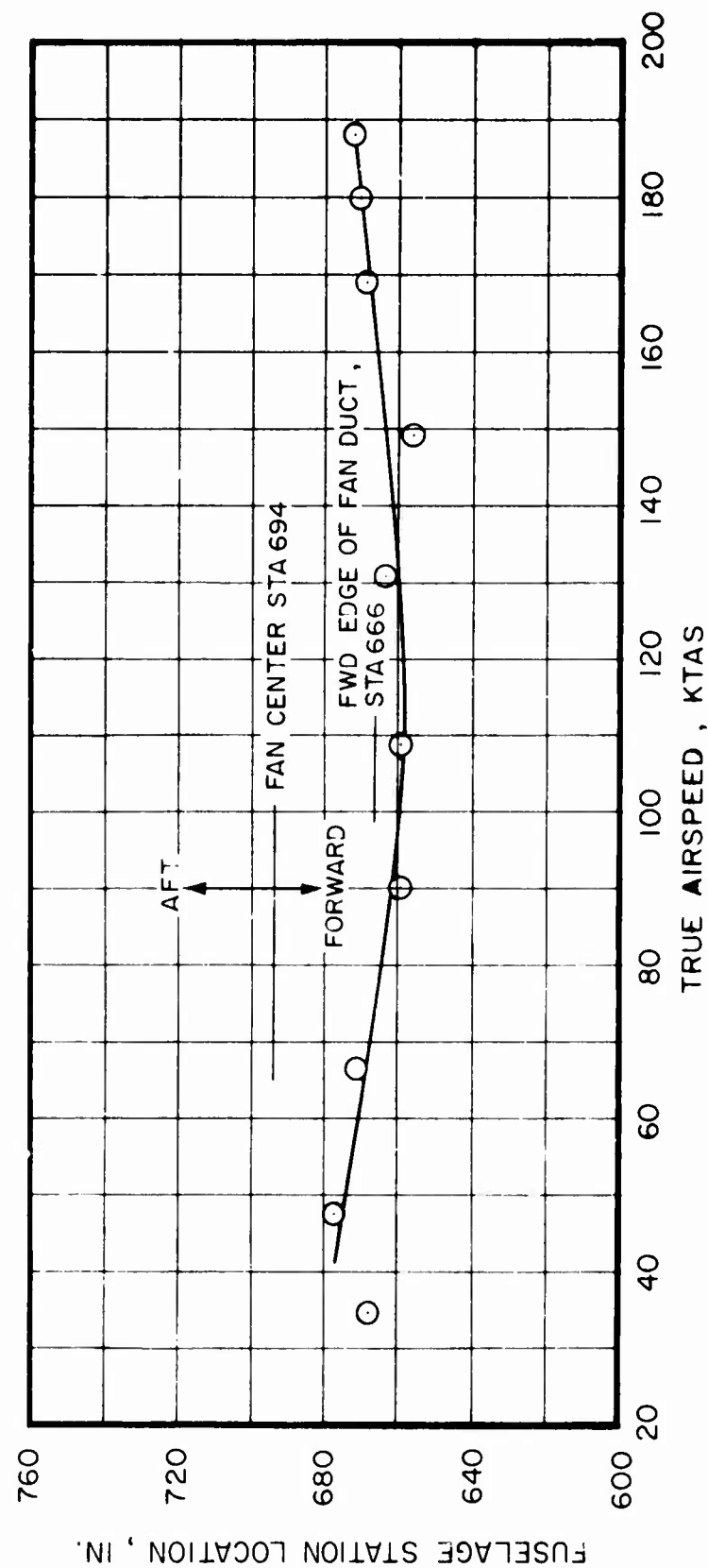


Figure 27. Station Location of Measured Thrust Vector Center;
GW = 16,200 lb, Density Altitude 3,000 ft.

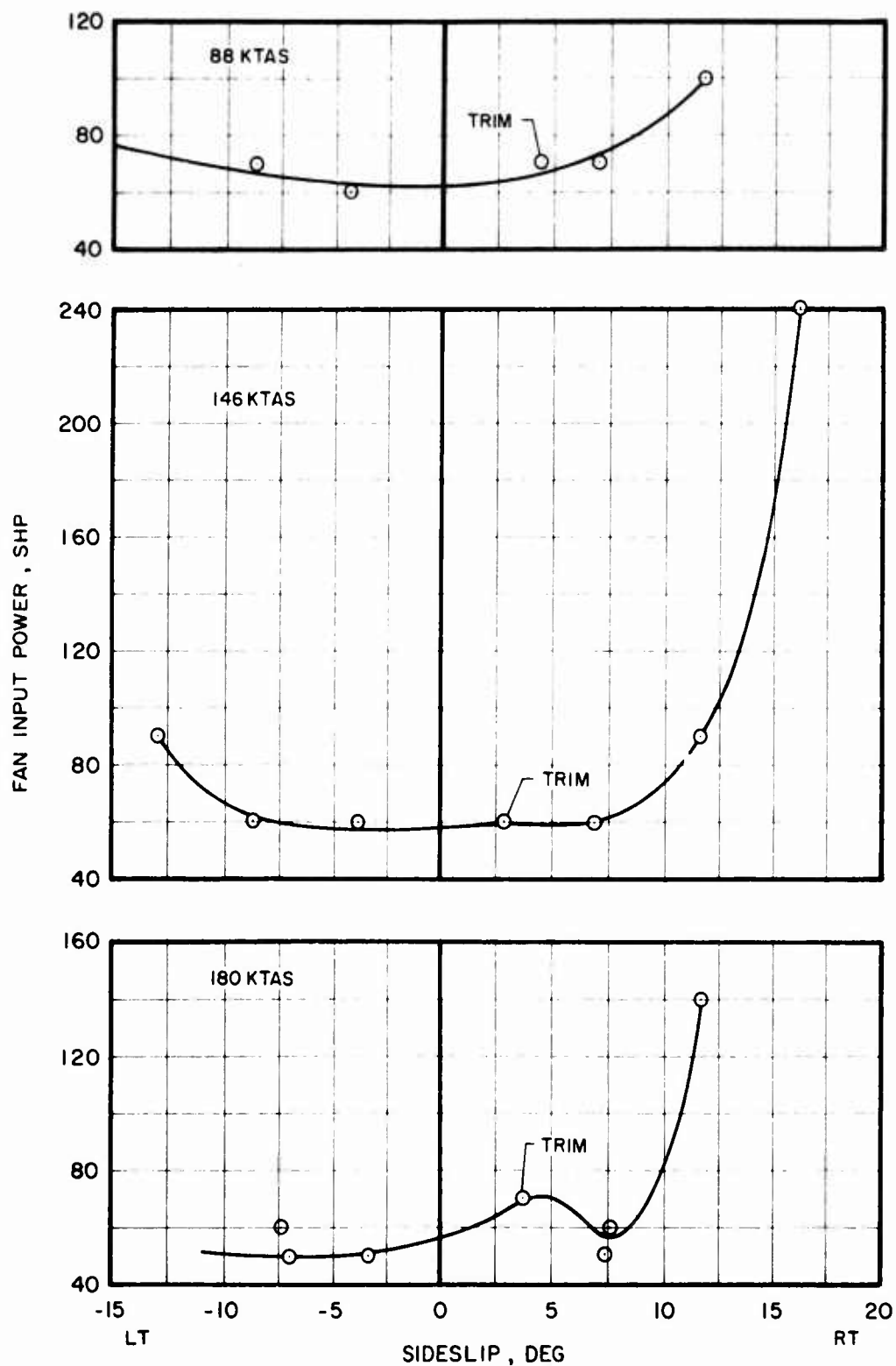


Figure 28. Fan Input Power vs Sideslip and Speed;
GW = 16,200 lb, Density Altitude 3,000 ft.

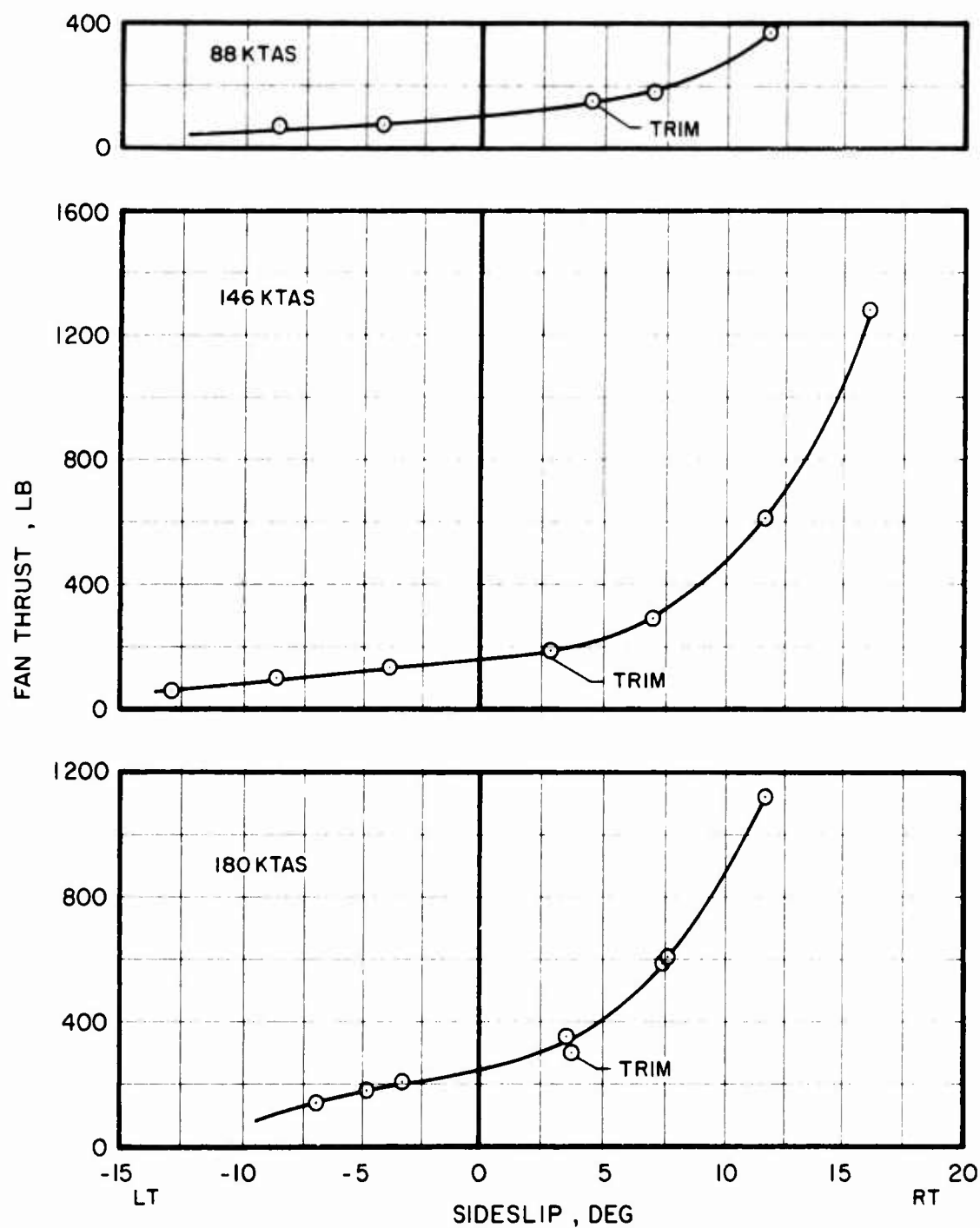


Figure 29. Fan Thrust vs Sideslip and Speed;
GW = 16,200 lb, Density Altitude 3,000 ft.

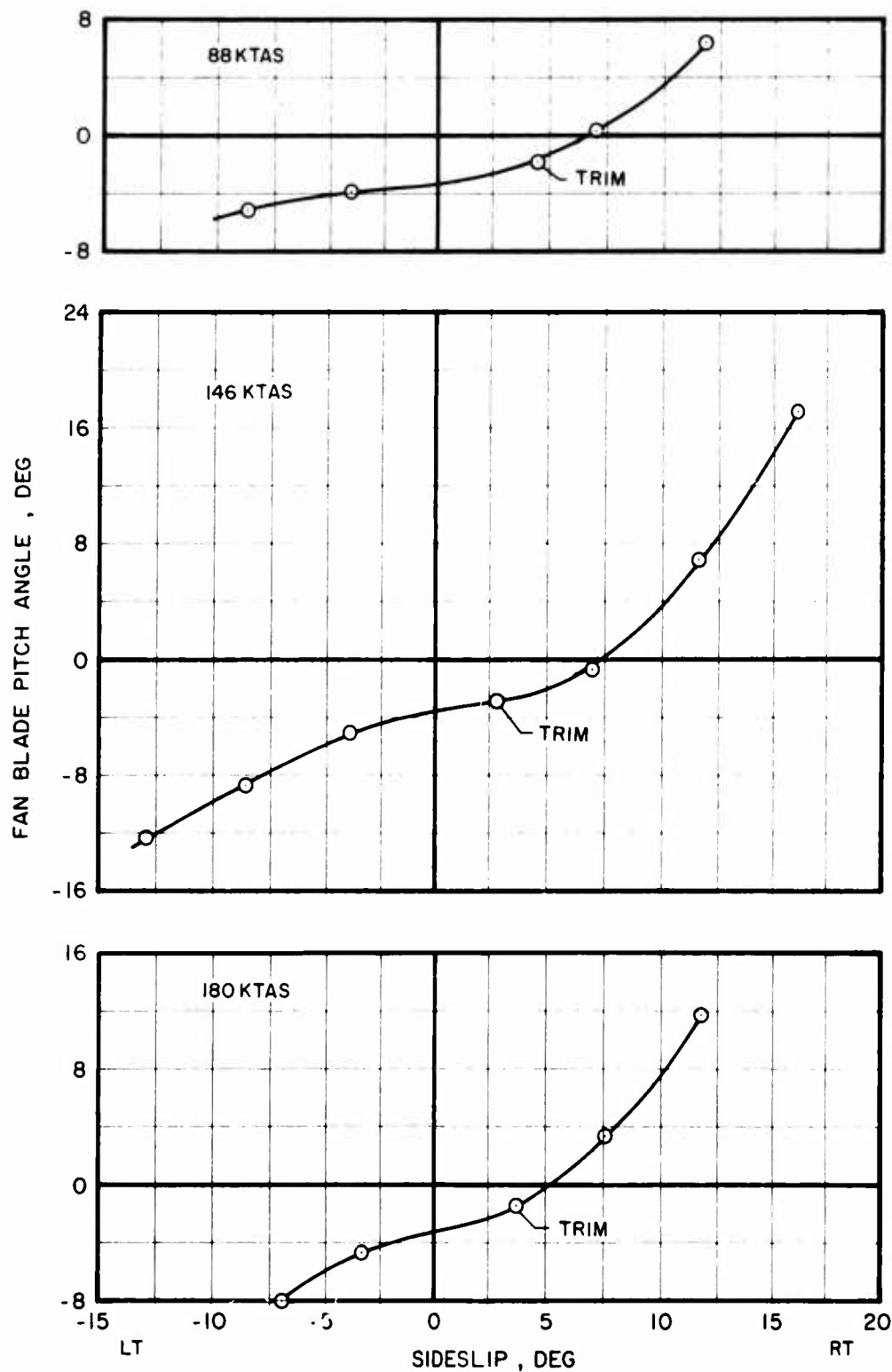


Figure 30. Fan Blade Pitch Angle vs Sideslip and Speed;
GW = 16,200 lb, Density Altitude 3,000 ft.

progressive with increasing left sideslip angle and also depends somewhat on airspeed. The total fan plus inlet lip thrust as measured is always positive although according to the blade pitch angle setting the fan itself is certainly providing negative thrust (fan efflux from the inlet side). This condition is recorded on the photograph in Figure 31 which shows the aircraft in a minus 10 deg (left; from trim) sideslips condition at an airspeed of about 180 KTAS. A close examination of the tufts on the fan inlet lip shows that the fan flow is reversed. This corresponds to the blade pitch angle setting shown on Figure 30. However, the fan efflux does not separate immediately from the well-rounded inlet lip, generating a suction force and causing the total fan thrust to be measured as still positive (this phenomenon will be discussed in the following section, Fan Inlet Behavior). The tufts on the upper vertical stabilizer indicate a flow separation on the upper fin. It is thought that the fan efflux is forced straight up the vertical fin, enhancing the flow separation and contributing to the loss in effectiveness of the upper vertical fin.

This condition, discussed above for level flight, is particularly pronounced whenever the fan operates at low or negative thrust levels, such as in part power descents and autorotation.

This flow separation on the upper fin is a major cause for the reduced static lateral stability of the aircraft and must definitely be avoided in future fan-in-fin configurations. This could be achieved by reducing incidence or introducing twist towards the tip of the vertical fin; another solution might be to install a flow divider fence or the horizontal stabilator part way up the vertical fin.

It is evident from Figure 31 that flow separation occurs only on the upper vertical fin while the flow over the lower vertical fin remains attached. The primary reason for this is that the flow induced by the horizontal stabilator is directed upwards (the stabilator produces negative lift), which enables the fan efflux to separate from the lower part of the inlet lip. Furthermore, the lower fin does not have an incidence of 2 deg (referred to chord line; the effective incidence is about 4 deg) as the upper fin and its effective angle of attack is therefore smaller, which delays the onset of flow separation.

In order to measure the fan and inlet lip thrust, the entire fan unit including the inlet lip was mounted in the airframe by means of three load cells. It was recognized that the duct, necessarily of light construction to minimize total weight, could distort due to aerodynamic loads or as a result of changes in length of the stationary fan vanes due to temperature changes, possibly leading to rubbing of the blades in the duct. For this reason, a rub strip was imbedded in the duct. To minimize performance losses, fan blade tip clearance was held between 0.05 and 0.15 inch.

The high aerodynamic forces generated on the forward and upper portion of the fan inlet lip and possibly gyroscopic effects did cause some deformations which led to fan blade rubbing against the duct. Blade rubbing

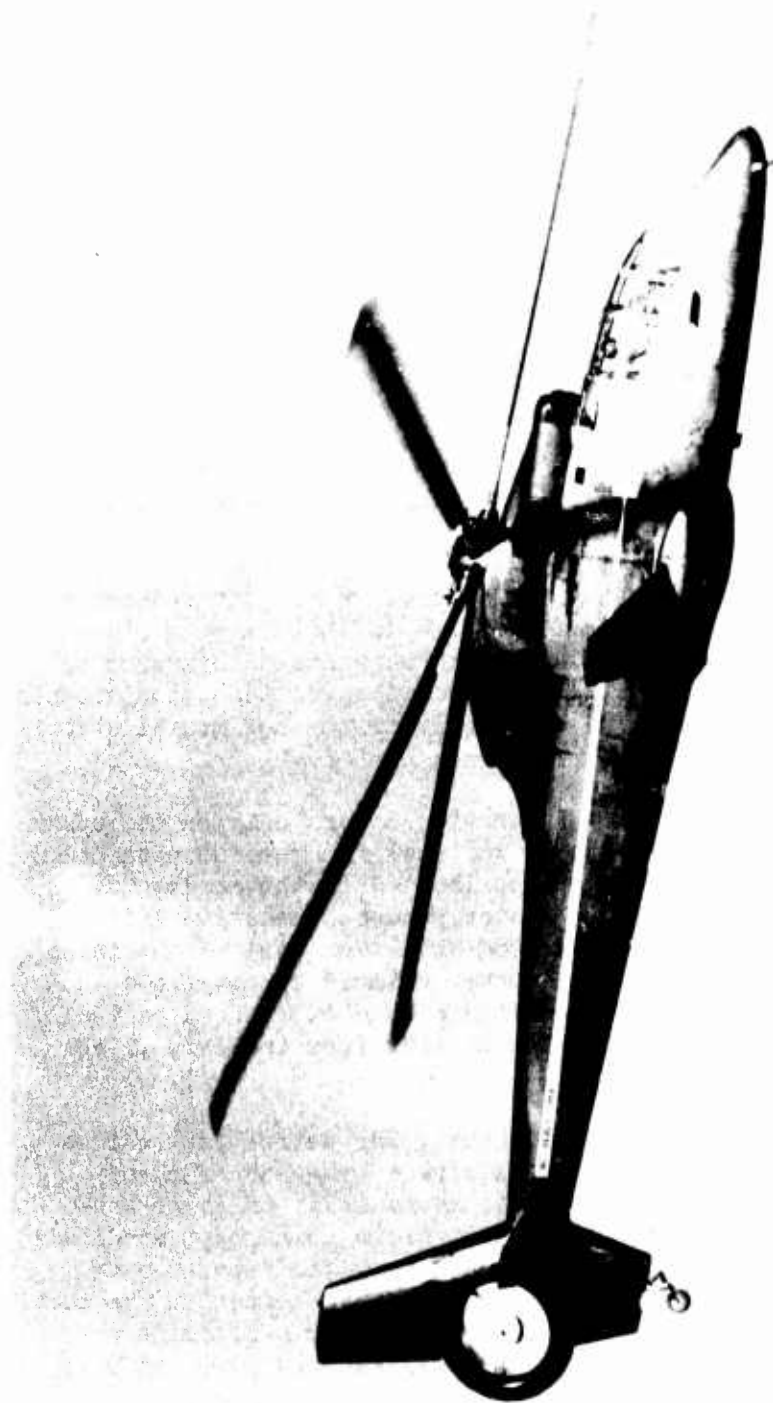


Figure 31. J-67 Pan-in-Pin Aircraft, Approximately 10 Deg Left Sideslip from Trim 2.
180 KIAS, Pan Inlet Side.

occurred during yawing maneuvers and in sideslips at speeds over 80 knots. The rubbing occurred in two areas of the duct, particularly in the forward and upper part, where the highest local thrust is generated. The depth of the rubbing grooves was generally about 0.02 inch with a maximum of .100 inch. As the rub areas were contained within the rub strip, no repair was considered necessary.

Future fan designs should provide for similar rub strips if close blade tip clearances are anticipated. However, if the shroud were integral to the airframe, instead of free floating as in the present design, the possibility of deformation under air pressure loads with consequent possibility of blade rubbing would be greatly reduced.

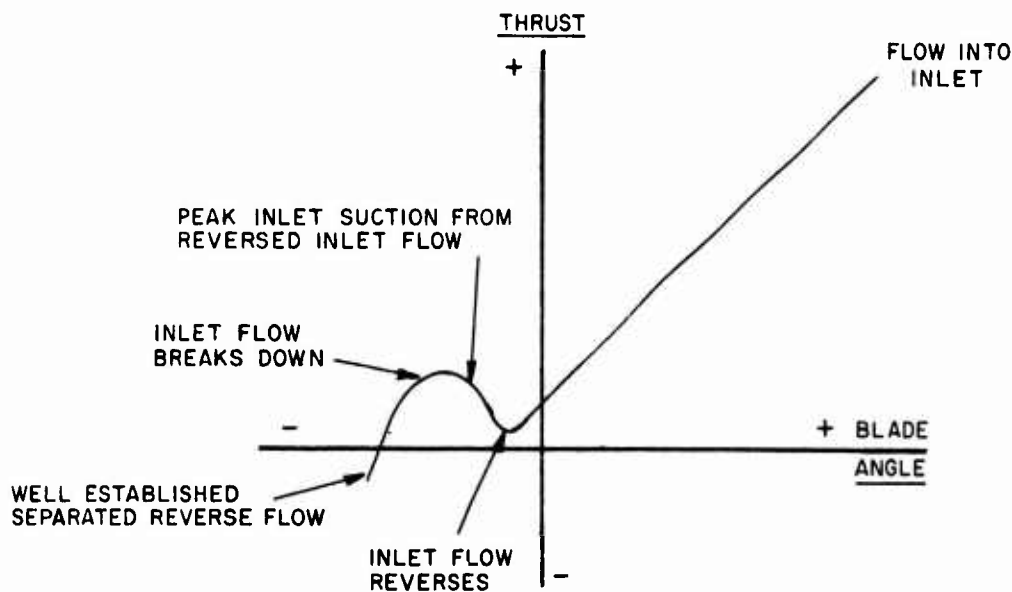
FAN INLET BEHAVIOR

Measured Data

During whirl testing of the fan-in-fin static test module, surface pressures were measured at the inlet, the surface surrounding the inlet, and the aft-facing cusp region. Figure 32 summarizes the azimuths at which pressure data were taken.

Static Performance

Figure 33 shows that in the absence of wind, the inlet flow field is well behaved as the blade angle (and hence thrust) is increased from a value where the thrust is nominally zero. Most noticeable is the increase in the height of the suction peak on the inlet lip and the intensification of the unfavorable pressure gradient approaching the fan. Despite this, there is no appearance of separated flow in the inlet. As flow in the fan is reversed, with increasingly negative blade angles, pressures on the inlet should remain low. This does not happen immediately. The reverse flow in the duct, instead of separating from the walls after passing through the fan, remains attached to the inlet (in the negative thrust range this becomes the exhaust side), creating a suction (positive) force, which at a blade angle of -15 deg is larger than the negative thrust being generated by the fan. The fan has to go to high negative angles (-25 deg) before the exhaust flow is able to break free from the inlet walls. When this happens, the suction force on the inlet is reduced and the negative thrust on the fan predominates. This explains the unusual thrust/blade angle characteristics noted on Figures 21 and 22 and summarized in the sketch below.



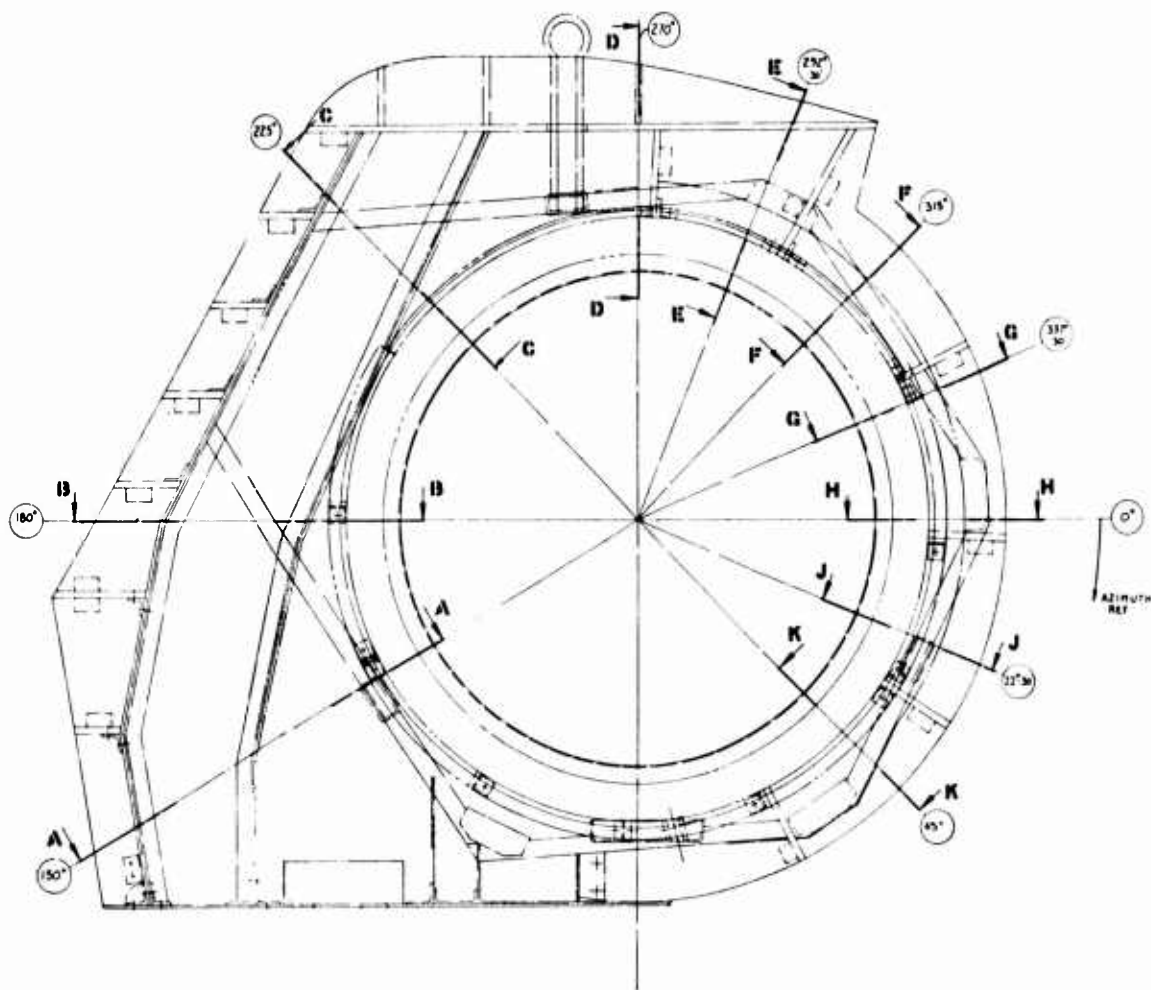


Figure 32. Schematic of Static Test Module With Pressure Tap Azimuths.

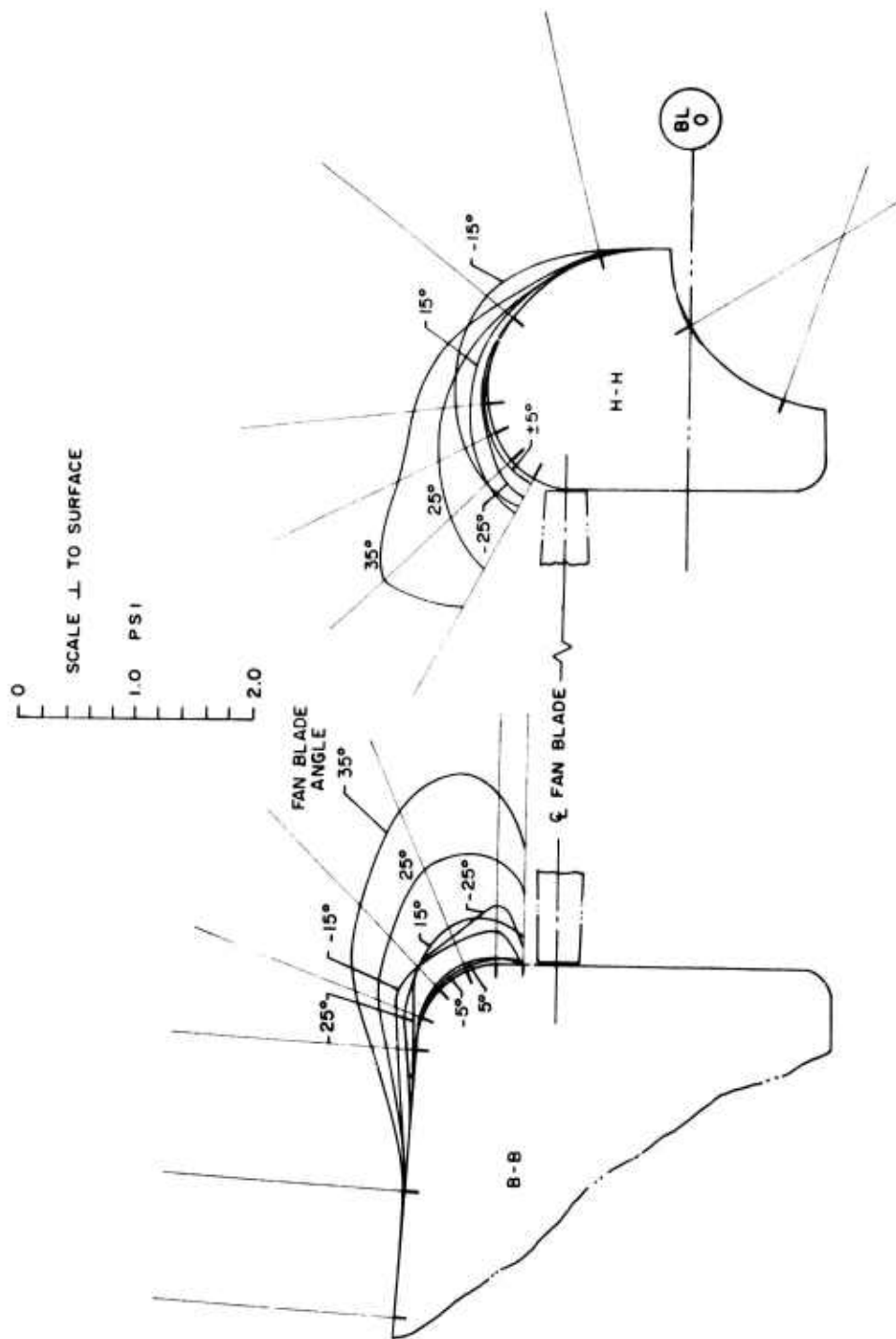


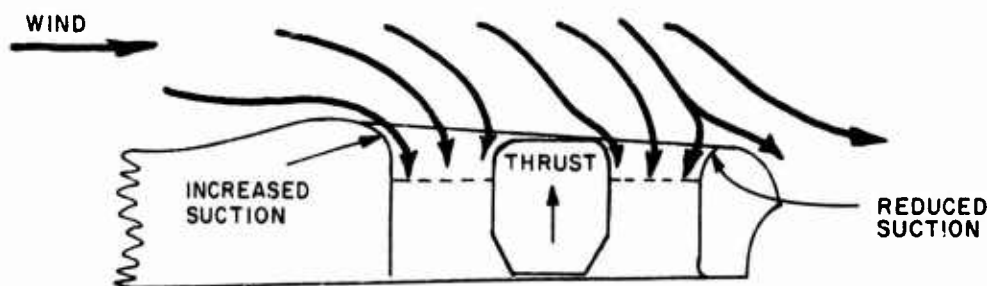
Figure 33. Variation of Fan Inlet Pressure Field With Fan Static Thrust.

The influence of the suction resulting from the reversed inlet flow shows clearly in Figure 34, which plots the component of the inlet pressure contributing to the thrust. The area under the curves represents the local induced thrust. As blade pitch is reduced, the suction peak falls and the induced thrust is reduced. At 5 deg blade angle, the inlet force is close to zero. For lower blade angles, the reversing flow should separate and produce little induced thrust. However, as is clear from the figure, it remains attached, but with the flow reversed, producing a significant amount of thrust until the flow breaks down somewhere between -15 deg and -25 deg. This confirms the qualitative observations made with tufts and smoke during the whirl test.

As would be expected, where the fan is producing positive thrust and the inlet flow is well established, the distribution of suction on the surface surrounding the fan is very symmetrical. The small differences that do exist are directly attributable to the variation in the depth of the duct at the particular section and to changes in surface curvature away from the inlet. It is interesting to note the proportion of the fan-induced suction force that is being felt by the lip (radius = 0.10 fan diameter) and the extent to which it is carried over onto the surrounding surface. An integration of the induced contribution at 25 deg blade angle on Figure 34 shows that of the total of 1750 pounds being measured by the test stand load cell, 846 pounds, or 48.5%, was the result of the suction on the surface surrounding the fan. Of the 846 pounds of induced thrust, 610 pounds was produced on the active portion of the inlet and would have been picked up by the three fan load cells. This means that, based on the measured pressure data, 1514 pounds of the total of 1750 pounds thrust indicated by the test stand instrumentation would have been measured by the three fan load cells.

Simulated Low-Speed Flight

The powerful effects of wind on the inlet flow field at positive fan thrust can be seen in the comparison of the data taken with the wind at 0 deg and 180 deg azimuth, equivalent to forward and rearward flight at approximately 35 knots, presented in Figure 35. As the wind is applied, the suction experienced by that segment of the inlet acting as the leading edge increases while the trailing edge suction decreases. This is consistent with the forces required to change the direction of the external flow streamlines and turn the airstream into the duct, as shown in the sketch below.



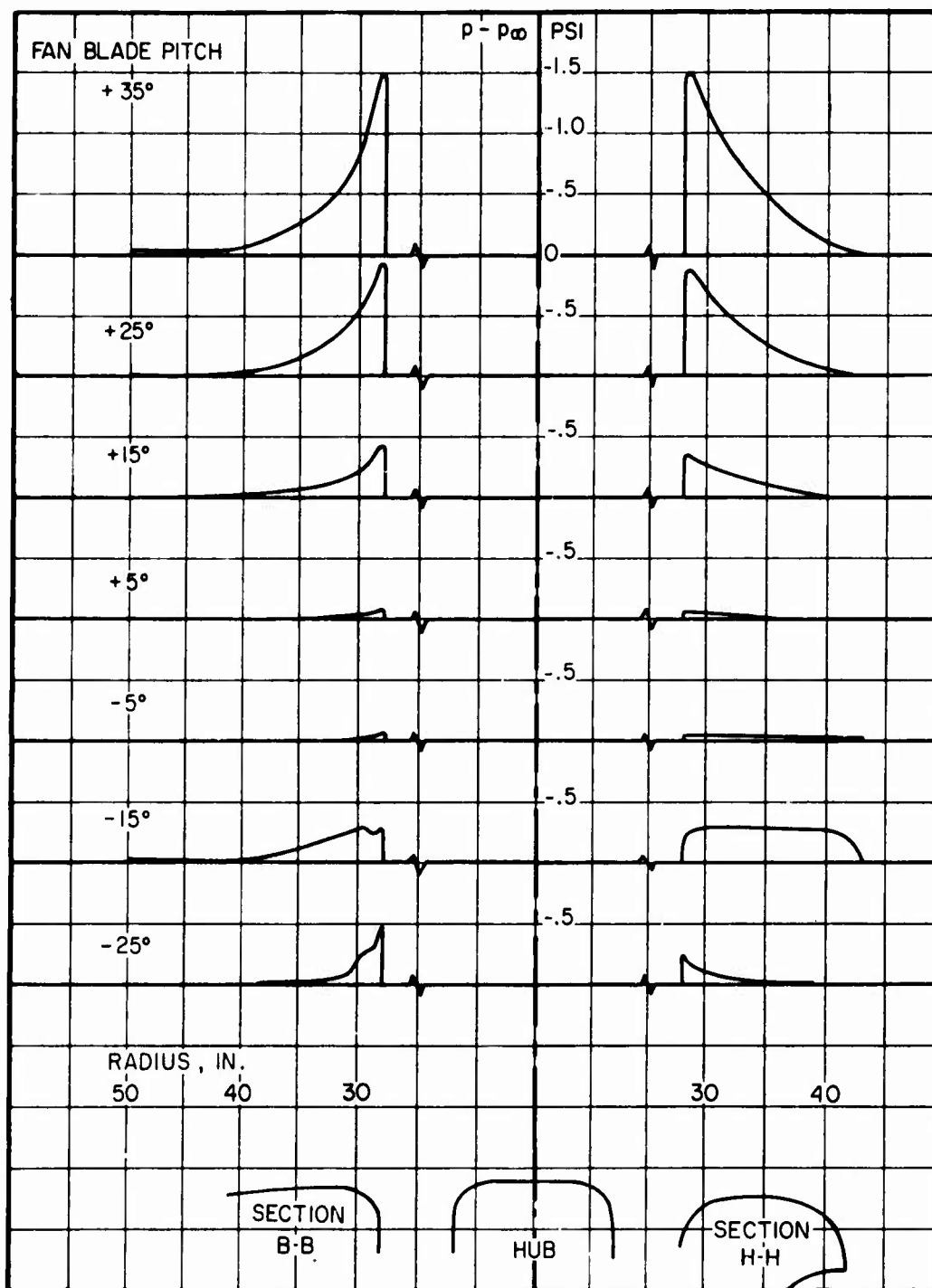


Figure 34. Variation of Thrust Component of Inlet Lip Section With Changing Blade Angle; Wind Velocity = 0.

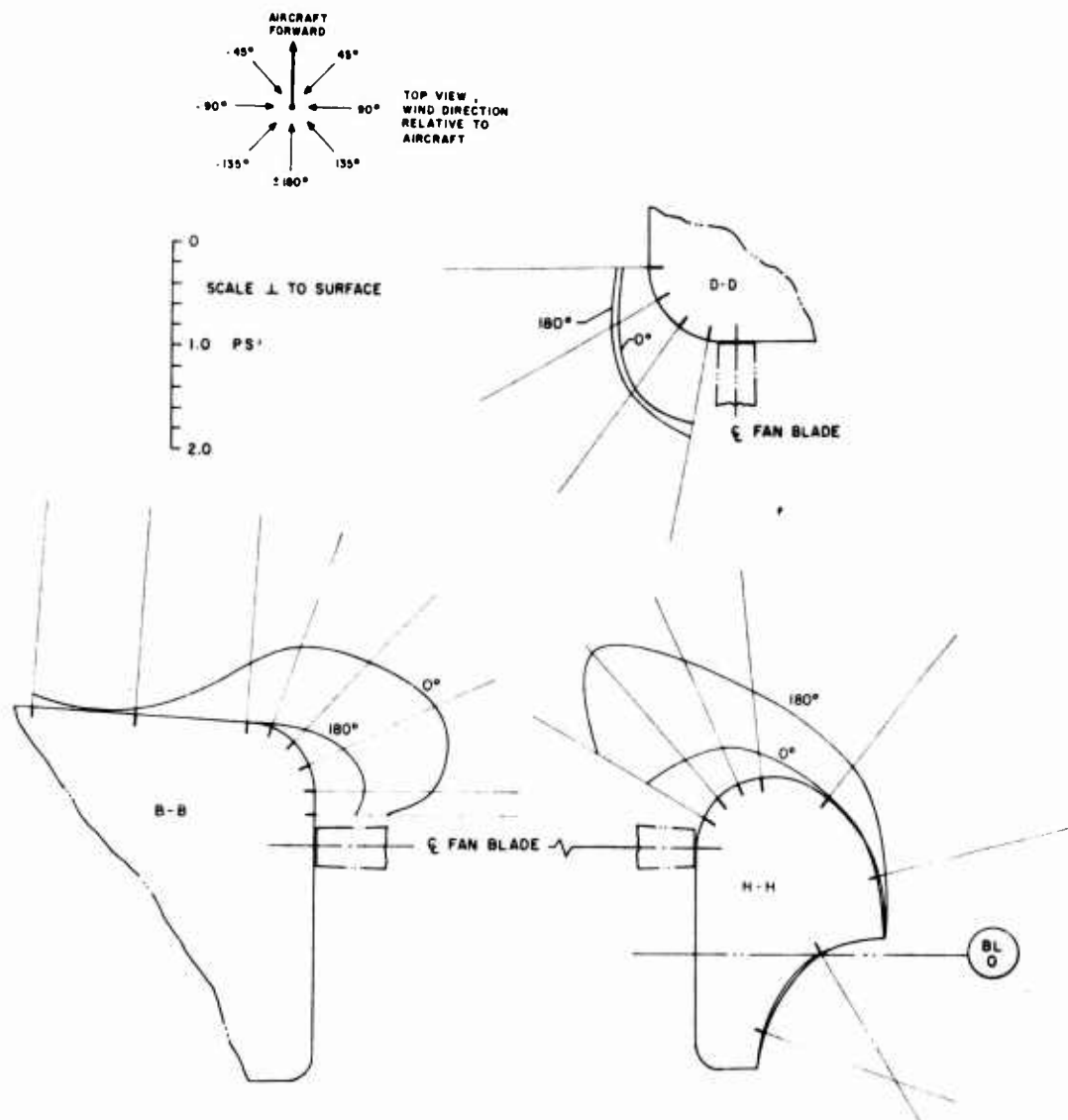


Figure 35. Variation of Fan Inlet Pressure Field, Simulated Forward and Rearward Flight, Positive Fan Thrust, Blade Angle = 25 deg, Wind Velocity = 35 Knots.

For the sections at 90 deg to the stream directions, section DD in Figure 32, the suction profiles are relatively unchanged in going from forward to rearward flight, and they compare well with the profiles noted at the station for the same total thrust condition, no winds. The data have been reported in terms of the thrust component for a range of relative headings in Figure 36, and the movement of the induced thrust toward the leading edge of the inlet is especially clear, as the relative wind moves from the trailing edge through a right cross wind toward the leading edge.

The major significance of the shift in suction toward the front of the inlet is that it is an indication of the tendency of the center of the lift of the system to move forward as speed increases. Placing the fan to the rear of the vertical surface, as has been done in the S-67 fan-in-fin aircraft application, minimizes the undesirable effects of this shift and takes maximum advantage of the extra induced lift forward. Obviously, if the fan were in the front of the surface, the area aft of the fan would experience a reduction in lift as speed increased. This is the lift droop noted in several fan-in-wing tunnel studies (Reference 4).

With the fan producing positive thrust, the inlet pressures appear relatively insensitive to small changes in wind direction. Figure 37 presents the effect of yaw angles up to 20 deg on the measured pressures. Apart from a slight increase in the height of the leading edge suction peak, the rest of the data fall within the expected level of scatter.

As would be expected, the inlet pressures show considerable variation when the test module is used to simulate quartering flight at 35 knots and, as was noted above and in Figure 38, the leading edge of the inlet experiences the highest suction. In simulated forward flight, with nose left 45 deg, the peak suction generated are greater than with 45 deg nose right. However, the change in level occurs well down into the duct, being associated with the turning of the flow. When the two cases are plotted in the side force coordinates, Figure 36, they are seen to result in almost equal thrust. The rearward flight 45 deg nose left inlet pressures are almost a mirror image of the forward flight profiles for the same yaw angle, with the minor differences in pressure distribution resulting from the changes in surrounding surface contour. With the fan at -25 deg blade angle, the inlet (now the exhaust) pressure distributions are much less sensitive to module (aircraft) attitude relative to the wind. Figures 39 and 40 summarize the reverse flow data. When the back flow in the duct is fully established at high negative blade angles, the trends of surface pressure with relative heading noted for the positive thrust direction are reversed. The increase in suction, although at a much lower level because of the largely separated exhaust flow, are now found in the downstream edge of the duct, as shown in the sketch on the following text page.

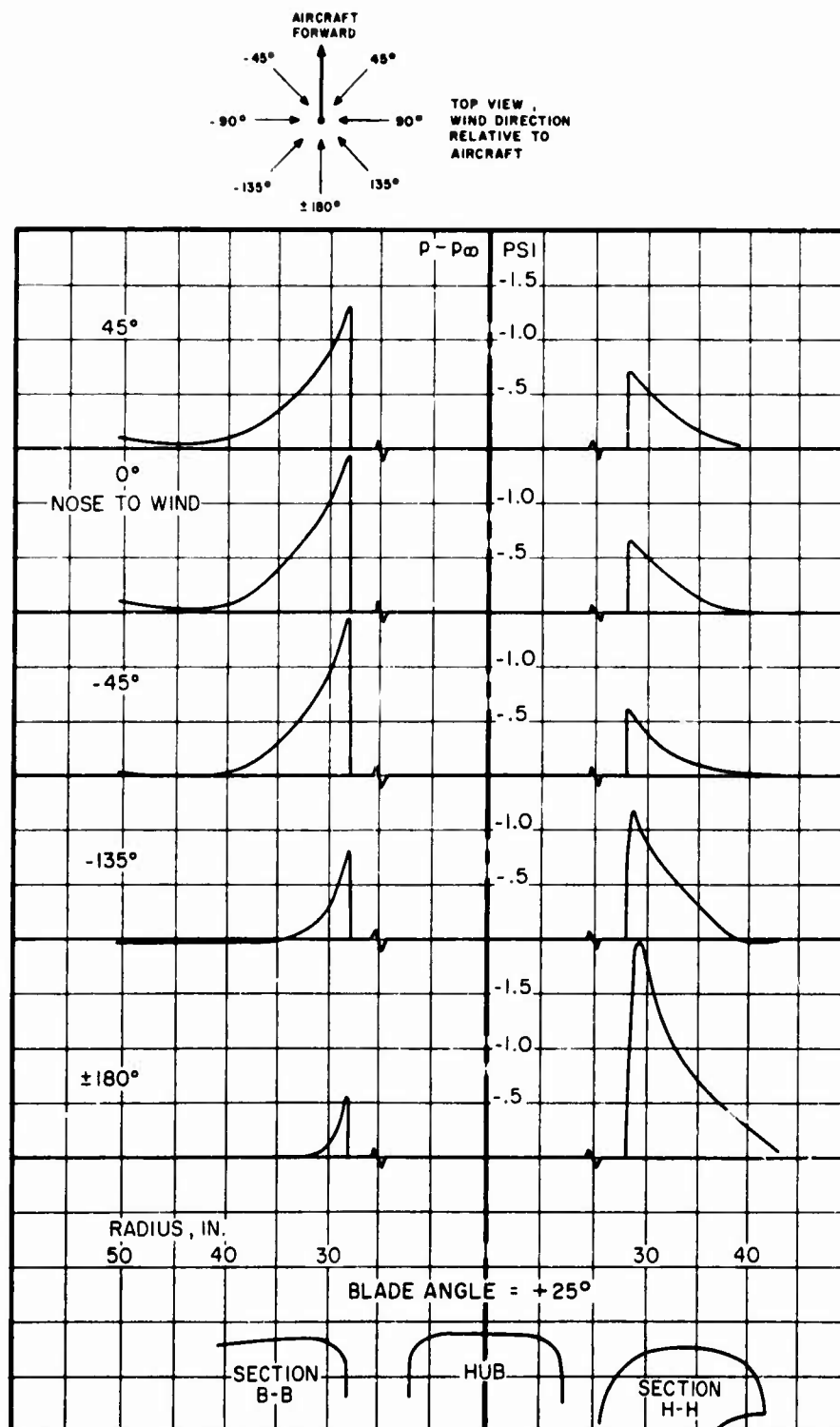


Figure 36. Variation of Components of Inlet Lip Suction With Simulated Aircraft Heading at High Thrust; Wind Velocity = 35 Knots.

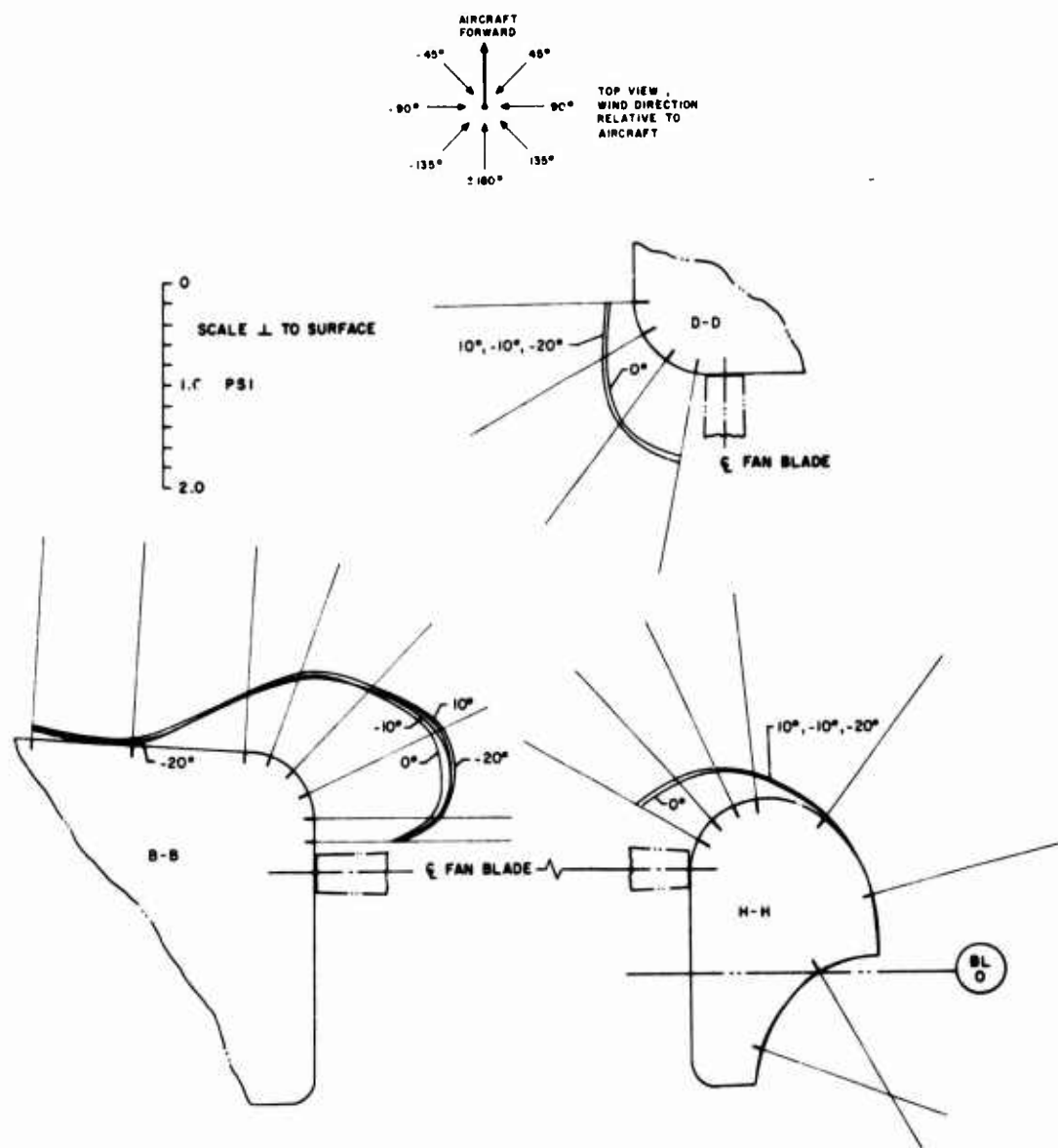


Figure 37. Variation of Fan Inlet Pressure Field, Simulated Sideslip Conditions, Positive Fan Thrust, Blade Angle = 25 deg, Wind Velocity = 35 Knots.

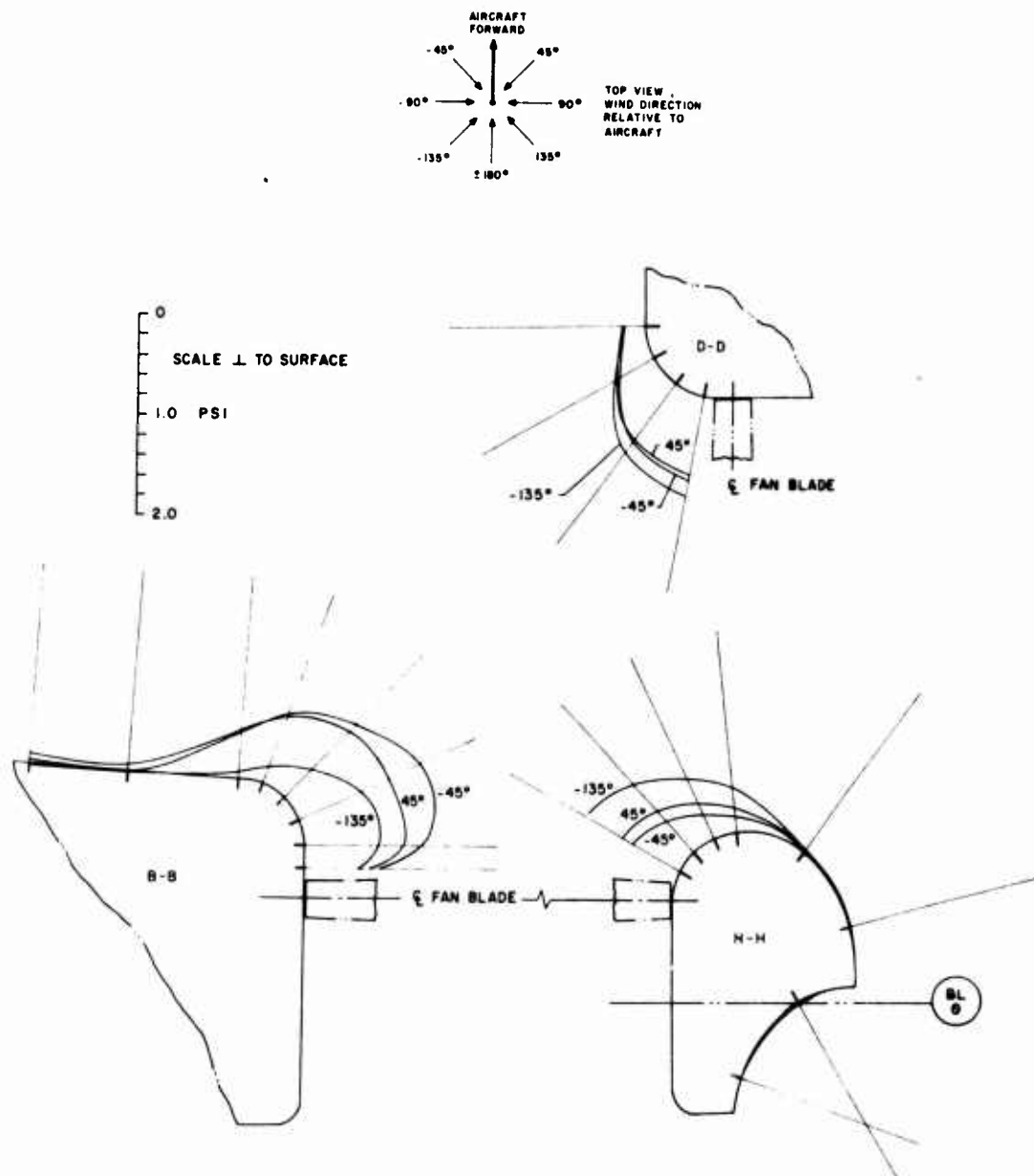


Figure 38. Variation of Fan Inlet Pressure Field, Simulated Quartering Flight at 35 Knots, Positive Fan Thrust, Blade Angle = 25 deg.

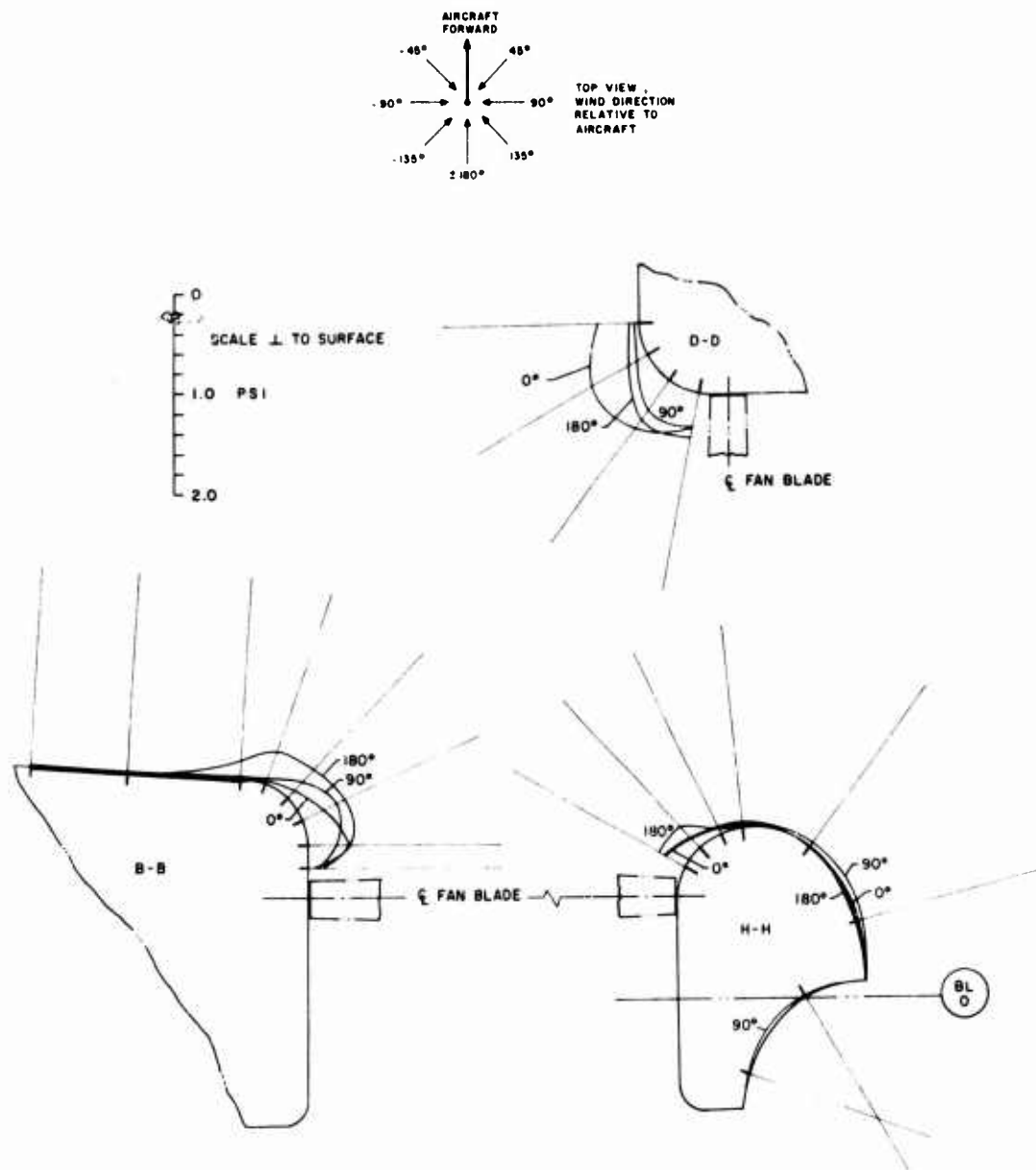


Figure 39. Variation of Fan Inlet Pressure Field, Simulated Forward, Rearward, and Sideward Flight at 35 Knots, Negative Fan Thrust, Blade Angle = -25 deg.

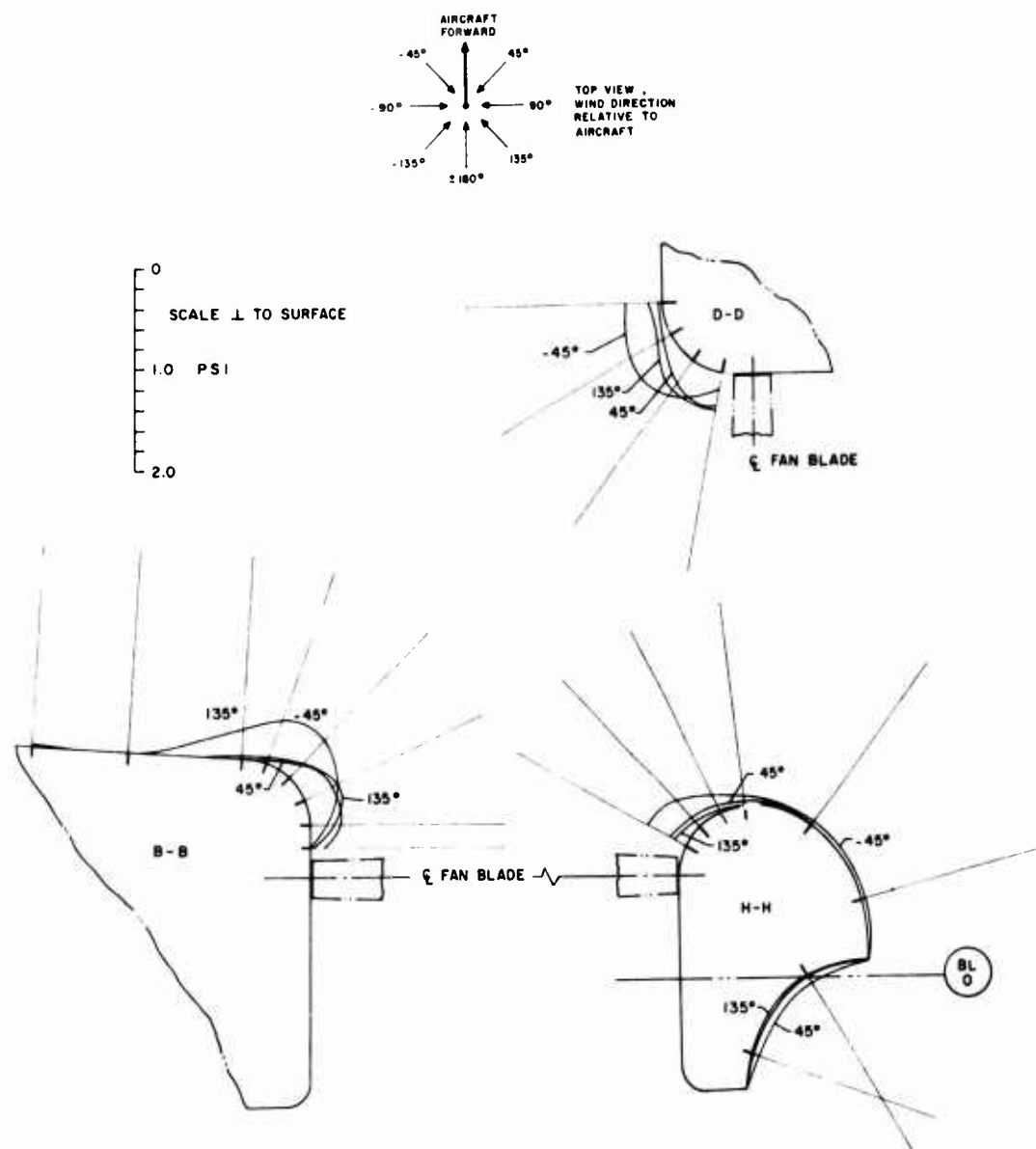
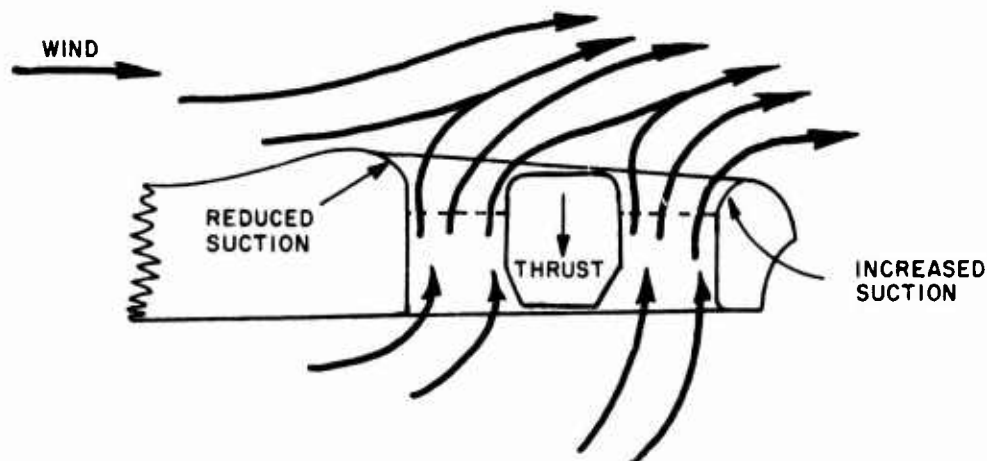


Figure 40. Variation of Fan Inlet Pressure Field, Simulated Sideslip Conditions, Negative Fan Thrust, Blade Angle = -25° , Wind Velocity = 35 Knots.



Pressures in the cusp region are uniformly low for flight at any of the conditions examined with either positive or negative fan thrust.

Correlation Between Observed and Predicted Behavior

As shown in the discussion of static performance above, almost 50% of the static thrust of the fan-in-fin comes from induced thrust on the inlet and surrounding surfaces. To achieve this result, considerable effort was devoted during the design phase of the program to the development and application of analytical tools to shape the duct for maximum effect. The data measured during the tests correlates well with the predicted inlet surface pressures; they confirm the accuracy of the design methodology and support its use in the design of inlets for ducted fan devices in the future. Figure 41 compares measured and predicted inlet pressures for two levels of fan static thrust. Figure 42 shows the level of correlation achieved in left sideward flight and forward flight at 35 knots. Agreement is generally good, the poorest correlation being with the left sideward flight condition. Here, the actual test setup with a limited diameter jet blowing onto the fan exhaust is far removed from the idealized model used in the analysis. It is interesting to note, however, that the disparity between predicted and measured pressures is in a direction that suggests that the blower jet is operating at somewhat less than 35 knots. This would be expected since, to model left sideward flight, the fan is exhausting its high energy jet directly into the blower output. The more significant static thrust and forward flight cases are well modeled, and correlation is good. Although no direct boundary layer data were taken during the whirl testing, the pressure data showed that attached flow was maintained on the inlet for all values of positive thrust. This had been a major design goal. Since the analysis is based on momentum exchange (mass flow) for a given thrust the blade angle as such does not appear in the prediction.

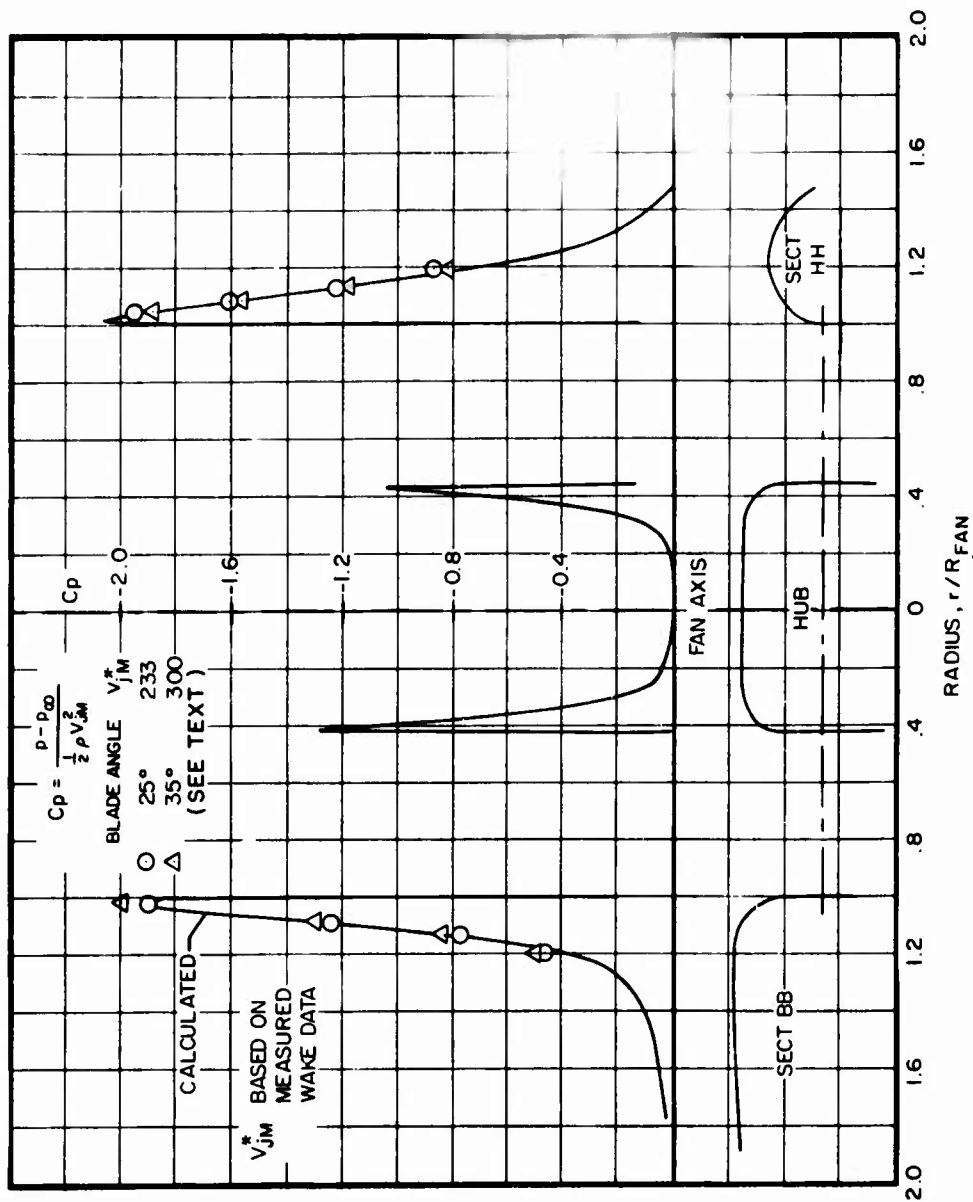


Figure 4.1. Comparison of Predicted and Measured Inlet Pressures, Static Thrust.

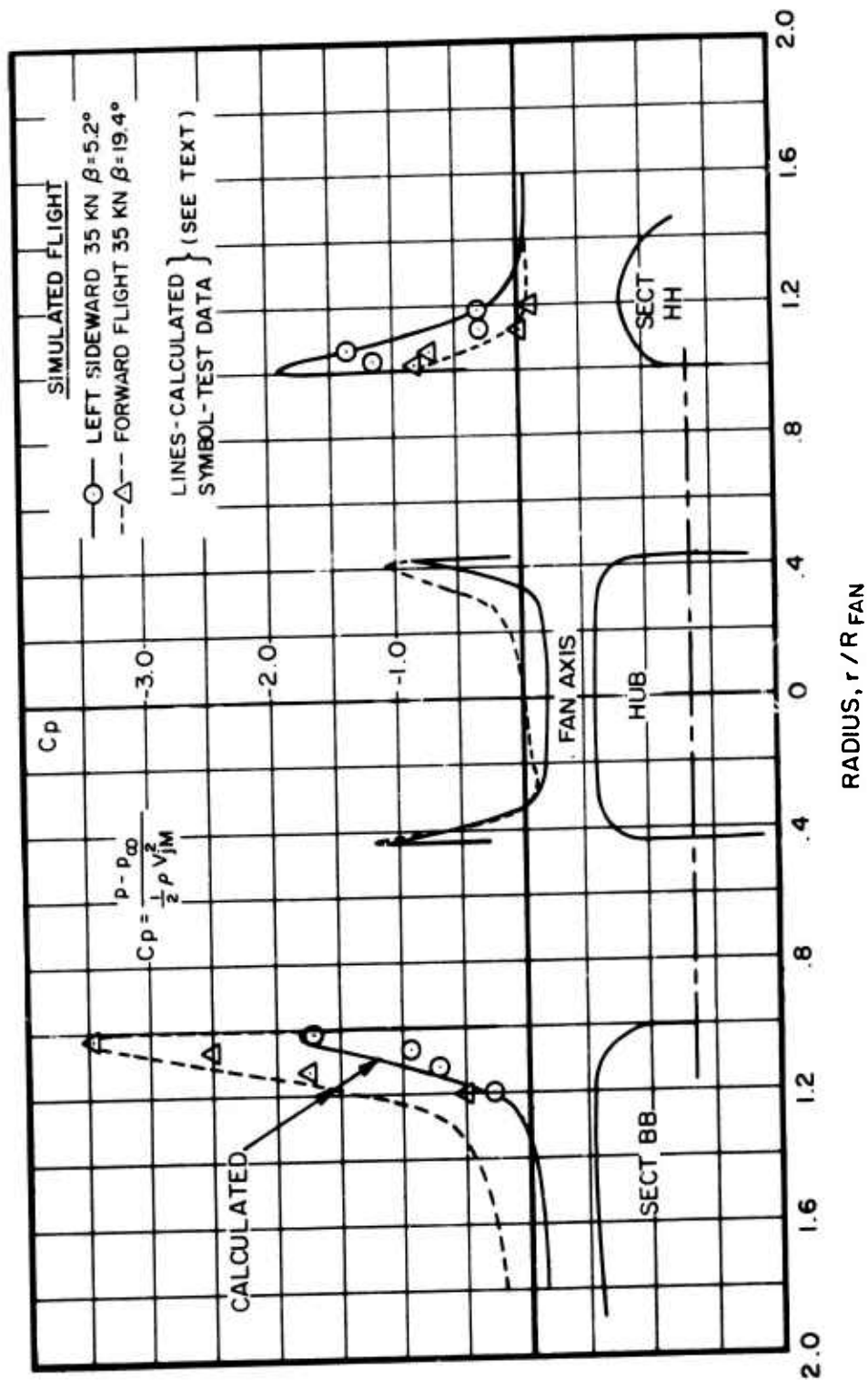


Figure 42. Comparison of Predicted and Measured Inlet Pressures; Airspeed = 35 Knots.

Consequently the experimental data in Figures 41 and 42 have been non-dimensionalised by the measured mean exit velocity to reduce them to the same base and allow comparison with the prediction.

The thrust level for any shroud design is set by specifying a value of fan mass flow. This defines a mean velocity in the plane of the fan. To check the validity of the mean flow assumptions in the analysis and to provide a data base for subsequent refinement of the fan design, the velocity profiles in the wake of the fan were measured. The wake velocity profiles for two levels of fan thrust are shown in Figure 43. They correspond to fan blade angles of 26 and 32 deg. The lower setting is close to the fan design point and, apart from some root and tip effects, the velocity profile is fairly uniform. At the high blade angle, there are indications of root stall, and much more lift is attributable to the outboard sections of the fan. Mean velocity trends from the wake survey data were used as the basis for the surface pressure correlation shown in Figures 41 and 42 and discussed above.

High-Speed Flight - Tuft Studies

In addition to satisfying the requirement to operate efficiently at low speed and high thrust, the inlet was designed to maintain attached, if not uniform, flow at high speed and low fan thrust. The aircraft was not pressure tapped, but it was possible to verify the achievement of the forward flight design goals from the tuft studies. Figure 44 is a photograph of the fan inlet for a 140 KIAS, trim condition. This condition was chosen, because it is close to the minimum fan thrust point. Apart from the expected small area of separated flow on the aft facing portions of the fan rear shroud, the flow is attached everywhere. In the most critical area, just inside the leading edge of the inlet lip, the tufts are steady and well aligned, indicating stable, attached flow.

Although not directly contributing to correlation of the analytic design method, the final three tuft photographs, Figures 45, 46, and 47, are presented because they validate the rationale used in design of the exhaust side of the fan and the integration of the fan assembly, the upper and lower stabilizer, and the fuselage termination. Use of the offset vertical stabilizers, the concave fairing around the fan exhaust, and the cusped trailing edge was justified in that together they would help guide flow into the aft region, reduce the extent of separated flow, and minimize drag.

Figure 45 is a view into the cusp at 160 KIAS. The tufts indicate that the lower surface cusp flow has been led up to almost the fan centerline before it has separated. The upper surface flow comes to within 30 deg of the centerline. Tufts on the aft edge of the inlet side appear to be attached to within 15 deg of the centerline. The extent of the attached flow in the cusp is confirmed by the view of the exhaust face given in Figure 46. Here the aircraft is flying level at 140 KIAS. Tufts on the aft tail cone and on the upper rim of the exit are streaming aft and down under the influence of the main rotor wake. The tufts on the upper portion of the rim being above the rotor wake are more aft directed. The picture also indicates

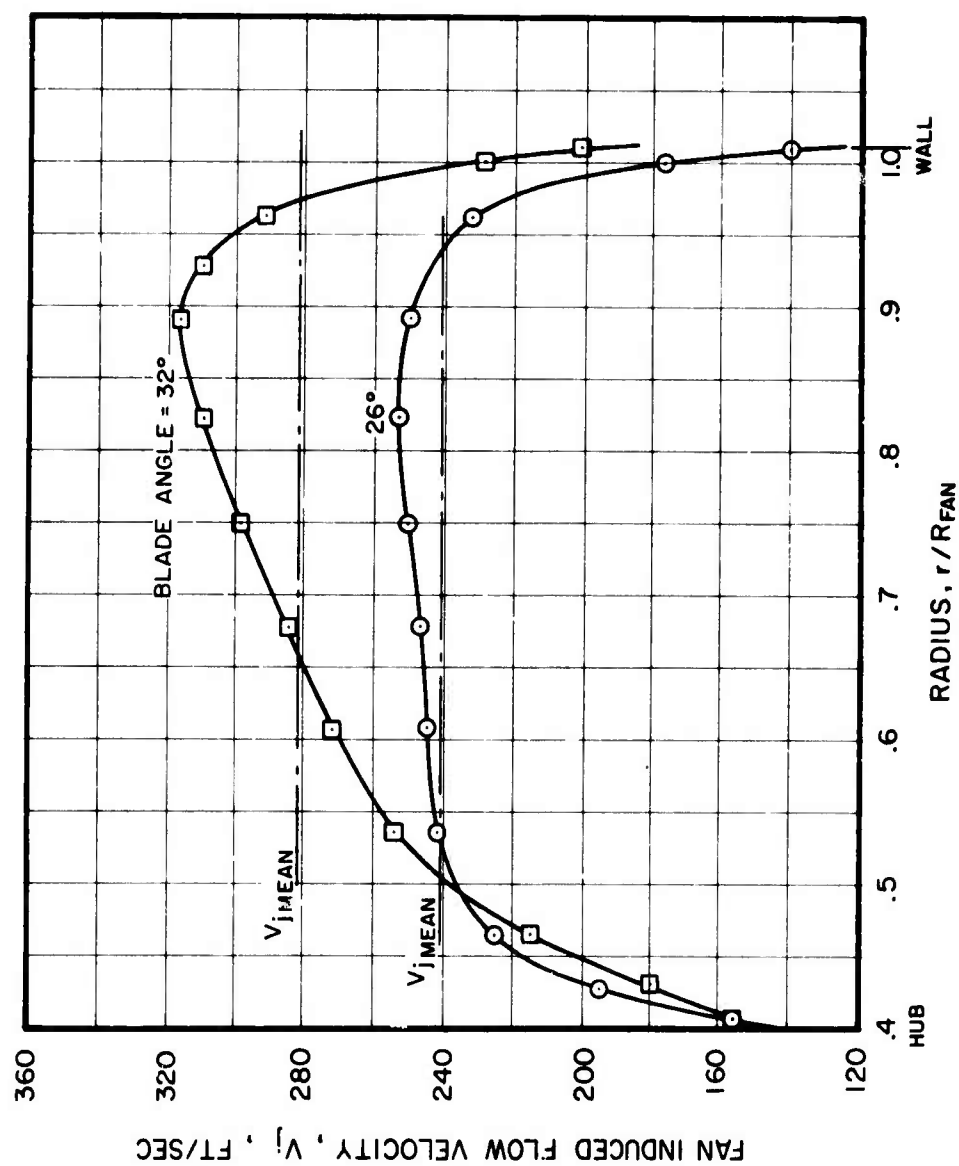


Figure 43. Typical Fan Wake Velocity Profiles.

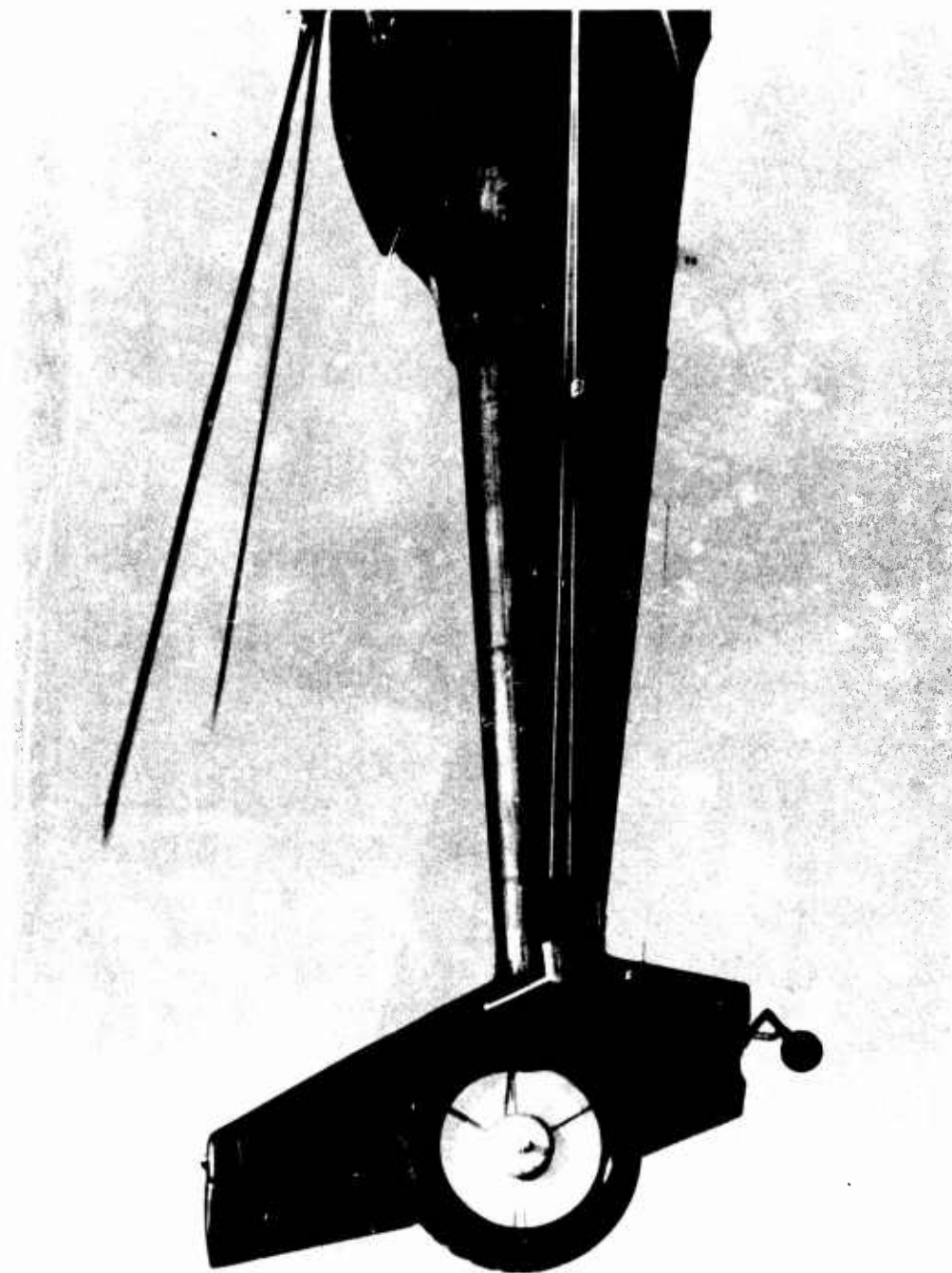


Figure 4.. Fan Inlet and Tufts at 140 KIAS.



Figure 1. Fan, pump and turbine at 1000 rpm.



Figure 46. Fan Exhaust and Tufts at 140 KIAS.

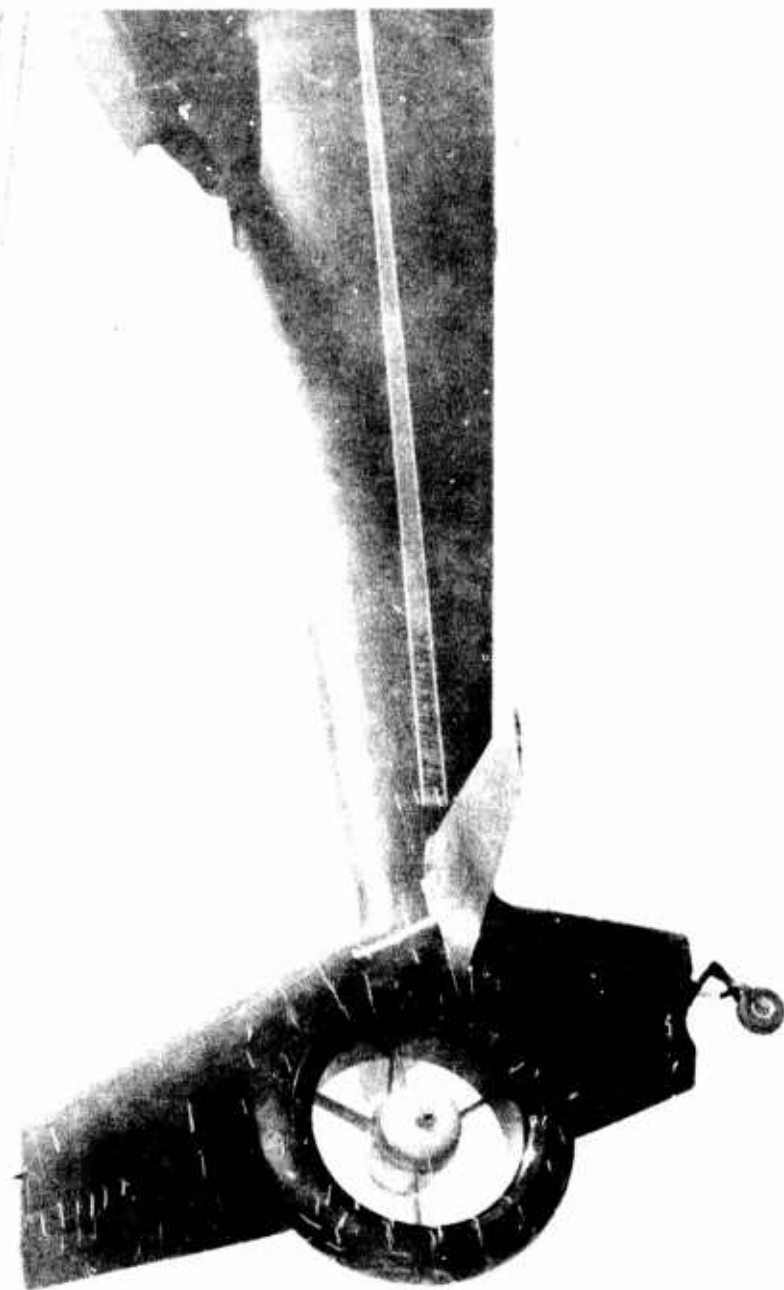


Figure 47. Fan Inlet and Tufts at 80 KIAS.

that there may be some leakage around the inboard end of the horizontal stabilizer, since a tuft on the tail just forward of the fan shroud is turned strongly down while the tuft on the stabilizer trailing edge close to the root is streaming out. The photograph of Figure 47 was taken at a lower speed, 80 KIAS, and confirms the integrity of the inlet flow field.

The tuft photographs are not conclusive evidence but they provide data that support the validity of the analysis used in the inlet design and the rationale that led to the somewhat novel fuselage termination.

S-67 FAN-IN-FIN HANDLING QUALITIES

The handling quality characteristics of the fan-in-fin, as determined by flight test, are compared with those of the tail rotor configuration. Test results are also compared with predictions and requirements of MIL-H-8501A (Reference 3) if a significant change was observed.

Time histories of aircraft rates, attitudes and control positions are presented for flight test conditions and maneuvers. Pitch, roll, and yaw rates were measured by body-oriented gyros installed at the aircraft's center of gravity. Pitch and roll attitudes were measured by gyros while yaw attitude was determined by integrating yaw rate. Longitudinal and lateral cyclic, collective stick, and yaw pedal positions were recorded by measuring the displacement of the auxiliary control servo outputs. Attitudes and control positions are expressed in absolute values for the plots while they are expressed as deviations from the initial trim position for the time histories. Aircraft altitude was maintained by reference to a radar altimeter that measured the distance between the ground and the fully extended landing gear wheels.

The relationship between the pilot's controls - main rotor collective, longitudinal and lateral cyclic, and pedals - and the outputs of the four auxiliary servos where control positions were recorded is linear, one-to-one.

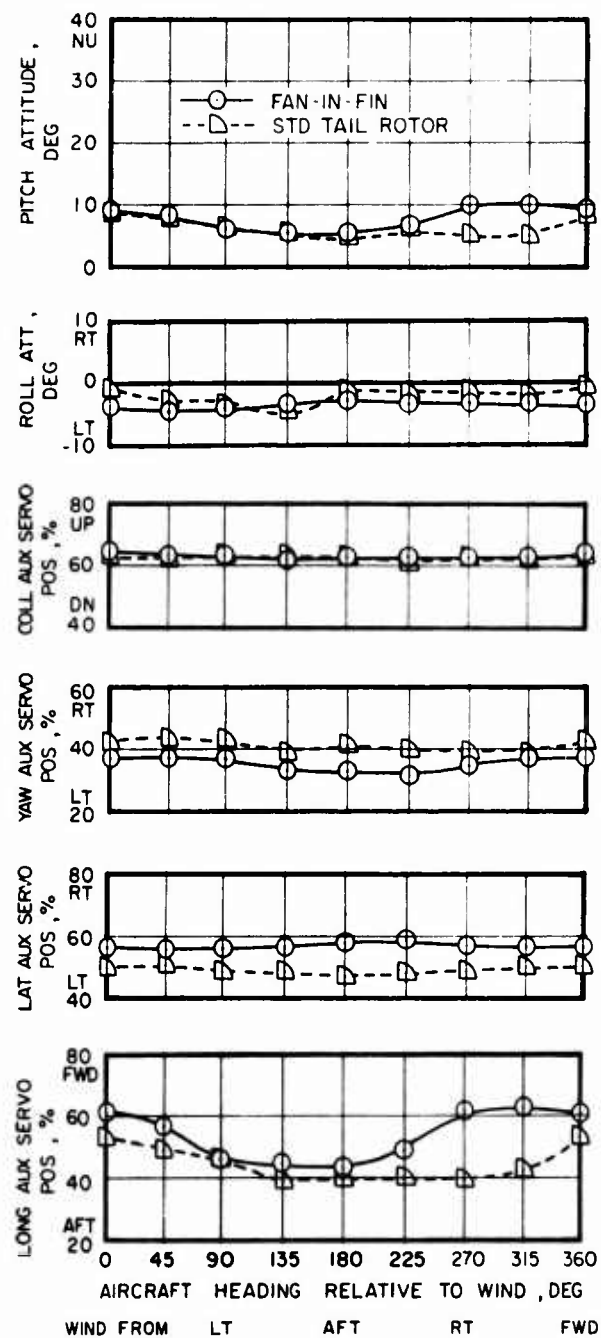
Critical Azimuth in Hover

The effects of wind velocity and direction on aircraft trim attitude and control positions are presented in Figure 48 for 20-foot wheel height hover (IGE) and in Figure 49 for 100-foot wheel height hover (OGE). The aircraft was trimmed in successive increments of 45 degree heading changes to the right in winds of 5 knots and 20 knots.

The critical azimuth test data show the effects of two configuration changes between the two aircraft. Less evident are effects caused by differences in characteristics between the fan and the tail rotor; these will be discussed subsequently in the sections on side flight and low-speed forward and rearward flight characteristics where they are better discernible.

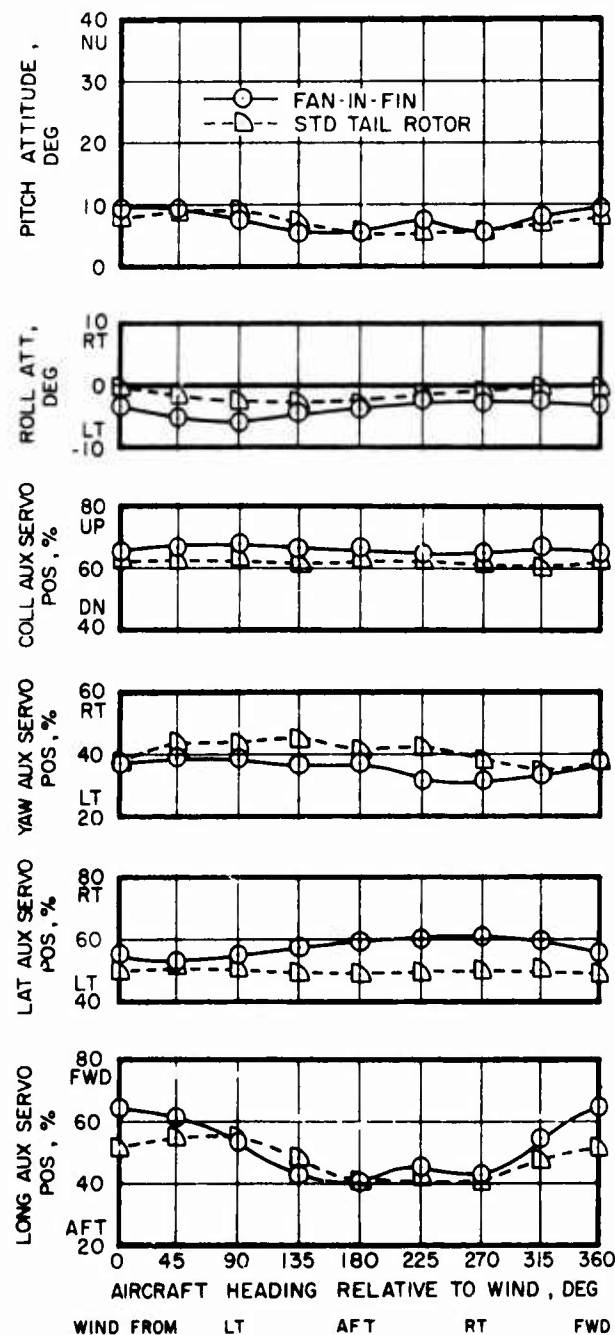
IGE and OGE, and for both wind velocities investigated, the fan-in-fin configuration hovers more left wheel low and requires more right lateral cyclic than the tail rotor configuration as a consequence of the installation of the fan at a lower waterline position.

At the low wind velocity of 5 knots, the fan-in-fin configuration shows a pronounced nose-up pitch attitude with the wind approaching from the forward and right quarter. This is a consequence of main rotor downwash impingement on the horizontal stabilator which in the fan-in-fin configuration is 11 inches further forward than in the tail rotor configuration; fan wake interaction with the stabilator is possibly a contributing factor. The difference is more obvious IGE than OGE because of the different main rotor



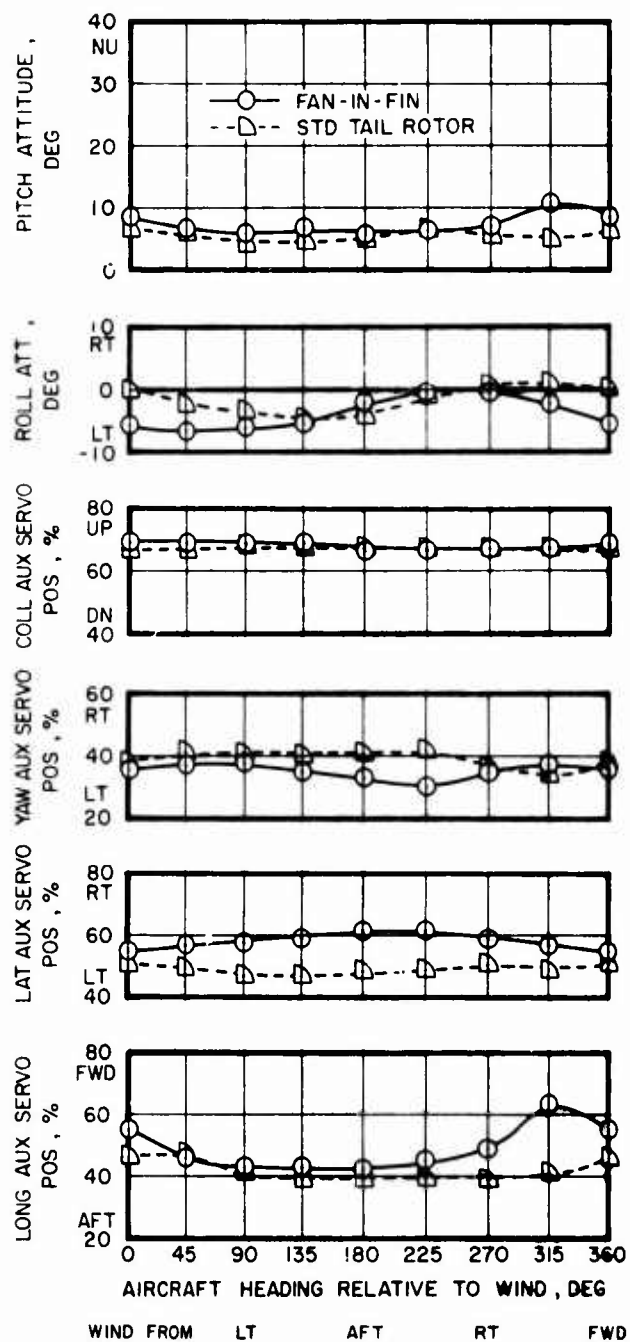
(a) 5-kn Wind

Figure 48. Comparison of Critical Azimuth in Hover, 20-ft Wheel Height.



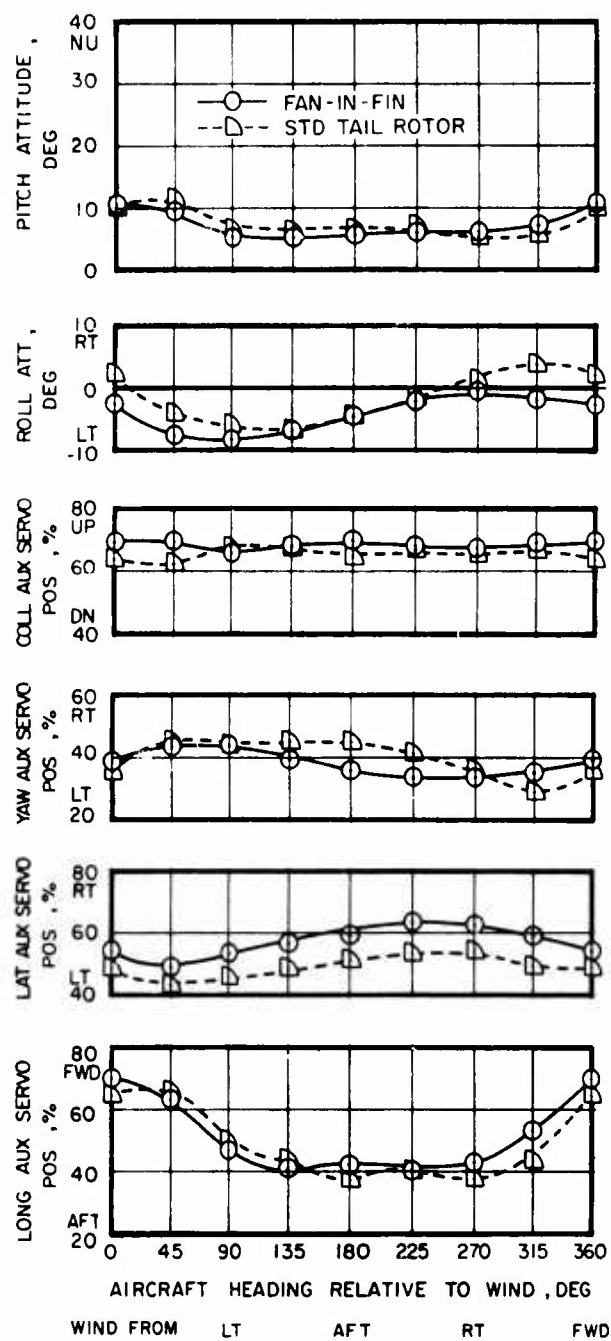
(b) 20-kn Wind

Figure 48. Concluded.



(a) 5-kn Wind

Figure 49. Comparison of Critical Azimuth in Hover, 100-ft Wheel Height.



(b) 20-kn Wind

Figure 49. Concluded.

downwash pattern. For the same aircraft heading relative to the wind but at a wind velocity of 20 knots, OGE and IGE, the main rotor downwash immerses the stabilator for both configurations and the differences in attitude and longitudinal cyclic position are greatly reduced.

These changes in pitch attitude were annoying to the pilot and could be avoided in future configurations by a more favorable location of the horizontal stabilator. In the tail rotor configuration, the effect of downwash impingement on the horizontal stabilator can be noticed but it is not of disturbing magnitude (Reference 6).

Adequate control margins remained for all conditions tested. No abrupt changes in pedal position were required to attain each trim position whether in or out of ground effect. However, to maintain a steady hover OGE with a 20-knot left crosswind, considerable pilot effort was required. This phenomenon is of particular significance in left side flight and will be discussed and explained in the section Side-Flight Characteristics.

Hovering Turns

Time histories for hover maneuverability characteristics are shown for both configurations on Figures 50 to 53. No difficulty in yaw control was encountered with either configuration; however, both configurations display aerodynamic control coupling modes.

Initiation of a left hover turn with the fan-in-fin results in a more rapid nose-down pitch moment than with the tail rotor. The correction applied by the pilot can be seen for both configurations in the change of the longitudinal auxiliary servo position. Even with this correction, the aircraft remained in a nose-low attitude throughout the turn with the fan-in-fin. This is a consequence of the increased left roll attitude in hover which results in a vertical fan thrust component that forces the nose down. In a right turn less fan thrust is required and the nose-down pitch moment is greatly reduced.

The lateral auxiliary servo position (pilot lateral cyclic position) is to the right of the trim position for a right turn with the fan-in-fin, and after the initial entry it is to the left of the trim position with the tail rotor. In a left turn, the servo position is to the left of trim for both configurations. This clearly shows that the aircraft wants to roll and translate in a direction away from the turn. With the tail rotor, the aircraft wants to roll and translate to the left for turns in either direction. This phenomenon is a consequence of the difference in vertical position of the fan and tail rotor.

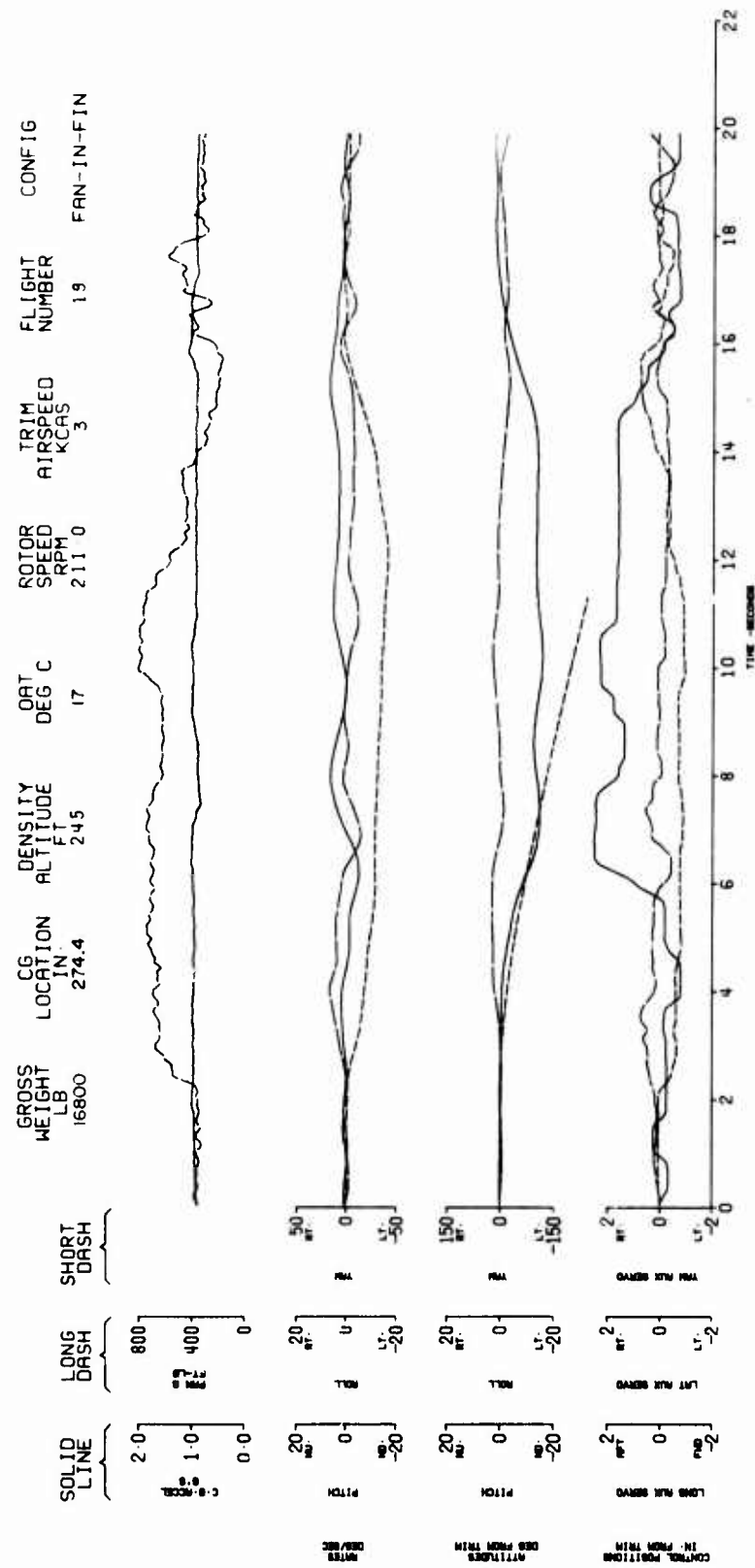


Figure 50. S-67 Fan-in-Fin, Left Hover Turn.

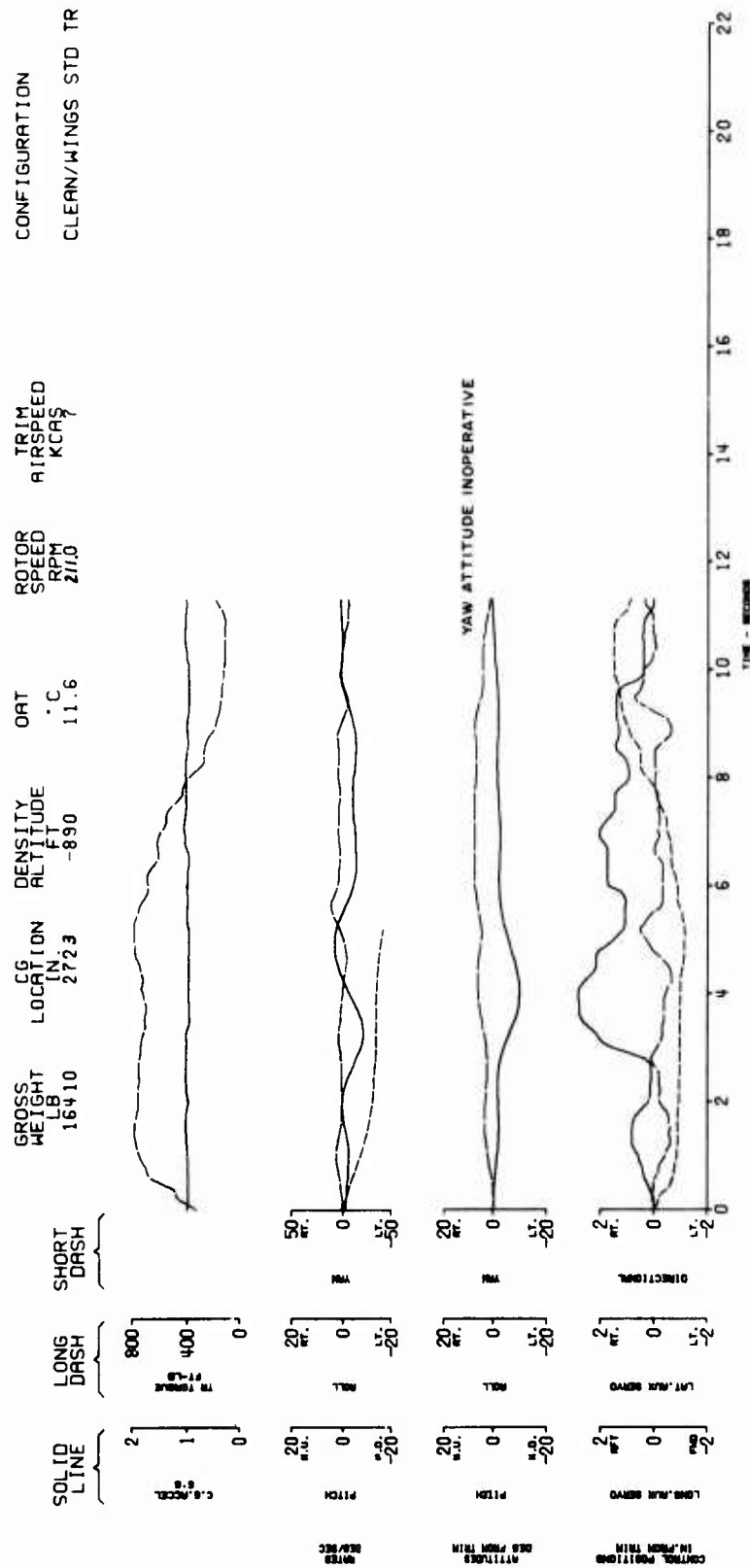


Figure 51. S-67 Tail Rotor, Left Hover Turn.

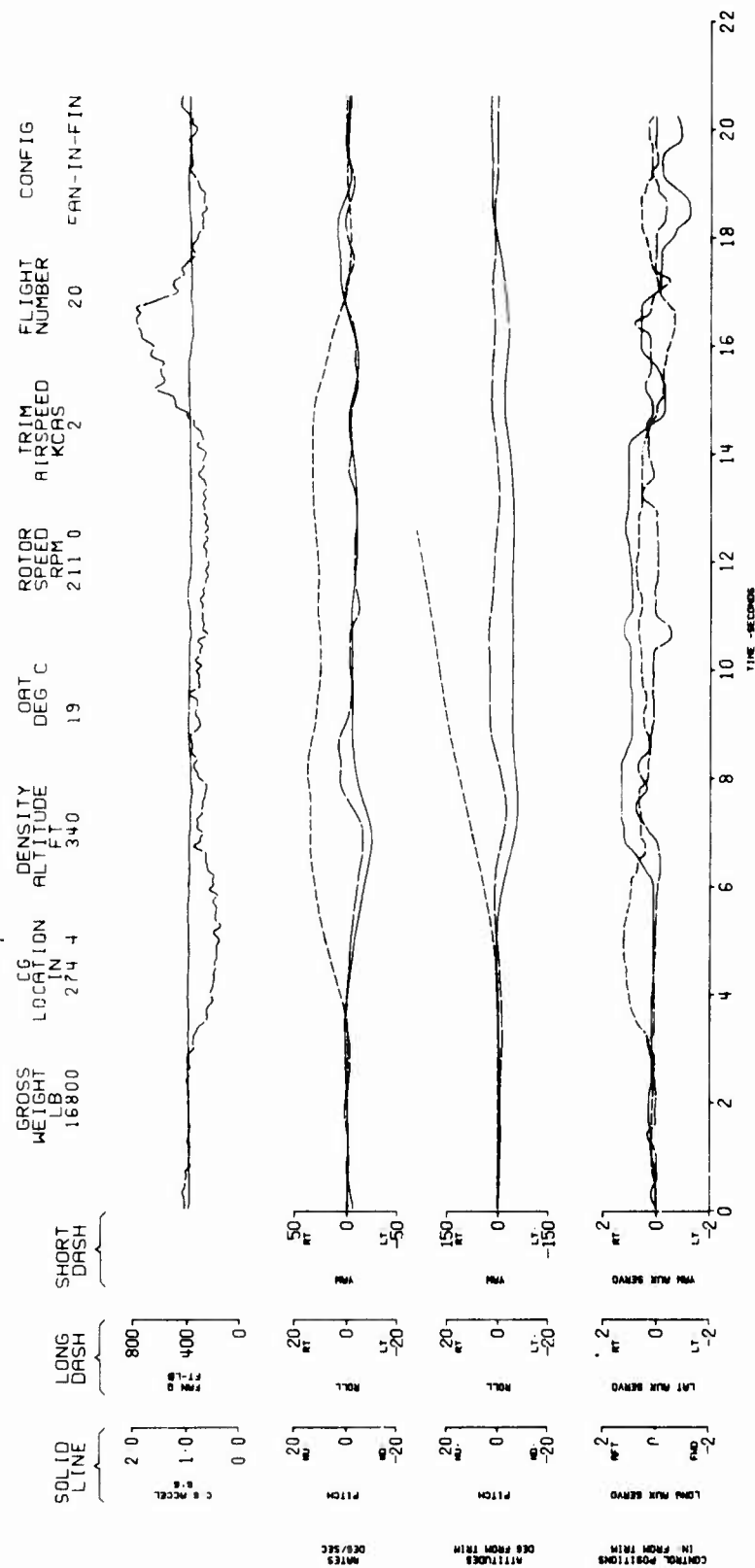


Figure 52. S-67 Fan-in-Fin, Right Hover Turn.

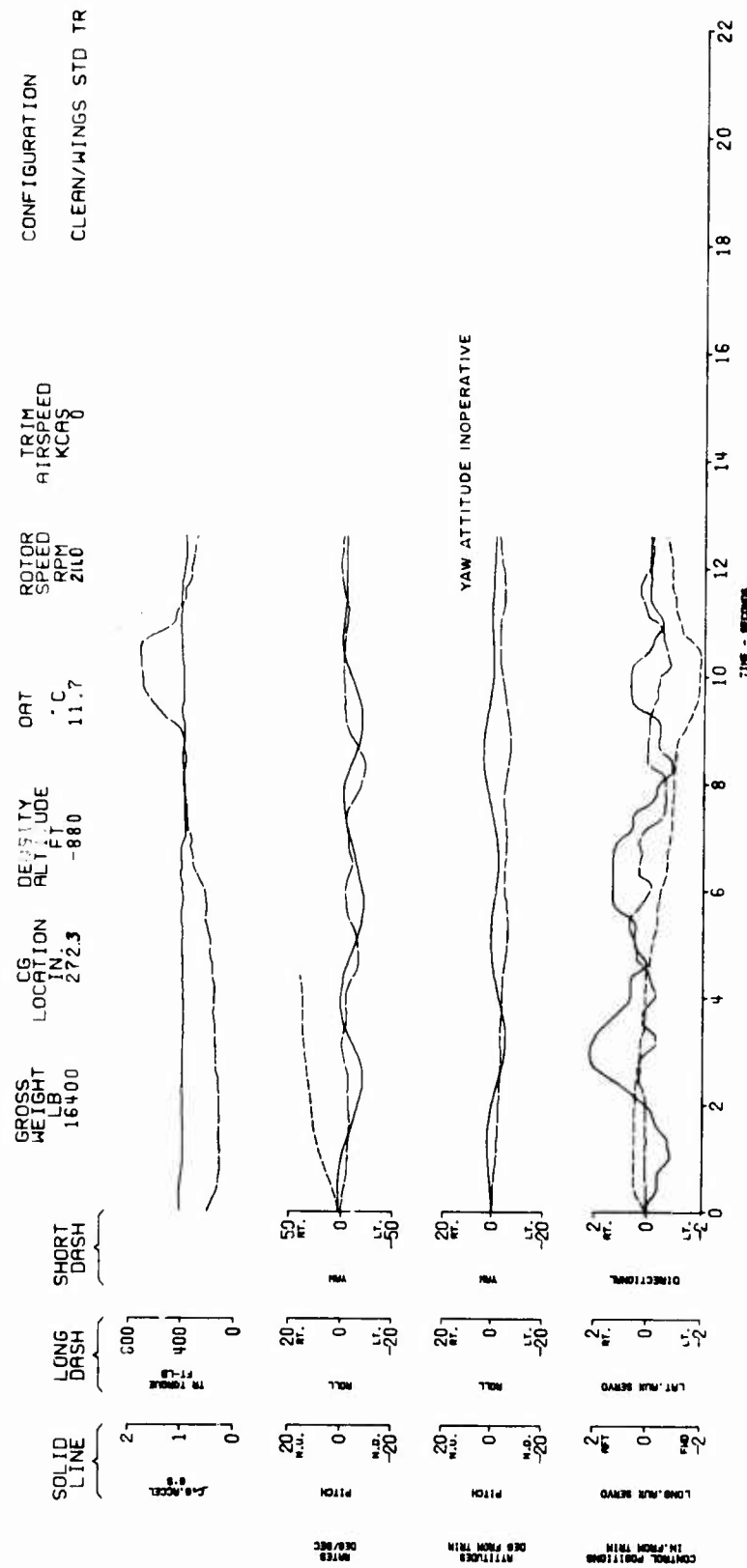
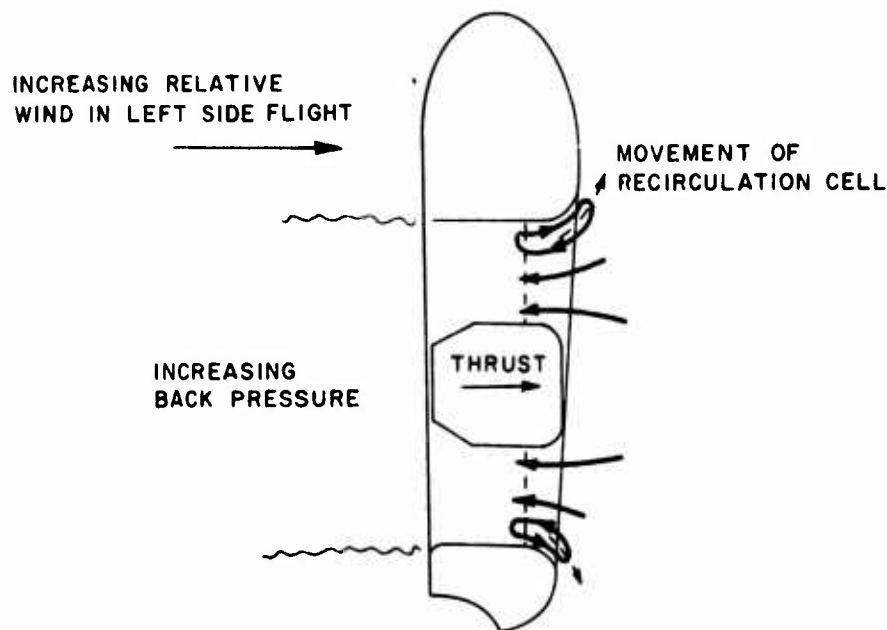


Figure 53. S-67 Tail Rotor, Right Hover Turn.

Side-Flight Characteristics

Left and right sideward flight characteristics are shown in Figure 54 for IGE and in Figure 55 for OGE conditions. The yaw auxiliary servo (pedal) position for IGE and OGE conditions show that considerably less right pedal is required for the fan-in-fin than for the tail rotor in left side flight. This difference is significant. The tail rotor configuration behaves as expected and the pedal position reflects the fact that the aerodynamic drag of the fin decreased tail rotor thrust requirements to below antitorque thrust levels in left side flight. This also occurs for the fan configuration but with increasing left side flight speed, the fan blade tips approach and then assume negative blade angles. This results in fan flow recirculation as indicated in the sketch below. With further



increases in left side-flight speed, the "effective" back pressure is increased and the recirculation region will tend to move out over the inlet. This results in progressive reduction in combined inlet and fan thrust. However, also with increases in left side-flight speed, the required total thrust decreases. The result is a nearly flat pedal position characteristic in the left side-flight range. The fan flow field in this flight condition is apparently not very stable and requires considerable pilot effort as was mentioned under critical azimuth in hover and also in Reference 5.

In IGE at 35 knots right side-flight speed, 26% pedal margin remained for the fan-in-fin, 12% more than for the tail rotor. At 35 knots left side-flight speed, 57% pedal margin remained for the fan-in-fin, 32% more than for the tail rotor. These results indicate a substantial increase in side-flight capability for this fan-in-fin configuration over the tail rotor configuration.

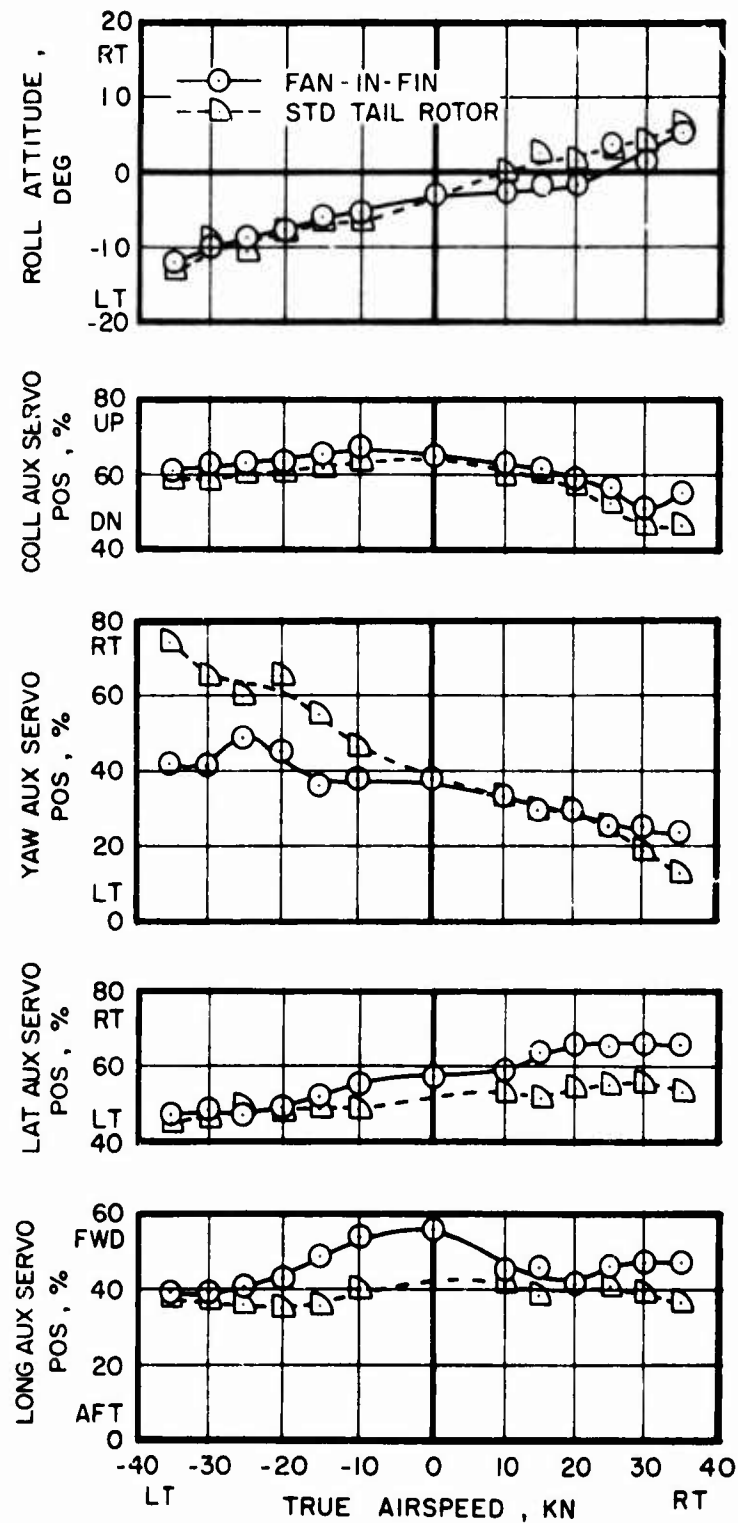


Figure 54. Comparison of Side-Flight Characteristics, 20-ft Wheel Height.

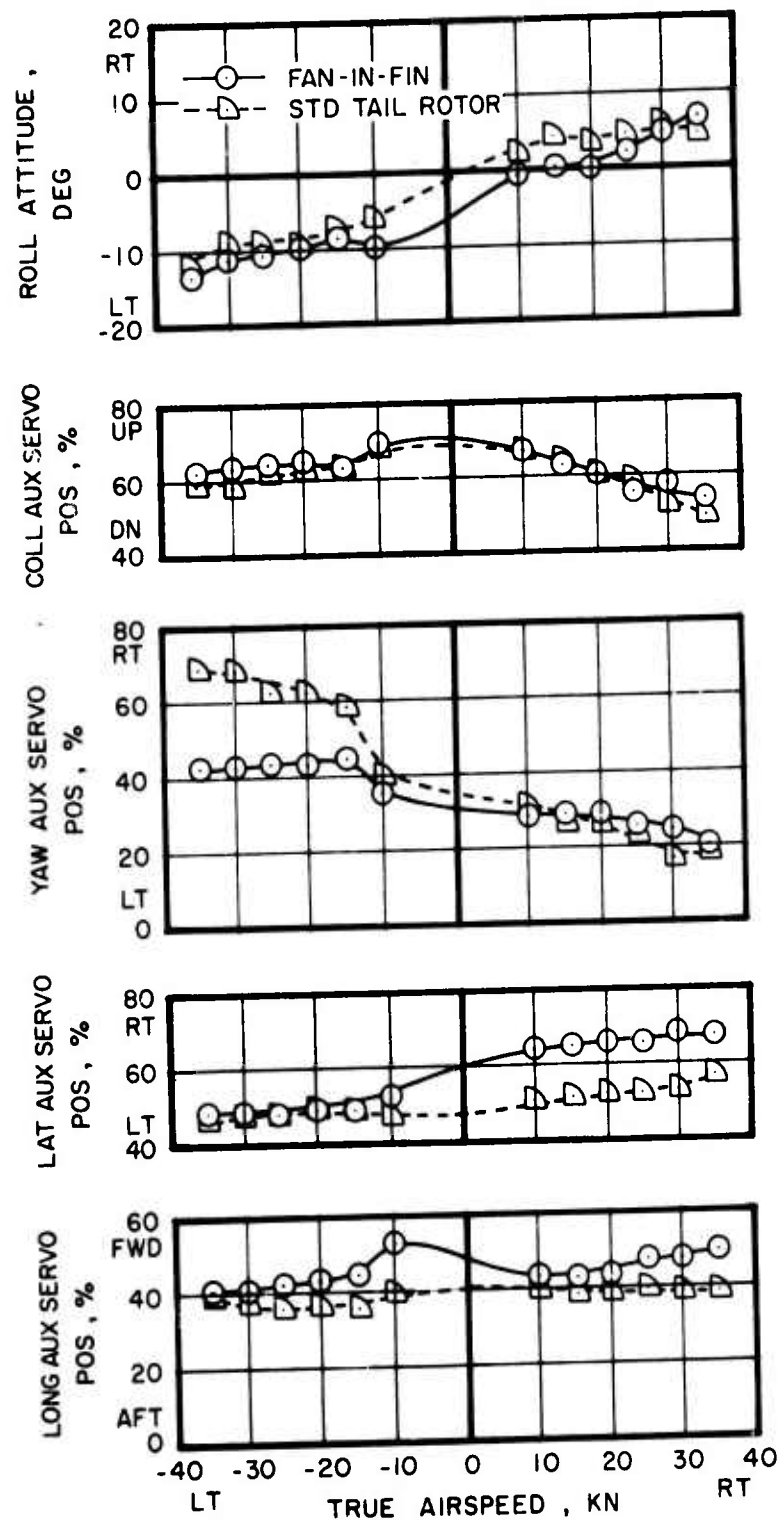


Figure 55. Comparison of Side-Flight Characteristics, 100-ft Wheel Height.

The variation of main rotor collective is normal and as expected, indicating more total power required when flying to the left than to the right. The lateral cyclic control positions in left side flight are quite similar for both configurations. The effect of the fan installation at a lower waterline position becomes evident in right side flight where more right cyclic must be applied.

The longitudinal cyclic position for the fan-in-fin configuration shows the application of forward cyclic required to compensate for the impingement of the main rotor downwash on the horizontal stabilator in the fan-in-fin configuration. As the aircraft moves either to the left or right from hover and the main rotor downwash is redirected, both forward cyclic position and nose-up attitude are reduced. Little change in either cyclic position or attitude is required for side flight with the tail rotor configuration.

Low-Speed Rearward and Forward Flight Characteristics

The low-speed rearward and forward flight trim characteristics are shown in Figure 56 for IGE and Figure 57 for OGE. Rearward flight control positions are as expected for both configurations. For the fan-in-fin configuration, servo (pedal) position remains essentially constant as speed increases to 30 knots rearward. This is due to the ineffectiveness of the vertical fin to produce a side force and is a manifestation of the lift droop effect discussed in the section entitled Fan Inlet Behavior/Simulated Low-Speed Flight and in Reference 4. The lift droop is a translational interference effect experienced by a fan-in-fin or fan-in-wing configuration aft of the fan. In rearward flight, the fan is now in the leading edge of the vertical surface and, as speed is increased, the area of the fin downstream of the fan experiences a reduction in induced thrust. To maintain the anti-torque force, the fan contribution must be increased. The pilot reported that rearward flight with the fan required less pedal effort to maintain a steady heading. Control margins for both configurations remain adequate, both to maintain flight and to execute recovery either to the left or right. Forward flight speed characteristics demonstrate the effect of main rotor downwash on the horizontal stabilator for both configurations. Peaks in both longitudinal control and attitude are seen as the aircraft translates from hover to 20 knots and are greater for OGE.

Level Flight Trim Characteristics

Level flight trim characteristics of the fan-in-fin and tail rotor configurations are compared in Figures 58 and 59. The higher collective pitch required by the fan-in-fin is due to the takeoff gross weight being 400 lb higher than for the tail rotor. There is a small difference in the lateral cyclic pitch required for trim at low speeds. This is because the fan is located closer to the roll axis, thus requiring less lateral cyclic pitch to compensate for changes in the roll moment caused by the fan antitorque thrust. At high speeds, the lateral cyclic pitch required for trim is essentially the same for the fan-in-fin and tail rotor, since both are unloaded by the vertical tail in forward flight.

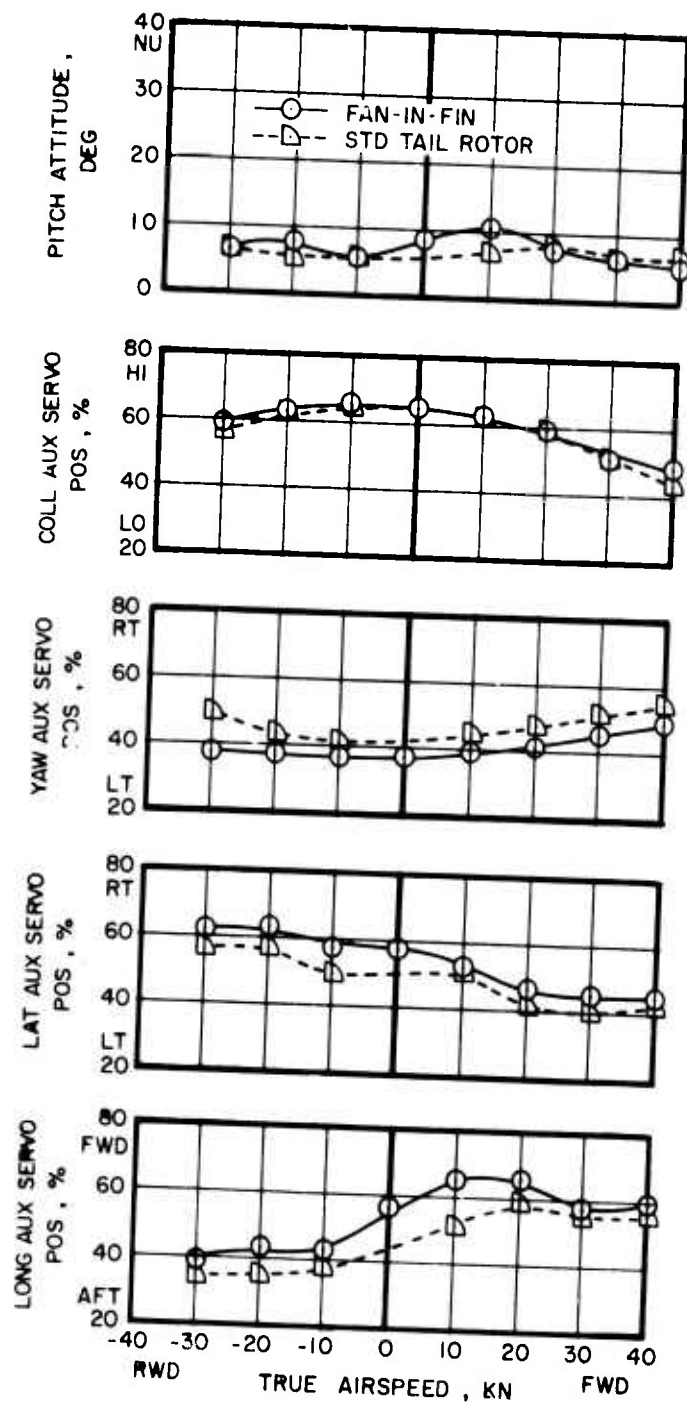


Figure 56. Comparison of Low-Speed Forward and Rearward Flight Characteristics, 20-ft Wheel Height.

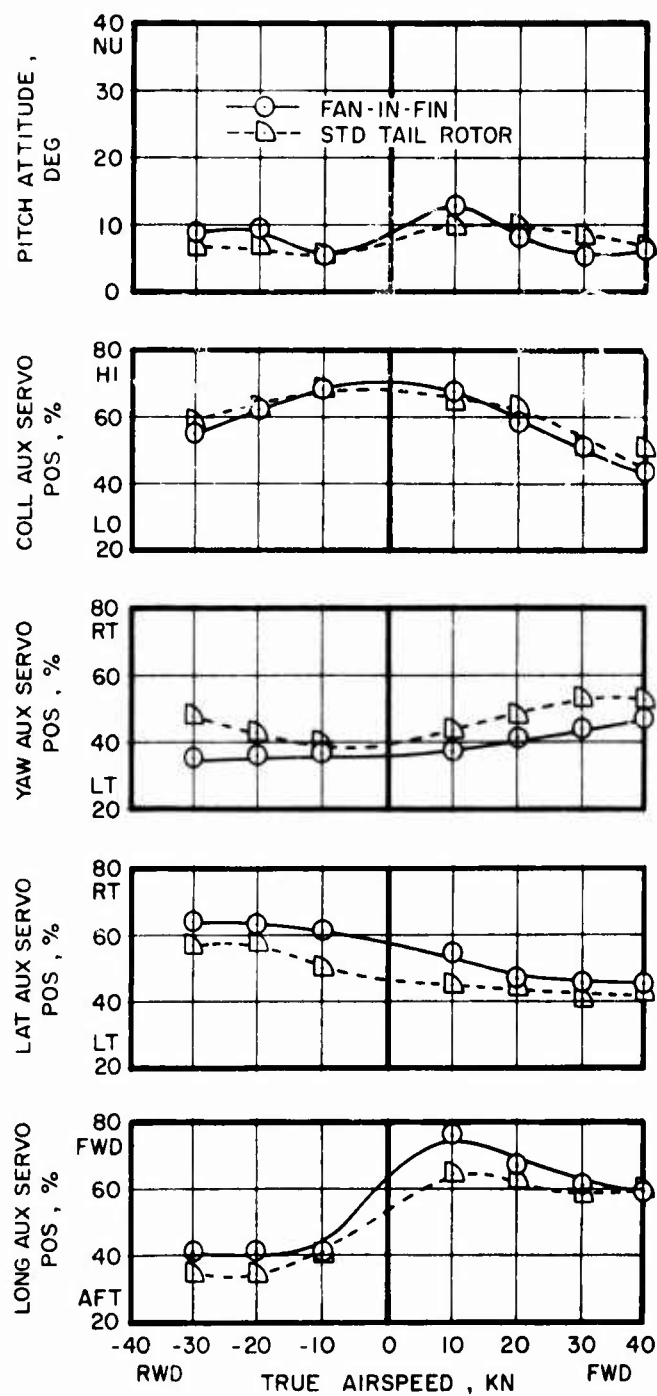


Figure 57. Comparison of Low-Speed Forward and Rearward Flight Characteristics, 100-ft Wheel Height.

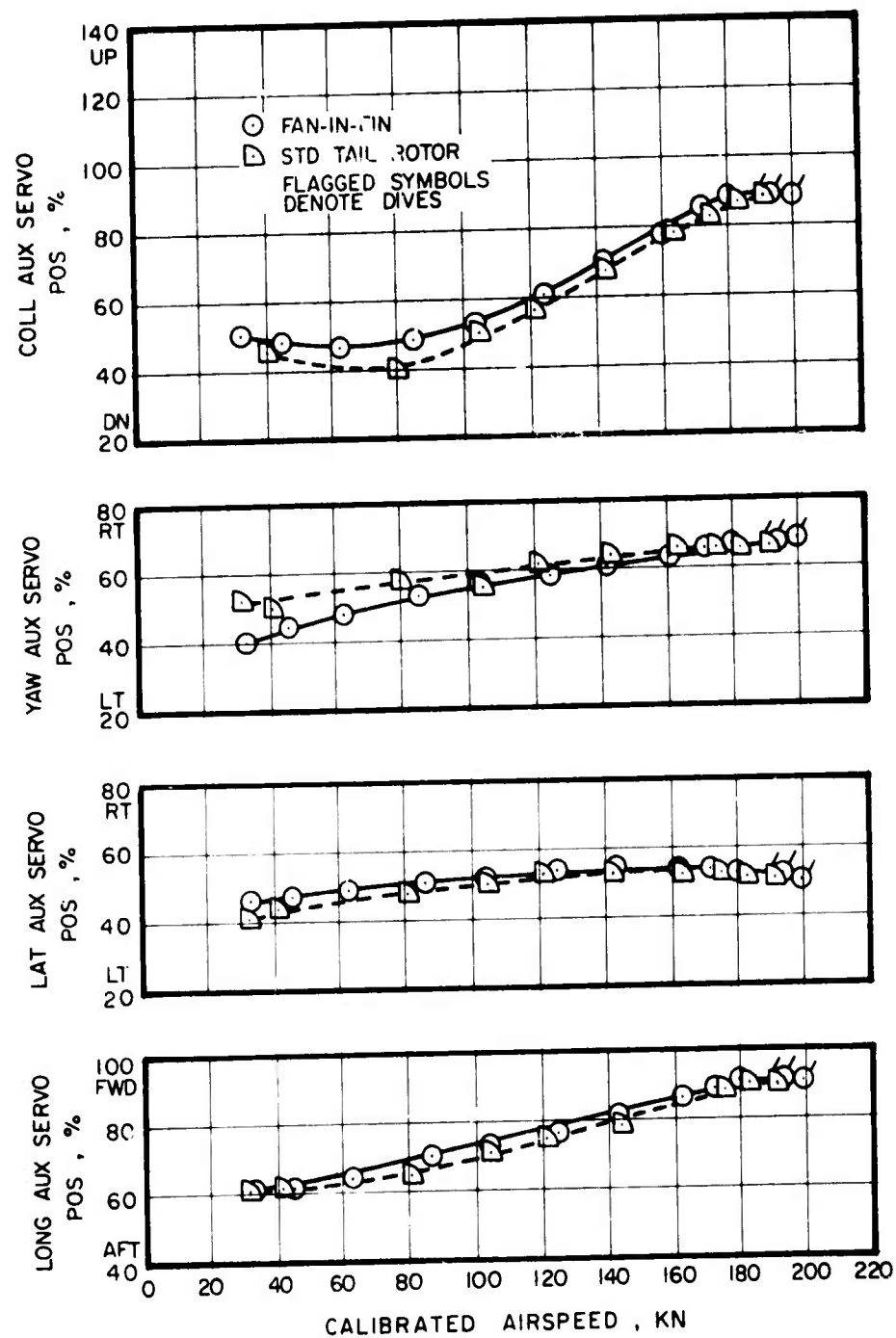


Figure 58. Comparison of Level Flight Controllability, Control Positions.

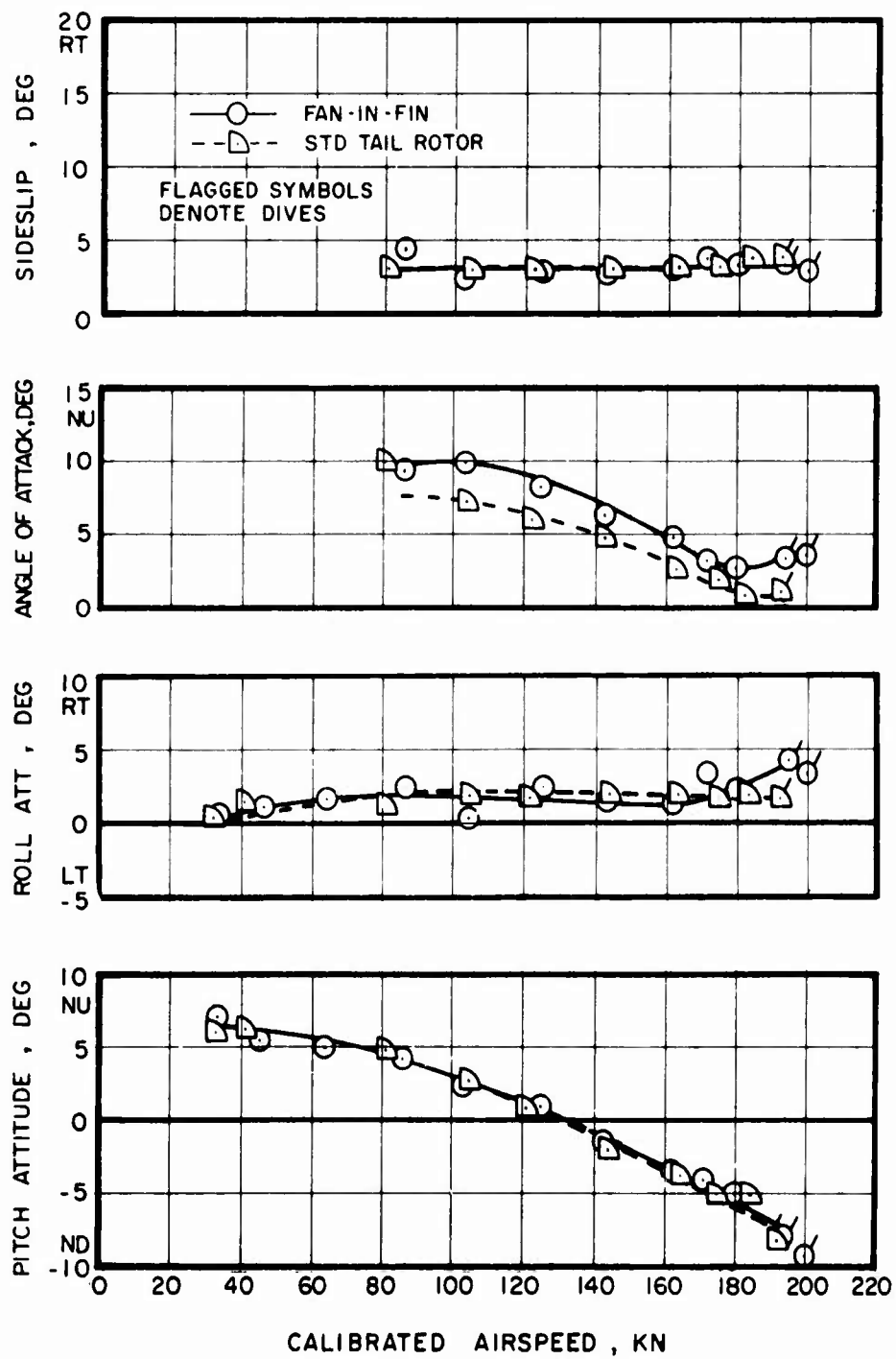


Figure 59. Comparison of Level Flight Controllability, Aircraft Attitudes.

Pedal position variation with speed is larger for the fan-in-fin than for the tail rotor. This is the result of an increase in the effectiveness of the leading edge of the fan inlet with speed which induces more mass flow through the fan. To compensate for this more right pedal is required as speed increases.

Level flight pitch and roll attitudes and sideslip angles are essentially the same for both configurations.

Static Lateral Directional Stability

The lateral directional stability of the fan-in-fin configuration did not match that of the tail rotor aircraft. This is apparent in two ways:

- . During sideslips, the aircraft displays almost indifferent yaw trim over a range of as much as 12 degrees, and reduced directional damping.
- . In cruise with wings level, the aircraft displays almost indifferent yaw trim over a range of about 4 degrees.

Static lateral directional stability characteristics are shown in Figures 60 through 67. Sideslip angles were established while maintaining a constant collective setting for each trim condition. The trim airspeed was maintained and altitude or rate of climb or descent permitted to vary. Sideslip angles achieved with the fan-in-fin were limited by the amount of roll the pilot would tolerate or by the aircraft's sideslip design envelope. The tail rotor configuration was limited by either the amount of roll or a tail rotor stress limit.

The variation in lateral control position with sideslip is essentially the same for both configurations and demonstrates positive dihedral effect. Longitudinal control gradients with sideslip are essentially the same for both configurations. The change in roll angle with sideslip (an indication of aircraft side-force characteristics) is also the same for both configurations. This roll attitude is characteristic of high values of projected side area of the fuselage.

The amount of steady fan thrust required to trim the aircraft in level flight sideslip conditions was shown earlier in the section Fan Forward Flight Performance and on Figure 29. These data show that to achieve left sideslip, very little fan thrust change is required. The reason for this has been identified as flow separation on the upper vertical fin, occurring progressively with increasing left sideslip angle and diminishing the effectiveness of the upper fin. This flow separation is not a consequence of airfoil stall. It is induced by efflux from the fan not readily separating from the well-rounded inlet (in left sideslip this becomes the exhaust) and following the contour of the fin into the region of reduced pressure on the lifting side of the fin. The extent of the resulting flow separation on the fin depends primarily on the amount of negative fan thrust, and therefore the slope of the pedal position gradient depends also on the level of fan thrust for any particular flight condition. At

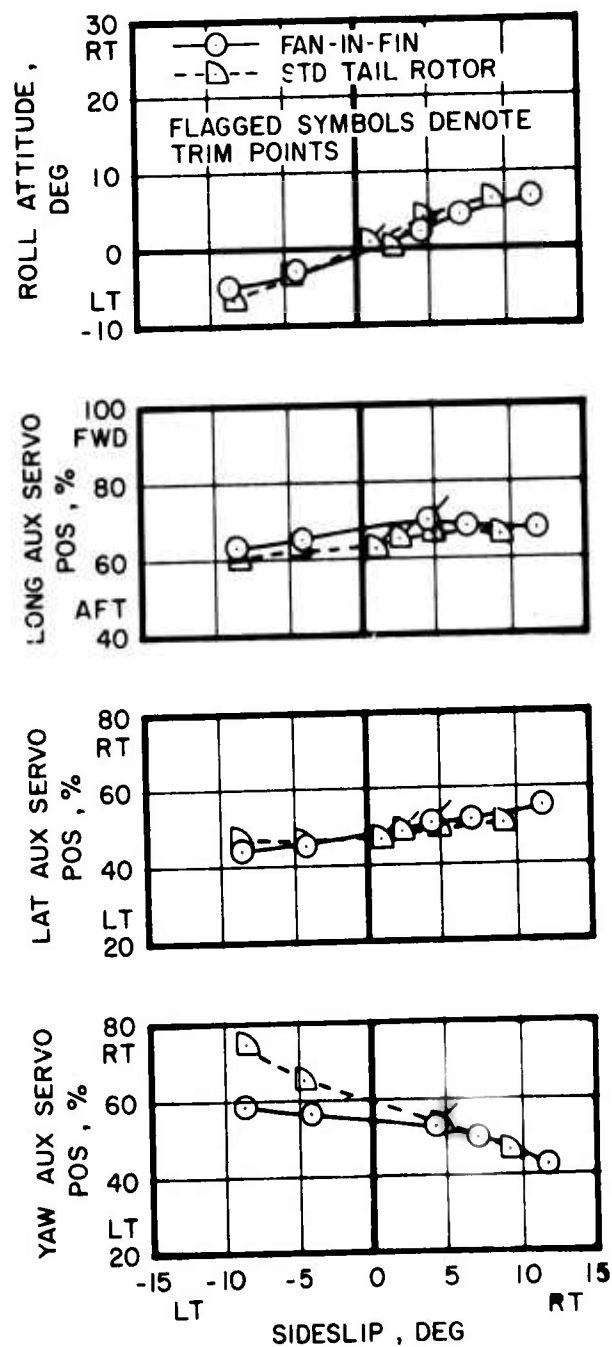


Figure 60. Comparison of Static Lateral Directional Stability, 80 KIAS, Level Flight.

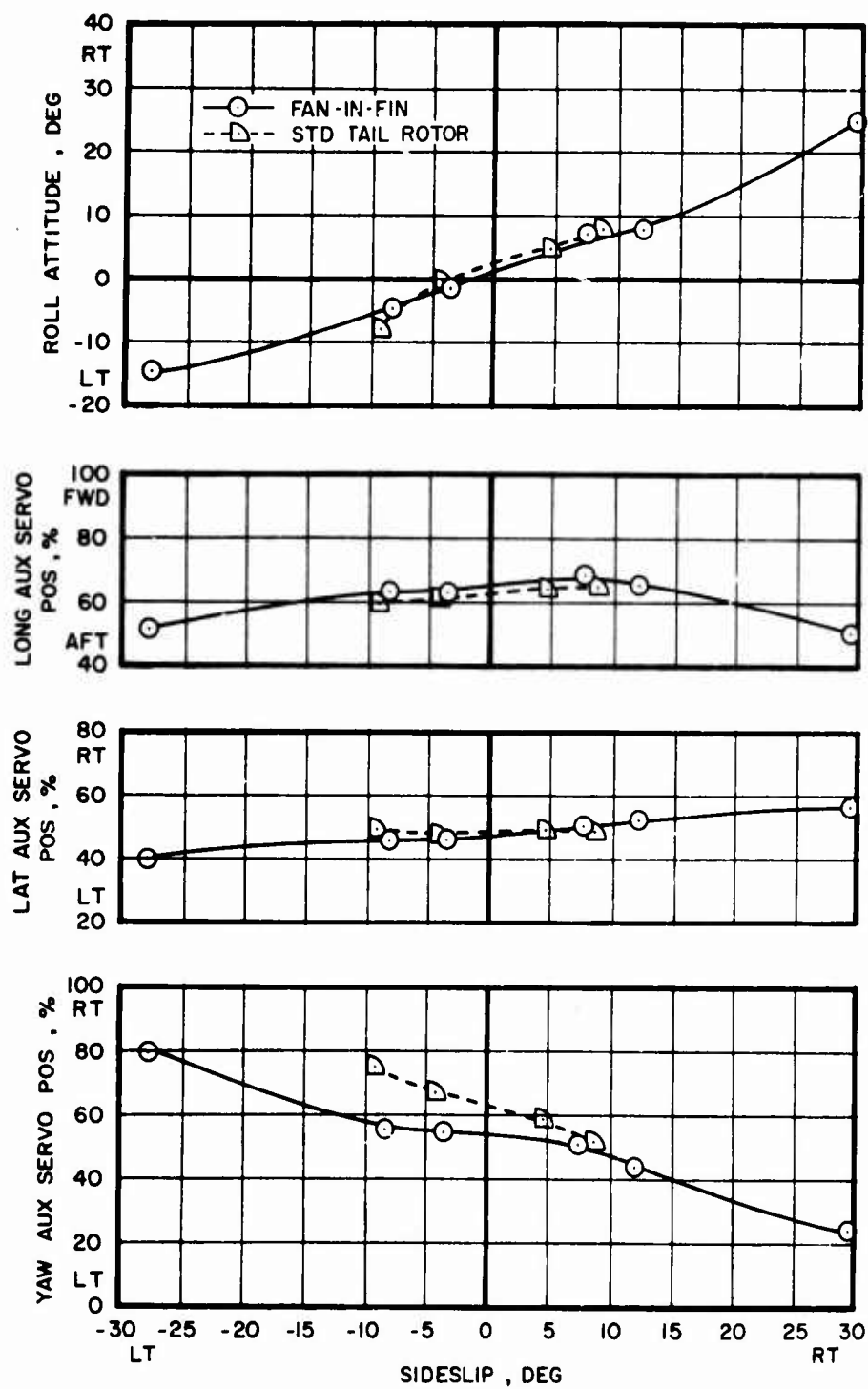


Figure 61. Comparison of Static Lateral Directional Stability, 80 KIAS, Partial Power Descent.

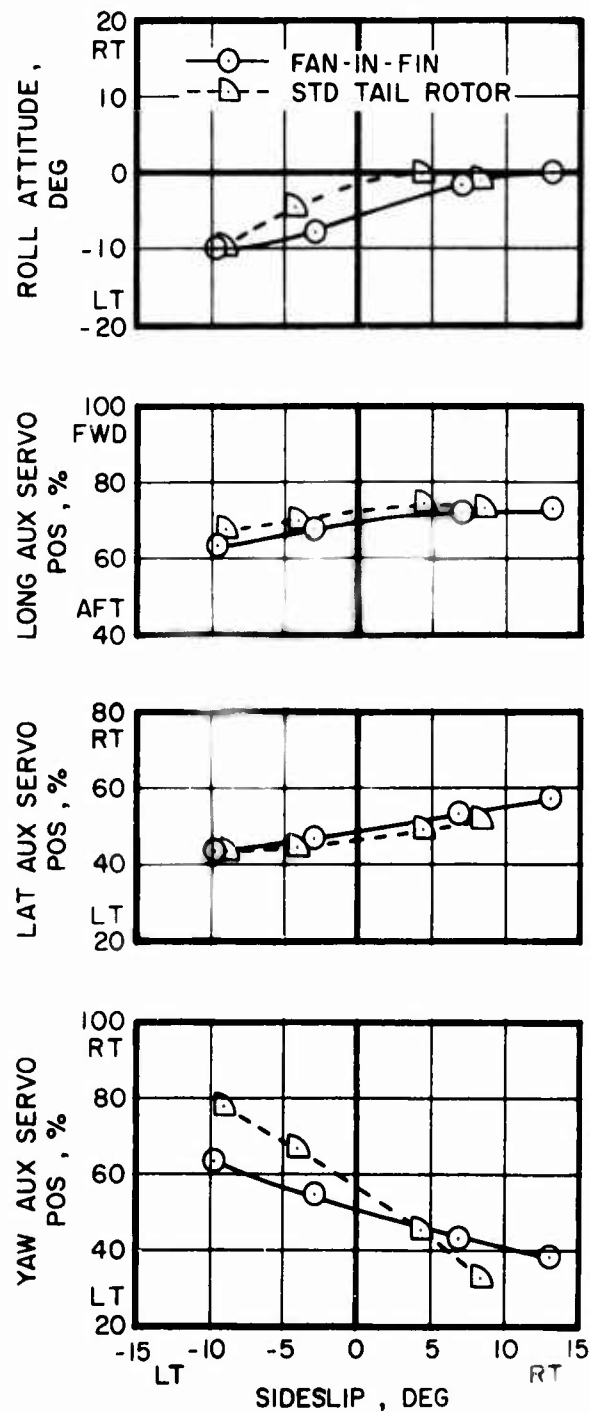


Figure 62. Comparison of Static Lateral Directional Stability, 80 KIAS, Climb.

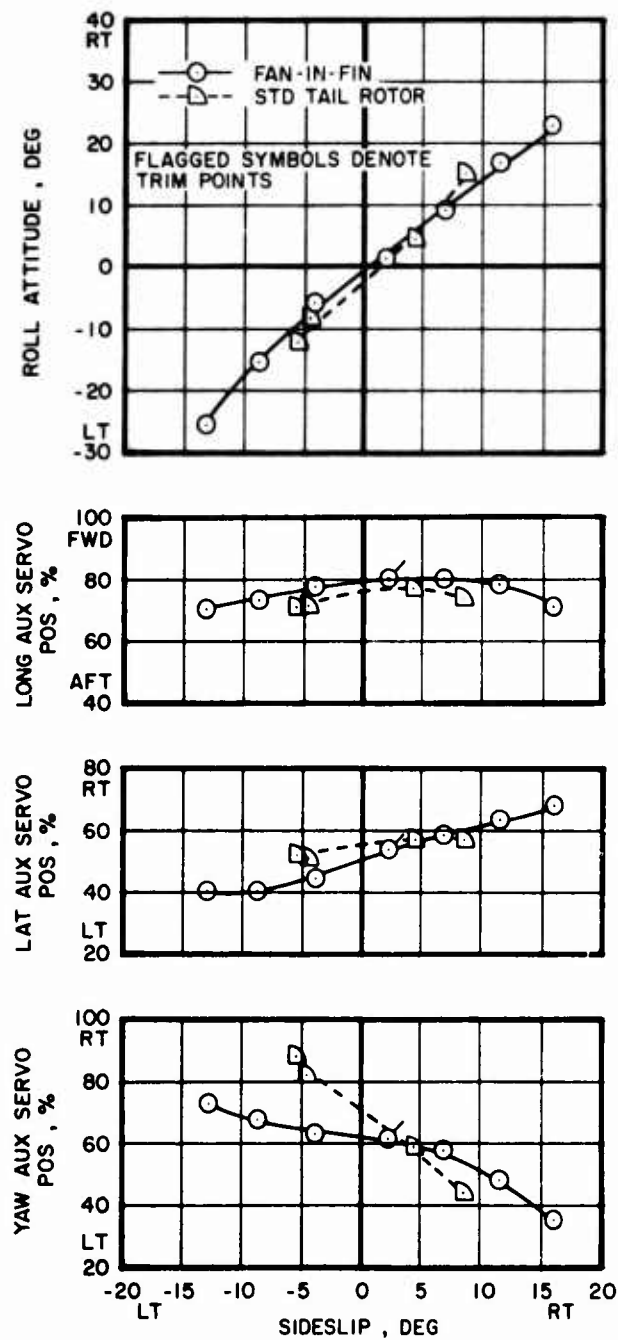


Figure 63. Comparison of Static Lateral Directional Stability, 140 KIAS, Level Flight.

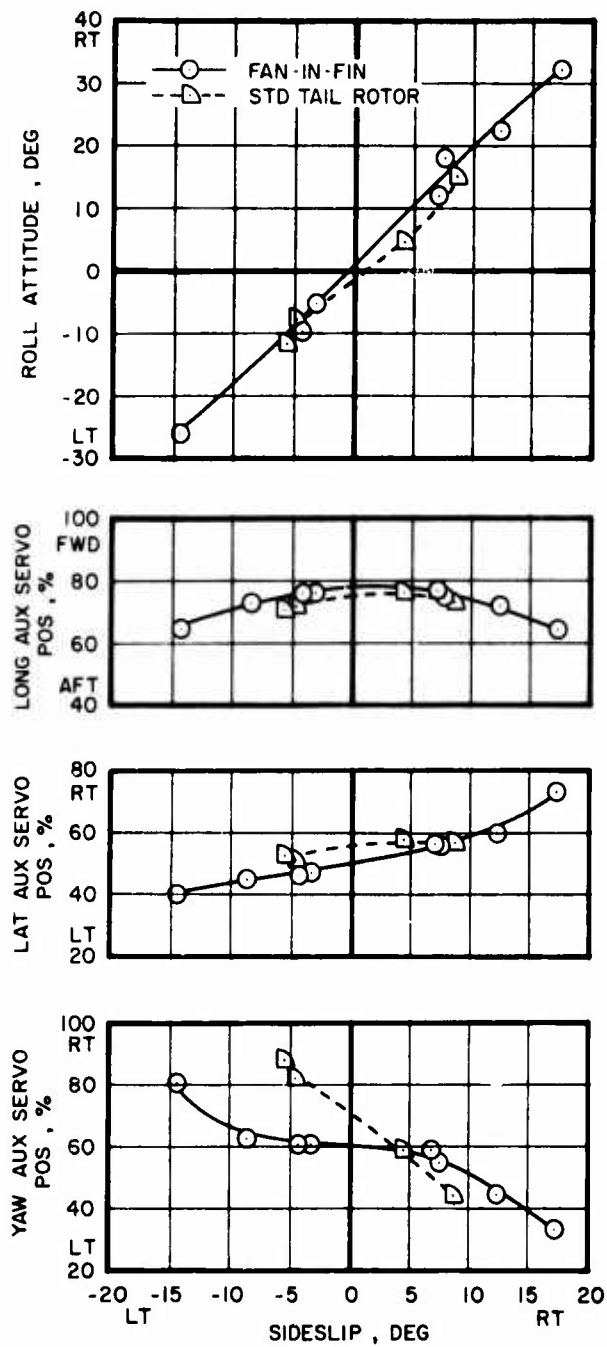


Figure 64. Comparison of Static Lateral Directional Stability, 140 KIAS, Partial Power Descent.

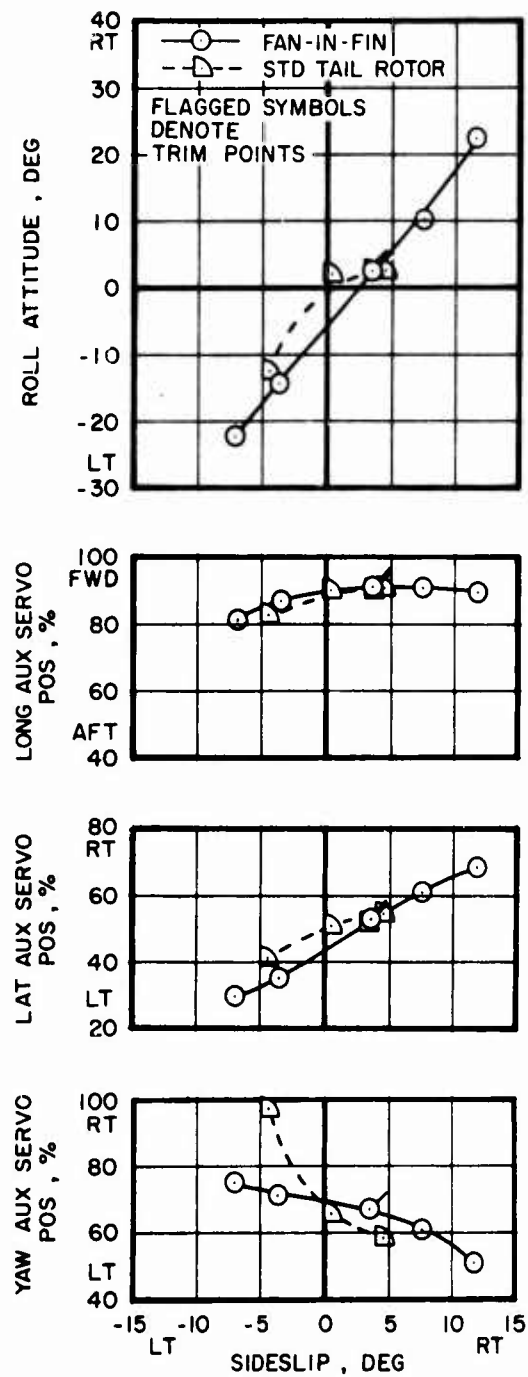


Figure 65. Comparison of Static Lateral Directional Stability, $V_{\max} = 190$ KTAS, Level Flight.

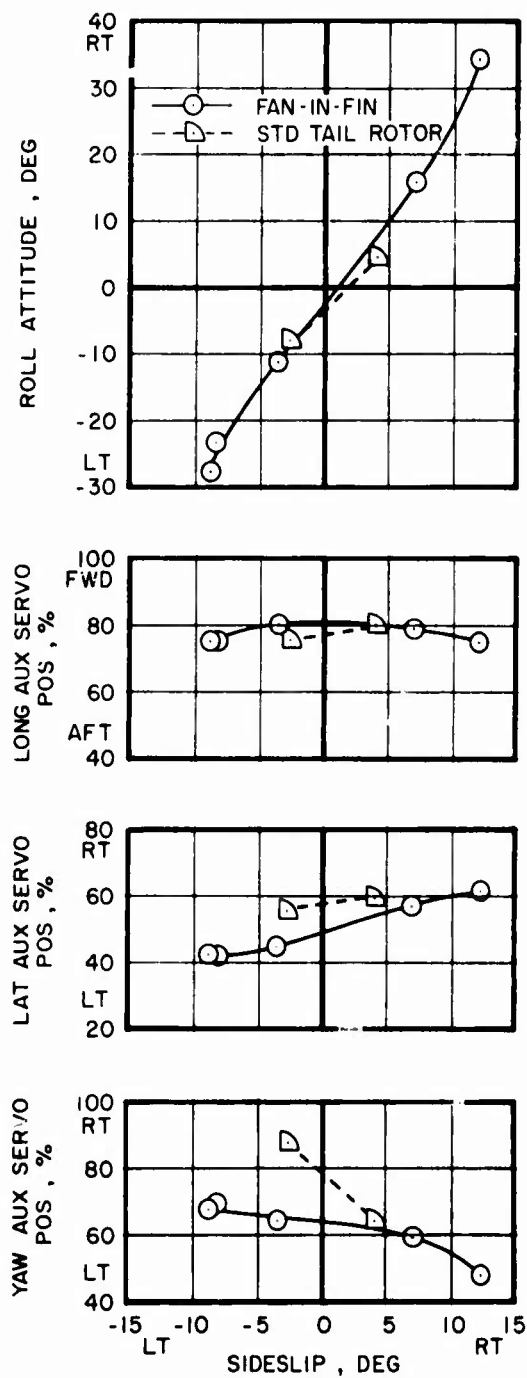


Figure 66. Comparison of Static Lateral Directional Stability, $V_{\max} = 190$ KTAS, Partial Power Descent.

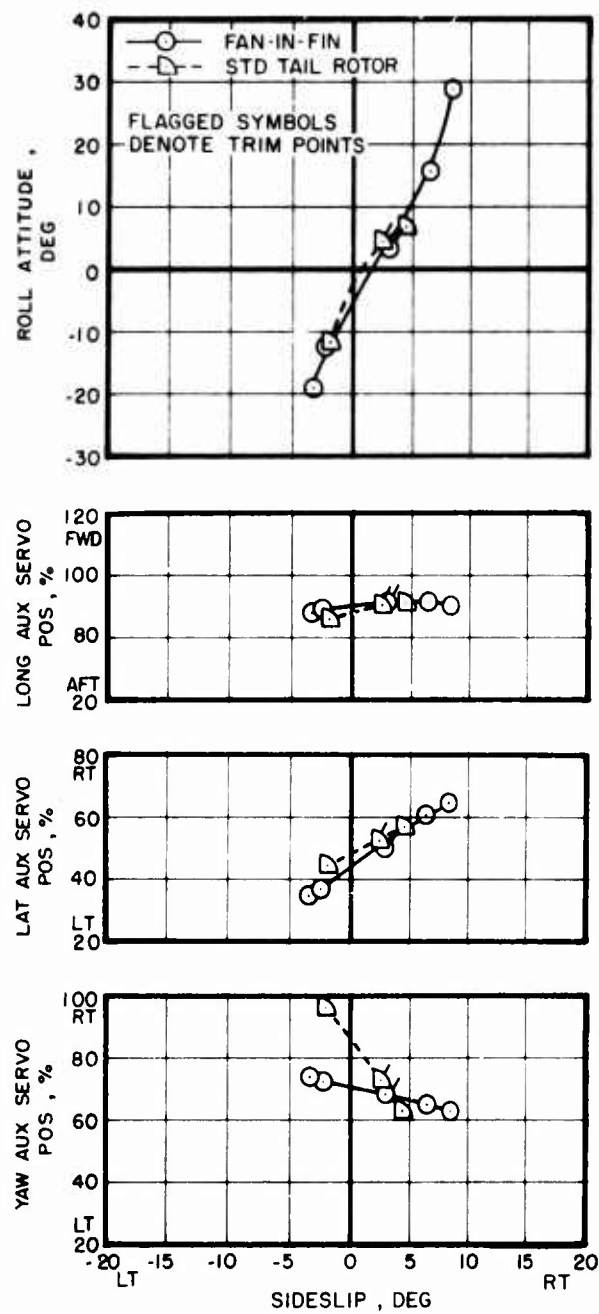


Figure 67. Comparison of Static Lateral Directional Stability, Dive at 111% Q, 209 KTAS.

80 KIAS, Figures 60, 61, and 62, the climb condition requires high positive fan thrust levels, there is no flow separation on the fin and the pedal (yaw aux. servo) position gradient is relatively steep. In partial power descent, the fan operates primarily at negative thrust levels, flow separation does occur to a varying degree and the pedal position gradient becomes shallow. The level flight condition is in between, showing a shallower pedal position gradient in left sideslip where the fan enters the negative thrust regime, and a steeper gradient in right sideslip where the fan operates at positive thrust levels. At 140 KIAS, Figures 63 and 64, the level flight condition shows again a steeper pedal position gradient in right sideslips where the fan operates at positive thrust levels and a shallower gradient in left sideslips where the fan operates at negative thrust levels. In partial power descent, the fan operates generally in the negative thrust regime and the pedal position gradient is shallow. Similar observations can be made on Figures 65 and 66 for V_{max} .

For all conditions tested, the fan-in-fin pedal position gradient is less steep than that of the tail rotor configuration. At 80 knots the fan-in-fin pedal position gradient is essentially neutral for small sideslip angles around trim and does not meet section 3.3.9 of MIL-H-8501A (Reference 3). At high speeds the pedal slope increases, but still remains relatively shallow, as shown in Figure 68. This results in difficulty in trimming the fan-in-fin configuration directionally.

Further examination of Figure 68 shows that the control gradient about the trim point is unsymmetrical. The regime of decreased pedal gradient extend approximately 10 deg to the left and 5 deg to the right of the trim point in level flight.

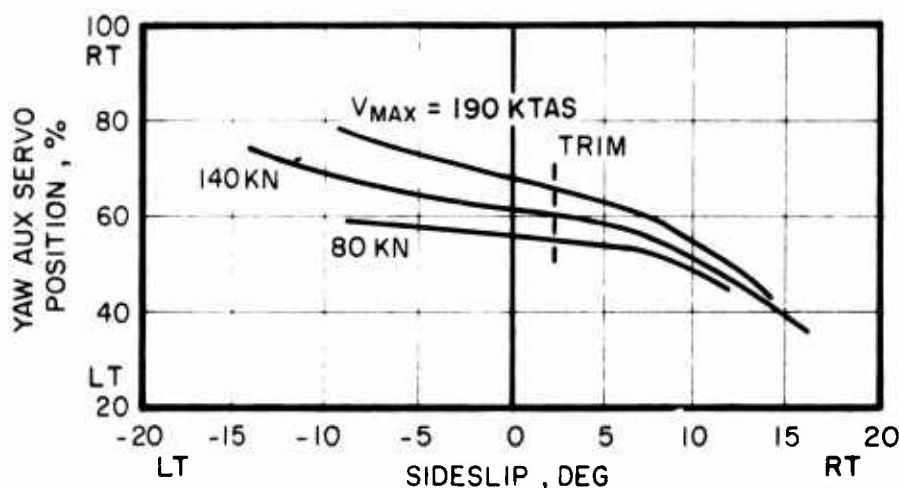


Figure 68. Variation of Sideslip With Pedal Position as Function of Airspeed, S-67 Fan-in-Fin.

In cruise with wings level, the aircraft tightens considerably and displays indifferent yaw stability over a range of only about two degrees to the left and right of the level flight trim point. This effect is believed to be caused by the interaction between fan-induced flow and the fan inlet flow field. It does not involve flow separation on the vertical fin and is therefore a different phenomenon than that experienced during sideslips.

The wind tunnel test airframe yawing moment data obtained with 1/12 scale models shows nearly identical behavior for the tail rotor configuration (without tail rotor) and the fan-in-fin configuration with the fan hole closed. With fan hole open, the slope of the yawing moment curve becomes less steep around trim attitude, but still shows fair stability. This would indicate a reduction in directional stiffness but not a dead band of indifferent yaw trim. However, the significant features not accounted for in the wind tunnel tests are the positive stability contribution of the tail rotor and the airflow effects of the fan.

The tail rotor is known to exhibit a significant restoring force. The thrust variation of the 10-ft-7-in. tail rotor, in response to deviation from trim at cruise (without pedal motion), is about 40 pounds per degree of displacement from trim, acting always in opposition to the displacement. This restoring force results from a thrust variation in response to inflow angle changes upon displacement from trim. It is the biggest single contribution to the lateral directional stability of a single rotor/tail rotor helicopter and provides damping as well.

By contrast, the fan appears either to have no restoring force capability whatsoever within a narrow range around trim or, in combination with the inlet behavior, to have an adverse effect large enough to counter the generally favorable yawing moment characteristics of the airframe. This is not apparent from the data points recorded during flight, since they are based on time-weighted averaging of parameters varying over the record interval (several seconds). But an observation in real time of the fan load cell traces and the sideslip trace, in level flight with wings level and pedals fixed, shows no noticeable fan thrust variation with sideslip angle within the yaw trim dead band. In this respect, the fan-in-fin is significantly different from the tail rotor.

The flow phenomenon that causes the indifferent yaw stability in cruise with wings level is not yet properly understood, largely because the aircraft instrumentation was not refined enough to permit detailed measurements of fan and inlet behavior. However, clues are present that lead to the following explanation, and it is offered as a tentative conclusion to be verified by additional testing on the aircraft or in a wind tunnel before design solutions can be explored.

In the absence of the fan, the duct and vertical fin would produce a restoring force in response to a yaw displacement. This was verified by the 1/12 scale model test with the fan hole open. As the aircraft yaws, the suction on the leading edge of the duct changes to produce some of this force. When the fan is present and operating at low thrust, the outboard portions of the blade are at negative pitch angles and are producing a

flow counter to the natural flow on the inlet. Consequently, the restoring force resulting from the inlet suction is neutralized. This tentative conclusion is supported by the load cell data, which show no appreciable variation in thrust during a yaw excursion with pedals fixed. This could only occur if the yaw-sensitive suction force on the inlet were cancelled out by the influence of the fan.

If this is the flow phenomenon that causes the dead band of indifferent yaw trim, even a liberal increase in vertical tail area will not solve the problem, but only diminish its magnitude at the expense of drag and side-flight capability. The real solution must be provided by measures that deal with the flow field itself.

At one time in the fan flight test program, the SAS yaw channel was activated to see if it could cope with the observed softness in yaw trim in forward flight. However, the SAS yaw channel authority proved too narrow and did not noticeably improve the aircraft's flying characteristics. No further investigations were conducted.

Forward Flight Dynamic Directional Stability

The directional dynamic stability of both configurations was evaluated by initiating a 1-inch, 1/2-second pulse through the directional controls. Responses were generated at 120 KIAS, 160 KIAS, and V_{max} for both configurations. The reduction in directional stability of the fan-in-fin compared to the tail rotor is clearly evident from Figures 69 to 80. The short-term response of the tail rotor aircraft is damped, while that of the fan-in-fin is oscillatory. Left pedal pulses excited the Dutch Roll mode of both aircraft at all speeds except on the tail rotor configuration at 80 knots. At 160 knots, both showed a strong tendency toward spiral divergence in addition to the Dutch Roll mode. Right pedal pulses excited the spiral divergence mode at all airspeeds tested for the fan-in-fin and at the two high-speed conditions for the tail rotor configuration. In these tests, the pilot maintained steady control positions with the tail rotor configuration. In the fan-in-fin, lateral control inputs were applied almost immediately to correct for the resulting roll motion.

Directional Control

Directional response to control in hover was evaluated by measuring the yaw displacement of the aircraft after applying one-inch pedal steps. The results of these tests are shown in Table 6 for both aircraft configurations and are compared with predictions and the requirements of MIL-H-8501A (Reference 3), section 3.3.5. As can be seen, both the fan-in-fin and tail rotor configurations exceed the required displacement. The fan-in-fin configuration displays higher levels of directional response and the results compare well with predictions although considerable scatter was observed in the data.

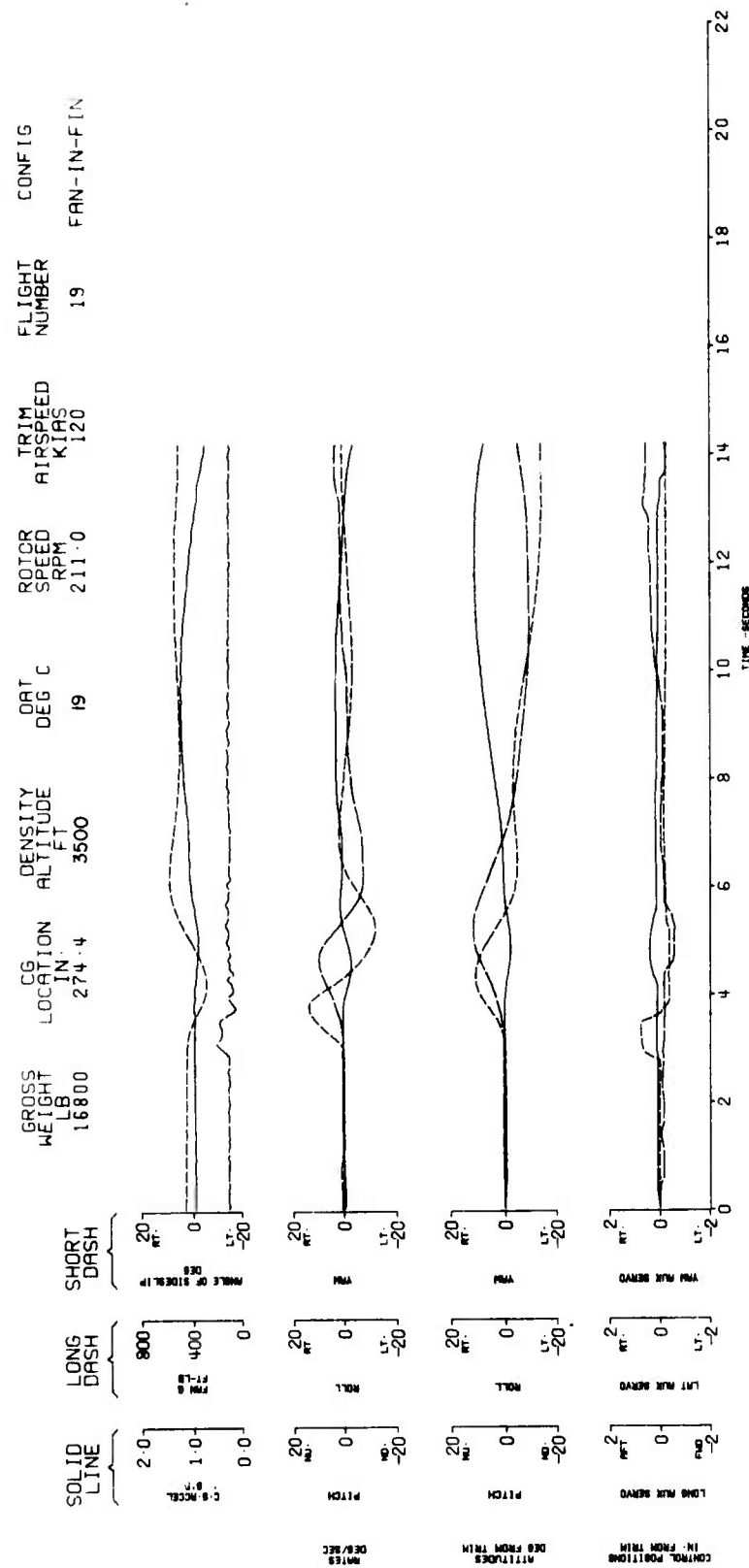
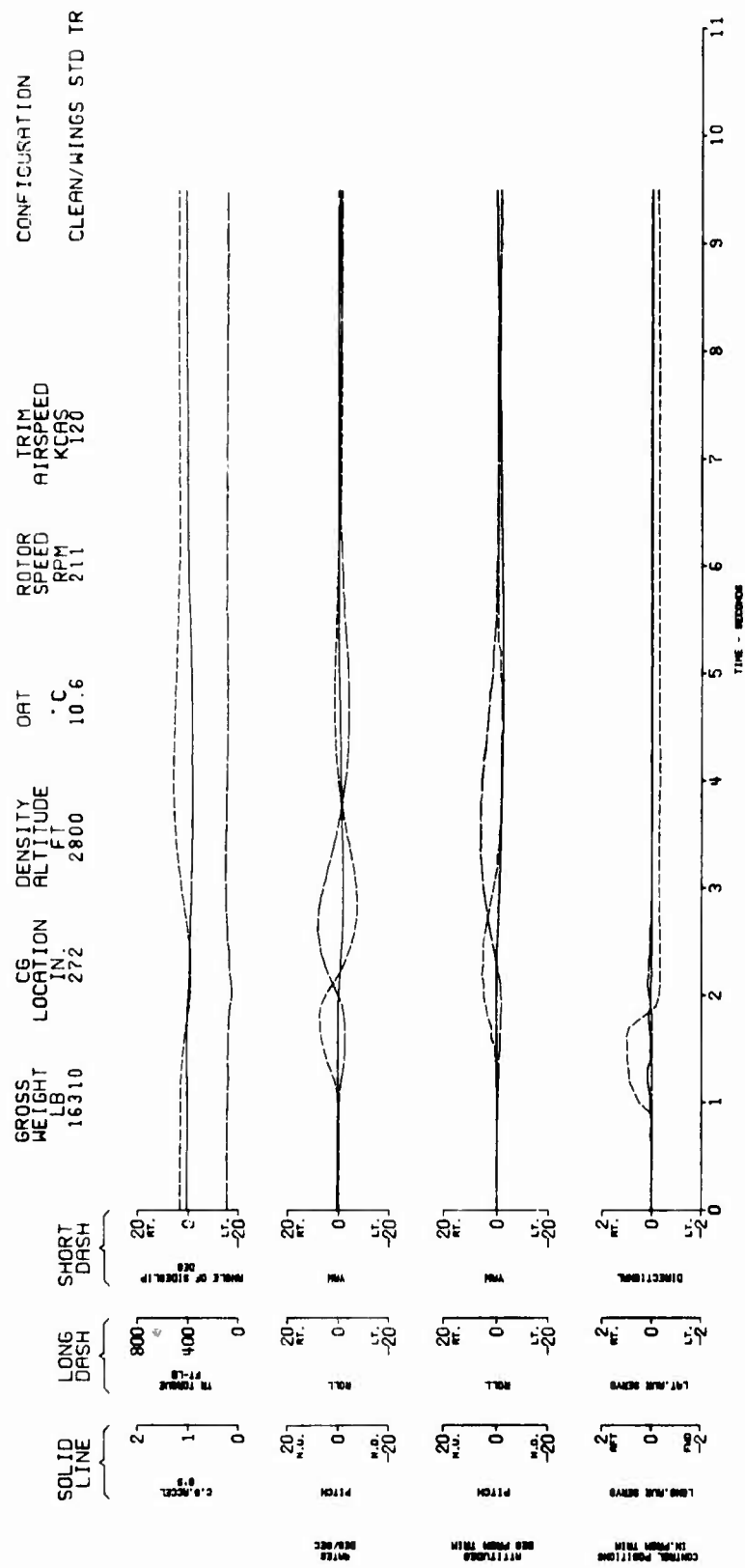


Figure 69. S-67 Fan-in-Fin, Level Flight 120 KIAS, 1-inch 1/2-sec Right Pedal Pulse.



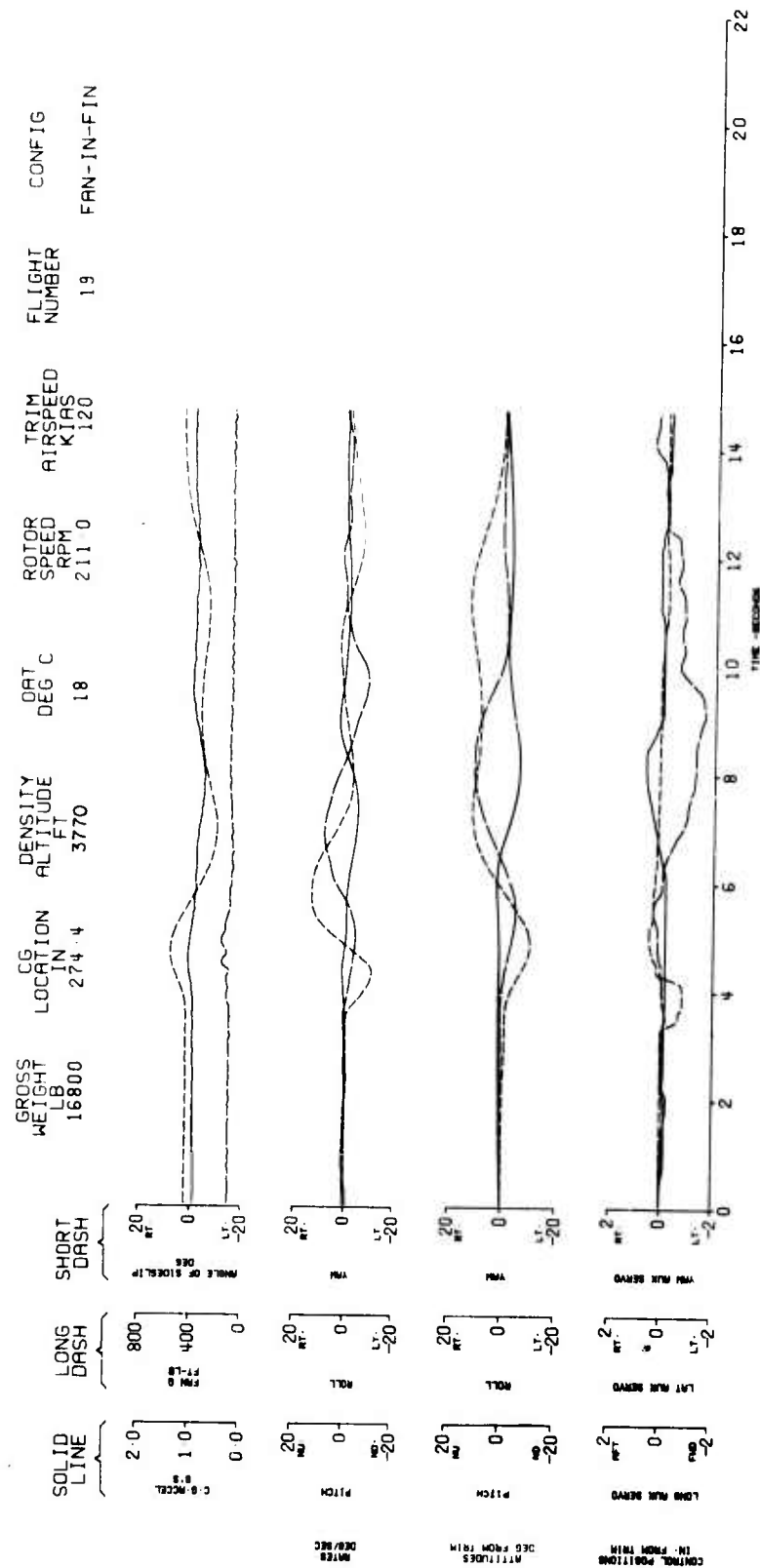


Figure 71. S-67 Fan-in-Fin, Level Flight 120 KIAS, 1-inch 1/2-sec Left Pedal Pulse.

CONFIGURATION
CLEAN/WINGS STD TR

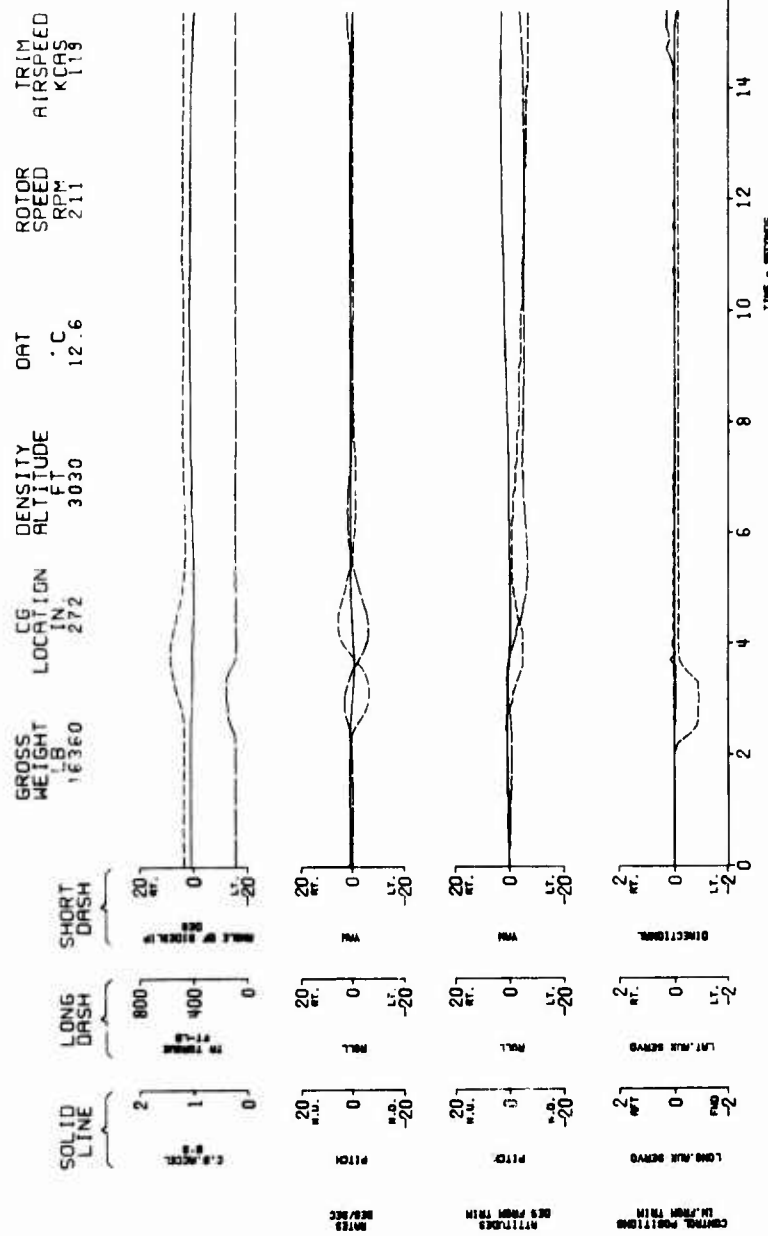


Figure 72. S-67 Tail Rotor, Level Flight 120 KIAS, 1-inch 1/2-sec Left Pedal Pulse.

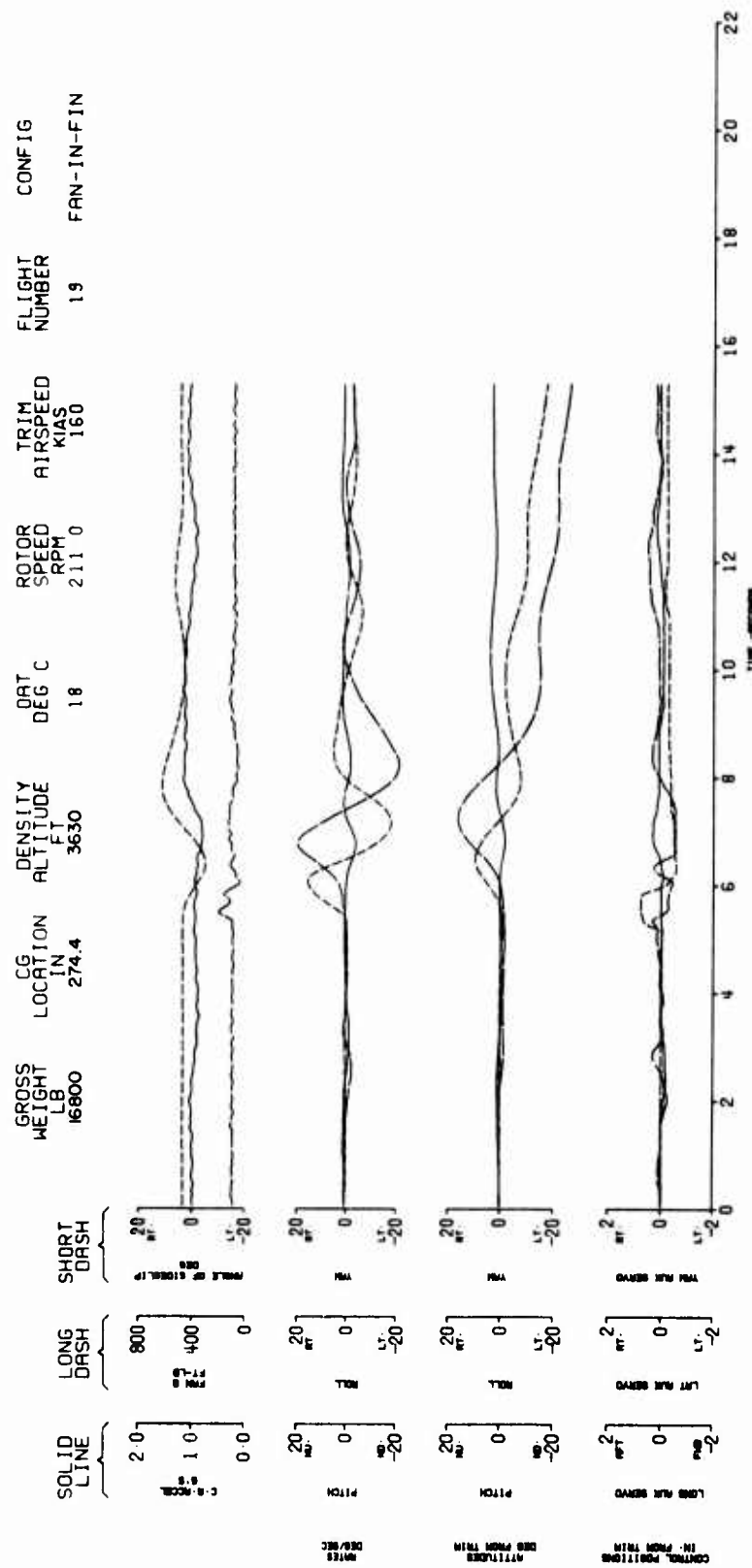


Figure 73. S-67 Fan-in-Fin, Level Flight 160 KIAS, 1-inch 1/2-sec Right Pedal Pulse.

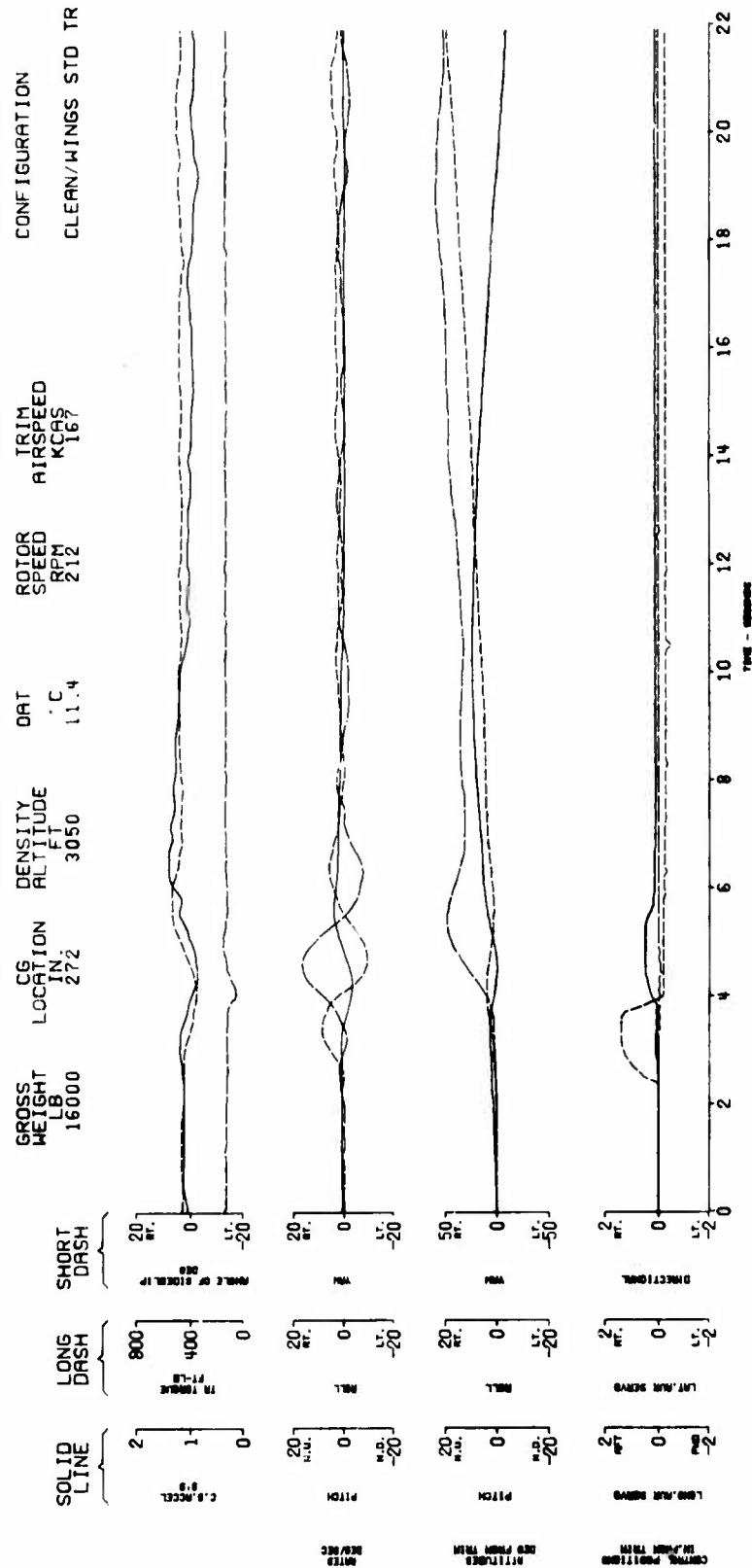


Figure 74. S-67 Tail Rotor, Level Flight 160 KIAS, 1-inch 1/2-sec Right Pedal Pulse.

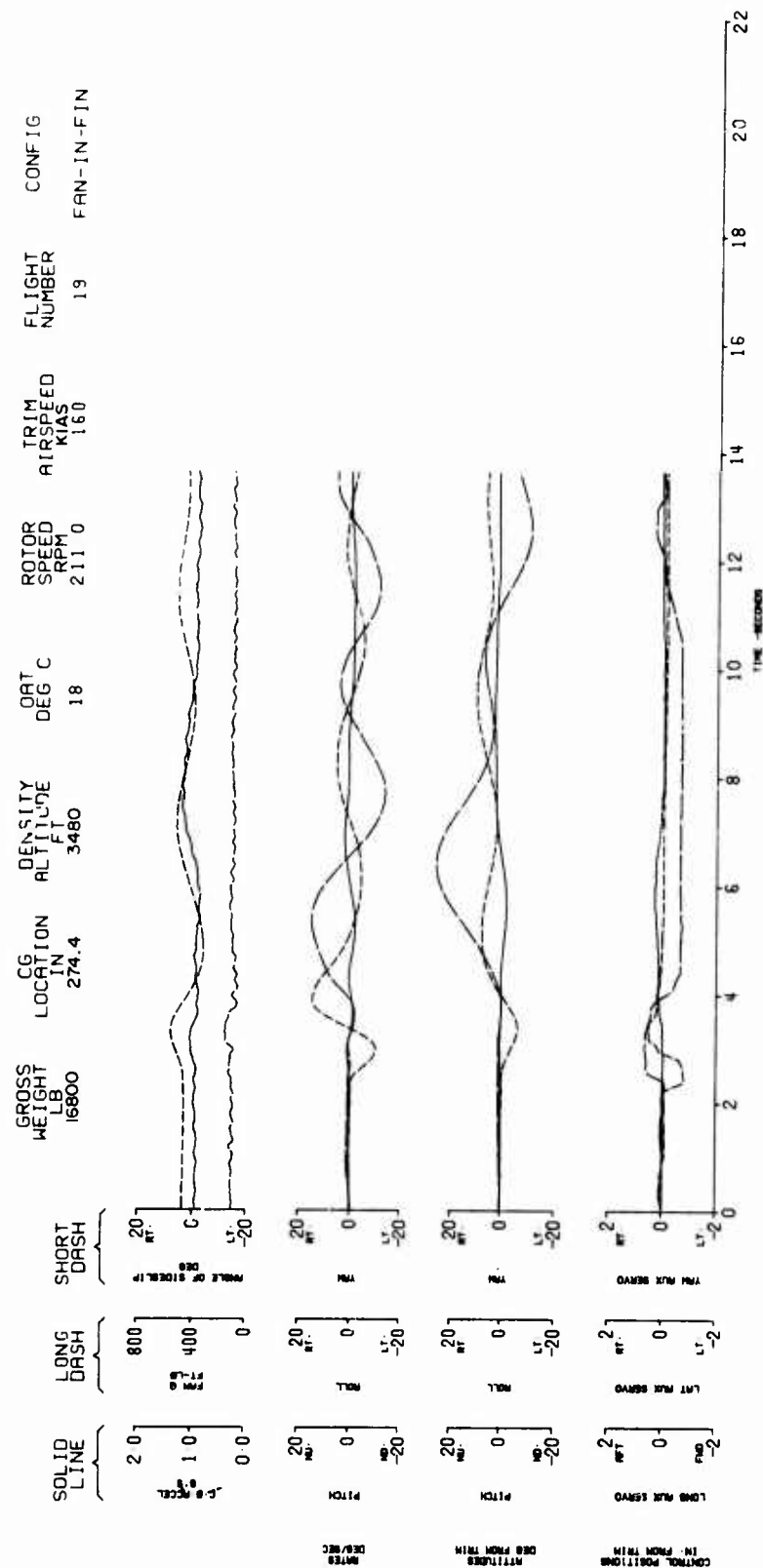


Figure 75. S-67 Fan-in-Fin, Level Flight 160 KIAS, 1-inch 1/2-sec Left Pedal Pulse.

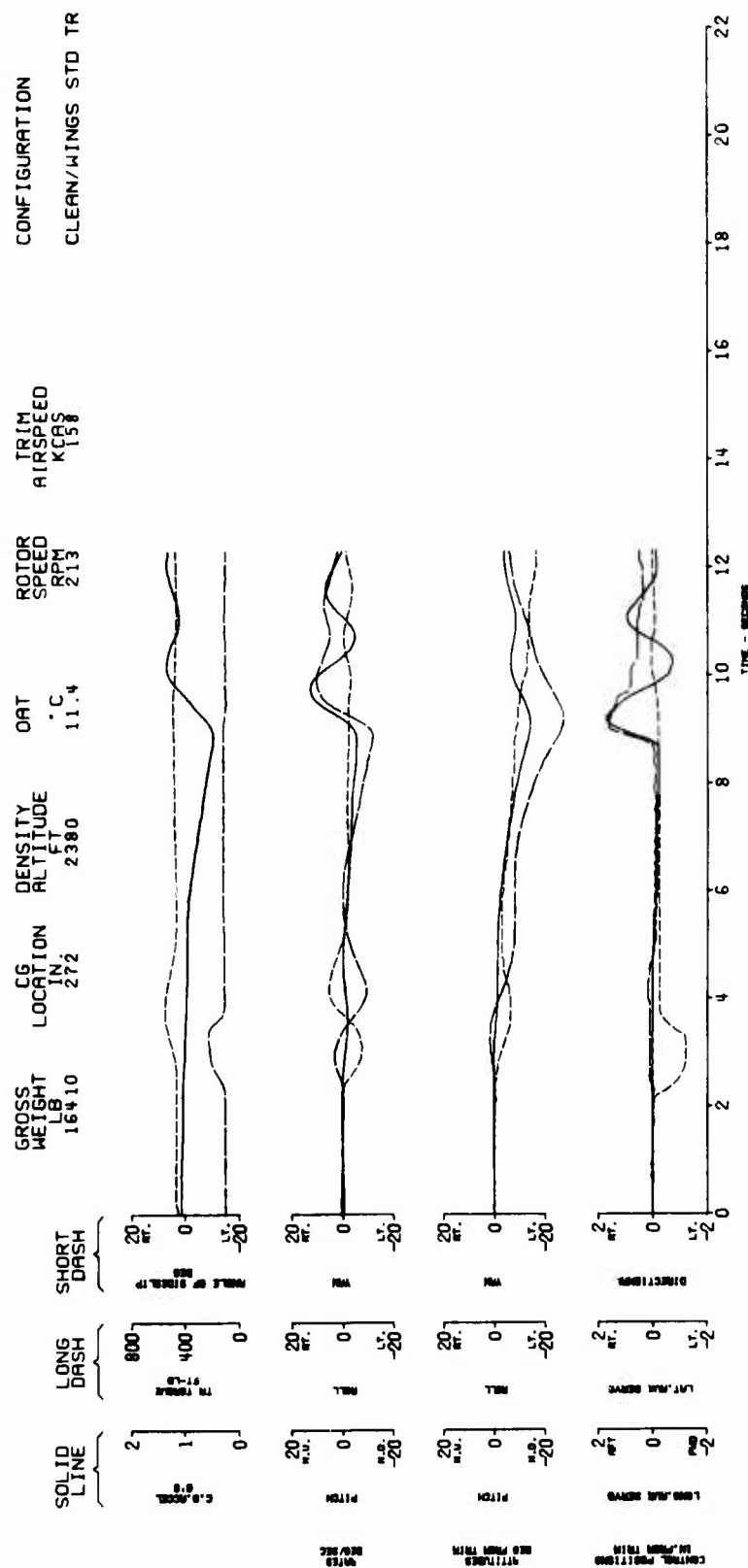


Figure 76. S-67 Tail Rotor, Level Flight 160 KIAS, 1-inch 1/2-sec Left Pedal Pulse.

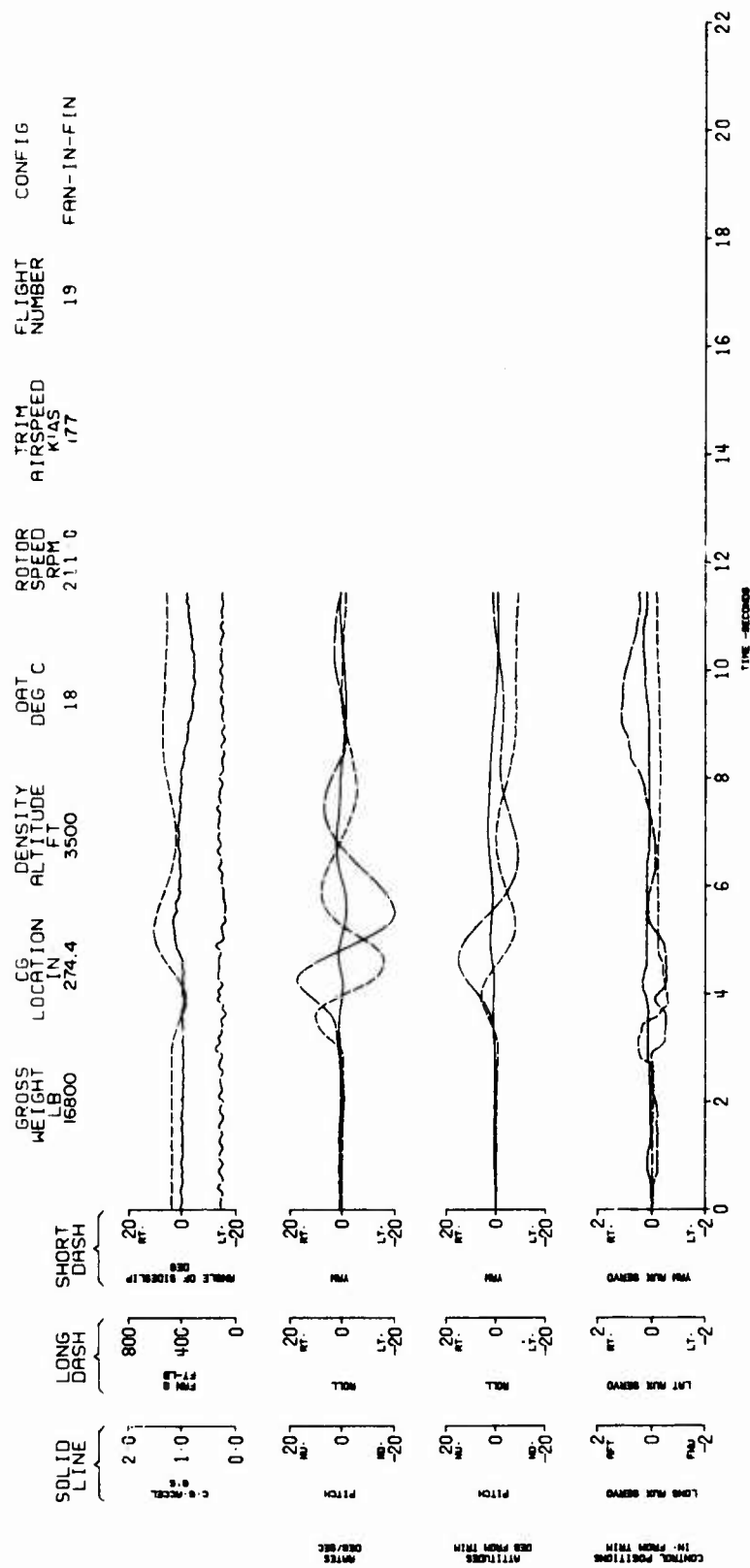


Figure 77. S-67 Fan-in-Fin, Level Flight 180 KIAS, 1-inch 1/2-sec Right Pedal Pulse.

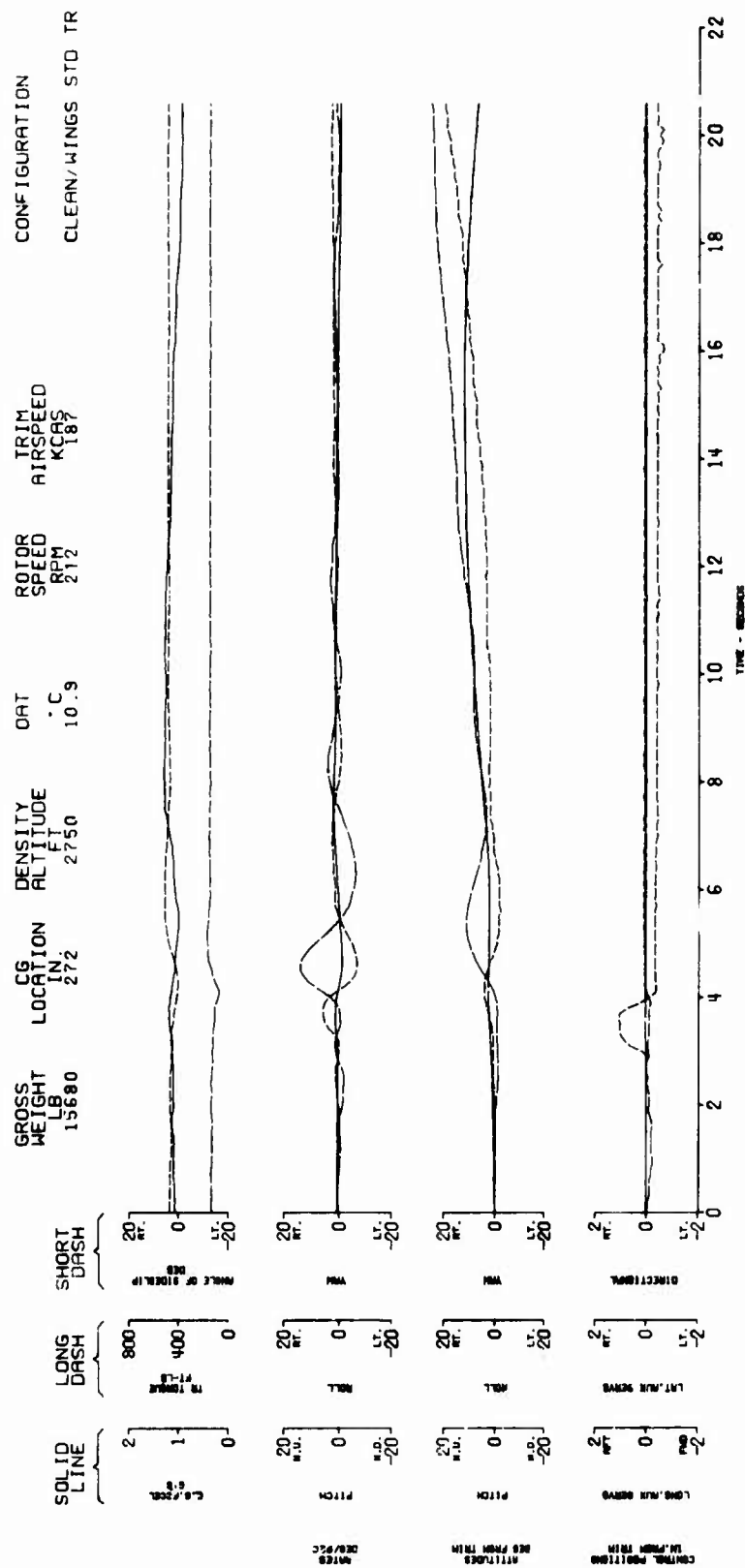


Figure 78. S-67 Tail Rotor, Level Flight 180 KIAS, 1-inch 1/2-sec Right Pedal Pulse.

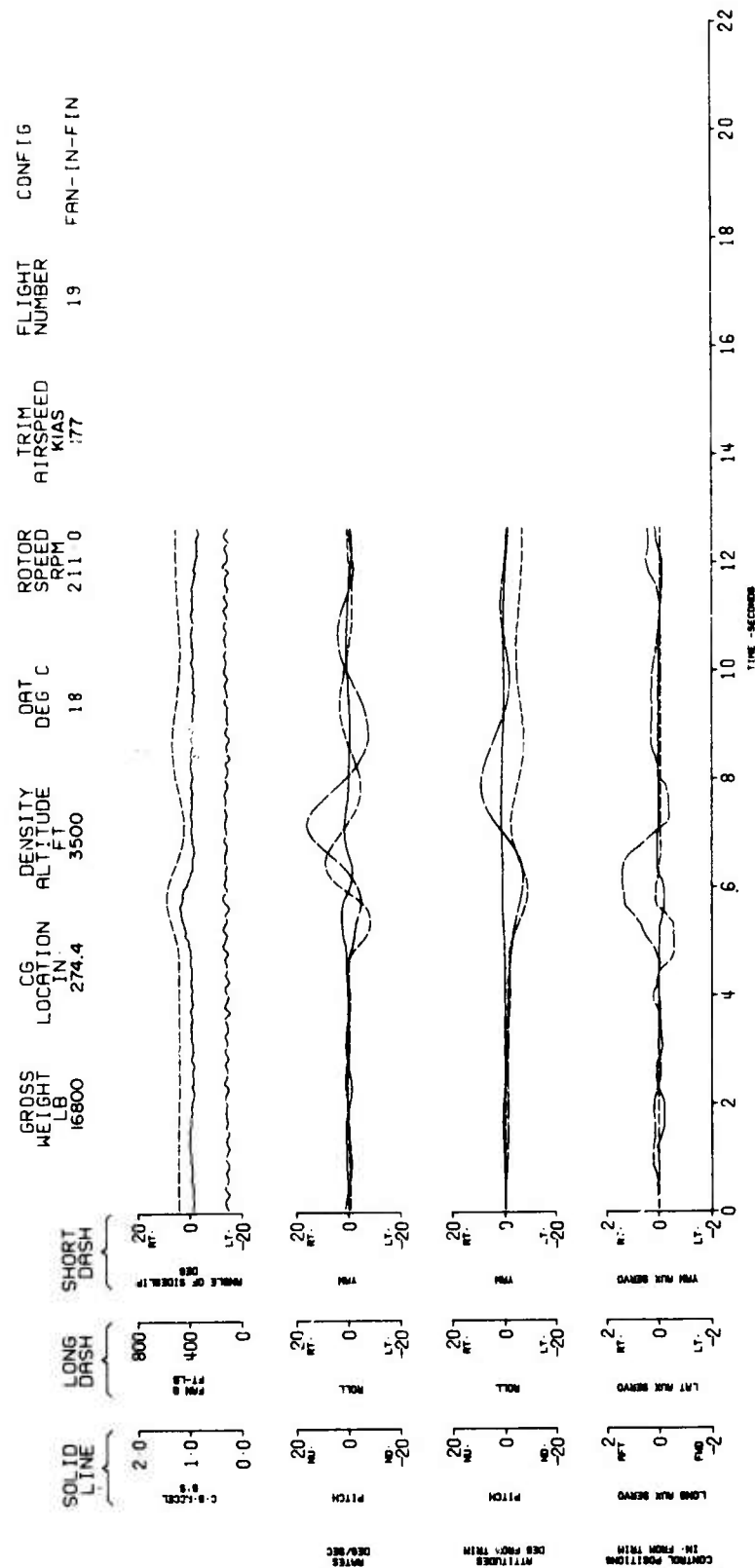


Figure 79. S-67 Fan-in-Fin, Level Flight 180 KIAS, 1-inch 1/2-sec Left Pedal Pulse.

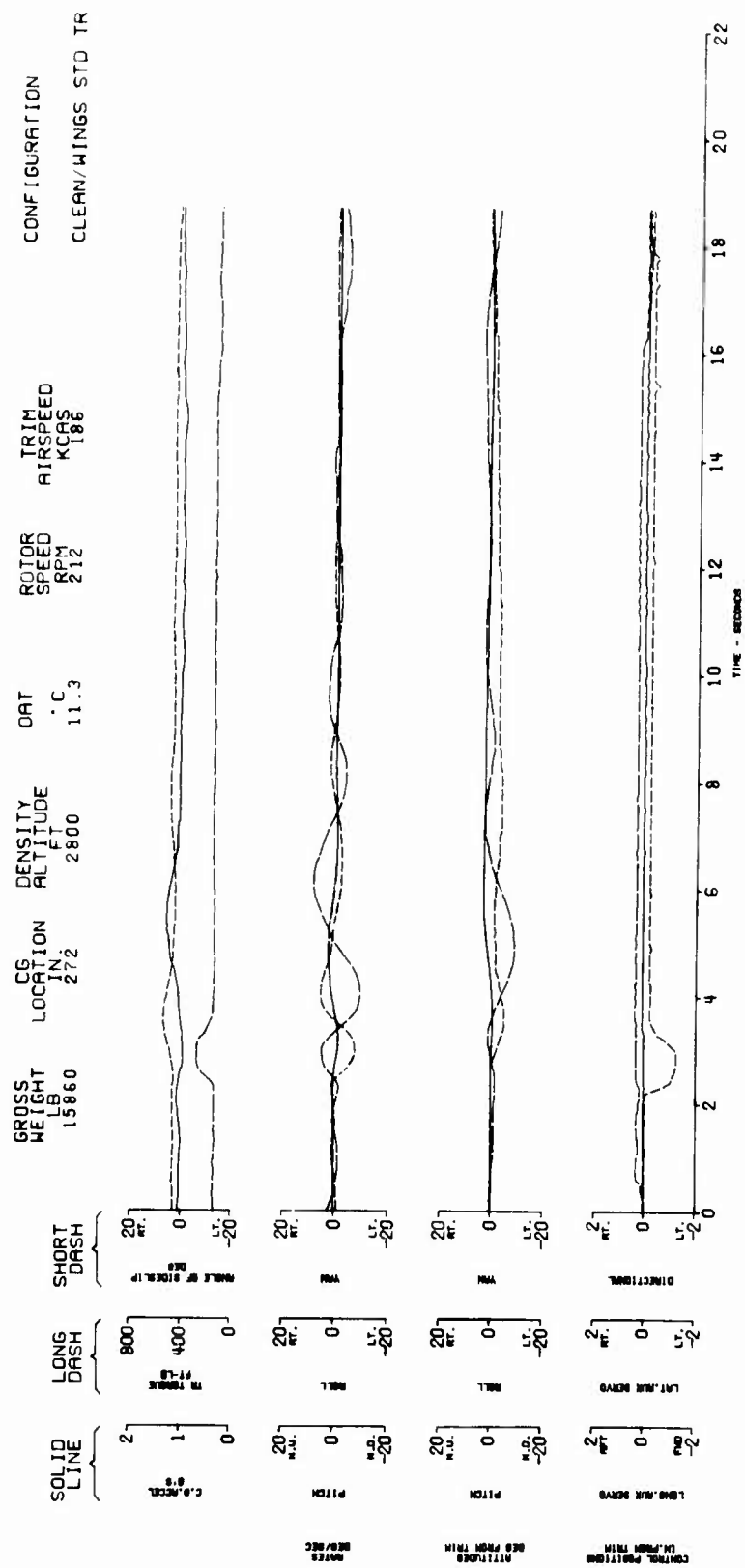


Figure 80. S-67 Tail Rotor, Level Flight 180 KIAS, 1-inch 1/2-sec Left Pedal Pulse.

TABLE 6. YAW DISPLACEMENT AFTER ONE
SECOND, ONE INCH PEDAL INPUT

CONFIGURATION	FAN-IN-FIN Degrees	TAIL ROTOR Degrees
MIL-H-8501A 1-inch	4.2	4.2
Predicted		
Left Pedal	8.104	-
Right Pedal	6.804	-
Flight Test Results		
Left Pedal	7.8	6.2
Right Pedal	7.8	6.2

The rapid applications of full directional control in hover or from a side-flight condition at 35 knots, section 3.3.5 and 3.3.6 in Reference 3, could not be evaluated because of a lubrication problem in the fan gearbox. Several times during maneuvers resulting in high centrifugal accelerations in the tail of the aircraft, the low oil pressure warning light for the fan gearbox illuminated. It went out immediately when the acceleration level decreased. The phenomenon was interpreted as resulting from oil in the sump sloshing away from the pump inlet as a consequence of high acceleration. The problem can be corrected by installing a baffle in the fan gearbox sump or a redesign of the oil inlet to the pump.

The values of directional control response for full application of directional control in hover and from a 35-knot side-flight condition were therefore calculated on the basis of test results. Figure 81 shows the calculated values of displacement achieved after 1 second versus right side-flight speed for the design conditions at 4000 feet, 95°F, at the design gross weight of 16,030 pounds (16,300 pounds for tail rotor configuration). The design goal for the fan-in-fin configuration was to meet the right side-flight and residual maneuvering capability requirement of MIL-H-8501A (Reference 3), section 3.3.6, and this has very nearly been achieved. In any case, the yaw control response provided by the fan in hovering and slow speed flight exceeds that of the tail rotor by an impressive margin.

Directional and Lateral Control Response

Directional control response as a function of airspeed is summarized in Figure 82. The pedal sensitivity of the fan-in-fin configuration is slightly higher than that of the tail rotor configuration but it has much less damping. For these reasons, the rates developed by the fan are higher than those for the tail rotor; however, for the fan, the peak rates develop about 0.8 second after control application, while the tail rotor rates peak after about 0.6 second. Therefore, the difference in displacement after 1 second is less than would be implied by the difference in peak rates on Figure 82. The lateral control response characteristics of the two configurations are essentially the same as is shown in Figure 83.

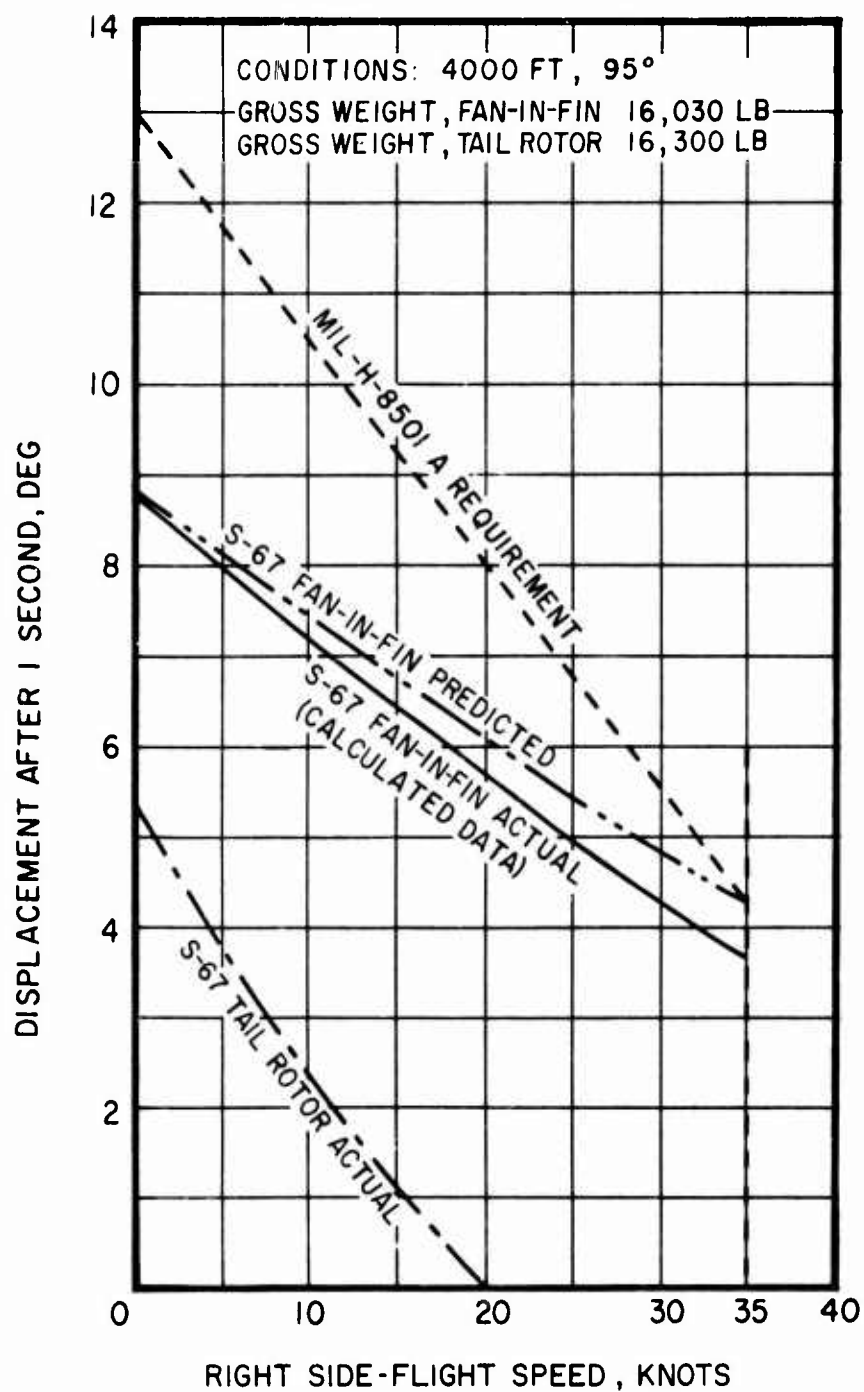


Figure 81. Comparison of Maneuvering Capability.

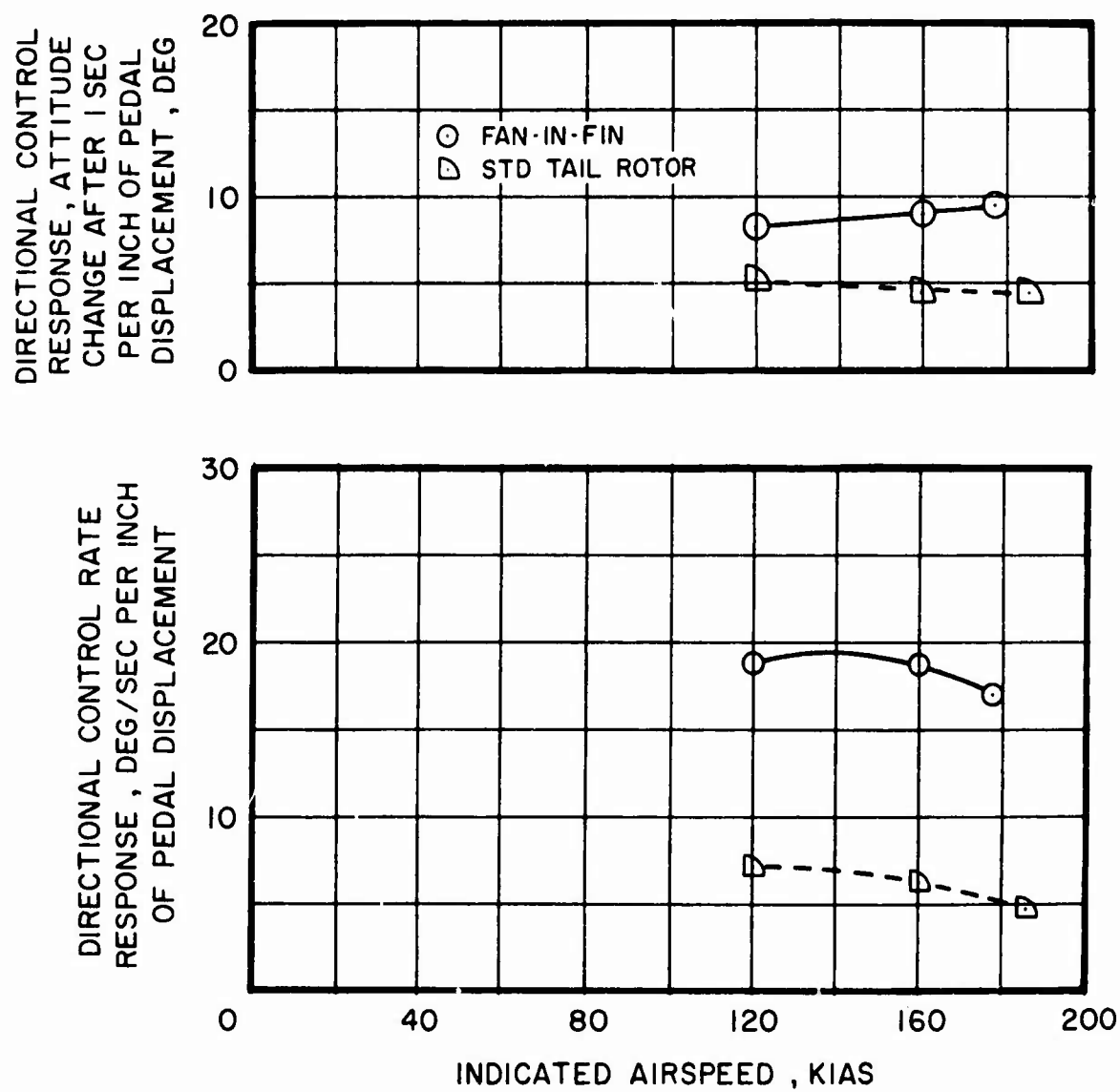


Figure 82. Comparison of Directional Control Response With Airspeed.

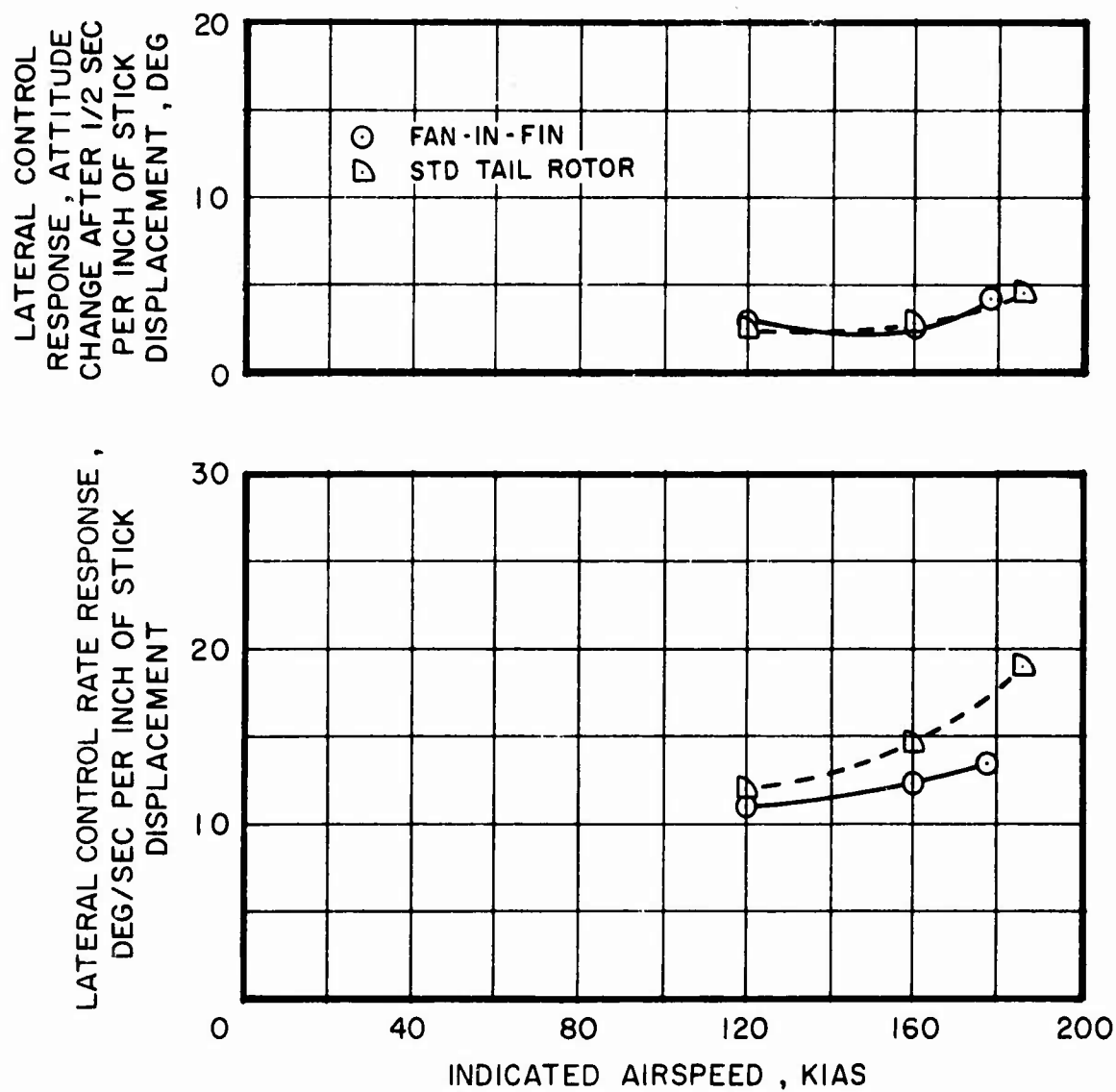


Figure 83. Comparison of Lateral Control Response With Airspeed.

Maneuvering Stability

Maneuvering stability characteristics were evaluated during wind-up turns and are summarized in Figures 84 to 86 for both configurations. The variation of longitudinal control position with normal acceleration was determined by trimming the aircraft in coordinated level flight at the desired speed and then rolling the aircraft to bank angles of 30 deg, 45 deg, and 60 deg in each direction. Collective control was fixed and airspeed held constant by losing altitude during the maneuver. The fan-in-fin aircraft longitudinal control gradient is essentially the same as that of the tail rotor configuration.

Adverse Yaw Characteristics

The adverse yaw characteristics of the two aircraft configurations were investigated by trimming the aircraft in a 30-deg bank angle turn and then applying a 2-inch lateral roll reversal holding pedals fixed. The change in sideslip which developed 1-1/2 seconds after the full control input (2-inch) is presented in tabular form in Table 7. As can be seen for most cases tested, the fan-in-fin configuration exhibits more adverse yaw than the tail rotor configuration.

TABLE 7. ADVERSE YAW COMPARISON: CHANGE
IN SIDESLIP 1-1/2 SECONDS AFTER
A 2-INCH LATERAL STEP INPUT

FORWARD SPEED KIAS	RIGHT ROLL REVERSAL		LEFT ROLL REVERSAL	
	Fan-In-Fin	Tail Rotor	Fan-In-Fin	Tail Rotor
100	-5.0	-4.0	5.5	3.5
180	-2.0	-1.0	2.0	2.0

Autotorotative Flight Characteristics

With speed brakes closed, autotorotative descents were flown at speeds of 20, 40, 80 and 120 KIAS to investigate directional control characteristics with the fan operating at near zero and negative blade angles. No difficulty was encountered during entry, flares, and power recoveries conducted at altitude. However, during descents up to 120 KIAS, aircraft directional response was sluggish and considerable pilot attention was required to maintain heading. This is caused by the reluctance of the fan flow to separate from the well rounded inlet lip at low negative fan thrust levels and probably by flow separation on the upper vertical fin at higher negative thrust levels. The minimum permissible rotor speed of 90% N_R was reached at 120 KIAS, the same as with the tail rotor configuration, which is therefore an operating limitation for both configurations with the speed brakes closed.

The autotorotative flight characteristics of the tail rotor configuration with speed brakes closed are good with precise directional control. However,

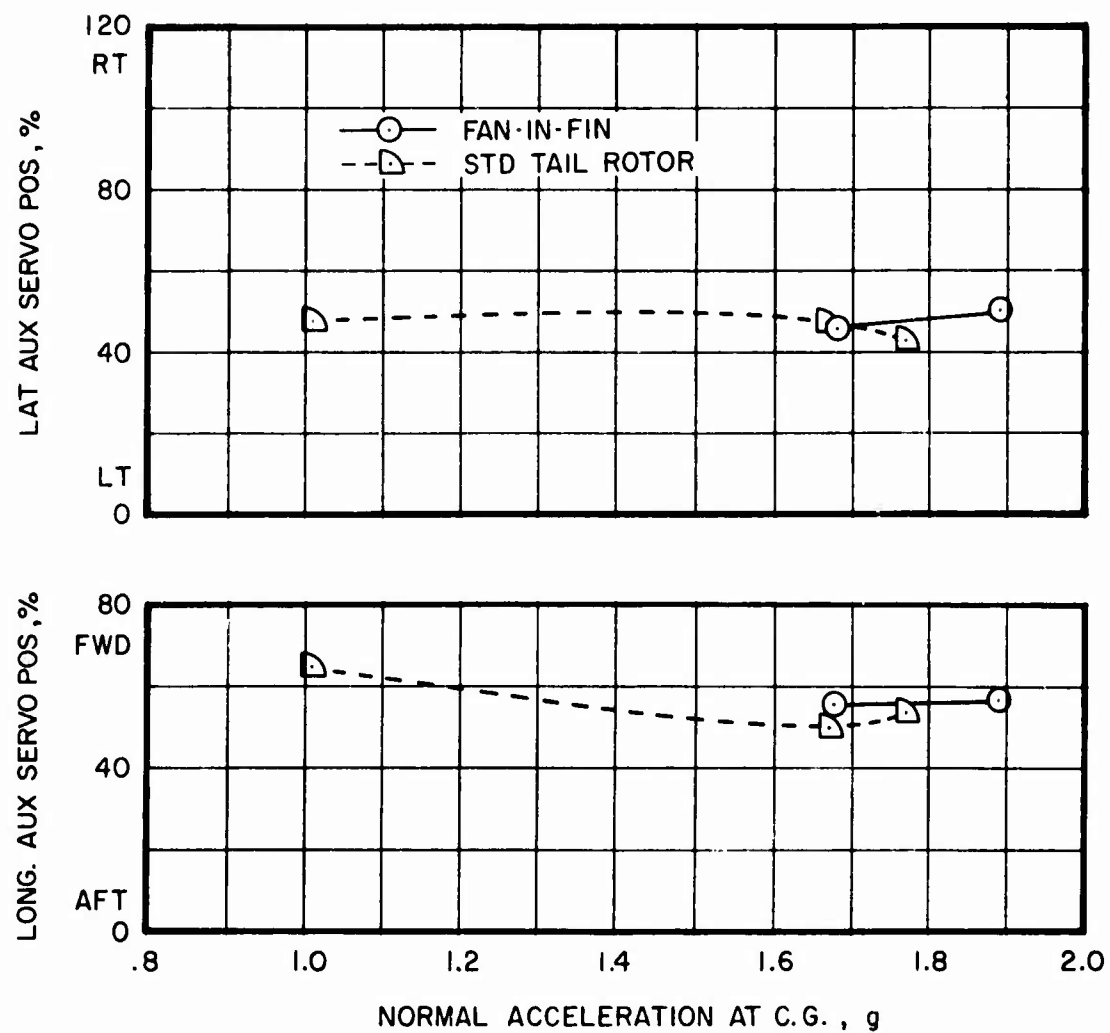


Figure 84. Comparison of Maneuvering Stability Characteristics at 80 KIAS.

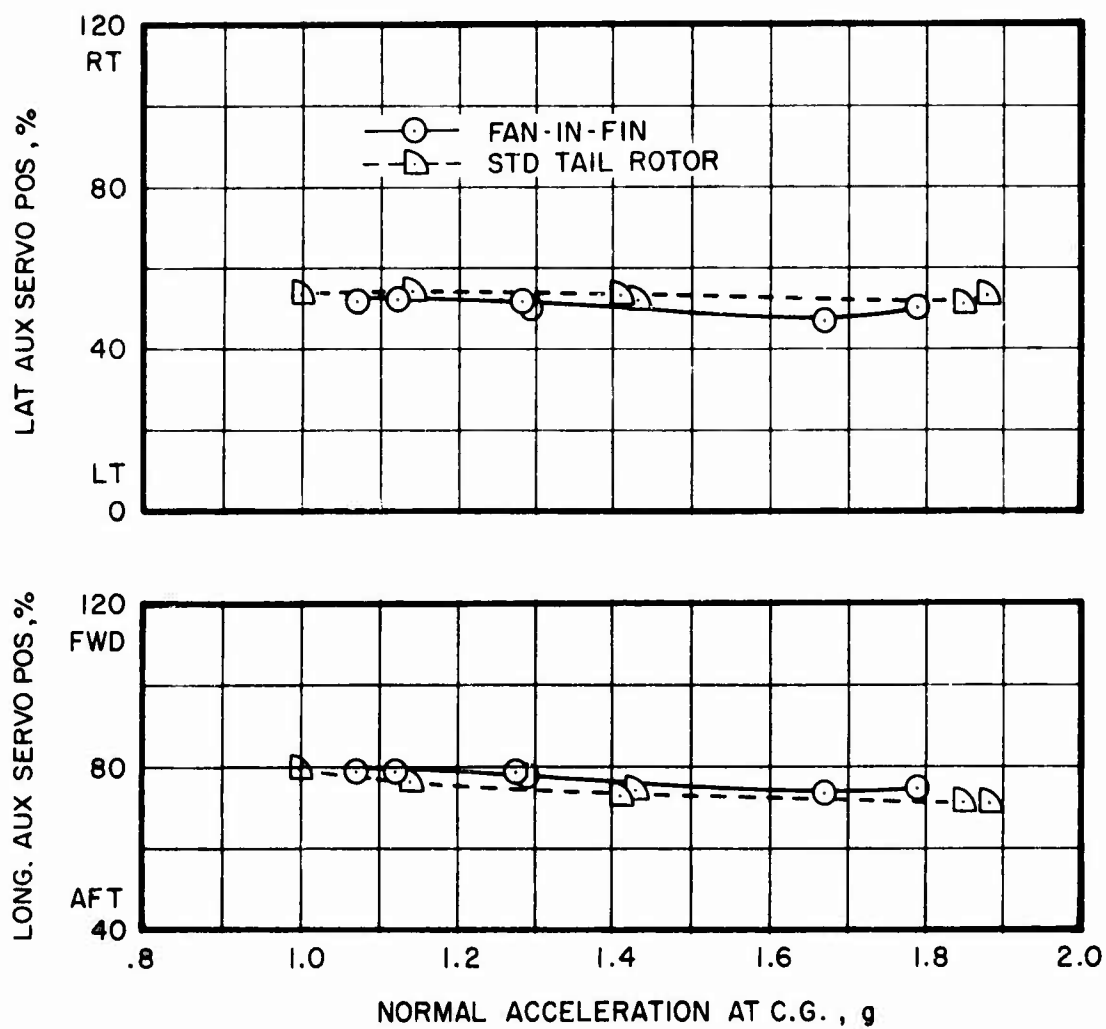


Figure 85. Comparison of Maneuvering Stability Characteristics at 140 KIAS.

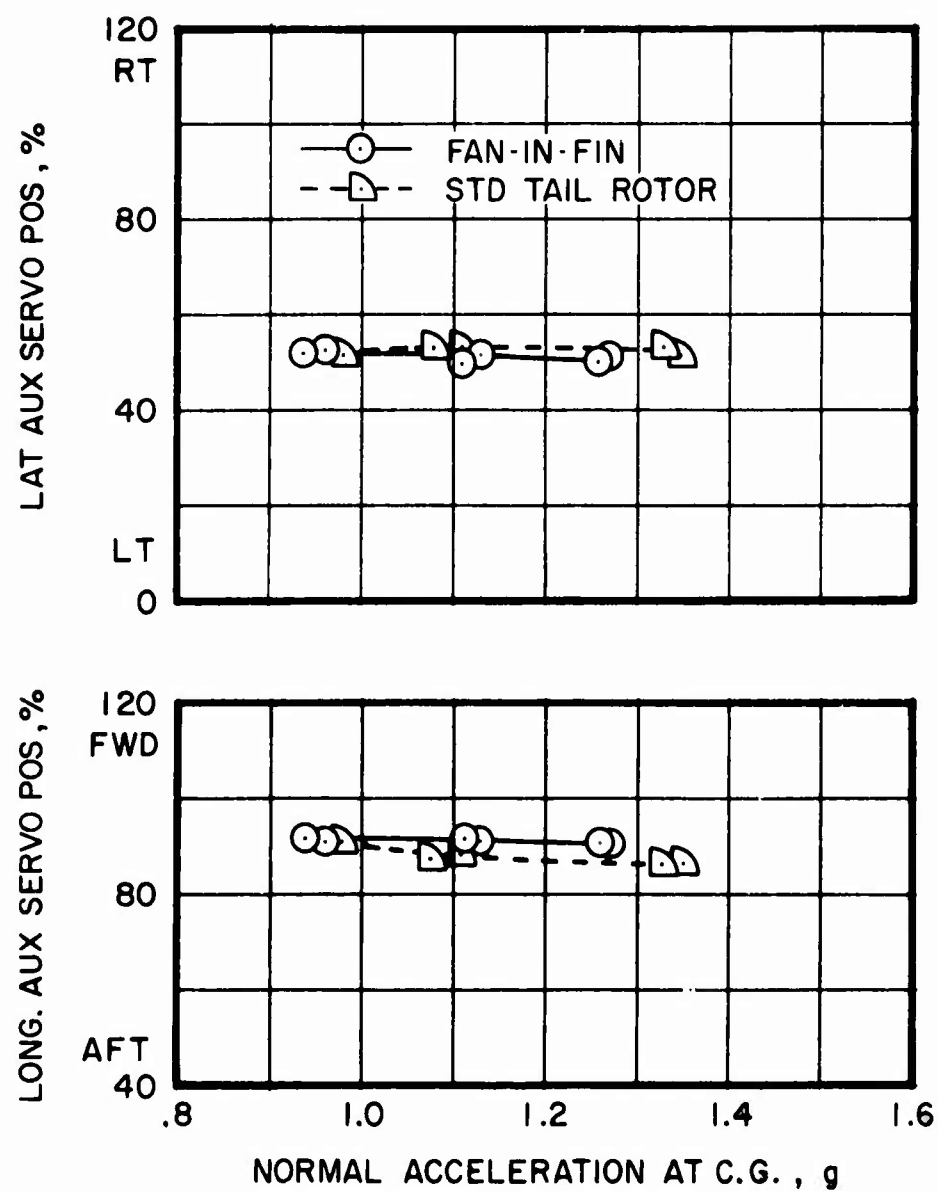


Figure 86. Comparison of Maneuvering Stability Characteristics at 177 KIAS.

in the tail rotor configuration both the upper and lower fins are cambered, requiring substantial right pedal to compensate for the fin force and maintain heading, with pedal runout occurring at about 130 KIAS. In the fan-in-fin configuration, the lower fin is symmetrical and adequate control margins remain over the entire autorotative speed range although the negative thrust capability of the fan is less than that of the tail rotor (-435 lb compared to -560 lb for the tail rotor at SLS).

With speed brakes open, the directional control characteristics for both configurations deteriorate as a consequence of the large mass of disturbed air engulfing the empennage section; however, the tail rotor configuration is less affected because of the larger diameter of the tail rotor and its installation at a higher waterline position.

The fan-in-fin configuration, with speed brakes open to eliminate wing lift, was tested at autorotative speeds up to 165 KIAS. The rotor speed remained at 98% N_R but rates of descent exceeded 6000 fpm. 165 KIAS is considered the maximum level flight condition at which an entry into autorotation can be performed followed by speed brake deployment, before blade stall becomes objectionable. Directional stability is poor at 120 KIAS and progressively deteriorates further with airspeed; however, control margins remain adequate.

No full autorotative roll-on landings were performed during this program. There was concern that the sluggish fan thrust response to control inputs and the fan thrust loss as a result of decay in rotor speed during autorotation would not permit adequate control during touchdown and rollout.

Taxi Characteristics

The S-67 fan-in-fin configuration displays insufficient directional control capability during taxi as a result of inadequate negative fan thrust and sluggish fan thrust response to control inputs. The inadequate negative fan thrust level available is a consequence of the limitation imposed by the use of the existing fan blade actuator.

The sluggish fan thrust response to control inputs at zero or low negative fan thrust levels is caused by the reluctance of the fan efflux to separate from the well-rounded inlet lip which in this operating regime becomes the exhaust. There is at this time no ready solution apparent to this problem that would not--like nonlinear control input or flow spoilers--impair fan operation in some other part of the aircraft operating envelope.

ACOUSTIC SIGNATURE

The series of noise measurements presented in Appendix C were undertaken to determine the noise levels and noise radiation characteristics of both the isolated fan and the S-67 fan-in-fin aircraft, and to compare the results with those from the isolated tail rotor and the S-67 tail rotor aircraft.

Measurements indicate that the fan is generally quieter than the tail rotor, yet most observers would judge it to be louder. The explanation is that the basic blade passage frequency of the fan, about 350 Hz, is clearly audible and detectable within the usual broad band helicopter noise. The distinctive sound of the fan can be identified even when several other tail-rotor helicopters are in the air simultaneously close to the S-67 fan-in-fin aircraft.

In Table 8, the total perceived noise levels of the S-67 fan-in-fin and the S-67 tail rotor aircraft configurations are compared for hovering flight. The data were recorded while the aircraft were in free hover at 100-ft wheel height and at gross weights of 15,800 lb. Microphones were placed at distances of 500 ft from a point directly below the aircraft at eight azimuth positions spaced at intervals of 45 deg. The table presents the recorded total aircraft noise levels in perceived noise levels (PNdB). The data show that during hover, the S-67 fan-in-fin is generally quieter than the S-67 tail rotor aircraft except in the left forward quadrant (fan exhaust side). The highest noise level of the fan-in-fin is about 3 dB lower than the highest noise level of the tail rotor configuration.

Table 9 presents cruise noise data acquired during passes at 200 ft altitude over a recording site at airspeeds of 80 KIAS, 120 KIAS, and 175 KIAS, at aircraft gross weights of approximately 16,000 lb. Noise measurements were taken during the aircraft's approach at distances of 2000 ft and 1000 ft from the recording site, when it was directly overhead, and when it had reached a distance of 1000 ft after the fly-over. The data are expressed in over-all sound pressure level (dB). A comparison of the data between the two aircraft configurations show that the S-67 fan-in-fin is louder than the S-67 tail rotor configuration at the relatively low sound pressure levels during approach and departure, but quieter when directly overhead.

TABLE 8. COMPARISON OF MEASURED TOTAL AIRCRAFT NOISE IN
HOVER OGE, 100-FT WHEEL HEIGHT, AT 500-FT DISTANCE

PERCEIVED NOISE LEVEL, PNdB

Microphone Location (At 500 Ft Distance) With Respect to Aircraft (45 deg Azimuth Spacing)	S-67 Tail Rotor Configuration PNdB	S-67 Fan-In-Fin Configuration PNdB
Forward	96	94
Right/Forward	96	95.8
Right (Fan/Tail Rotor Inflow Side)	100.5	97
Right/Aft	100.5	99
Aft	102	99
Left/Aft	101	98
Left (Fan/Tail Rotor Exhaust Side)	97	98
Left/Forward	96.5	98

TABLE 9. COMPARISON OF MEASURED TOTAL AIRCRAFT NOISE
DURING FLY OVER AT 200-FT ALTITUDE

Over-All Sound Pressure Level, dB
(dB Ref: 0.0002 bar)

Fly-Over Airspeeds: 80 KIAS, 120 KIAS, 175 KIAS

Measurements: - During Approach at 2000 Ft and
1000 Ft Distance
- Directly Overhead
- 1000 Ft Past Overhead

Airspeed During Fly-Over	Distance From Measurement Location	S-67 Tail Rotor Configuration	S-67 Fan-In-Fin Configuration
80 KIAS	Approach, 2000 Ft	71.5	75.0
	Approach, 1000 Ft	78.5	80.5
	Overhead	91.0	90.0
	Past Overhead, 1000 Ft	74.0	80.5
120 KIAS	Approach, 2000 Ft	76.5	80.0
	Approach, 1000 Ft	80.0	83.5
	Overhead	94.0	89.5
	Past Overhead, 1000 Ft	73.5	79.0
175 KIAS	Approach, 2000 Ft	85.0	92.0
	Approach, 1000 Ft	90.5	95.2
	Overhead	101.0	100.5
	Past Overhead, 1000 Ft	78.5	78.5

IMPLICATIONS FOR S-67 FLIGHT ENVELOPE

The normal operating limitations of the S-67 aircraft were observed throughout the entire flight test program. Within the scope of the planned fan-in-fin flight tests, a suitable recommended aircraft flight test envelope was established. This envelope is essentially the same as that for the tail rotor configuration, except as defined below.

Autorotation

1. Maximum Autorotation Airspeed with speed brakes closed was defined as 120 KIAS (same as tail rotor). Limitations: Minimum allowable power-off rotor speed of about 90% N_R at the test gross weight.
2. Maximum Autorotation Airspeed with speed brakes open was defined as 165 KIAS (120 KIAS for tail rotor). Limitations: Practicality of the condition, defined by rate of descent in excess of 6000 fpm at 98% rotor speed and only a small margin (lower rotor speed and/or higher airspeed) remaining before blade stall becomes objectionable. No control or structural limits were encountered during these maneuvers.
3. Auterotative Landings - No full autorotation landings were performed because of the known insufficient right directional control power and sluggish fan response experienced during ground operations (taxi turns). Autorotation roll-out would occur at rotor speeds well below 104% and possibly less than 90% rotor speed. A build-up test sequence would have been required to investigate the feasibility and techniques of performing this type of maneuver, and this was beyond the scope of the program.

Sideslip Envelope

Aircraft maximum sideslip angles were defined for level flight to V max and 200 KIAS dives and for partial power descents to V max (177 KIAS), as shown in Figure 87. Limitation: Practicality of the condition, defined by uncomfortable roll attitudes (30 to 35 deg) and slip angles beyond any flight requirement. Roll-to-slip angle ratios at 140 KIAS and V max were approximately 2:1 and 3:1 respectively. No control or structural limits were encountered during autorotations and climbs at 80 KIAS.

Ground Taxi

Recovery from a left taxi turn at normal rates required nearly full right pedal travel. Limitations: Maximum taxi turn rates of 15 deg/sec in winds of 8-12 knots and 20 deg/sec in winds of 0-7 knots were limited by insufficient directional control power. It should be noted that turn recoveries, if led with pedal well ahead of intended headings, can be performed safely at the maximum turn rates defined herein.

Low-Speed Maneuvers

Sideward Flight maneuvers (limited to 35 knots by scope of program) were performed to the left and right with adequate control available. Recoveries

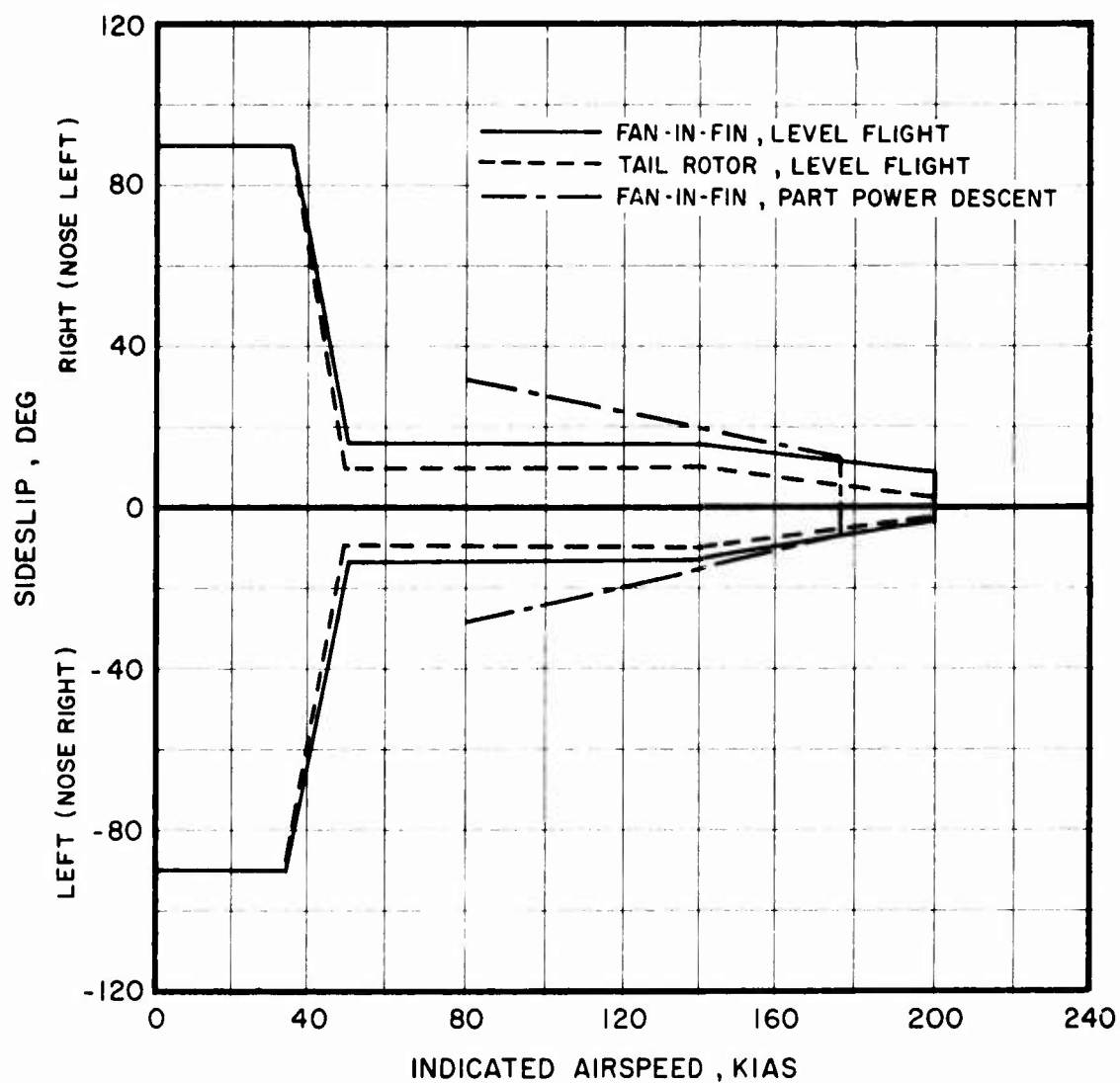


Figure 87. S-67 Sideslip vs Speed Envelope.

from 20-30 knots rearward flight should be initiated only to the right to prevent temporary fan gearbox oil pressure loss (fan oil pump inlet redesign could alleviate this limitation). The severity of the recovery from left or right sideward flight at rapid hovering turn maneuvers could also create a momentary loss of fan gearbox oil pressure.

Approaches to a hover or landing following failure of a single stage of fan servo should be conducted only into a head wind or a left cross-wind since a left turn into a 12-knot wind stopped at 90 deg of turn until considerably more left pedal was added. This was essentially as predicted due to directional control cable stretch.

Main rotor droop stop contact during recoveries from low-speed translational flight may occur due to the excessive aircraft pitch-up tendency with power application and resultant application of forward longitudinal cyclic control. This presents a flight limitation on the aircraft.

OPERATIONAL POTENTIAL

APPLICATIONS

The fan-in-fin concept offers considerable operational advantages over conventional tail rotors. The greatest potential for this design is improved safety for ground personnel and reduced attrition due to elimination of tail rotor strikes.

It is generally accepted that future Army helicopter operations will be conducted principally in the nap of the earth (NOE) mode, taking advantage of terrain to reduce combat losses. Early experience in Vietnam taught that flying at altitude was an appropriate tactic, but the realities of radar-directed automatic weapons and heat-seeking missiles demand a change.

In recent years, field experiments have indicated that the average Army aviator today cannot possibly survive in the low NOE flight profile without extensive and formal training. Methods, techniques, and equipment must be used that can facilitate this training and prepare pilots for operation in a mid-intensity conflict. The fan-in-fin is a helicopter design feature that will facilitate NOE flight and NOE flight training.

In Vietnam most tail rotor blade strikes occurred during hover and parking operations. In 1969 alone, tail rotor strikes were the direct cause of 250 accidents. In addition, 11 persons were injured or killed as a result of being struck by rotating tail rotor blades. Accident reports cite such examples as one aircraft backing into another, suffering damage while backing out of revetment areas, landing in confined areas with insufficient tail rotor clearance, and tail rotor strikes of high tension wires on takeoff. Total destruction of aircraft often resulted. It can be expected that the ducted fan will decrease the severity of damage suffered in such accidents.

Nap-of-earth flight demands close crew coordination, alert undivided attention to terrain avoidance, and primarily head-out-of-the cockpit procedures. This precision is even more demanding at night. Army field experiments have shown that it is almost impossible to maintain a precise hover position at night without outside visual references; small movements, descent rates, lateral movements, and drift are virtually unnoticeable. Reduction of the hazards of tail rotor strikes in these confined area operations will reduce crew workload and fatigue, increase safety and survivability, and improve mission reliability and availability.

U. S. Army flight experiments are currently under way to determine capabilities of the attack helicopter team concept in a night anti-armor role. In addition to day NOE, night flight, as close to the ground as vegetation and obstacles permit, is also a required capability for survival on the mid-intensity battlefield. Where previously less than 10% of an aviator's flight time occurred during darkness, one-third to one-half of his combat time may now require night flight.

By U. S. Army estimates, approximately 75% of helicopter primary mission flight time in future combat operation may be conducted in the low-speed NOE and hover mode. The excellent maneuver capability, in combination with the reduced susceptibility to damage, that the fan-in-fin can provide should make this concept attractive for application to future Army Helicopters operating in a combat zone.

RELIABILITY AND MAINTAINABILITY

The total number of operating hours of the fan in the S-67 aircraft is 35.1 hours, of which 29 hours are flight time and 6.1 hours are ground tie-down test time. During this time, no problems were encountered with the fan. Partial disassembly inspection, performed every 10 hours of fan operating time, showed the hardware to be in excellent condition. There was no indication of unusual wear, overheating, or other adverse effects.

The maintenance required for the flight fan was limited to periodic disassembly inspection, with no need for spare parts or repair actions. On the basis of this limited experience, visual inspection intervals are projected to be extended from 10-hour intervals to a much longer interval for any future test program involving the fan.

It would be inappropriate, from this limited test experience on a single unit, to make reliability and maintenance predictions for large-scale field service of fans, because the data are statistically insignificant. In addition, the fan is not representative of a production configuration in several respects, and its installation in the airframe incorporating a thrust measurement system is not typical. In addition, the main rotor bifilar vibration was not retuned for the fan installation, so aircraft vibration characteristics, which are of predominant importance for reliability, are not representative of a helicopter designed initially with a fan.

A substantial amount of operational experience with a fan-in-fin has been acquired by the French SA-341 Gazelle. The reliability of the Fenestron appears to be good, and maintenance requirements are comparable to those of a tail rotor.

Yet, there are considerable differences in the mechanical implementation of the fan-in-fin concept. The fenestron has 13 blades, each retained by a tension-torsion strap and guided in a dry Teflon bearing permitting blade pitch-angle changes. The fan has 7 blades, each retained by an oil-lubricated ball bearing to react centrifugal loads and bending moments, and to permit blade pitch-angle changes. These are differences in detail design which do not permit application to one design of operational experience acquired with the other. Which one of the two approaches is better is as yet undetermined.

In comparing a tail rotor installation with a fan installation, it should be noted that many tail rotors need to be installed on pylons to provide the necessary ground clearance, while for a fan this can be avoided. The fan installation eliminates the intermediate gearbox and the shaft between the intermediate and tail gearbox, resulting in reduced maintenance requirements and inevitably higher reliability.

Apart from differences in rotational speed, the drive system bevel gearbox is essentially similar for the tail rotor and the fan. Also, the means of controlling blade pitch angle are similar up to the output of the servo, which is necessary in either case. The essential differences between fan and tail rotor appear in the blades and in the blade pitch-change mechanism. As there are different concepts in fan detail design, there are different concepts in tail rotors: flapping hinge, teetering, and cross-beam tail rotors, involving different types of blade design. Any meaningful comparison between fan and tail rotor in the area of reliability and maintainability would, therefore, have to involve specific designs.

Strictly on the basis of the number of parts involved (blades and blade pitch-change mechanism), the fan should fare no better than the tail rotor despite the fact that the blade pitch-change mechanism of the fan is usually protected by a fairing. However, the fact that there is no blade flapping or other out-of-plane motion in the fan should result in a much more favorable vibration environment that could easily compensate for the disadvantage of the higher number of parts. Omitting the retuning of the main rotor bifilar vibration absorber during this program resulted in increased vibration levels caused by the main rotor throughout the airframe and masked the fan's own vibration environment. In view of the potential benefits to reliability and maintainability, the main rotor bifilar vibration absorber should be retuned for any further flight testing of the S-67 fan-in-fin aircraft, and the resulting vibration environment should be carefully monitored.

ABRASION

Despite the higher inflow velocities it is not expected that blade abrasion will be a problem in the operational use of the fan-in-fin. This was confirmed by the limited flight testing on the S-67 which resulted in no noticeable abrasion. When the fan is operating at normal RPM, close to the equivalent tail rotor speed, the inevitably higher disc loading of the fan results in increased inflow velocities and up to a 20% increase in the relative kinetic energy of any abrading particles carried by the air. This is not felt to be significant. As with a tail rotor, however, abrasion protection will be required in unfavorable environments such as would be met in desert operation.

During both ground and flight testing inlet abrasion was negligible and is not expected to present any operational problems. Abrasion levels in service would be roughly equivalent to those met in forward facing engine inlets.

CONCLUSIONS AND RECOMMENDATIONS

LIMITS OF COMPARISON

Before final conclusions can be drawn from the results of this program, it is valuable to review some of the basic differences between the tail rotor and the fan as used in the S-67 airframe.

The 10-ft 7-in. tail rotor was not specifically designed for the S-67 aircraft. It is a standard SH-3D production part which, with some limitations, proved to be adequate for the higher speed of the S-67. Tail rotor mechanical stress limitations restricted the aircraft's side-flight capability; thrust capability or control range restricted the side-slip envelope, autorotation entry speed, and high-power climbs. By contrast, the fan was designed to supply the higher thrust levels required for an enlarged operating envelope and to accommodate the associated increased stress levels. Thus, it would obviously be wrong to credit the fan itself for actual or potential expansion of the flight envelope. The important fact is not that the fan outperformed the tail rotor, but that it did so without major problems.

On the other hand, experimental modification of an existing helicopter to serve as a test bed for a novel component may have deprived the fan of the opportunity to show itself in the best light. Most of the differences noted in aircraft characteristics point in the direction that the fan configuration is worse than the tail rotor. In fact, most of these differences, except for reduced lateral directional instability, result from aircraft problems associated with design around constraints imposed by test bed and existing hardware. Thus, it is essential to make a clear distinction between aircraft problems and fan problems. As an example, it is reasonable to assume that the fan, without flapping hinges and therefore with one degree of freedom less, would run more smoothly than the tail rotor. However, the vibration data recorded in the tail section of the fan-in-fin aircraft are dominated by increased levels of main rotor n-per-revolution vibration. The main rotor bifilar vibration absorber was not retuned for the fan-in-fin configuration, and this omission sufficiently upset the tuning that previously existed between the main rotor, airframe, and tail rotor, to mask the fan's own vibration characteristics.

The primary advantage claimed for the fan in comparison with the tail rotor is its reduced susceptibility to damage in ground operations and increased safety for ground personnel. This advantage was not demonstrated in this program, nor was such a demonstration an objective of this program.

CONCLUSIONS

1. The fan-in-fin is an acceptable alternate for the tail rotor in applications where a small decrease in hover performance can be tolerated.
2. The fan-in-fin configuration suffered from main rotor downwash impingement effects on the horizontal stabilator in the slow speed regime as

a consequence of the forward shift of the stabilator. This problem is not caused primarily by the fan.

3. This fan could provide full directional control without a rudder within the flight envelope explored (See Appendix B).
4. The fan-in-fin aircraft configuration demonstrated a considerable decrease in directional stability. The primary reason for this decrease is loss of effectiveness of the upper vertical fin as a result of flow separation in left sideslip caused by fan efflux at negative fan thrust.
5. In cruise condition with wings level, the fan-in-fin aircraft demonstrated decreased directional stability resulting in difficulty to obtain and hold precise yaw trim within a narrow range. The reason for this characteristic is interaction of fan blade induced flow with the fan inlet flow field.
6. The fan-in-fin aircraft showed a reduction in maximum level flight speed from 193 KTAS to 190 KTAS as a consequence of parasite and momentum drag increases. The parasite drag increases are associated with the experimental installation and might be avoided in production configurations.
7. The results of the tethered hover performance measurements are inconclusive owing to the uncertainties of the method employed. Using an incremental approach that is based on the test results, the hover gross weight capability of the fan-in-fin configuration is shown to be reduced by about 1½% as compared to the tail rotor configuration.
8. Fan performance was remarkably free of aerodynamic problems. Based on correlation with observed fan and inlet performance, and the results of tuft studies in forward flight, the analysis used in the design is considered to model the flow field properly.
9. Even though an observer might judge the fan to be louder than the tail rotor and it had a distinctive sound that made it easily recognizable, noise measurements showed it to be quieter than the tail rotor.
10. The fan-in-fin aircraft configuration had insufficient negative thrust capability for taxi operation as a consequence of constraints imposed by the hydraulic fan blade actuator. Insufficient negative fan thrust at reduced rotational speeds prevented full autorotative roll-on landings.
11. Directional control during taxi was marginal as a consequence of sluggish fan thrust response to control inputs. This is a consequence of reverse flow effects when operating a fan with highly twisted blades in a duct optimised for flow predominantly in one direction.
12. The S-67 fan-in-fin aircraft configuration demonstrated an improved side-flight capability with large control margins remaining.

RECOMMENDATIONS

1. The feasibility of relocating the horizontal stabilator should be investigated to eliminate the disturbing interference between main rotor wake and horizontal stabilator and possibly the fan wake and horizontal stabilator in low-speed maneuvers.
2. Fan controls should be modified to provide more negative thrust margin.
3. Reduced fan blade twist, possibly in combination with increased blade root chord, should be investigated to realize potentially beneficial effects on fan noise characteristics and fan thrust response.
4. A full-scale wind tunnel test program should be instituted to determine the reasons for, and define possible design approaches to overcome, some of the problems peculiar to the fan encountered during the flight test program. The following specific areas should be investigated:
 - . Flow separation on the upper vertical fin caused by reversed fan flow, identified as the major cause of the reduced lateral directional stability.
 - . Interaction of fan and fan inlet flow field, identified as the cause of unprecise yaw trim in cruising flight.
 - . Inlet flow behavior at low negative thrust levels, identified as the cause of the sluggish fan thrust response to control inputs in operating conditions requiring near-zero and low absolute values of negative thrust.

LIST OF REFERENCES

1. Grumm, Arthur W., and Herrick, Groves E., ADVANCED ANTITORQUE CONCEPTS STUDY, Sikorsky Aircraft, USAAMRDL Technical Report 71-23, Eustis Directorate, U.S. Army Air Mobility Research and Development Laboratory, Fort Eustis, Virginia, July 1971, AD 72960.
2. Velazquez, J. L., ADVANCED ANTITORQUE CONCEPTS STUDY, Lockheed California Co., USAAMRDL Technical Report 71-44, Eustis Directorate, U.S. Army Air Mobility Research and Development Laboratory, Fort Eustis, Virginia, August 1971, AD 731493.
3. HELICOPTER FLYING AND GROUND HANDLING QUALITIES: GENERAL REQUIREMENTS FOR, MIL-H-8501 A, Military Specification, U.S. Government Printing Office, Washington, D. C., April 1968.
4. Hickey, D. H., and Ellis, D. R., WIND TUNNEL TESTS OF A SEMISPAN WING WITH A FAN ROTATING IN THE PLANE OF THE WING, NASA TN D-88, October 1959.
5. Kelley, H. L., and West, T.C., FLIGHT INVESTIGATION OF EFFECTS OF A FAN-IN-FIN YAW CONTROL CONCEPT ON HELICOPTER FLYING-QUALITY CHARACTERISTICS, Langley Directorate, U.S. Army Air Mobility R&D Laboratory, Hampton, Va., NASA TN D-7452, March 1974.
6. Kaplita, T. T., INVESTIGATION OF THE STABILATOR ON THE S-67 AIRCRAFT, Sikorsky Aircraft Division of United Aircraft Corporation, SER-67006, USAAMRDL Technical Report 71-55, Eustis Directorate, U.S. Army Air Mobility Research and Development Laboratory, Fort Eustis, Virginia, October 1971, AD 735766.
7. O'Conner, S. I., and Fowler, D. W., S-67 AIRCRAFT FEEL AUGMENTATION SYSTEM FLIGHT EVALUATION, Sikorsky Aircraft, Division of United Aircraft Corporation, SER-67009, USAAMRDL Technical Report 72-41, Eustis Directorate, U. S. Army Air Mobility Research and Development Laboratory, Fort Eustis, Virginia, August 1972, AD 749284.
8. Monteleone, R. A., INVESTIGATION OF THE MANEUVERABILITY OF THE S-67 WINGED HELICOPTER, Sikorsky Aircraft Division of United Aircraft Corporation, SER-67008, USAAMRDL Technical Report 73-51, Eustis Directorate, U.S. Army Air Mobility Research and Development Laboratory, Fort Eustis, Virginia, June 1973, AD 767559.

APPENDIX A. FAN DESIGN AND DESCRIPTION

FAN DESIGN APPROACH

Aircraft systems studies showed that the fan, while meeting thrust requirements to satisfy the adopted yaw control criteria, could be designed within a range of diameters limited on the low side by available power and on the high side by fan weight or the aircraft aft center-of-gravity limit (at low fuel state). The smallest possible diameter of 4 ft 8 in. was chosen primarily because compactness enhances the lower susceptibility of the fan to damage in accidents by comparison with the tail rotor. Compactness, therefore, becomes a design objective for the fan. Criteria contributing to this choice were lower drag in cruise and higher useful load, the lower power available to the main rotor being a lesser penalty to the aircraft than the higher fan weight associated with a larger fan diameter.

It was realized during preliminary design that the fan to be built for this program would be primarily a research tool and therefore not necessarily optimum for other purposes though entirely flightworthy and meeting performance requirements. Its design was based on a conservative approach consistent with the necessarily limited development program planned. This approach was intended to provide a cost effective, highly reliable fan for purposes of research.

This approach entailed using the following:

- . Solid aluminum blades rather than higher cost, lightweight, composite spar-shell blades.
- . Milled parts rather than castings and forgings.
- . Conservative design practices with respect to operating stress levels rather than designing to minimum weight.
- . Minimum machining for weight reduction purposes.

As currently designed for the S-67 fan-in-fin aircraft, the fan weighs 332 pounds, including fan rotor, actuator, support vanes, and fluids, but excluding shroud and mounting provisions. Based on current technology and results of the flight evaluation, a study has been conducted that predicts a possible minimum weight of 160 pounds for a fan of this capacity. The technology items considered in the study were as follows:

- . High-pressure blade pitch-change actuator integral with the fan.
- . Lightweight aluminum spar, fiber glass shell blade design. This item is of particular significance because of its impact on the actuator and structural components.
- . Precision castings and forgings with appropriate consideration given to weight control.

- . All components sized to aerodynamic requirements and structural loads established during the flight evaluation.
- . Experimental stress analysis techniques to confirm structural integrity and identify areas of practical weight reduction.

FAN DESIGN AND OPERATION

The fan assembly is shown on Figure A-1. It consists of a self-lubricated controllable pitch tractor fan with seven blades, a right angle gearbox with a self-contained lubrication system, and a blade pitch change system.

Power is supplied to the fan from the tail drive shaft through a spiral bevel gear mesh with a reduction ratio of 39/41. The input pinion interfaces with the aircraft drive shaft through a flexible coupling.

The gearbox utilizes a pressure lubrication system which includes a lubrication and scavenge pump, pressure regulating valve, and a chip detector. Oil is routed to orifices at each tailshaft bearing and to a spray bar for gear lubrication. The hot oil from the gears and bearings drains to a sump located at the bottom of the gearbox where it is scavenged and pumped to a reservoir. Measurements of oil pressure and temperature as well as chip detection are provided. Lubrication of the blade retention and part of the pitch change system is provided by oil retained within the hub and separate from the gearbox lubrication system.

Oil cooling is accomplished by convection between the gearbox housing and air passing over the housing. Cooling air is directed into the centerbody aft of the fan blades, flows over the gearbox, and is ejected overboard at the rear of the centerbody.

The fan assembly is centered within the shroud (see Figure 5) by three equally spaced support vanes which are attached to the gearbox housing at the inner end and to the airframe mount points at the outer end. The shroud is attached to the three static support vanes but is free-floating with respect to the airframe. It consists of the well-rounded inlet lip, the center duct, and the exhaust lip. The complete fan and shroud assembly is installed in the airframe at the tips of the static support vanes by means of two-point attachments. Tangential links react the drag loads and axial links incorporating a load cell react the thrust loads. These load cells permit measurement of the combined fan and inlet lip thrust.

Blade pitch change is accomplished by a CH-53 tail rotor tandem hydraulic actuator with servo valve and linkage assembly which is supplied by two independent airframe hydraulic systems.

FAN BLADE CHARACTERISTICS

Pertinent fan blade characteristics are shown in Figure A-2.

The fan blade was designed to operate under an optimum free vortex distribution of loading. The resulting design maintains the free vortex loading

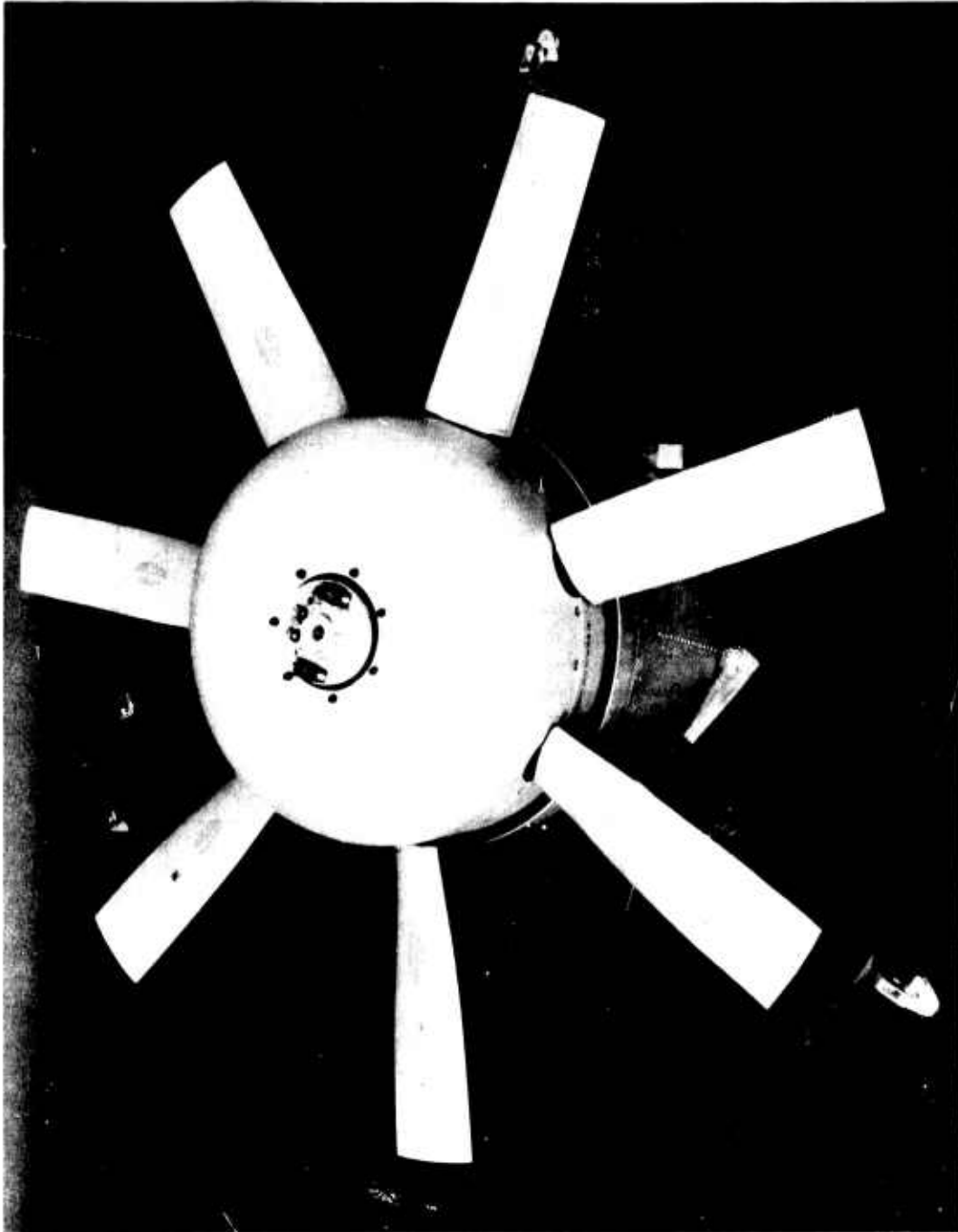
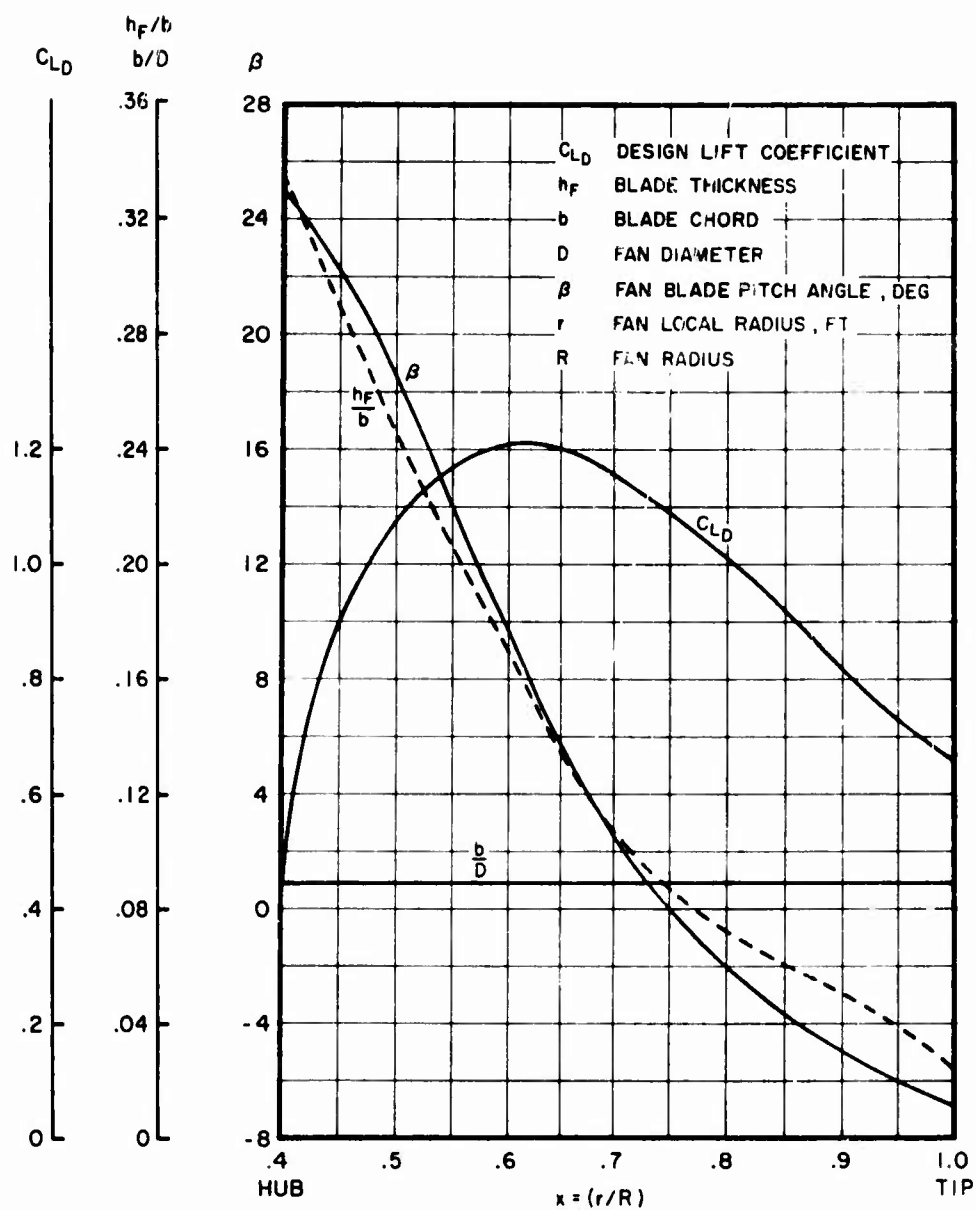


Figure A-1. Fan Assembly.



NACA 16 - SERIES AIRFOIL SECTIONS

$$C_{L_i} = 4 \int_{x=0.4}^{x=1} C_{LD} x^3 dx = 0.9$$

Figure A-2. Fan Blade Characteristics, $C_{L_i} = 0.9$.

distribution from approximately $r/R = 0.6$ to the blade tip, $r/R = 1.0$. The high required loading could not be obtained inboard because of the high blade thickness and limited chord. The integrated lift coefficient of the blade ($C_{L_i} = 0.9$) is a compromise determined by the shape of the thrust/power curve. High values of C_{L_i} reduce fan power requirements at high positive thrust but power requirements increase in the negative thrust regime. The blade twist distribution is optimised for the fan design condition, right side flight at 35 knots. The blade feathering axis was chosen to coincide with the 50% chord line in order to minimize blade tip losses over the entire blade angle range although this results in high blade centrifugal twisting moments. Blade chord is constant to avoid any further increases in these moments and to remain within the force and stroke capability of the designated blade pitch change actuator. Blade thickness is kept to a minimum consistent with structural requirements.

It was realized that some improvement to performance could be achieved by a wider blade root chord, and that some reduction in noise would be possible with less blade twist (the latter measure would benefit handling qualities as well). However, the constraints imposed by the bore and stroke capability of the blade pitch change actuator prevented any further increases to blade chord, and the limited power available to the fan required high blade twist to meet performance.

The minimum number of fan blades required to meet performance with the available power while remaining within the capability of the blade pitch change actuator is seven. There was no apparent advantage in adopting a higher number of blades, so the smallest possible number was chosen.

EXCERPTS FROM FAN SPECIFICATION

Axis Convention (with respect to aircraft)

- X: Longitudinal axis, plus aft
Y: Lateral axis, plus left (looking forward)
Z: Vertical axis, plus up

Design Limit Conditions

The angular rates for structural design, acting separately, are listed below:

$$\dot{\alpha}_x = \pm 150 \text{ deg/sec for } .00014 \text{ sec/hr}$$

$$\dot{\alpha}_y = \pm 60 \text{ deg/sec}$$

$$\dot{\alpha}_z = \pm 60 \text{ deg/sec for } .0008 \text{ sec/hr}$$

The fan shall be designed (structural integrity and mounting) to the following crash loads. The values are ultimate, acting separately:

$$N_x = 8.0g$$

$$N_y = \pm 3.0g$$

$$N_z = 8.0g$$

Flight Vibration Environment (Main Rotor or Aircraft Induced)

Vibration	Frequency	Amplitude (\pm g's)
5-per-revolution vertical	17.5 Hz	1.2 g's*
5-per-revolution lateral	17.5 Hz	.5 g's
Tail shake	5.7 Hz	.5 g's

* This value is typically .5 g's below 140 knots.

Rotational Speed

The normal rotational speed of the fan shall be 2997 RPM (equivalent to a tip speed of 732 ft/sec at 104% N_R). The maximum power-on RPM shall be 3199 (782 ft/sec at 111% N_R). The maximum power-off RPM (at design limit rotor speed) shall be 3372 (824 ft/sec at 117% N_R). The minimum power-off RPM shall be 2623 (641 ft/sec at 91% N_R). The minimum power-on RPM shall be 2766 (676 ft/sec at 96% N_R). The maximum fan acceleration is 105 rad/sec².

Installed Fan System Stability

The installed fan shall be free from mechanical instability and from weaving and flutter during all operating conditions. The installed fan blades shall be free of flutter, divergence and any other aeroelastic instability at rotational speeds up to 1.15 times the design limit rotor speed without power at 1.15 V_D . (1.15 times 3372 RPM equals 3878 RPM at 1.15 times 200 knots equals 230 knots). There shall be no significant resonances of the fan throughout the operating range of the helicopter, as defined herein.

Fan Unbalance

The maximum fan rotating system static unbalance shall not exceed 0.1 in.-lbs. Capability for "fine tune" balance on the aircraft shall be provided. Aerodynamic balance will be controlled to comply with the requirements of paragraph "Installed Fan System Stability" (above). Blade pitch spread shall not exceed 0.3 deg measured at the 75% blade radius station.

Environmental Requirements

The fan shall be capable of operating in ambient temperatures from -65°F to 130°F and from sea level to 10,000 feet. In addition, the fan system shall operate from 0 to -0.5g for 5 seconds, for sustained conditions between $\pm 15^\circ$ of pitch attitude and for sustained conditions between $\pm 25^\circ$ of uncoordinated roll attitude.

Fan Fatigue Life

The fan shall have a minimum 3 sigma fatigue life of 3600 hours and a bearing calculated B_{10} life of 3600 hours. The operating spectrum for the bearing life calculations is shown in the Table Speed/Time/Usage Spectrum (below). The operating spectrum for the fatigue life calculation is shown in Table Spectrum of Time at Inflow Conditions (second below).

Speed/Time/Usage Spectrum

Mission Time Distribution

<u>Condition</u>	<u>% Time</u>
Hover	5.0
Hover, Left turn	2.5
Hover, Right turn	2.5
Ascent	2.25
Transition	0.5
Descent	2.25
Cruise	81.675
V _{max}	2.5
Dive	0.825

Speed Distribution

<u>Airspeed</u>	<u>% Mission</u>
0 KTAS	10.0
70	5.0
100	11.7
130	53.5
180	16.5
185	2.5
200	0.8

Spectrum of Time at Inflow Conditions

<u>Inflow Conditions</u>	<u>% Time</u>
Hover	5.
Hover and Left Yaw	2.5
Hover and Right Yaw	2.5
Left Side Flight 35 Knots	0.001
Right Side Flight 35 Knots	0.0023
Trimmed Forward Flight 35 Knots	1.0
Left Yaw 45° at 50 Knots	0.0005
Right Yaw 45° at 50 Knots	0.005
Trimmed Flight at 50 Knots	4.0
Trimmed Flight at 100 Knots	11.7
Left Yaw 30° at 100 Knots	0.0005
Right Yaw 30° at 100 Knots	0.0005
Left Yaw 15° at 150 Knots	0.0005
Right Yaw 15° at 150 Knots	0.0005
Trimmed Flight at 150 Knots	70.0
Left Yaw 5° at 200 Knots	0.0001
Right Yaw 5° at 200 Knots	0.0001
Trimmed Flight at 200 Knots	3.275
Roll Maneuvers at 150 deg/sec	0.014

APPENDIX B. RUDDER EVALUATION

DESCRIPTION

The rudder with an area of 10 ft² is installed at the trailing edge of the upper vertical fin and is equipped with a tab to reduce flight control loads. The rudder is operated in unison with the fan and can travel 20 deg to the left and right of neutral. It can be biased up to 8 deg trailing edge left or right from the unbiased position by an electrically operated actuator controlled from the cockpit.

The reasoning behind combining fan and rudder for directional control was that fan flow behavior and fan performance was too uncertain to be relied upon exclusively at the anticipated level flight and dive speeds (in excess of 200 KTAS).

FLIGHT TESTS

For the early flights, fan gain was set at 100% (full range) with rudder travel at ± 20 deg from neutral. As the speed envelope expanded, the pilots reported that yaw control was overly sensitive, and above 150 KTAS was objectionable. As a corrective measure, the rudder travel was reduced to ± 12 deg from neutral, which brought considerable improvement as well as the desire to carry this measure one step further, namely, to lock the rudder. The rudder was locked in neutral position and the aircraft flew, performed, and handled well throughout the entire flight envelope, including dives, climbs, sideslips, descents, and autorotation.

The intention had been to investigate various combinations of reduced fan gain with different rudder bias settings until the optimum combination emerged. In light of the favorable finding that the fan could satisfy directional control requirements without the assistance of the rudder, the program was reoriented to eliminate the rudder from the flight control system. The data presented in the basic report apply to this condition which is an optimum cruise configuration for 160 KTAS, 3000 ft density altitude, and a gross weight of 16,000 lb.

CONCLUSION

The fan could handle directional control requirements without assistance from a rudder within the flight envelope explored. At speeds beyond those flown during this program, such as achieved by helicopters with auxiliary propulsion, the need for a rudder must again be investigated.

APPENDIX C. ACOUSTIC EVALUATION

The acoustic signature of the fan was assessed on three different occasions. Isolated fan noise was measured during the static performance tests on Sikorsky's tail rotor test stand, with the fan installed in a simulated fin module. A second noise survey was conducted during the aircraft tie-down tests. The third series of signature measurements was made during flight tests in hover and forward flight.

The basis for comparison is similar acoustic data taken under practically identical conditions with the S-67 tail rotor configuration. For isolated tail rotor noise, previously measured data were used. When measured data were not available, a mean value between SH-3 tail rotors with 10-ft 4-in. and 11-ft diameters was used.

ISOLATED FAN NOISE

Fan noise was measured while the fan was undergoing static tests on Sikorsky's tail rotor test stand, operating at rotor speeds of 2720, 3000, and 3300 RPM. Noise measurements were obtained on a 10-ft radius from the center of the fan rotor. This selection of measurement location eliminated the normal ground reflection problems associated with conventional, lower frequency rotors. Three data stations were monitored: (1) 45 deg off the tip path plane on the major lobe side of the fan (exhaust side), (2) directly on the tip path plane, and (3) 45 deg off the tip path plane on the minor lobe (inlet) side of the fan. At least ten blade pitch settings were evaluated for each rotor speed. Winds were less than five knots.

The tests indicate that the fan-in-fin is quieter when operating at high thrust levels (fan blade pitch angles from 10 deg to 25 deg) than at low thrust levels. Although this behavior is the opposite of that noted for tail rotors and conventional fans (where an increase in thrust raises the noise levels), it is not surprising in view of the high blade twist design employed. The high blade twist became necessary to meet the thrust levels required within the constraints imposed by the available power and the force and stroke limitations of the existing actuator.

A comparison of the fan-in-fin and the tail rotor at the same thrust values shows the fan to be up to 12 PNdB quieter at a 500-ft distance as is shown in Figure C-1. At low blade pitch angle values (-20 deg to +5 deg, fan thrust levels below 500 lbs), the fan generates noise levels above those of the tail rotor.

Figure C-2 shows the lobal patterns (patterns of constant noise levels) of the isolated shrouded fan and the isolated 10-ft 7-in. tail rotor. Both lobal patterns are calculated for a thrust level of 1000 lb. It is interesting to note that the fan generates a very similar lobal pattern but without the reductions observed for the tail rotor in the extension of the rotational or tip path plane.

Figures C-3, C-4, and C-5 show the PNdB levels of the fan-in fin obtained at the three measurement stations described previously. Figures C-3 and

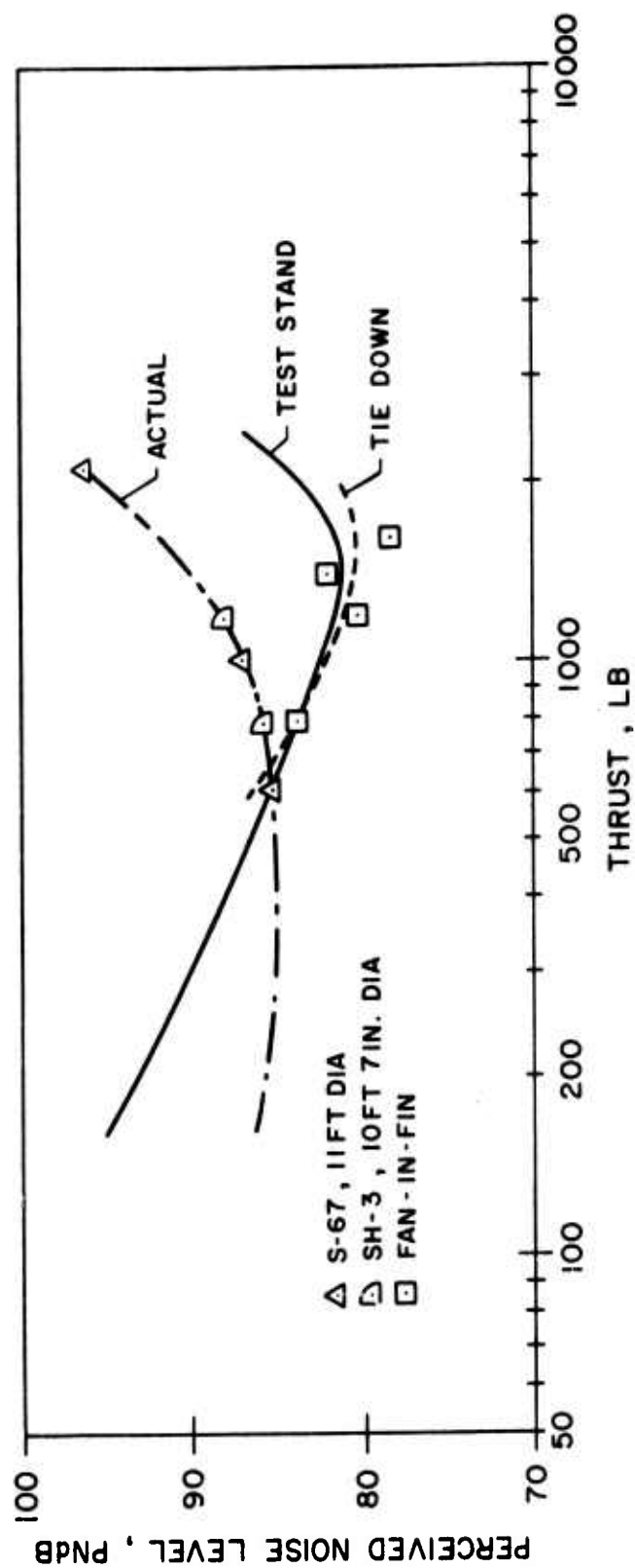
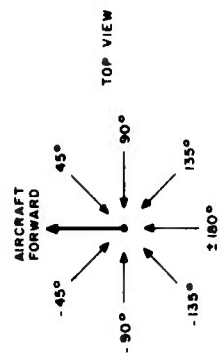


Figure C-1. Fan and Tail Rotor Perceived Noise Levels vs Thrust, Exit Side, -45-deg Azimuth (45 deg Off Tip Path Plane), 500-ft Distance.

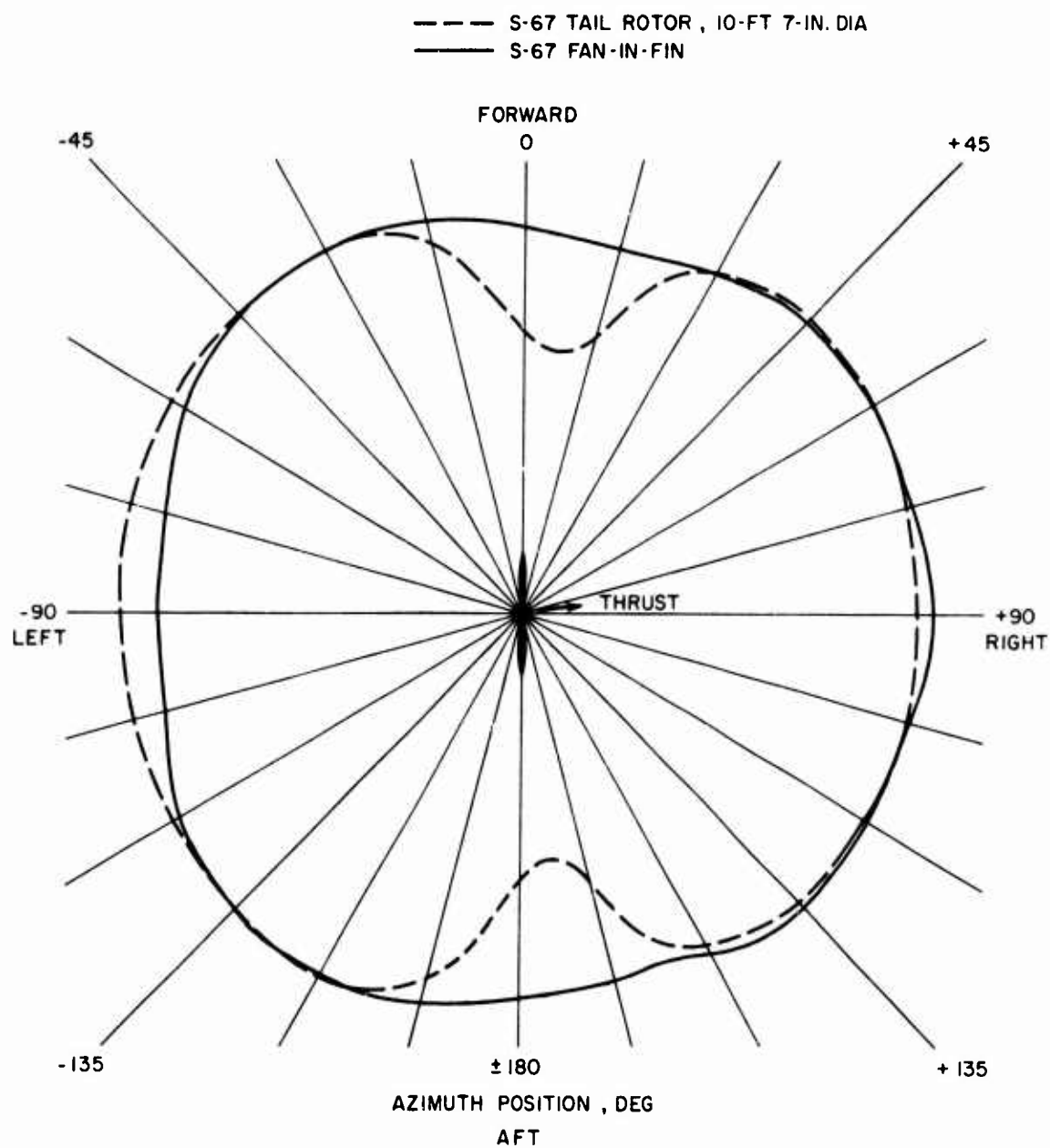


Figure C-2. Calculated Lobal Patterns (Constant Noise Levels) for the Isolated Fan and Tail Rotor, Thrust \approx 1000 lb.

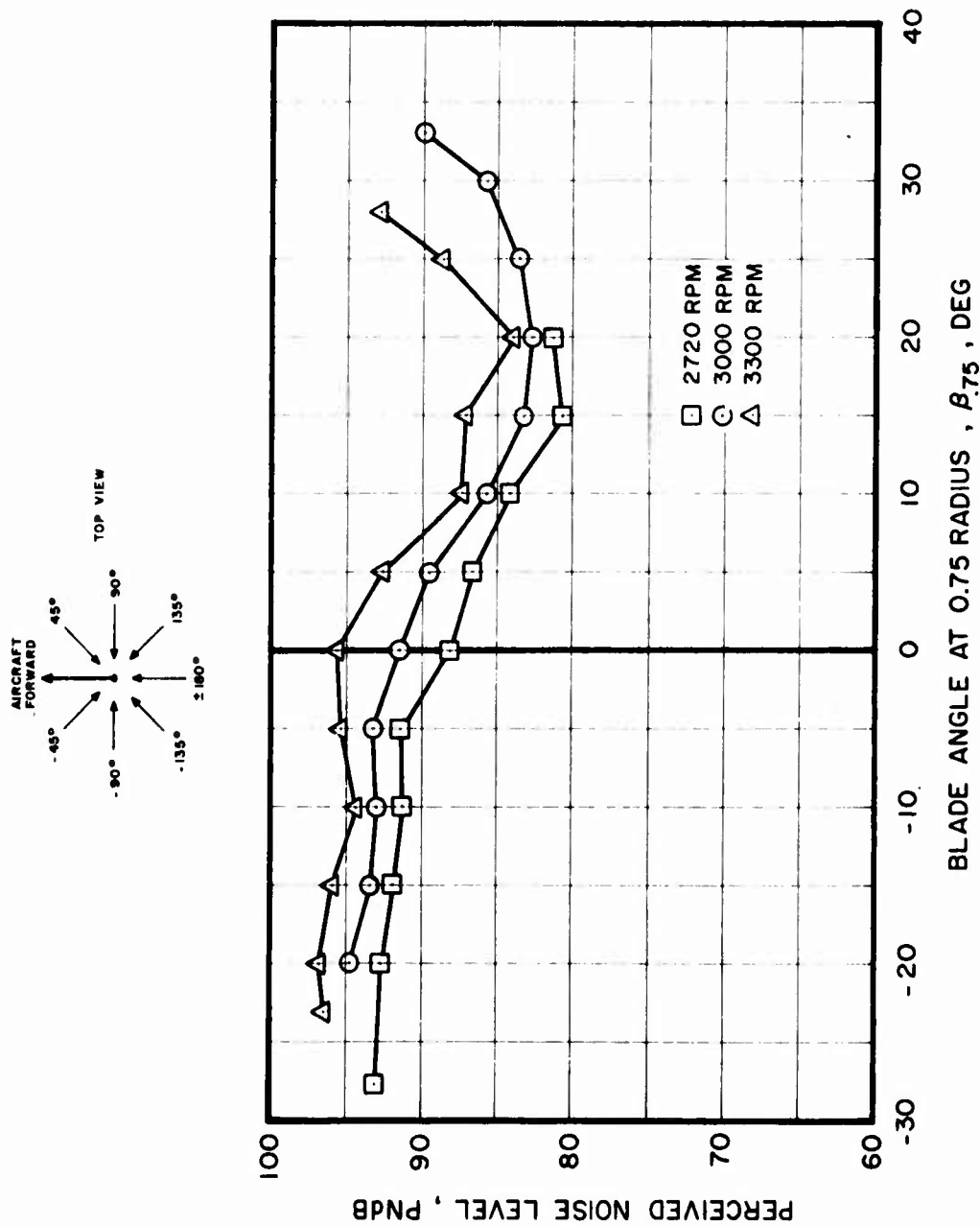


Figure C-3. Fan-in-Fin, Test Stand, PNdB vs Fan Blade Pitch Angle, Exit Side, -135-deg Azimuth (45 deg Off Fan Tip Path Plane), 500-ft Distance.

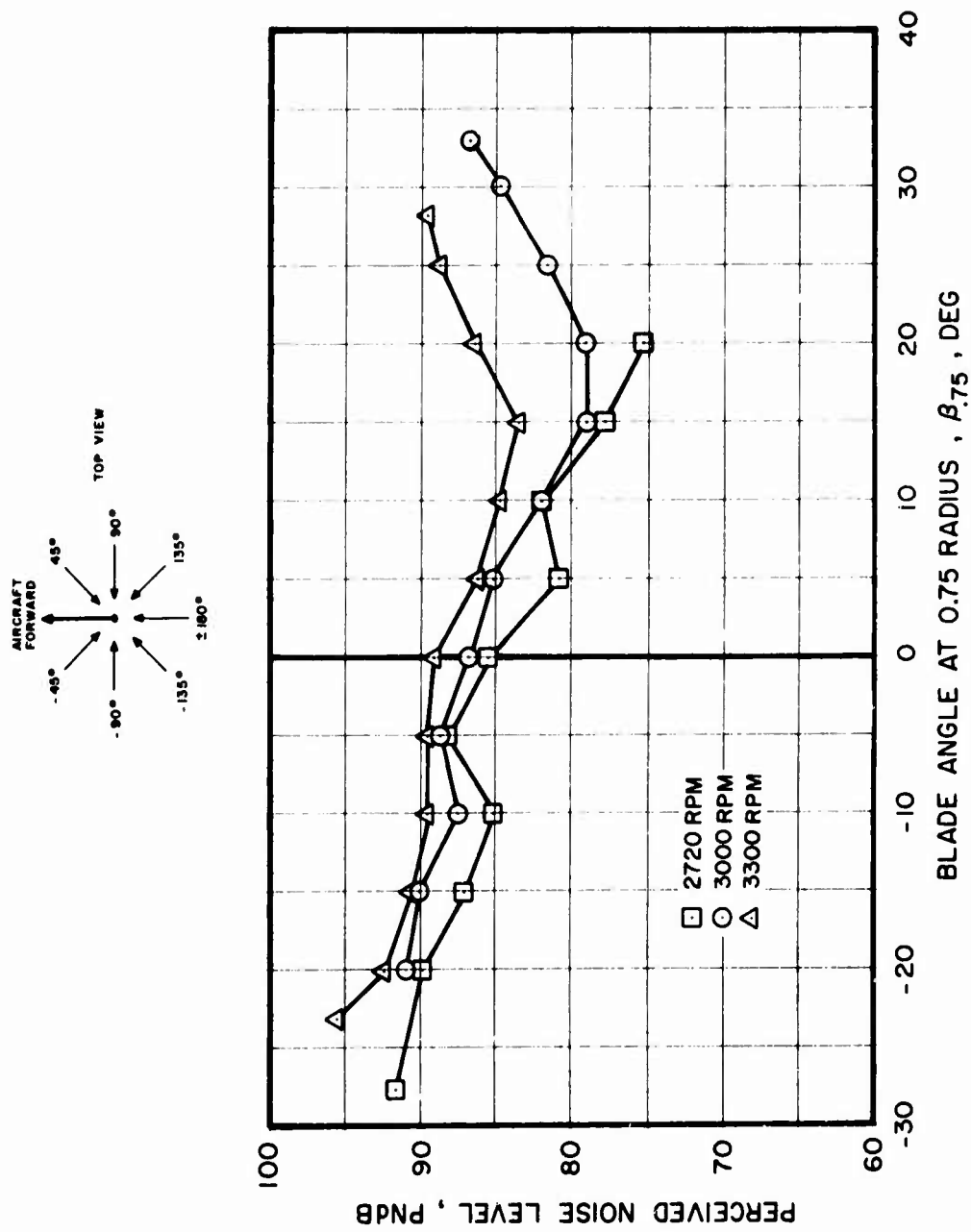


Figure C-4. Fan-in-Fin, Test Stand, PNdB vs Fan Blade Pitch Angle, ± 180 -deg Azimuth (On Fan Tip Path Plane), 500-ft Distance.

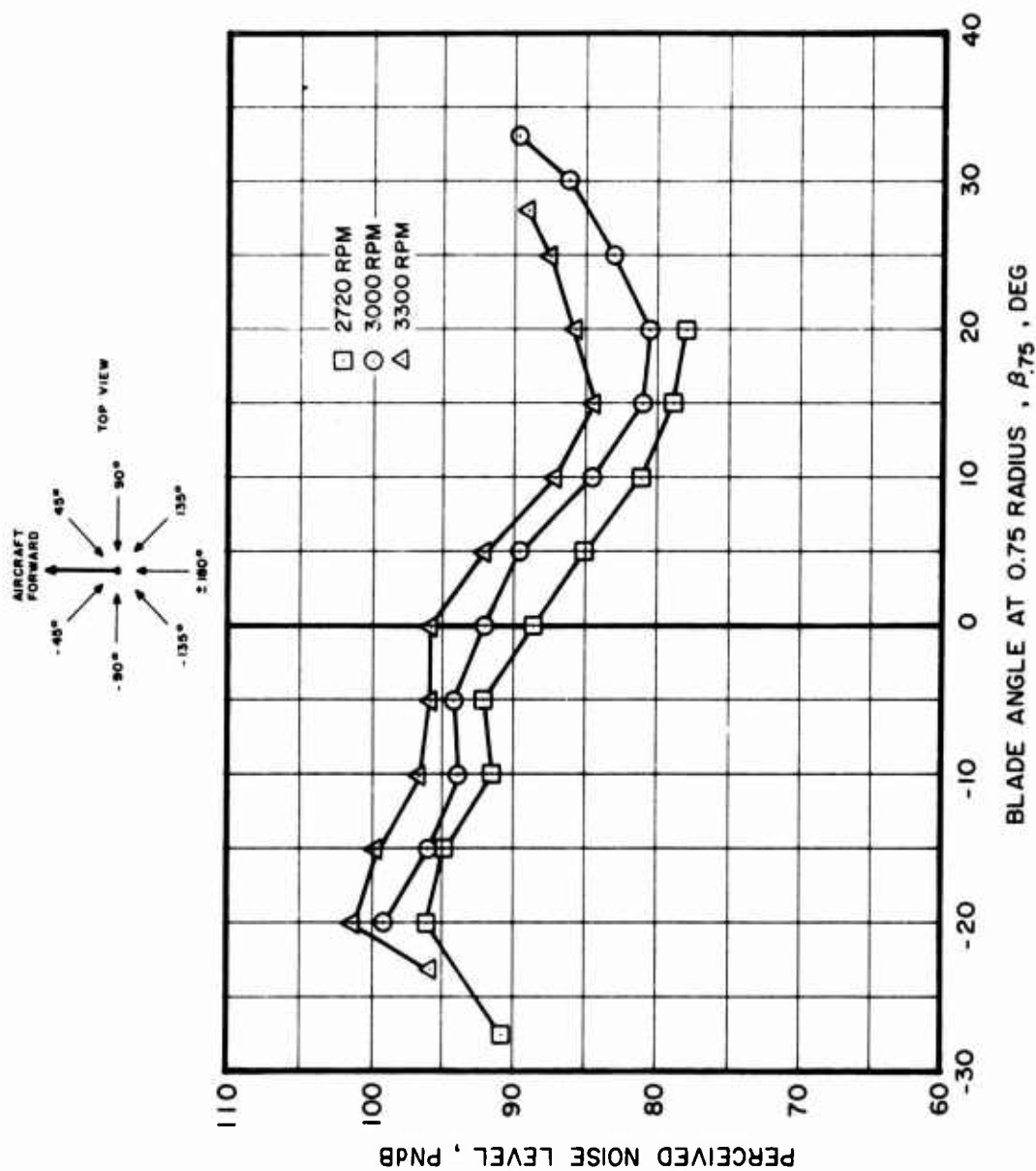


Figure C-5. Fan-in-Fin, Test Stand, PNdB vs Fan Blade Pitch Angle, Intake Side, +135-deg Azimuth (45 deg Off Fan Tip Path Plane), 500-ft Distance.

C-5 show an increase in noise level as RPM is increased. Figure C-4 has the same general trending but shows some variations that may be attributed to distortion of the airflow by the shroud. In the normal operating range of the fan (10 deg to 25 deg pitch), a decrease in noise level with increasing pitch is evident at each measurement location, independent of rotor speed, as is shown in Figure C-6. This appears to be a general characteristic of the fan, related to the highly twisted blades used. Figure C-7 shows the relationship between fan blade pitch and thrust for the three rotor speeds.

Figure C-8 is a 1/10 octave band spectra comparison between the tail rotor and the fan-in-fin, both generating 1000 pounds of thrust on the test stand (typical for anti-torque thrust in hover). An almost constant reduction is achieved by the fan throughout the indicated frequency range. Only in the fundamental harmonic region of the fan (350 Hz) is the level greater than that of the SH-3 tail rotor. This comparison, when related to perceived noise level, resulted in a 12 PNdB reduction at a 500-ft distance.

AIRCRAFT TIE-DOWN TESTS

For the aircraft tie-down tests, no main rotor blades were installed, and only a single engine was used. Three data stations were monitored: (1) 45 deg off the tip path plane on the major lobe (exhaust) side of the fan, (2) directly on the tip path plane, and (3) 45 deg off the tip path plane on the minor lobe (inlet) side of the fan. All data were obtained at a radius of 15 ft from the center of the fan. A fan speed of 2997 RPM (104% N_R) was maintained, and various horsepower settings were evaluated. Winds were less than 5 knots.

From the data obtained, it was concluded that test-stand and aircraft-mounted configurations could be compared at only one azimuthal location, since the spectra at the remaining two locations were masked by engine noise. Pertinent fan-in-fin ground run data are lower by 1 PNdB than similar data obtained with the fan installed on the tail rotor test stand. However, the fan-in-fin did generate less noise at a 500-ft sideline distance (up to 12 PNdB) than the S-67 tail rotor.

Ground run azimuthal data free from any additional noise contributions are almost identical to the fan installation on the test stand at comparable thrust levels, within a band of 1 PNdB (Figure C-1). Other azimuthal data cannot be compared directly due to masking by the engine, which was used for powering the fan during ground runup.

The data presented in Figure C-1 are representative of the -45-deg azimuthal location (exhaust side of fan). This data point was picked for comparison, because it is the only one that is not influenced by other noise sources. This point is also the only one that substantiates the theory that noise levels should not change between test-stand installation and tie-down evaluation. As is evident by the data presented in Figure C-1, the installed test stand fan noise levels and tie-down fan noise levels are similar, resulting in a 12 PNdB reduction in maximum level over previously taken S-67 tail rotor data at comparable thrust values.

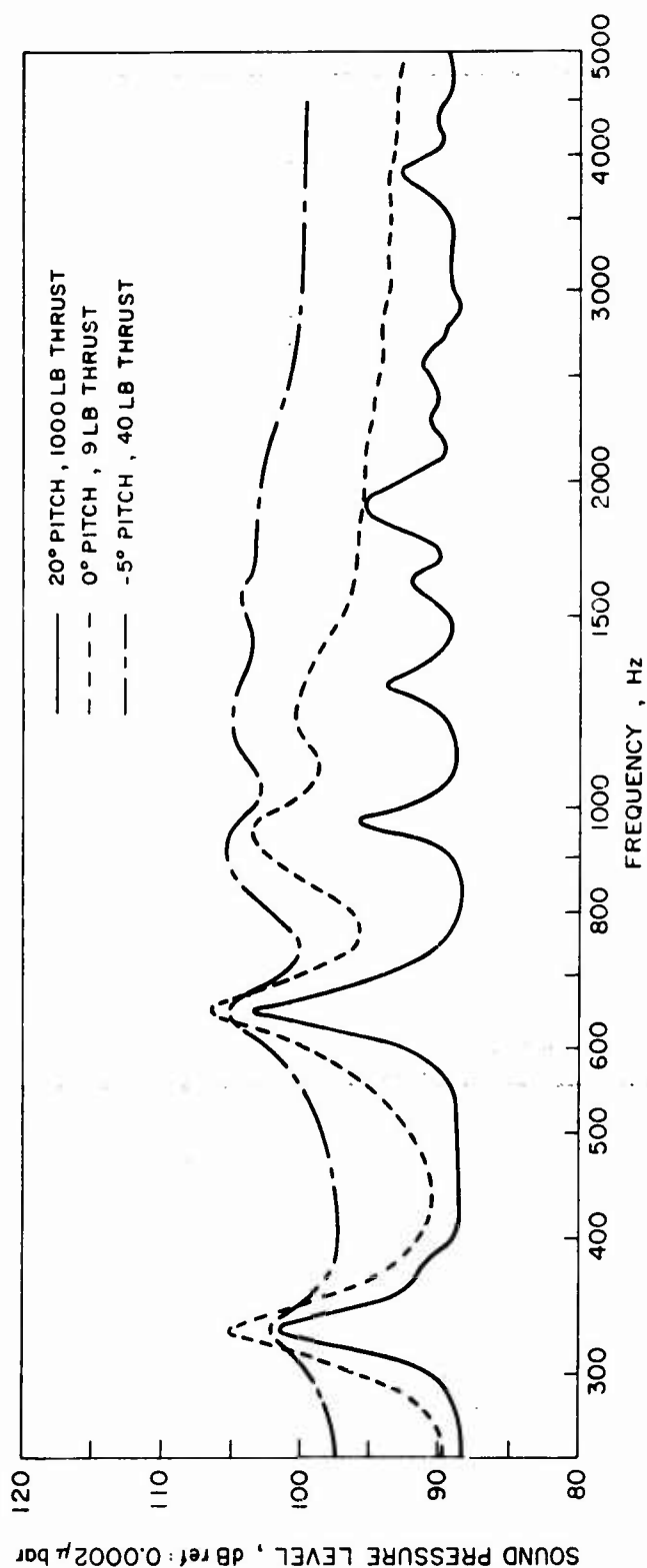
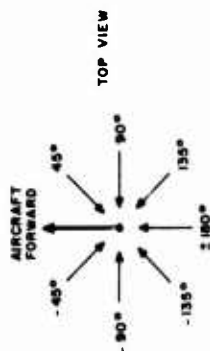


Figure C-6. Fan-in-Fin, Test Stand, Sound Pressure Level vs Frequency, Exit Side, -135-deg Azimuth (45 deg Off Fan Tip Path Plane), 500-ft Distance, 2997 RPM.

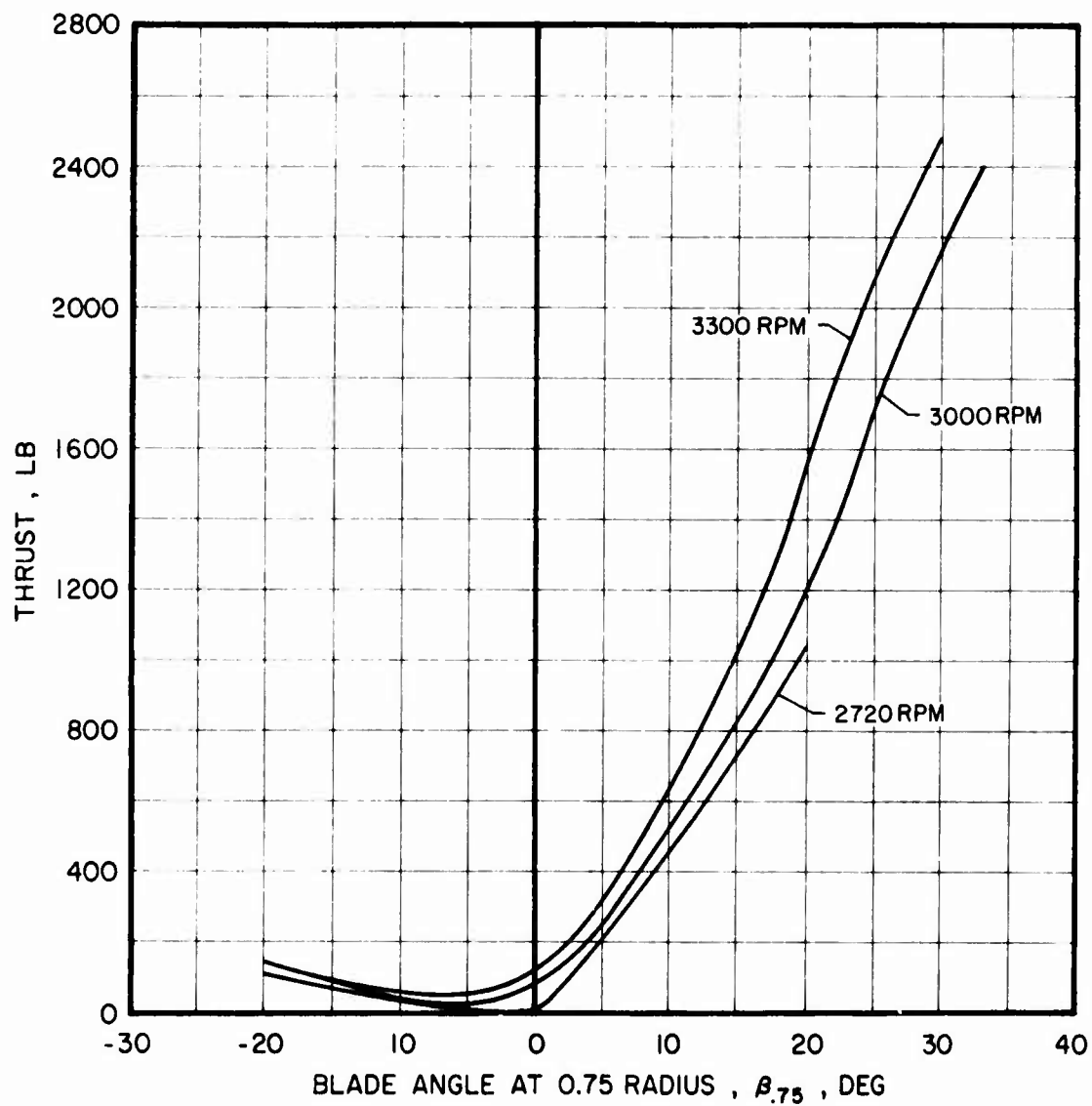


Figure C-7. Fan-in-Fin, Test Stand, Relationship Between Fan Blade Pitch Angle, Rotational Speed, and Total Thrust, SLS, 104% N_R .

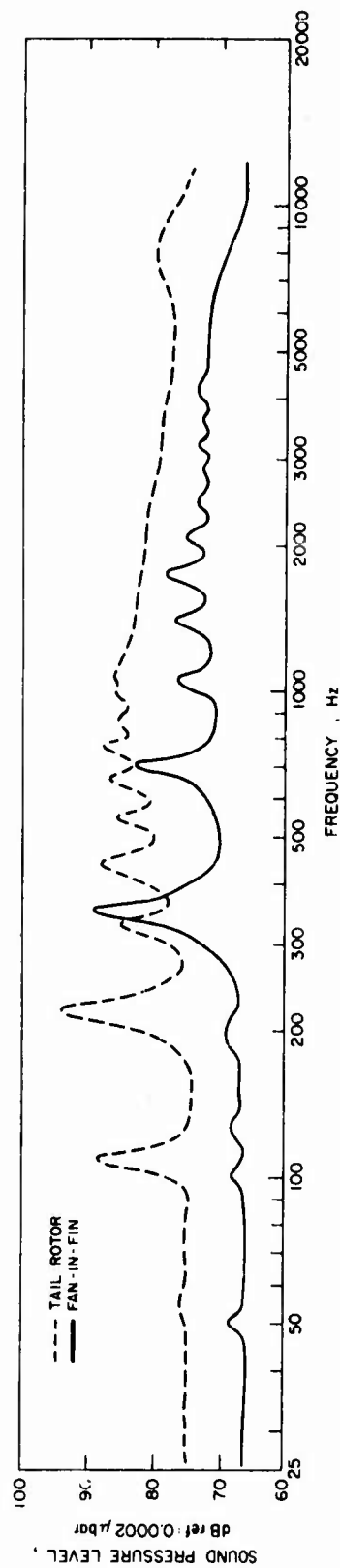


Figure C-8. Fan-in-Fin, Test Stand, 1/10 Octave Band Spectra Comparison With Tail Rotor at 1000 lb Thrust, 2997 RPM Fan, 1214 RPM Tail Rotor, 500-ft Distance.

In Figure C-9, perceived noise level vs. fan thrust is shown for the fan module test stand installation and the aircraft tie-down test at low positive and negative fan thrust levels typical for taxi conditions, at the -45-deg azimuth location. Wind was less than 5 knots. The data correlate well within the usual scatter observed for such tests.

FLIGHT NOISE SURVEY TEST

The flight portion of the fan-in-fin noise survey program was conducted at Sikorsky Memorial Airport in Stratford, Connecticut. The complete acoustical flight test program consisted of a hover survey and flyover data points at various airspeeds. In the area used for the flyover program, traffic variations altered the ambient noise level and made it necessary to take additional data. For the same reason, it was impossible to make subjective evaluations of aural detectability. The baseline S-67 data were obtained at Oxford Airport, Oxford, Connecticut, which has low ambient levels and a minimum amount of traffic, making conditions excellent for noise testing.

Comparative measured data taken during OGE hover (100-ft altitude) are presented in Figure C-10. These data show the fan to be quieter (a maximum of 3.5 PNdB) at all locations measured except at -90 deg and -45 deg. At the -90-deg and -135-deg azimuthal locations, the fan is louder by about 2.5 PNdB. However, the maximum noise level of the fan was lower than that of the tail rotor by about 3 PNdB.

The data measured during level cruise at 200-ft altitude are presented in the form of preferred octave band time histories in Figures C-11 through C-13. These data extend from a position 2000 ft before and 1000 ft past the directly overhead position. The data were acquired at constant recorder speed and the reduction in the distance scale on the plots with increasing aircraft speed is an indication of the shorter time taken by the aircraft to cover the 3000-ft distance. At each of the three airspeeds, a reduction of as much as 3 PNdB is obtained at the directly overhead position. At a position 1000 ft before overhead, the tail rotor is quieter by as much as 3.1 PNdB for the 80-knot and 120-knot cases, but becomes louder at the 175-knot pass by 2.7 PNdB. These noise levels are primarily controlled by the 500 Hz, 1000 Hz, and 2000 Hz octave bands. The difference in level of the 31.5 Hz and 63 Hz octave bands seems to be larger than the mid-octave levels but does not significantly affect the calculated PNL.

Aural detection time could not be obtained during the fan flight test program due to high ambient noise conditions at the test site. However, calculated aural detection times were made at an airspeed of 120 knots, using the ambient levels obtained at Sikorsky Memorial Airport. The results show the aircraft with either the fan or the tail rotor to have the same detection times (39.5 sec), detection being determined primarily by main rotor noise in both cases.

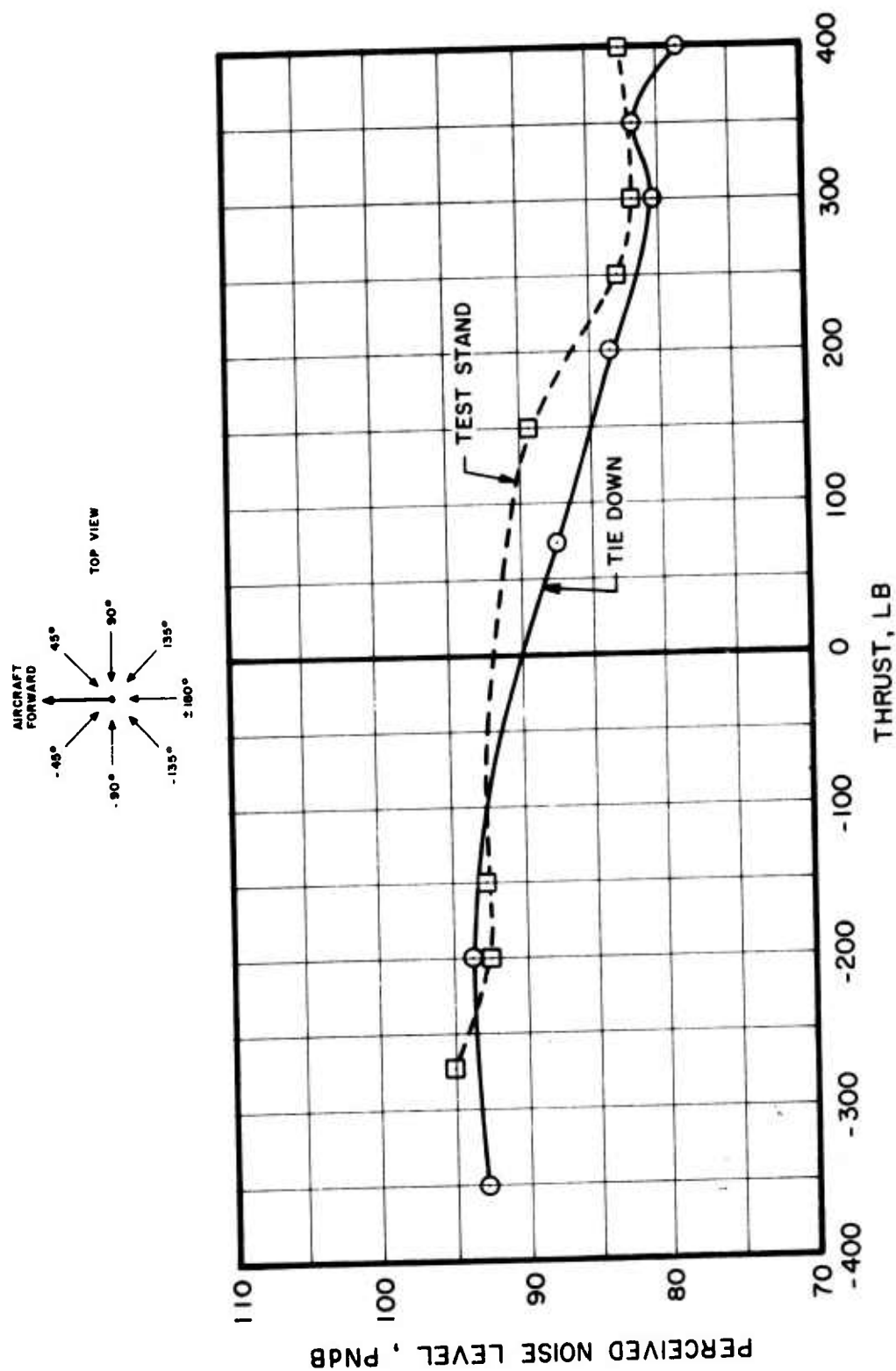


Figure C-9. Fan-in-Fin, Comparison of Perceived Noise Level vs Fan Thrust Between Test Stand and Aircraft Tie-Down Tests, -45-deg Azimuth, 2997 RPM, 500-ft Distance.

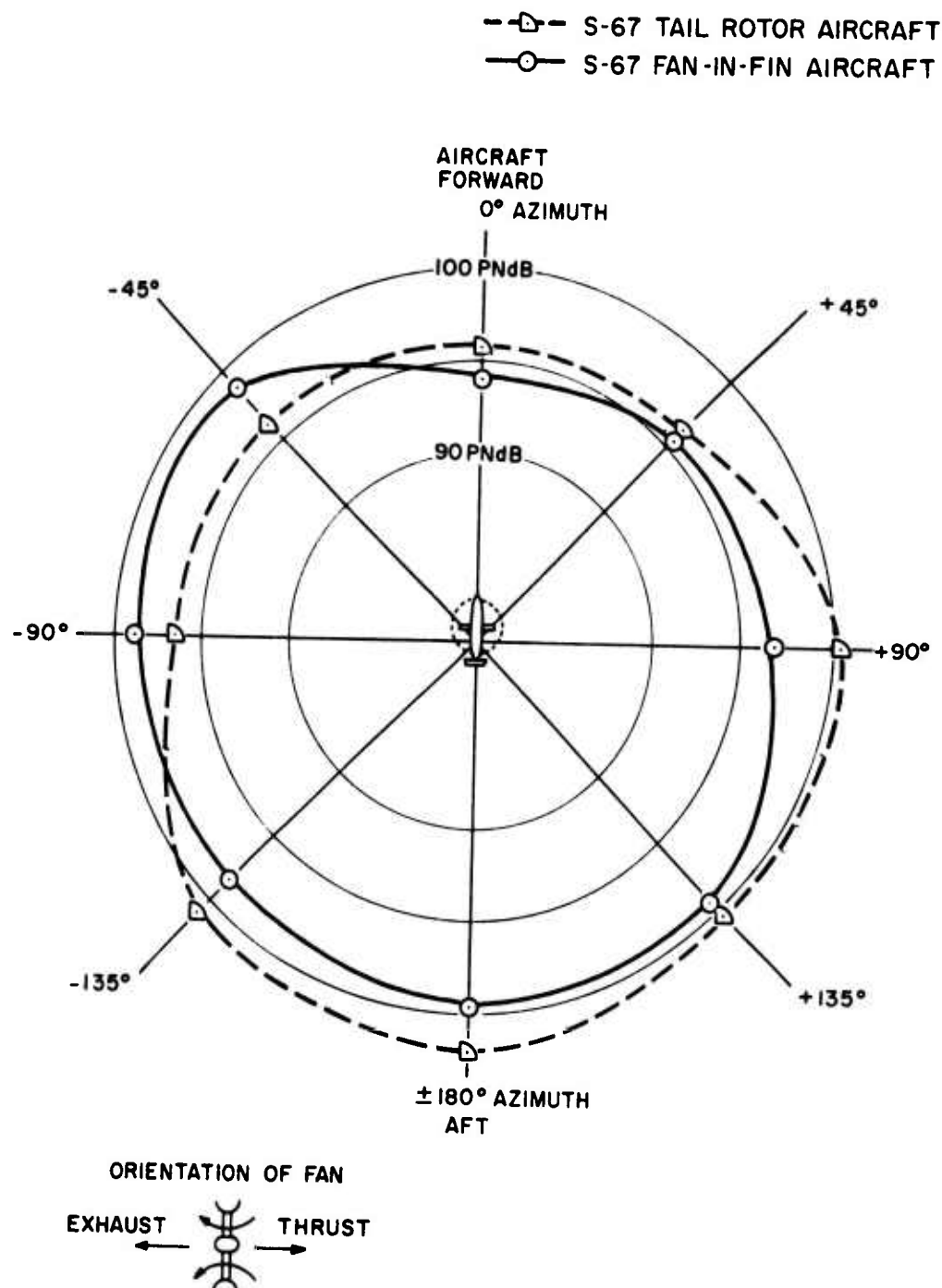
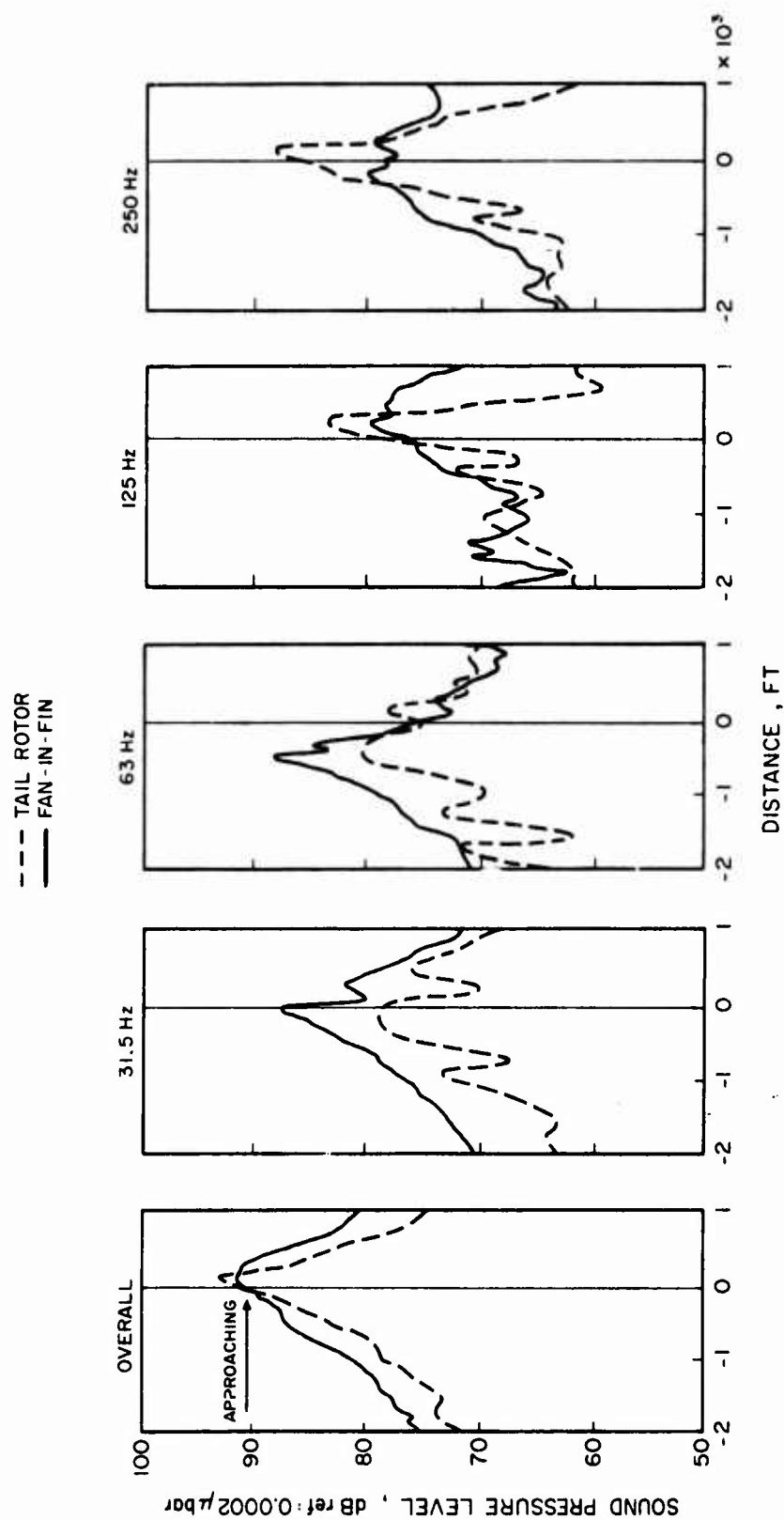
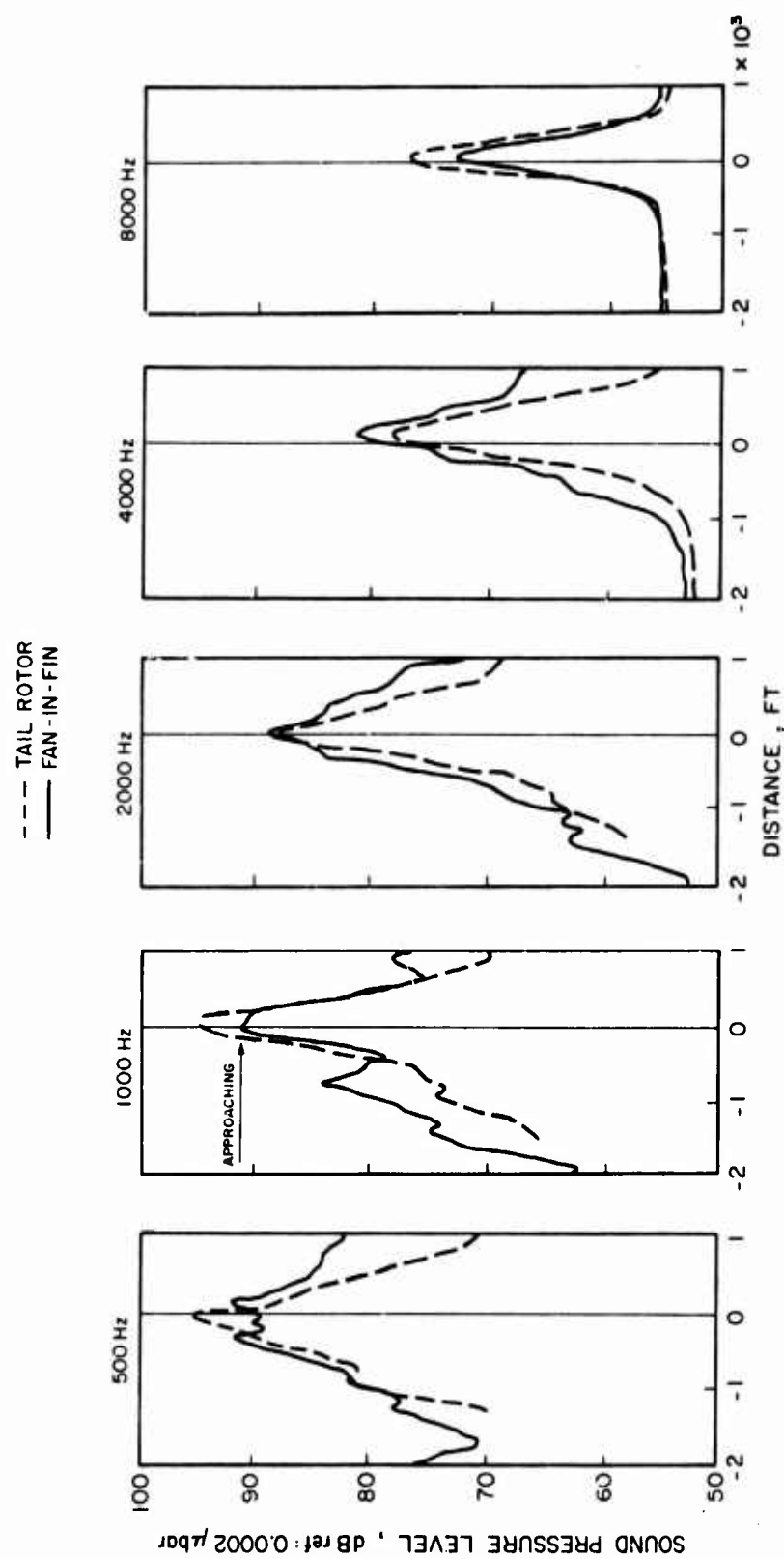


Figure C-10. Comparison of S-67 Aircraft Perceived Noise Levels in Hovering Flight, 100-ft Altitude, at 500-ft Distance.



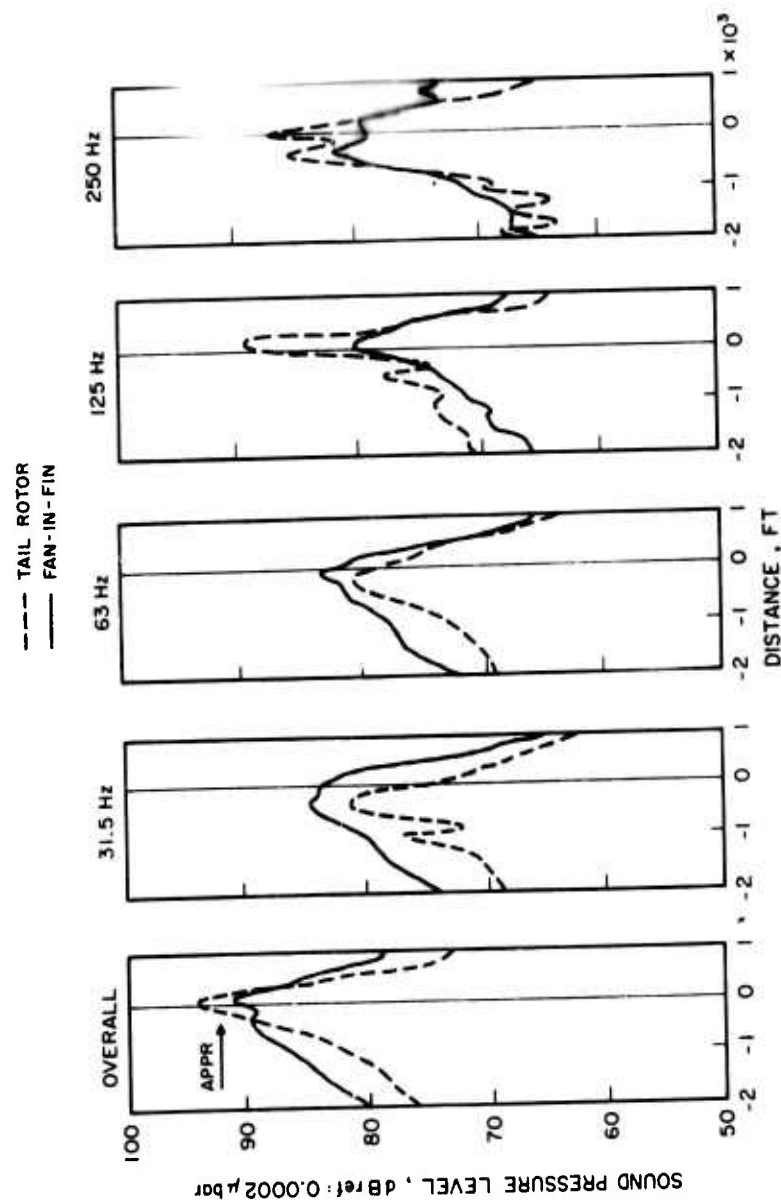
(a)

Figure C-11. S-67 Aircraft Sound Pressure Level vs Distance, 80-KIAS Fly-Over.



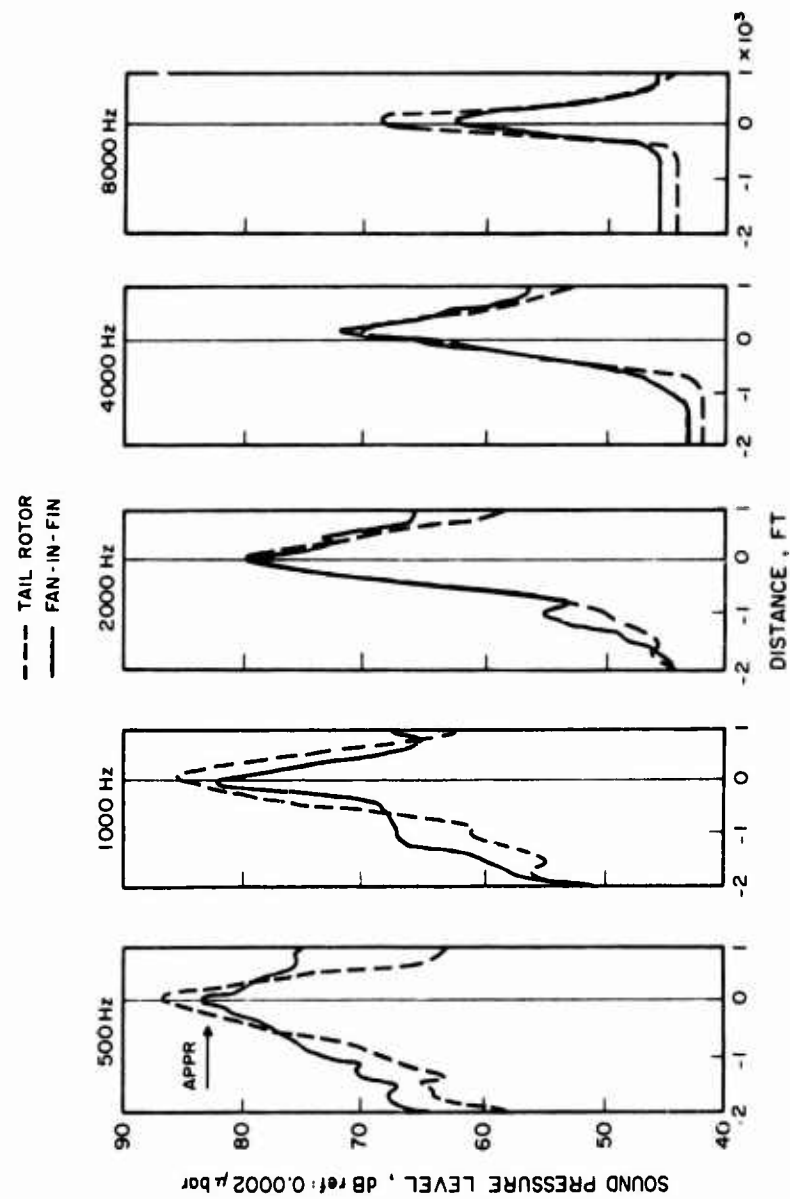
(b)

Figure C-11. Concluded.



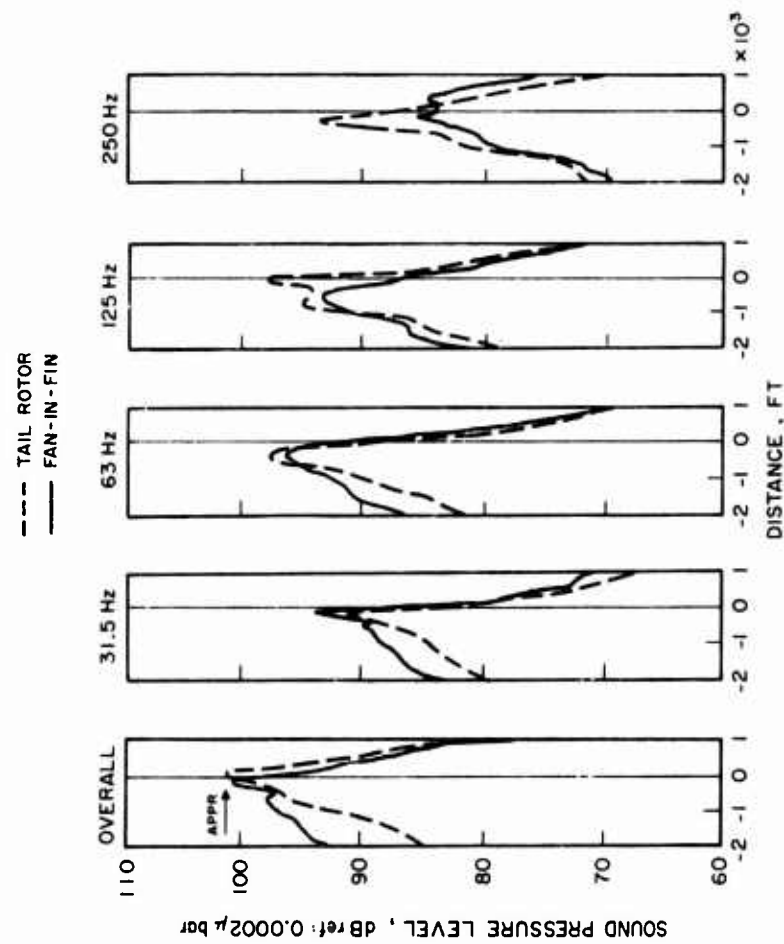
(a)

Figure C-12. S-67 Aircraft Sound Pressure Level vs Distance, 120-KIAS Fly-Over.



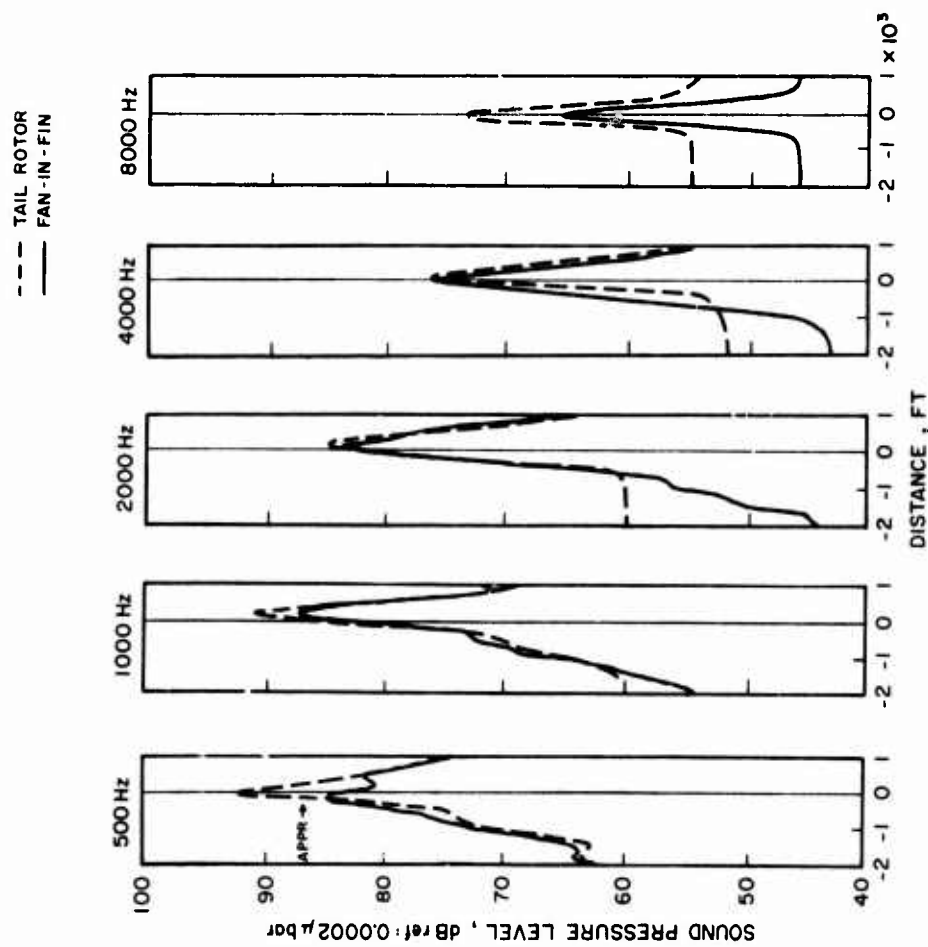
(b)

Figure C-12. Concluded.



(a)

Figure C-13. S-67 Aircraft Sound Pressure Level vs Distance, 175-KIAS Fly-Over.



(b)

Figure C-13. Concluded.

APPENDIX D. EVALUATION OF A COLLECTIVE FORCE AUGMENTATION SYSTEM

PREFACE

A collective force augmentation system (CFAS) was fitted in the S-67 helicopter and flight tested during the S-67 fan-in-fin flight test program on a noninterference basis.

The S-67 helicopter is equipped with a cruise guide indicator (CGI) system that visually displays main rotor loads to the pilot on a cockpit indicator; the display is expressed as the percentage of actual main rotor servo vibratory pushrod load compared with a reference load. The collective force augmentation system was added to provide an artificial force to the collective stick, supplying a force cue rather than a visual display to the pilot as an indication of main rotor loads. Thus, the pilot is made aware of high rotor load conditions without having to focus his attention on a cockpit indicator. High load factors experienced during maneuvering flight with correspondingly high rotor forces cause the CFAS to displace the collective stick downwards.

The CFAS had in-flight adjustable controls for threshold (start) and slope. System behavior varied as a function of control panel potentiometer settings. At high settings, unstable or oscillatory response was obtained in the collective channel. At low settings, the aircraft response differed from the CFAS off condition only in that collective stick damping was present. Due to limited time of the CFAS portion of the fan-in-fin program, it was impossible to fully evaluate the system, but enough has been learned to consider it as a likely candidate for collective channel control. Minor changes in circuitry were made during the flight test program as inputs from pilots were received.

FOREWORD

This Appendix presents design and installation descriptions, and flight test results of the CFAS portion of the fan-in-fin program. Sikorsky Aircraft was the contractor, and the S-67 Blackhawk was utilized for the installation of the system. Components of the system were designed, manufactured, and installed at Sikorsky Aircraft. The flight test program totaled 1.5 flight hours and consisted of gain optimization while in high rotor load environments. The program was conducted at the contractor's facility for the Eustis Directorate, U. S. Army Air Mobility Research and Development Laboratory, Fort Eustis, Virginia, under Modification P00005 of Contract DAAJ02-72-C-0050, DA Project 1F163204D157.

Mr. J. Whitman and Mr. H. Murray were the Army technical representatives, and Mr. D. Simon was the Army project pilot.

INTRODUCTION

The collective force augmentation system (CFAS) is designed to provide collective stick trim beeping capability, and an increased heads up capability for the crew by providing cues to the pilots via the collective

stick during high performance flight. During maneuvers in a winged helicopter, the collective stick is used to adjust the distribution of lifting force between the rotor and the wing. Lowering the collective stick reduces rotor loads and increases wing lift, but also reduces forward velocity. The best maneuvering performance is achieved, therefore, by lowering the collective just far enough to avoid excessive rotor loads. In most helicopters, the degree of adjustment required can be estimated by the level of airframe vibration induced by blade stall. In the S-67, because of the efficiency of the main rotor bifilar vibration absorber, this airframe vibration cue is virtually nonexistent, and pilots heretofore have relied heavily upon the cruise guide indicator (CGI) to provide a visual cue of impending blade stall and high rotor stress.

As part of the preparation for the U. S. Army evaluation of the S-67 force augmentation system (FAS), Reference 7, a collective stick shaker was installed in the aircraft. This device applied a small n-per-revolution vibration to the collective stick whenever rotor loads exceeded a preset threshold. It was intended to replace the vibratory cue that the bifilar absorber masked. Army evaluation pilots rated the effect as a definite improvement. It reduced the attention to the CGI that was previously required. The device, however, has an inherent shortcoming in that it produces a stick vibratory cue, perceived by the pilot as an on-off function. The information is sufficient to warn the pilot to lower the collective, but does not indicate to him the amount of stick displacement necessary to simultaneously unload the rotor while maintaining maximum available performance. In the Army evaluation, pilots found that they often lowered the collective stick too far. They avoided excessive rotor loads, but could not take advantage of the total performance capability available (Reference 8). CFAS was designed to provide force cues to the collective stick as a function of CGI information to overcome these shortcomings. Some of the items to be accomplished in the program were:

- . Determine the extent to which CFAS improves the maneuvering handling qualities of an attack helicopter.
- . Define the force level (lb/% CGI) to be utilized.
- . Evaluate the variable rate-force beeper as an improvement over the conventional beeper.

SCOPE OF PROGRAM

The CFAS program consisted of three phases of operation: First, fabricating electronic modules, installing wiring, modifying the auxiliary servo and collective stick grips, installing the CFAS control panel, and providing the necessary interfacing with the new equipment.

The second phase consisted of ground checking and failure demonstration. Data was taken and seen to agree with expected results.

The third phase was the flight test portion in which gain optimization was performed. A matrix of start and slope values was defined. The pilot flew

these values under high main rotor loading and nominal values were found.

The CFAS was built as a prototype breadboard system and was flown in that manner, although a production configuration would be a comparatively easy task to define. New electronic modules were housed in the existing FAS amplifier. Interfacing was provided between the modules, CFAS control panel, cyclic and collective stick functions, and the existing CGI system.

SYSTEM DESCRIPTION

Design and Operation

The block diagram of CFAS is shown in Figure D-1. A stick trim function is provided by circuitry installed in the FAS computer. Trim position is held by utilizing a stick position sensor. Stick movement from the trim position is transformed into an electrical signal which is utilized by the stick force characteristics to reposition the stick via the auxiliary servo. The stick force characteristics are shown in Figure D-2, and depict the force experienced by the pilot when positioning the collective stick against trim. The force characteristic is the combination of shaping circuitry in the FAS computer and friction present in the control system. Repositioning the stick to a new position can be accomplished by either utilizing the trim release switch or beeper switch, both located on the collective stick grip. Depressing the trim release allows manual positioning of the stick by synchronizing stick position until the button is released. Beeping the stick is accomplished by applying force to the beeper switch. Unlike conventional make-and-brake toggle switches, the switch utilized is one which is force operated, producing a rate of movement of the collective proportional to the amount of force applied to the switch. The maximum rate is set at 1.0 inch per second.

In conjunction with the stick trim system, the cruise guide amplifier produces a signal used to position the collective stick as a function of a percentage of cruise guide. Rotor loads are measured at the stationary star, and the electrically amplified signal from the cruise guide amplifier is used in the CFAS shaping circuitry to produce a signal. The signal is electrically added to the stick trim information dropping the collective for increasing cruise guide indications. The resulting force (pull) required by the pilot to keep the stick from dropping is shown in Figure D-3.

During flight testing, the cruise guide force characteristics were adjustable by the pilot for optimization. As shown in Figure D-4, the CFAS control panel permitted adjusting the start point to a specified displacement and/or force by adjusting the gain for cruise guide indications between the start value and 60% cruise guide. For values above 60%, the circuitry is designed to produce a relatively fast collective response of 0.5 lb/% due to impending blade stall.

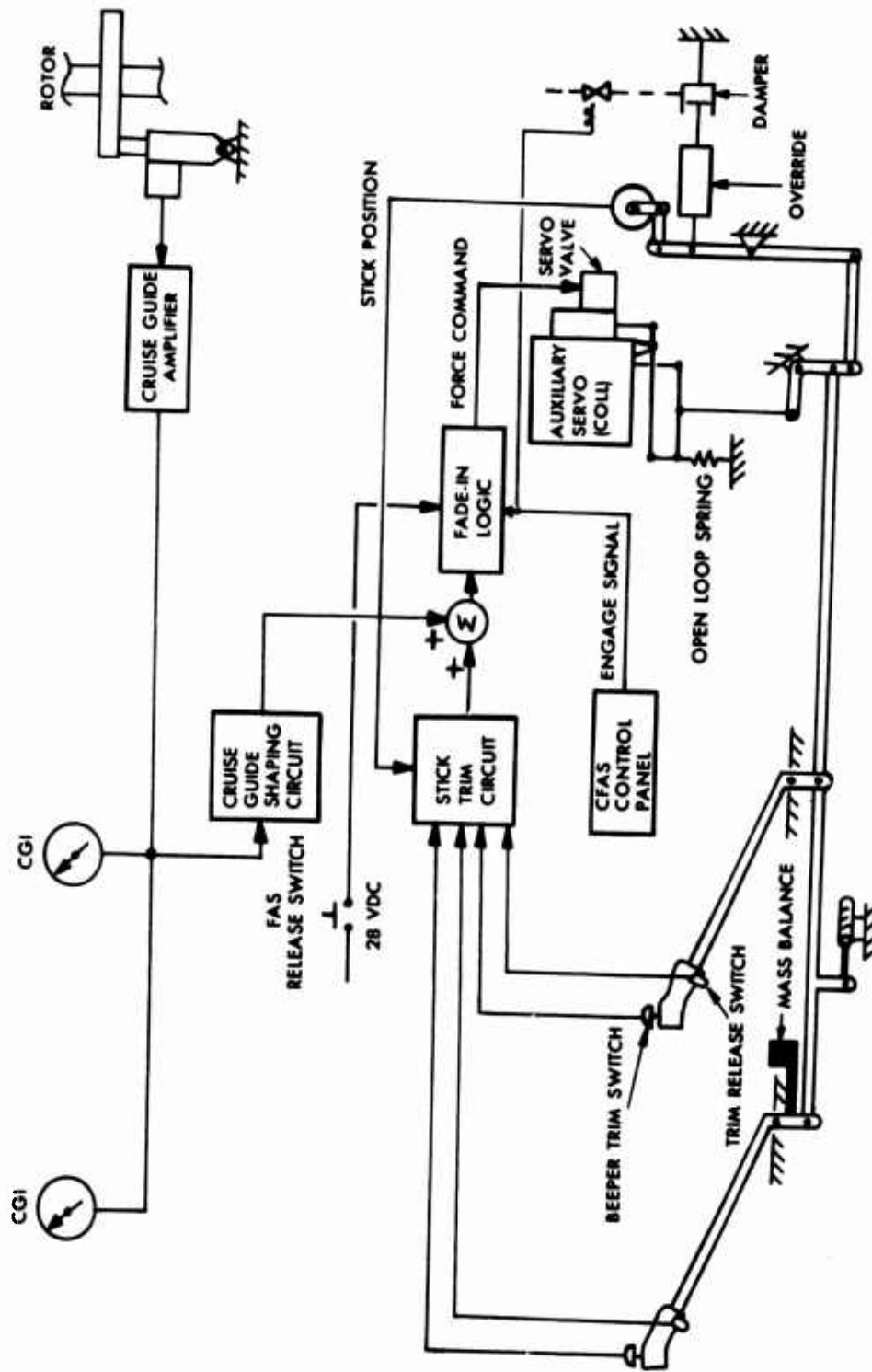


Figure D-1. CFAS Block Diagram.

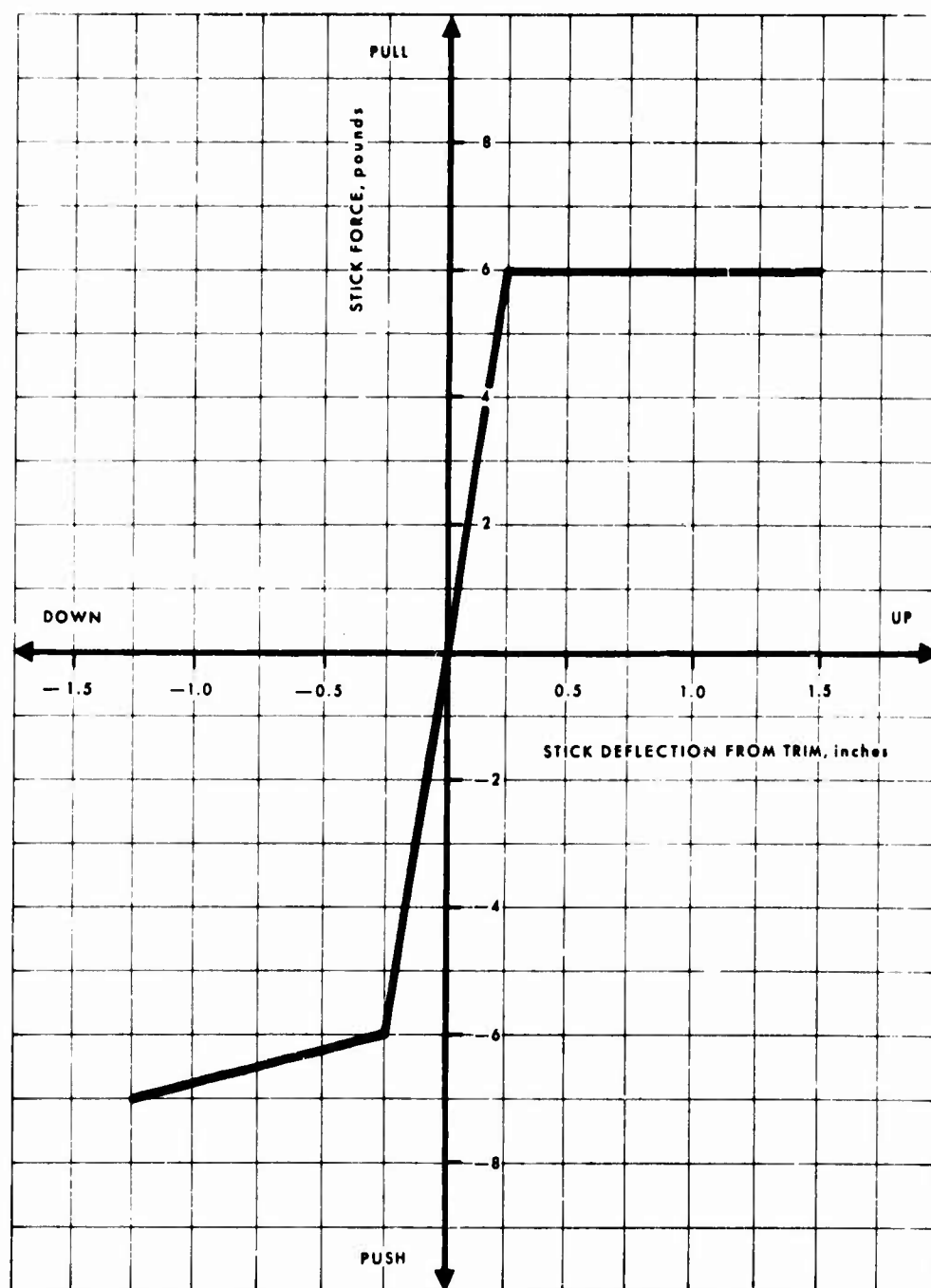


Figure D-2. Typical Stick Force Characteristic.

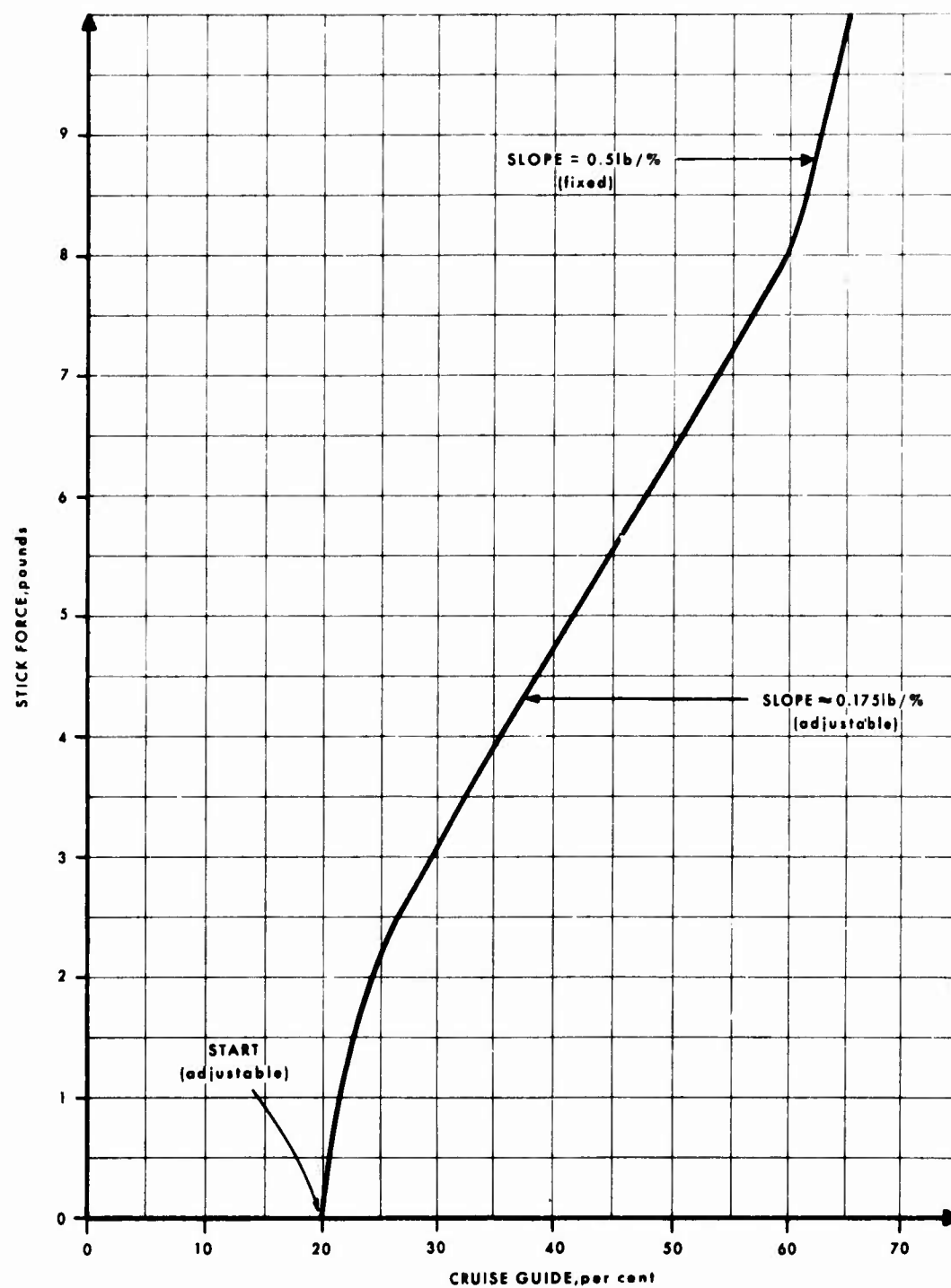


Figure D-3. Cruise Guide Force Characteristic.

Implementation of the CFAS required modifications as defined below and shown in Figure D-5.

A standard servo valve was utilized on the collective auxiliary servo to provide a means of applying stick force by commanding compression of the open loop spring.

The addition of a damper/override spring assembly was required. Its purpose was to provide a smoothing effect for pilot inputs and to limit the rate of stick motion in the event of a CFAS malfunction. The damper force is 6.0 pounds per inch per second.

Mass balancing the collective stick with the friction lock set to zero was also necessary. To reduce friction, the cable connecting the collective sticks was replaced by hard linkage.

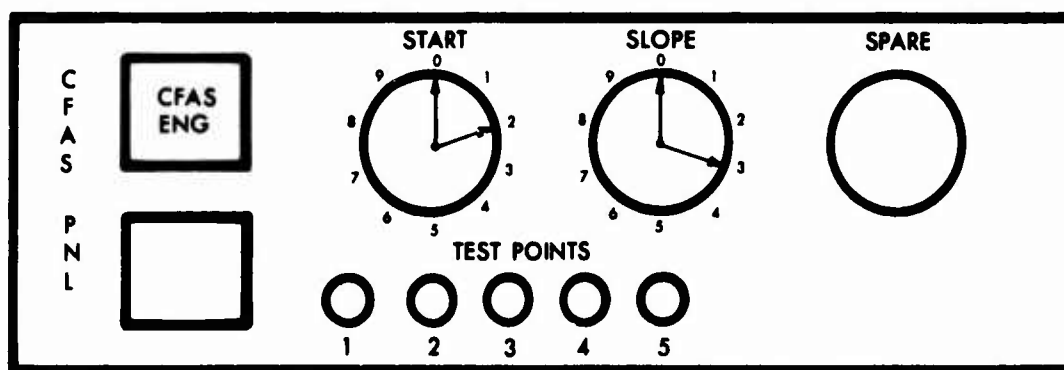


Figure D-4. CFAS Control Panel.

CFAS Fault Protection

The CFAS utilizes single channel electronics, and no failure monitoring or automatic shutdown is necessary. The concept of applying stick force and providing stick position control through use of the open loop spring with single channel electronics is utilized in all standard S-61 aircraft equipped with a collective AFCS. In these systems, the rate of stick motion for a hardover input is a function of the friction setting. Using a low friction setting, the stick can move full travel in about 1.0 second; with friction off, stop to stop time is about 0.5 second. In the CFAS, the hydraulic damper limits the maximum stick rate in the event of a hardover to about 20% per second, as shown in Figure D-6. Furthermore,

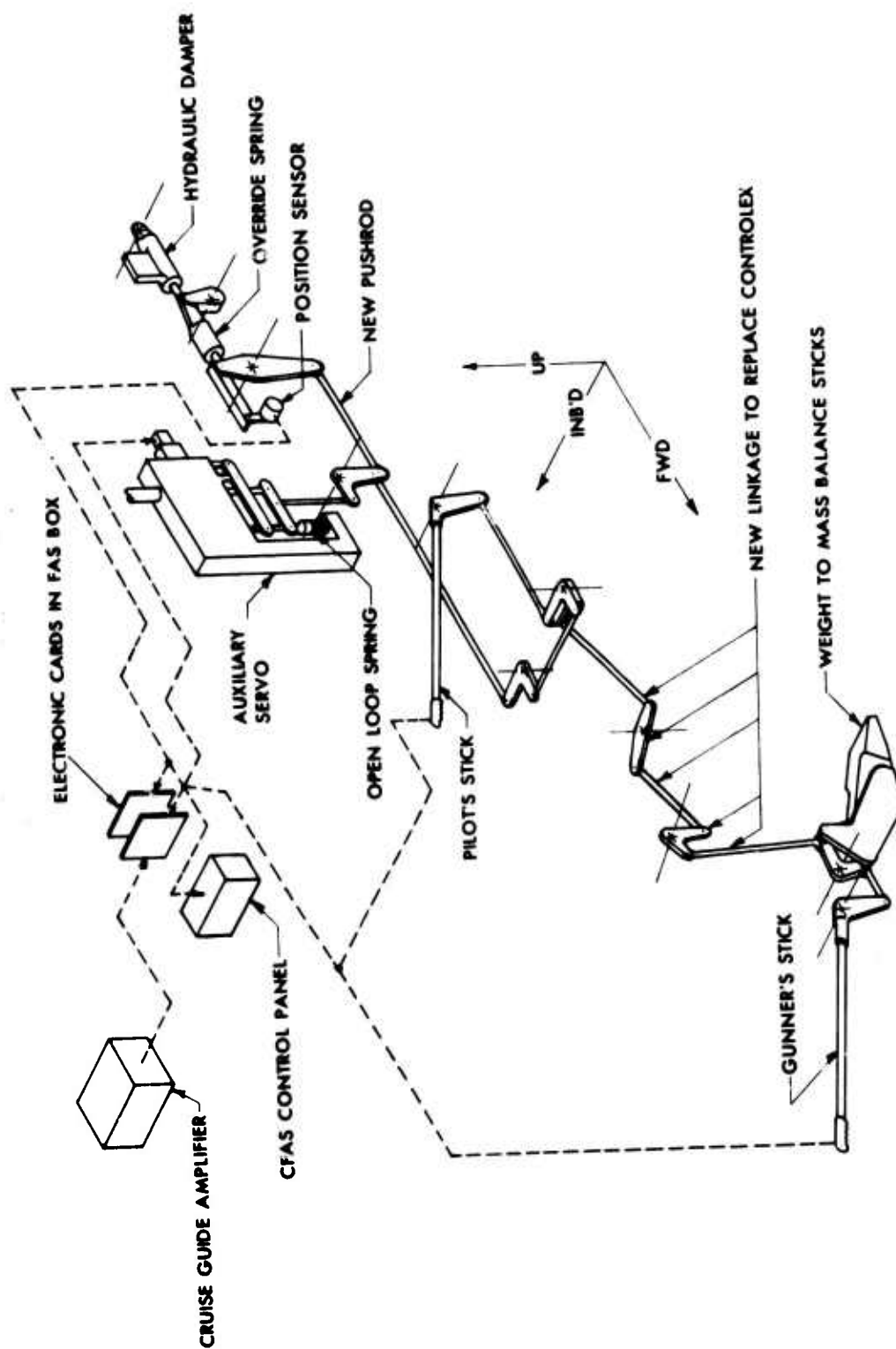


Figure D-5. CFAS Controls Schematic.

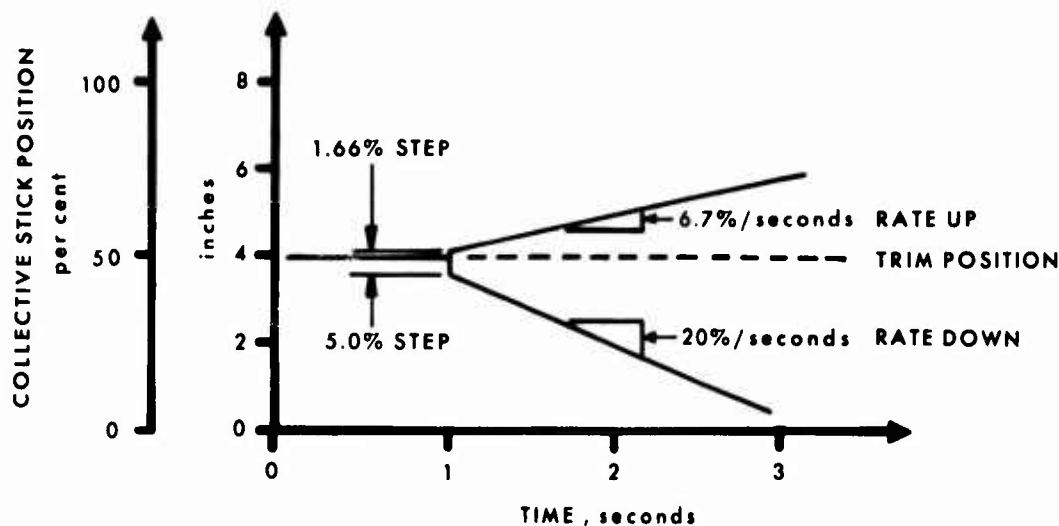


Figure D-6. CFAS Worst Case Hardover.

under normal operating conditions, electrical up-collective hardovers are limited by circuitry to approximately 6.7% per second. Figure D-6 shows hardover initiation at time = 1.0 second. The initial step is due to the authority of the series servovalve and occurs without stick motion while subsequent motion takes place as the stick moves against the hydraulic damper. The pilot can override the collective motion at any time with a maximum force of 10.0 pounds. Safety of flight for the CFAS, therefore, is achieved by an authority limit worst case of an initial 5% servo motion, by a worst case hardover stick rate of 20% per second, and by manual override capability. In addition, the pilot may disengage the CFAS force command by depressing the FAS release switch on the cyclic grip. This action removes electrical signals to the collective stick, but allows the hydraulic damper to function, smoothing the stick response. The removal of the damper as well as all electrical signals to the collective stick is accomplished by disengaging CFAS from the CFAS control panel.

RESULTS AND DISCUSSION

Flight Evaluation

Optimization of CFAS's cockpit and adjustable parameters was accomplished by flying prescribed combinations of the start and slope settings located

on the CFAS control panel. The settings were chosen at both high and low extremes as well as mid-position values.

Start settings of 1.0 to 3.0 (cruise guide readings of 10% to 30%) were evaluated. Slope settings of 1.0 to 6.0, resulting in pounds of collective force per percent cruise guide, were used. Due to the time limitations imposed by the fan-in-fin schedule, the CFAS was investigated only in the maneuver-entry regime. Turn entries were initiated from trim level flight at 140 knots airspeed with a collective setting which provided 70% torque.

Start values flown were 1.0, 2.0, and 3.0. Slope values were 1.0, 3.0, and 6.0. These values were evaluated in a 3-x-3 matrix. Qualitatively, for the maneuvering case only, a start of 2.0 and a slope of 3.0 proved to be the best combination (see Figure D-3).

It is important to note that CFAS was evaluated in the open loop mode only, that is, as an autopilot aid without pilot input. As such, it performed the task of limiting control system loads during maneuvering flight as well as the pilot/stick shaker combination. It had the advantage that, as opposed to the human pilot, it never became distracted or tired.

The CFAS was not evaluated at high gross weight, high altitude cruise conditions during this program. However, cross-country flight under these conditions conducted earlier in light to moderate turbulence (normal thermal activity) produced cruise guide excursions to 80 - 100% from a trim value of 30%. An operational CFAS must not have a threshold below control system endurance loads, yet must be responsive enough to limit excursions within reason.

When maneuvering the S-67 at lower collective settings, it is possible to increase the main rotor rotating control loads (push rods), to a limit value before the stationary control loads reach a limit. Since the cruise guide is based on stationary system vibratory loads, this presents a problem for the present CFAS design. Since the case of reaching either a rotating or stationary control system limit as a function of collective position is not peculiar to only the S-67 helicopter, an effective CFAS must be flexible enough to sense the critical parameter in each case.

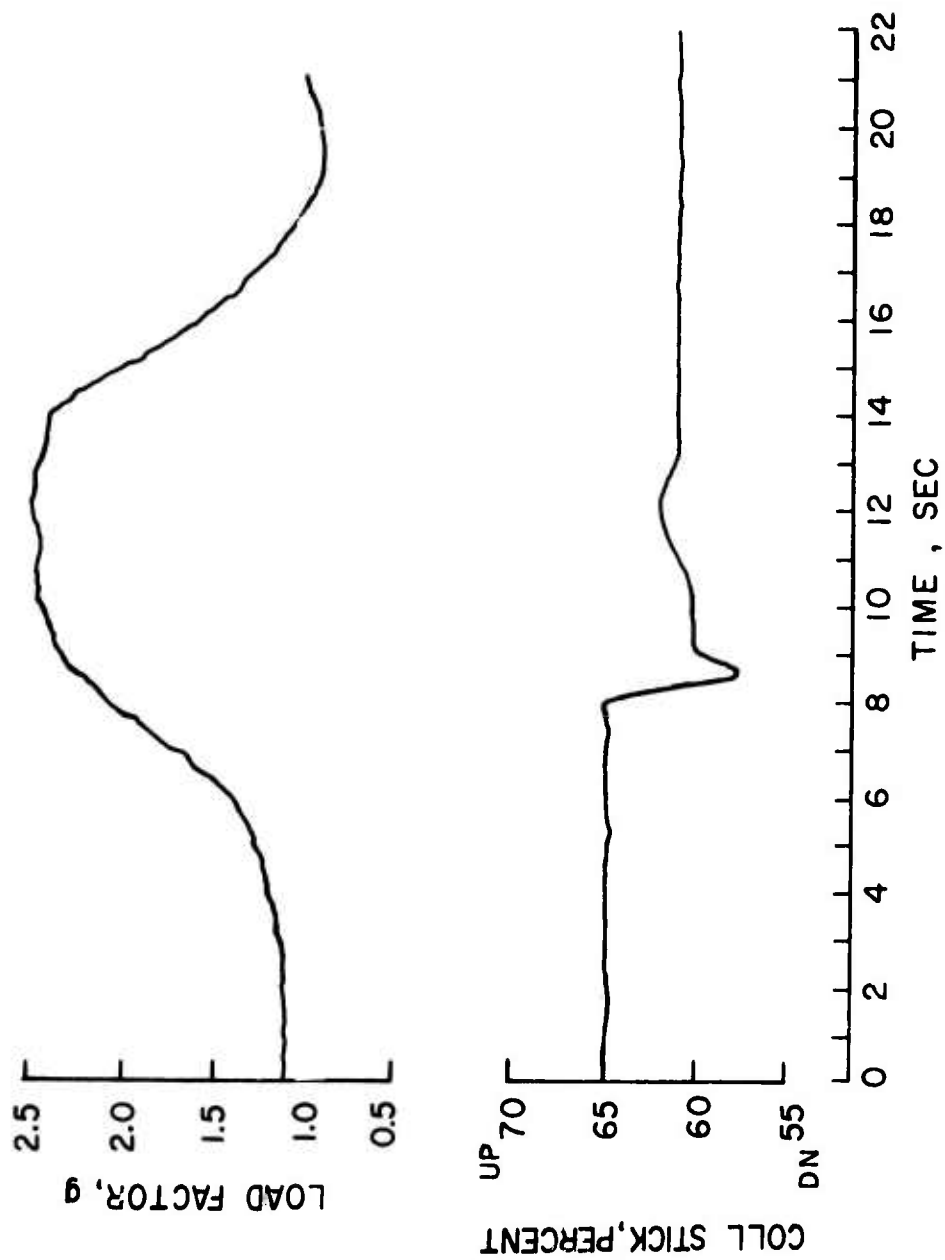
Flight Test Results

Nominal knob potentiometer settings determined during the flight test program were:

Start potentiometer - 20% of full scale

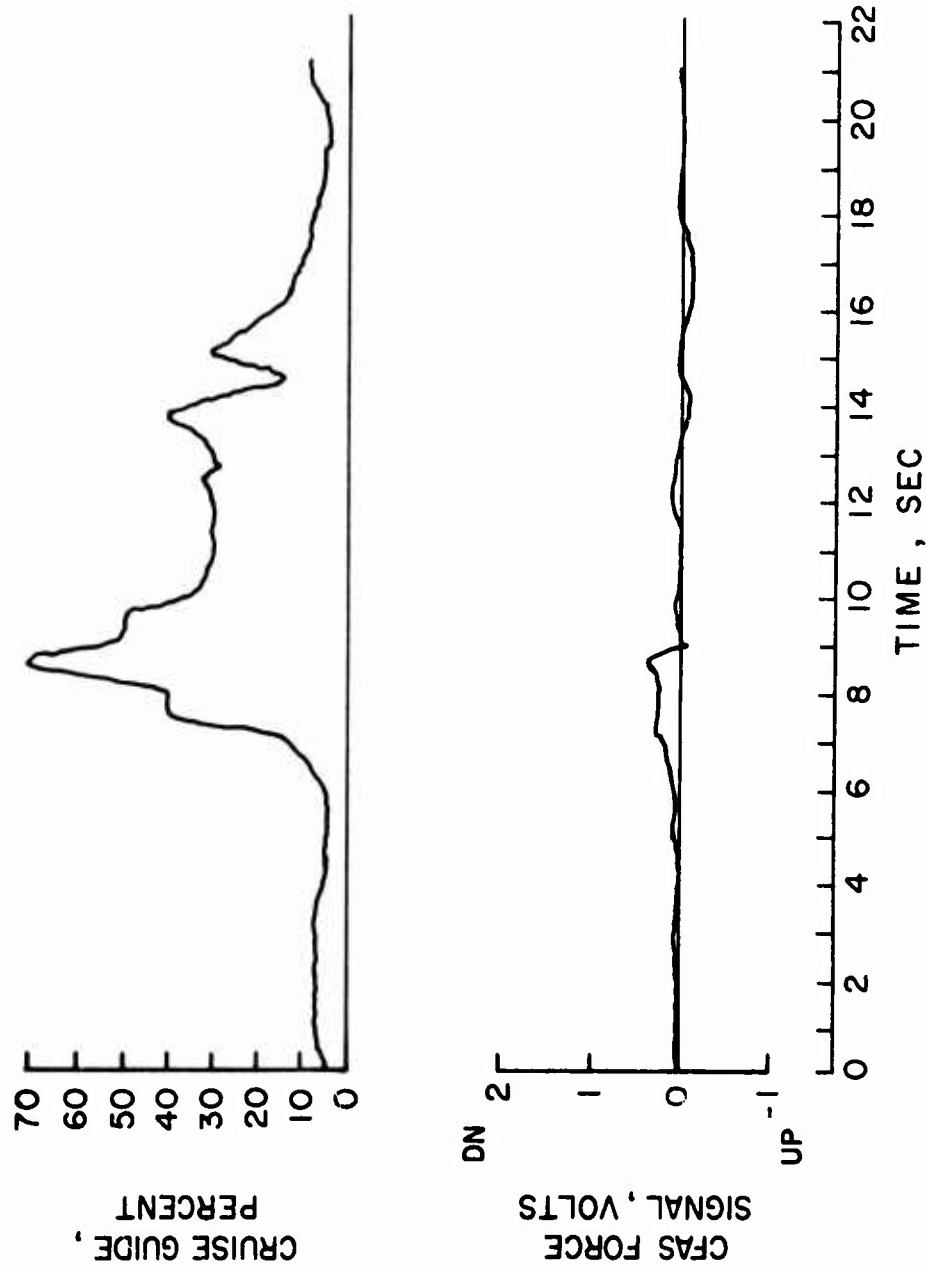
Slope potentiometer - 30% of full scale.

These values correspond to the graph shown in Figure D-3. The flight test results shown in Figure D-7 were taken with the nominal settings, and show the relationship between pitch attitude, roll attitude, collective stick position, cruise guide indicator output, collective force augmentation system output, and load factor. The flight test results, Figure D-7,



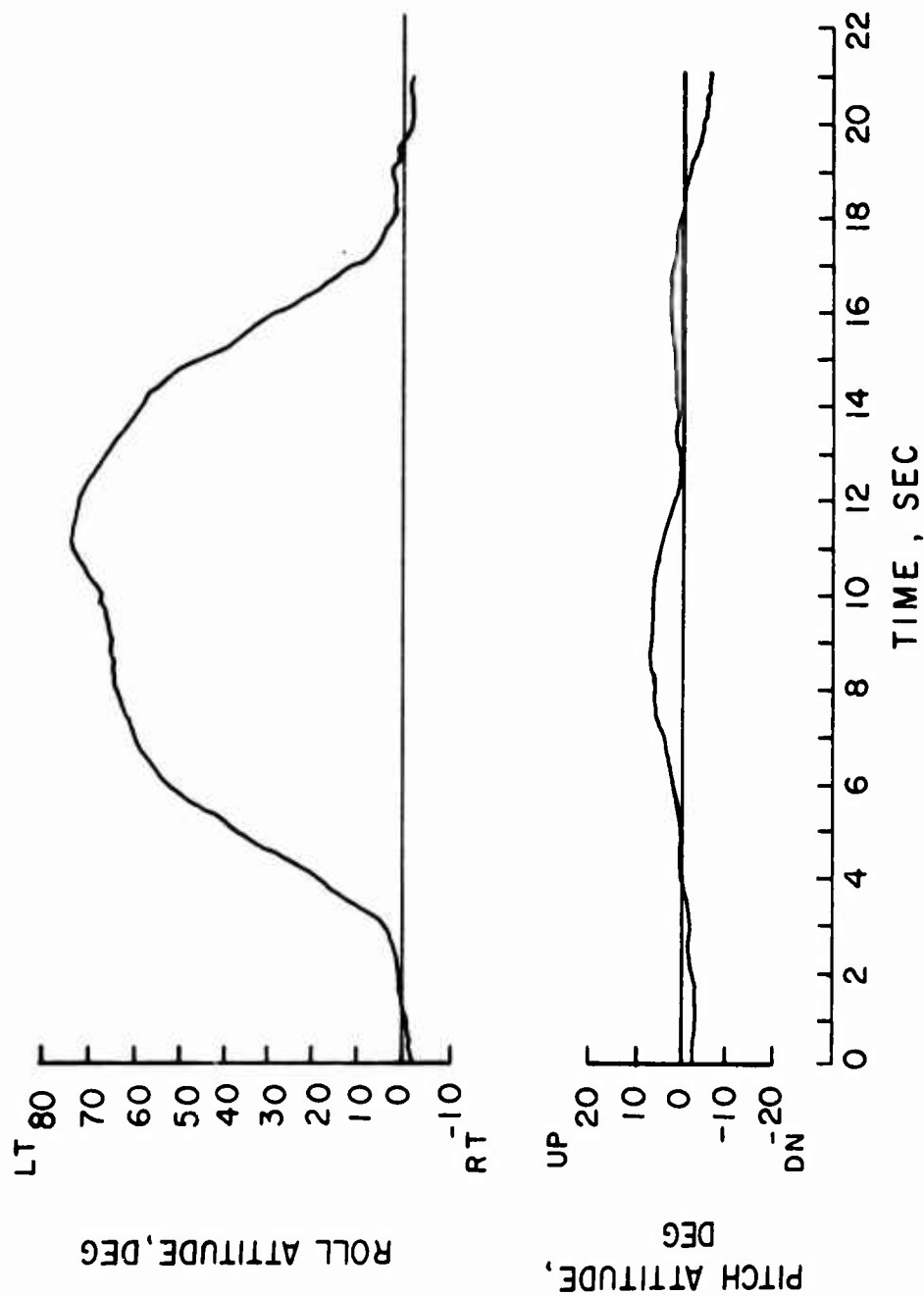
(a)

Figure D-7. CFAS Flight Test Evaluation Results.



(b)

Figure D-7. Continued.



(c)

Figure D-7. Concluded.

indicate that the CFAS is at least as responsive as the pilot in maintaining acceptable rotor loads.

CONCLUSIONS AND RECOMMENDATIONS, CFAS

In the allotted time given to CFAS development, it has been shown that the system is capable of limiting rotor loads by effectively controlling the collective stick. Further development could include modifying the gain characteristics of CFAS and possibly providing more anticipation as blade stall is approached. Rotating control loads, while presently monitored in the S-67 cockpit, could be used as an input to the CFAS in an either/or configuration with stationary loads. In that way, either stationary vibratory loads or rotating push rod loads would consequently affect the collective stick.

Further development of the CFAS should also include an evaluation of the force feel characteristics of the collective stick, much the same as cyclic FAS. Flights should also be made at heavy gross weight and high altitude.

LIST OF SYMBOLS

AUX	auxiliary
b	fan blade chord, in.
B_{10}	bearing life expectancy during which 90% of a given group of bearings will remain in service, hours
B.L.	butt line (location reference)
CFAS	collective force augmentation system
C.G.	center of gravity
CGI	cruise guide indicator
C_{L_D}	design lift coefficient
C_{L_i}	integrated lift coefficient
D	main rotor diameter or fan diameter, ft
deg	degree, angular
DN	down
FAS	force augmentation system
fpm	feet per minute
FWD	forward
GW	gross weight, pounds
g	load factor
h	height of main rotor above ground, ft
h_f	fan blade thickness, in.
Hz	hertz, cycles per second
IGE	in ground effect
I_{xx}	roll moment of inertia, slug-ft ²
I_{yy}	pitch moment of inertia, slug-ft ²
I_{zz}	yaw moment of inertia, slug-ft ²
I_{xz}	cross product of inertia, slug-ft ²

LIST OF SYMBOLS (CONTINUED)

KCAS	calibrated airspeed, nautical miles per hour
KIAS	indicated airspeed, nautical miles per hour
knots	nautical miles per hour
KTAS	true airspeed, nautical miles per hour
LT	left (side)
M	Mach number (main rotor blade tips)
MRHP	main rotor power, HP
N	number of main rotor blades
n	blade passage frequency
ND	nose down
NOE	nap of the earth (mode)
N_R	nominal operating rotational speed (100 percent for SH-3/S-61 series aircraft, 104 percent for S-67)
NU	nose up
OGE	out of ground effect
PED	pedal
PNdB	unit of perceived noise level
PNL	perceived noise level, PNdB
Q	engine or gearbox torque, ft-lb, or % rated torque
R	main rotor radius or fan radius, ft
r	fan local radius, ft
rad	radian
RT	right (side)
RPM	revolutions per minute
SAS	stability augmentation system
SHP	shaft horsepower, engine output or fan input

LIST OF SYMBOLS (CONTINUED)

SLS	sea level standard conditions (0 ft, 59°F)
STA	station (location reference)
STD TR	standard tail rotor
T	air temperature, ° Rankine
T ₀	air temperature, 519 ° Rankine
V	airspeed, ft/sec
V _D	dive speed, KTAS (200 KTAS for S-67)
V _h	maximum level flight speed at maximum continuous torque (Q = 86%), KTAS
V _j	fan induced flow velocity, ft/sec
V _{max}	maximum level flight speed at maximum torque (Q = 111%), KTAS
W.L.	waterline (location reference)
X	longitudinal axis (plus aft)
x	r/R, fan local radius/fan radius
Y	lateral axis (plus left, looking forward)
Z	vertical axis (plus up)
$\dot{\alpha}$	angular rate, deg/sec
β	fan blade pitch angle, deg
$\beta.75$	fan blade pitch angle, deg, at 75% blade radius
ρ	air density, slugs/ft ³
ρ_0	air density at SLS, slugs/ft ³
θ	air temperature ratio, T/T ₀
ΩR	tip speed, main rotor or fan, ft/sec